



SCUOLA INTERNAZIONALE SUPERIORE
DI STUDI AVANZATI

DOCTORAL THESIS

Matter Fields in Asymptotically Safe
Quantum Field Theories of Gravity

Author:
Peter LABUS

Supervisor:
Prof. Dr. Roberto PERCACCI

*A thesis submitted in fulfilment of the requirements
for the degree of Doctor of Philosophy*

in the

Astroparticle Physics Group
Department of Physics

August 2017

PHD PROGRAMME IN ASTROPARTICLE PHYSICS, SISSA TRIESTE, ITALY.

The research for this PhD thesis project was carried out under the supervision of Prof. Dr. Roberto Percacci with financial support of a SISSA PhD Fellowship.

September 2017.

Abstract

In this doctoral thesis we present the research of Refs. [1–4] concerning the asymptotic safety scenario in quantum gravity. We motivate the theoretical and conceptual need for the existence of a theory of quantum gravity, and explain how such a theory might be realised through the construction of an ultraviolet complete quantum field theory defined via a high-energy interacting fixed point.

In particular, we give a pedagogical introduction to the functional renormalisation group, as well as fixed points and critical phenomena. Thereafter we investigate the issue of background independence, which is introduced when constructing a scale-dependent effective action of a gauge theory using the background field formalism through the introduction of an infrared cutoff operator and the gauge fixing procedure. To this end we study simultaneous solutions of the flow equation combined with so-called modified split Ward identities in a conformally truncated theory in the derivative expansion.

In the main part of this thesis we study the dynamics of a gravitational system coupled to a number of scalar fields. In doing so, we find scaling solutions in a fully functional truncation using the derivative expansion and background field approximation on a d -dimensional sphere. We then study a similar system using the vertex expansion in a fully dynamical fluctuation field calculation. This is done in the exponential as well as the linear parametrisation of the metric, using different gauge fixing procedures. We find that the overall behaviour is very similar in both cases. We furthermore find however that the contribution of the scalar fields to the gravitational coupling differs in its sign compared to older results obtained in a background field approximation. To correct this behaviour, we supplement the background field equations with modified split Ward identities, with the aim to obtain the fluctuation field behaviour from a background approximation. This seems to give satisfactory results in the case of the cosmological constant, whilst the running of Newton's constant still differs significantly.

Acknowledgements

First and foremost I would like to thank my supervisor Roberto Percacci for outstanding support and guidance during my three years of research at SISSA.

It is furthermore with great pleasure that I acknowledge the help and support of my collaborators Pietro Donà, Astrid Eichhorn, Tim R. Morris, Jan M. Pawłowski, Manuel Reichert, Zoë Slade and Gian Paolo Vacca in quantum gravity, as well as Bartosz Kostrzewa, Stefan Krieg, Thomas Luu and Carsten Urbach during my stays in Bonn and Jülich where I was working on lattice quantum chromodynamics.

Last, but not least, I would like to thank Alfio Bonanno and Frank Saueressig for evaluating this thesis.

Peter Labus, September 2017.

Contents

Abstract	ii
Acknowledgements	iv
Introduction	ix
The need for quantum gravity	ix
Outline of the thesis	xii
List of publications	xiii
1 Asymptotic Safety and the Functional Renormalisation Group	1
1.1 Functional renormalisation group	1
Observables in quantum field theories [1] Smooth cutoff operators [3] Effective average action and its exact flow [7] Approximation schemes [10]	
1.2 Asymptotic safety	13
Fixed points and fundamental quantum field theories [13] Case study: scalar field theory [21]	
2 Background Independence in Quantum Gravity	29
2.1 Conformally reduced gravity at order derivative-squared	30
2.2 Compatibility of the msWI with the flow equation	32
Compatibility at the exact level [32] Compatibility versus derivative expansion [35] Compatibility at order derivative-squared [36] Incompatibility implies no solutions [38]	

	Required form of the cutoff profile [39]	
2.3	LPA equations	40
	Demonstration of background independence forbidding fixed points in general [40] Confirmation of no solutions if the msWI is incompatible with the flow [41] Background independence at vanishing anomalous dimension [42]	
2.4	Polynomial truncations	43
	Counting argument [44]	
2.5	Towards background independence in full quantum gravity	46
3	Non-minimally Scalar-Tensor Theory	51
3.1	Flow equations	52
3.2	Scaling solutions	54
3.3	Large N_s limit	55
3.4	Stability analysis	56
3.5	Gravitationally dressed Wilson-Fisher fixed point	57
3.6	Scalar-free cutoff	58
4	Dynamics of Gravity-Matter Vertices	61
4.1	Matter-gravity flow setup	62
	Truncation [62] Projection rules [64]	
4.2	Results for beta functions and anomalous dimensions	65
	Anomalous dimensions [65] Flow of the graviton-matter coupling [67] Beta function for the graviton-matter coupling [67]	
4.3	Results for the pure gravity case	69
4.4	Results for the interacting matter-gravity system	72
	Fixed-point results without scalar anomalous dimension [72] Fixed-point results including scalar anomalous dimension [74] Background beta functions [76]	
5	Effective Universality in Quantum Gravity	79
5.1	Matter-gravity flow setup	80
5.2	Effective universality for the scalar contribution to the Newton coupling	81
5.3	Threshold effects	83
5.4	Effective universality	84
	Effective gravitational coupling [85] Large N_s limit [85]	
5.5	Level-1 improvement	86
	Background field approximation and Ward identities [87] Background flow equations [89] Fluctuation couplings via Ward identities [89]	

	Conclusions	90
	Bibliography	97
	Appendices	109
A	Exponential parametrisation	111
A.1	Basic definitions	111
A.2	York decomposition	112
A.3	Gauge fixing and ghost sector	113
	Conventional gauge fixing [113] Gauge transformation properties [114] Unimodular gauge [115]	
A.4	Variations of Christoffel symbols and curvature invariants	116
A.5	Hessian of the Einstein-Hilbert action and propagators	118
	Hessian with and without York decomposition [118] Propagators in the conventional gauges [119] Propagators in the unimodular gauge [120]	
B	Scalar-tensor theories	121
B.1	Derivation of the Hessian	121
B.2	Derivation of the flow equations	123
C	Running of interaction vertices	125
C.1	Interaction vertices	125
C.2	Calculating Feynman diagrams	129
D	Modified Ward identities in Yang-Mills theory	131
E	Modified Ward identities from heat kernel techniques	135
	Declaration of Authorship	141

This page intentionally left blank.

Introduction

The need for quantum gravity

The undoubtedly most influential achievements of twentieth century theoretical physics are the discovery and understanding of quantum mechanics—including the subsequent construction of quantum field theories—as well as the development of general relativity.

The study of quantum field theories in particular has led to the construction of the standard model of particle physics that describes the three—believed to be—fundamental strong, weak and electro-magnetic interactions. Its theory predicts various particles that have subsequently been discovered by experiments, such as the W and Z bosons, gluons (via jets), the top and charm quarks, and very recently the Higgs boson. The sector of strong interactions also predicts confinement of quarks to form hadrons, and certain observables of the electromagnetic interactions provide the best agreement between prediction and experiment for any man-made theory (e.g. anomalous magnetic dipole moment of the electron).

The general theory of relativity on the other hand, which is a classical theory of gravitation, has had comparable success and its classical predictions such as the perihelion precession of Mercury's orbit, the deflection of light by the Sun and the gravitational redshift of light have long satisfactorily been confirmed by experiments. More recent experimental/observational tests of the theory include gravitational lensing, frame-dragging (Lense-Thirring precession), the cosmological predictions of structure formation and the recent discovery of gravitational waves.

However, there are still unresolved issues, both in the standard model as well as in general relativity. The standard model, for instance, suffers from a number of phenomenological issues such as the precise mechanism to generate the masses of neutrinos, the structure of dark matter and dark energy, the mechanism for CP violation needed for early universe baryogenesis, and the properties of the axion. Examples of more conceptually related issues include the triviality problem, the stability of the Higgs potential, the hierarchy problem, the cosmological constant problem, as

well as the origin of the symmetry structure and matter content of the standard model.

Some of these issues are likely to be resolved by extensions of the standard model with new matter degrees of freedom, new symmetries and new dynamics. Others, however, such as the cosmological constant problem or the nature of dark energy, and even the stability of the Higgs sector in the ultraviolet (UV) seem to be intricately connected to the gravitational interaction.

But even general relativity by itself clearly reveals boundaries of its applicability. Most notably, this includes the existence of singularities of physical quantities in the cases of cosmological and black hole solutions of the theory. Trying to apply the machinery of quantum mechanics to (ordinary) matter degrees of freedom whilst keeping the treatment of the gravitational interaction classical has led to the development of quantum field theory on curved backgrounds. This approach has been used in the context of early Universe cosmology and cosmological inflation with great (apparent) success. It however has introduced a great many new questions within the physics (and in particular thermodynamics) of black holes. This includes the no-hair theorems, as well as the information paradox.

The general consensus on how to resolve these issues is the quantisation of gravitation itself—often referred to as quantum gravity. Apart from the observation that all other known interactions are described by quantum mechanics, there are usually three arguments brought forward in favour of this approach.¹First of all, Einstein's field equations

$$R_{\mu\nu} - \frac{1}{2} R g_{\mu\nu} = \frac{8\pi G_N}{c^4} T_{\mu\nu},$$

the classical equations of motion of general relativity, couple geometry, *i.e.* the gravitational field described by the Einstein tensor $G_{\mu\nu} = R_{\mu\nu} - \frac{1}{2} R g_{\mu\nu}$ to the energy-momentum tensor $T_{\mu\nu}$ of the present matter content. But since ordinary matter is described by quantum mechanics, the latter is actually a tensor of linear operators rather than of c -numbers. One way to make Einstein's field equations consistent would thus be to cast the Einstein tensor to an operator as well, *i.e.* quantising the gravitational field.

The second argument, is of similar spirit: Since we know of situations where both gravitational as well as quantum mechanical phenomena are strong, we need a theory that can consistently describe both phenomena at the same time. Namely, in black hole thermodynamics, the Hawking temperature of ordinary matter evaporating from a black hole is given by:

$$T_H = \frac{h c^3}{G_N k_B} \frac{1}{4M}.$$

Clearly, in natural units quantum mechanical, gravitational, special relativistic and statistical phenomena are of the same order of magnitude. Since however in quantum mechanics particles have mass associated with them, and mass couples to gravity, interactions have to be treated by their full non-linear dynamics given by general relativity, *i.e.* taking back-reactions of the gravitational field into account. But since the matter field follows a quantum mechanical probability distribution the interfering gravitational field must possess a similar probabilistic description as well.

Finally, gravitational waves must necessarily consist of elementary excitations, called gravitons, otherwise they could be used to determine the path of an electron in a double-slit experiment

¹Strictly speaking, all of the following arguments only show that there should be a probabilistic theory of gravitation that is compatible with the known framework of quantum mechanics used for the other known interactions. However, gravity need not be neither quantised nor even a fundamental interaction.

without disturbing the interference pattern of the electron field behind the slits. This would however violate Heisenberg's uncertainty principle.

There have been many approaches towards a theory of quantum gravity most notably M-theory, and its low energy limit supergravity, as well as approaches of canonical quantisation including loop quantum gravity, its path integral formulation of spin foams and group field theory. Furthermore, there are theories using an underlying lattice regularisation such as causal dynamical triangulation and Regge calculus. There are also approaches emphasising more of the geometrical nature of general relativity such as causal sets. All of these formulations are going beyond the framework of quantum field theories, however, in spite of its successful application within the standard model.

An exception is the so-called asymptotic safety scenario which we want to study in this thesis. To understand its core idea, let us recall the modern view of quantum field theories. In contrast to the original understanding that a quantum field theory has to be (perturbatively) renormalisable in order to be a useful tool to predict physical quantities, today we regard quantum field theories as either fundamental or effective, depending on their ultraviolet behaviour. Namely, any theory without a mathematically well-behaved (*i.e.* finite) ultraviolet limit, or one with infinitely many relevant directions, may be called effective. However, effective field theories are far from futile. This is because, as long as the energy scale is kept below a certain ultraviolet cutoff, effective field theories allow to predict physical observables up to a given precision after fixing only a finite number of parameters (for instance through a number of independent experiments).

Effective quantum field theories have been used with great success in chiral perturbation theory, inflation and even general relativity.² However, they do not allow to extrapolate predictions towards arbitrary energy scales: this is because of the dependence of observables on infinitely many parameters, which would require infinitely many, independent experiments to fix them. Fundamental theories on the other hand only have a finite number of relevant directions which is to say, they have predictive power at all energy scales after measuring only a finite number of parameters. Long-known examples of the latter are perturbatively renormalisable theories without Landau poles—these include the class of Yang-Mills theories, which have proven to be an excellent tool, for instance to describe the strong interactions through quantum chromodynamics. However, since the late 1970s it is known that this scenario is not applicable to Einstein gravity, and that the latter is not perturbatively renormalisable.

The perturbative renormalisability of Yang-Mills theories may equally well be viewed as a collective fixed point of the beta functions of all couplings³ of the theory in the ultraviolet. That means that the energy scale-dependence of the couplings becomes self-similar (*i.e.* stable) when approaching arbitrary high energies. In Yang-Mills theories this is trivially satisfied, because the essential coupling converges to zero at high energies: quarks and gluons stop interacting with each other and become free, which is known as asymptotic freedom. The fixed point in this case is called *free* or *Gaussian*, and it allows the theory to be studied perturbatively in the ultraviolet. However, the values of the couplings at the fixed point do not have to be zero for the theory to be well-behaved in the ultraviolet—it suffices for them to remain finite. In the latter case the field degrees of freedom will interact with each other at high energies, which is why the fixed point is called *interacting*.

²Actually, it is fair to say that the effective field theory of Einstein gravity is the best known theory of quantum gravity today. Not only does it combine quantum field theory with gravity in a true sense, it also allowed the calculation of (at least in principle) falsifiable results, for instance in form of corrections to the Newtonian potential.

³Strictly speaking it is enough for all *essential* couplings to have a fixed point, that is products and quotients of bare couplings that appear in physical observables such as cross sections.

Although in the case of gravity no ultraviolet Gaussian fixed point can exist, because the theory is perturbatively non-renormalisable, there still may be an interacting fixed point. The possibility of such a scenario to indeed take place for gravity was first proposed by Steven Weinberg in 1979, *cf.* Ref. [5]. It is since referred to as asymptotic safety following the case of asymptotic freedom discovered earlier. The first approach to apply this idea to construct an ultraviolet complete quantum field theory of gravity using the exact renormalisation group equation was subsequently done in 1996 by Martin Reuter, *cf.* Ref. [6]. Since then, a considerable amount of evidence has been found to support that such a theory could be constructed in the case of pure gravity.

It is important to mention that the value of the couplings at the fixed point is not *a priori* restricted in any way. In particular, the relevant dimensionless values may be of order one or greater, forbidding a conventional perturbative study of the theory at the fixed point by expanding physical observables in powers of the coupling. This is why the space of all quantum field theories of gravity must be scanned for candidate theories with non-perturbative tools. Of such there are only a few available, none of which is as matured as the perturbative tools developed in the last century, yet. The most notable non-perturbative tools are the conformal bootstrap, the lattice, entanglement entropy and the functional renormalisation group. The latter is the traditional tool which has been used in the vast majority of research concerning asymptotic safety in gravity and it is the one we will use throughout this thesis as well.

Outline of the thesis

One of the main open issues in asymptotic safety in quantum gravity is the inclusion of matter field degrees of freedom. Most of this thesis will deal with this issue in one way or another.

This is interesting and relevant for a number of reasons. First of all, one may argue, that having an ultraviolet complete quantum field theory of gravity alone is not enough for at least two reasons: (a) the inclusion of matter fields introduces new couplings into the theory which may behave very differently from the ones which couple gravitons to one another and thus may interfere with asymptotic safety of pure gravity, or destabilise fixed points entirely; (b) the generally accepted *effectiveness* of the standard model has to be dealt with. In principle it is possible that gravity could cure the instabilities of the Higgs sector and hence an asymptotically safe quantum field theory of everything could serve as a nice and elegant ultraviolet completion of the standard model.

Initial studies of the inclusion of matter fields have indeed revealed that a large number of scalar fields may destabilise gravitational fixed points and thus predict an upper bound for the number of scalar matter fields present in the Universe, *cf.* Ref. [7]. This is especially relevant for (effective) cosmological theories and (possibly supersymmetric) grand unified theories which usually incorporate large numbers of scalar fields. However, there are still many technical details that need to be addressed in order to solidify these predictions.

A second major reason to study the behaviour of matter fields within a gravitational quantum field theory concerns the ability to compare predictions of the theory with experiments and observations. This is in particular true for astrophysical systems and cosmological tests, where couplings between matter and gravity can be measured much more accurately than observables coming from purely gravitational effects. This includes the equivalence principle, perturbations of the cosmic microwave background, implications for inflationary models as well as even collider experiments.

A second issue we will be (much less) concerned about in this thesis is one of more technical nature. Namely, we will study some of the implications, that the use of the well-known background

main topic	chapter	parametrisation	expansion scheme	reference
	Ch. 1	general	general	
background independence	Ch. 2	any	derivative	[3]
	Ch. 3	exponential	derivative	[1]
scalar matter + gravity	Ch. 4	exponential	vertex	[2]
	Ch. 5	linear	vertex	[4]

Figure 1: Overview of the chapter contents of the thesis including its main topic, some information about technical details used in the calculations and the original reference (where applicable).

field method in quantum field theory has on renormalisation group properties when defining an energy scale with respect to this very background.⁴ This may be regarded as a mathematical consistency condition and could give interesting insides about the appropriate description of the renormalisation group, when applied to gravitational theories.

The thesis is organised as follows:

Chapter 1 provides a technical introduction to asymptotic safety and the functional renormalisation group. We will establish most of the mathematical notions used in later chapters, including truncation schemes, forms of cutoffs and field parametrisations, as well as basic concepts of critical phenomena. This chapter includes a detailed case study of a scalar field theory.

Chapter 2 presents the foundation of the modified split Ward identities and its application to insure background independence. We study the implications of the combination of flow equation and Ward identity in the context of conformally reduced quantum gravity.

Chapter 3 studies scalar fields non-minimally coupled to a curved background in a background calculation using heat kernel techniques. We find functional fixed point solutions and study their linearised behaviour in more details. We discover various upper bounds for the number of scalar fields when demanding asymptotic safety for the combined system.

Chapter 4 augments the previous chapter by studying the dynamics of a three-leg vertex consisting of two massless scalar fields minimally coupled to the spin-two mode of a graviton about a flat background. We find qualitatively similar results as previously, and in particular observe that too many scalar fields induce a destabilising effect on fixed points.

Chapter 5 repeats the calculation of chapter 4 with different technical choices such as field parametrisation and cutoff. This shall give an idea about the robustness of the results obtained so far and the validity of the upper bounds. We also use the Ward identity to remove background dependencies due to the cutoff operator.

List of publications

The work presented in this thesis is based on the following publications:

⁴*A priori*, this has nothing to do with diffeomorphism invariance of the quantum theory, which is emphasised by other approaches such as loop quantum gravity, and may or may not hold at the fixed point in asymptotic safety.

- Peter Labus, Roberto Percacci, and Gian Paolo Vacca. Asymptotic safety in $O(N)$ scalar models coupled to gravity. *Phys. Lett.*, B753:274–281, 2016, arXiv:1505.05393 [hep-th]
- Pietro Donà, Astrid Eichhorn, Peter Labus, and Roberto Percacci. Asymptotic safety in an interacting system of gravity and scalar matter. *Phys. Rev.*, D93(4):044049, 2016, arXiv:1512.01589 [gr-qc]. [Erratum: *Phys. Rev.*, D93(12):129904, 2016]
- Peter Labus, Tim R. Morris, and Zoë H. Slade. Background independence in a background dependent renormalization group. *Phys. Rev.*, D94(2):024007, 2016, arXiv:1603.04772 [hep-th]
- Astrid Eichhorn, Peter Labus, Jan M. Pawłowski, and Manuel Reichert. Effective universality in gravity-matter flows. 2017. *In preparation*.

An overview, including the main subject of each chapter, technical details of the respective calculations, as well as the main source of reference, may be found in Fig. 1.

Most of the diagrams, tables, figures and plots in the original sources have been recreated for this thesis using `TikZ` and `PGFPLOTS`, with the exception of Fig. 3.1 which was originally created using Wolfram Mathematica 10.0, and was reproduced here from Ref. [1]. All typesetting has been done with `LATEX`.

1. Asymptotic Safety and the Functional RG

In this chapter we will explain the idea of asymptotic safety in a more rigorous way than in the introduction, and in particular introduce the notation used in the rest of this thesis. To this end, we will first study the functional renormalisation group equation and its related concepts. Although the framework of asymptotic safety is quite generic and could well be studied with other non-perturbative tools, the language of the renormalisation group turns out to be particularly useful to explain the core ideas of asymptotic safety. Our presentation is heavily influenced by Refs. [8, 9].

1.1 Functional renormalisation group

In this first section we will introduce the functional renormalisation group as a tool to solve generic quantum field theories. In particular, we will see how to formalise Wilson’s idea of a coarse-graining procedure for the action of a quantum field theory by introducing smooth energy scale-dependent infrared cutoff operators: We will then introduce a scale-dependent effective average action and derive its exact renormalisation group equation. Finally, we will discuss some strategies how to obtain approximate solutions to the exact equation. For reviews of the topics, *cf.* [10–14].

1.1.1 Observables in quantum field theories

In order to solve a quantum field theory, one has to be able to calculate any physical observable the theory may predict. This will in particular include the existence of particles—elementary or bound—as well as their properties, such as masses or charges, but also their behaviour when interacting amongst each other, which can be quantified using cross-sections. All of these observables may be expressed using the kinematics of the theory, as well as its dynamical content, the latter of which is completely encoded in the so-called n -point correlation functions

$$C_n(x_1, x_2, \dots, x_n) = \langle \Phi(x_1) \Phi(x_2) \dots \Phi(x_n) \rangle, \quad (1.1)$$

where the variables Φ represent (possibly distinct) quantum fields, which may additionally carry indices of space-time or internal symmetries. The correlation functions are functional expectation values of products of n field operators at different space-time positions and they may be calculated using the path integral formalism via

$$\langle \Phi(x_1) \Phi(x_2) \dots \Phi(x_n) \rangle = \frac{1}{Z} \int \mathcal{D}\Phi \Phi(x_1) \Phi(x_2) \dots \Phi(x_n) e^{-S[\Phi]}, \quad (1.2)$$

where the partition function $Z = \int \mathcal{D}\Phi e^{-S[\Phi]}$ serves as a normalisation constant, $\mathcal{D}\Phi$ represents the integration measure, and $e^{-S[\Phi]}$ is the Euclidean Boltzmann factor—the (quantum) probability distribution which weights every field configuration in the path integral according to its classical action.

A more elegant way to obtain any n -point correlation function is by means of the generating functional $W[J]$ which is the logarithm of the partition function, to the latter of which a source term has been added:¹

$$Z[J] = e^{W[J]} = \int \mathcal{D}\Phi e^{-S[\Phi] + \int d^d x J(x) \Phi(x)}. \quad (1.3)$$

Taking derivatives with respect to the source term J and evaluating the expression at $J = 0$ yields an efficient procedure to obtain any correlation function:

$$C_n(x_1, x_2, \dots, x_n) = \frac{\delta W}{\delta J(x_1) \delta J(x_2) \dots \delta J(x_n)} \Big|_{J=0}. \quad (1.4)$$

Solving a quantum field theory can thus equivalently be viewed as calculating the generating functional (or its image under some one-to-one mapping, such as the Legendre transformation). One very common way to do so approximately, is through perturbation theory. There, one separates the action into a kinetic term, which describes the freely propagating fields, and a potential term, which in turn includes the vertices of the theory, *i.e.* the way fields interact amongst themselves. It is then the latter that is expanded in powers of some small quantity, such as a coupling parameter, in order to calculate perturbations around the free theory. Not only does this approach rely on the existence of a small expansion parameter, it is also by its very nature bound to hide non-analytic (or non-perturbative) dependencies of observables within the quantum field theory.

An alternative method to calculate the generating functional is based on Wilson's idea of a functional renormalisation group. In order to construct it, we first need to define an energy scale-dependent action S_Λ . It is obtained via integrating out only those momentum modes $|q|$ in the path integral that are higher² than some given cutoff scale Λ

$$e^{-S_\Lambda[\Phi]} = \int_{\Lambda \leq |q| \leq \Lambda_{UV}} \mathcal{D}\Phi e^{-S[\Phi]}. \quad (1.5)$$

The partition function may then be recovered by integrating out the remaining modes

$$Z = \int_{0 \leq |q| \leq \Lambda} \mathcal{D}\Phi e^{-S_\Lambda[\Phi]}. \quad (1.6)$$

¹Summation over distinct fields and symmetry indices is implicitly understood.

²In addition we have to regularise the theory in the ultraviolet, for instance via a cutoff Λ_{UV} . However, the details of such a procedure are irrelevant for the renormalisation group equation discussed here, as will become clear shortly.

In this way, we can define a scale-dependent generating functional which describes physics at same given energy scale Λ . In particular, we may quantify the dependence of S_Λ on the energy scale through its beta functional $dS_\Lambda/d\Lambda$, which can be obtained via

$$\frac{dS_\Lambda}{d\Lambda} = \lim_{\delta\Lambda \rightarrow 0} \frac{S_{\Lambda+\delta\Lambda} - S_\Lambda}{\delta\Lambda}. \quad (1.7)$$

Note that this equation will become a first-order integro-differential equation once the definition of S_Λ is employed on its right hand side. Wilson's renormalisation group thus gives us another strategy to solve a quantum field theory. In order to do so, we have to find the solution to the renormalisation group equation with the boundary condition $S_{\Lambda_{UV}} = S$, and subsequently integrate towards the infrared, $W = -\lim_{\Lambda \rightarrow 0} S_\Lambda$.

Although this approach does not seem any easier than calculating the original generating functional W directly, it does offer a number of advantages:

- The renormalisation group is conceptually simple and physically intuitive.
- The renormalisation group is non-perturbative. In particular, it does not rely on the use of a small expansion parameter.
- The renormalisation group equation has a simple one-loop form.³
- The resulting beta function is finite. In particular, ultraviolet divergences that may appear in S_Λ cancel out when taking the difference on the right hand side of the renormalisation group equation.

Note that the cutoff Λ may be thought of as an ultraviolet cutoff, since for any given S_Λ , it cuts off the high momentum modes in the path integral, when calculating the partition function. However, in the definition of S_Λ itself, it is an infrared cutoff for the high energy modes that get integrated out. For the differential equation that is the renormalisation group equation, this distinction clearly does not play any rôle. To formalise Wilson's idea and establish a tool for practical calculations, we will introduce a smooth infrared cutoff (opposed to the sharp cutoff used before) and use the Legendre transform of the generating function W to derive an exact functional renormalisation group equation.

1.1.2 Smooth cutoff operators

Our aim for this subsection is it to introduce a concept of a scale-dependent classical (or bare) action which can then be integrated over in the path integral to obtain a scale-dependent quantum action.

In order to do this, for any given energy scale k we want to distinguish modes with low momenta $|q| < k$ and modes with high momenta $|q| > k$. Since it is the high momentum modes we want to integrate out, they should remain undisturbed by the cutoff procedure, *i.e.* propagate as given by the theory. The low momentum modes however, should be suppressed, *i.e.* they should not propagate. Furthermore, we want to alter only the propagation of a given mode, and not its interaction structure. This is why we choose to add to the classical action a cutoff term that is bilinear in the fields which we want to regulate.

³This can be seen by rewriting the numerator of the right hand side in a perturbative loop expansion. Since the integral is linear in its upper and lower boundary, one integrates over a momentum shell of thickness $\delta q = \delta\Lambda$, such that in each diagram closed loops contribute $\delta\Lambda/q \rightarrow 0$, which leaves a one-loop contribution only.

In the most general case of a quantum field theory in curved space-time, we have to choose a first or second order differential operator Δ which we leave unspecified for the moment. Then we have to calculate the eigenspectrum of the latter

$$\Delta \varphi_n = \lambda_n \varphi_n. \quad (1.8)$$

Next we can expand the quantum field $\varphi(x)$ we want to regularise in terms of its generalised Fourier coefficients ϕ_n as

$$\varphi(x) = \sum_n \phi_n \varphi_n(x), \quad (1.9)$$

where for the moment we assumed a discrete spectrum of Δ which we label by integers n . We will outline the case of a scalar field here first, and comment on how to generalise this procedure to other types of fields at the end of the subsection. The cutoff term we want to add to the classical action, can then be written in its most general form in two distinct ways

$$\Delta S_k[\varphi] = \frac{1}{2} \int d^d x \varphi(x) R_k[\Delta] \varphi(x) = \frac{1}{2} \sum_n \phi_n R_k(\lambda_n) \phi_n. \quad (1.10)$$

The second expression is often the most convenient form of the cutoff term when it comes to evaluating functional traces, as the ones that will appear in the functional renormalisation group equation, see below. Since it is common practise, we will denote the cutoff kernel $R_k[\Delta]$ and its Fourier transform with the same symbol, and add its explicit argument as appropriate.

For a physically more transparent presentation, let us now specialise to the case of a flat space-time and $\Delta = \partial^\mu \partial_\mu$. The generalised Fourier transformation in this case simply becomes the usual continuous transformation and the cutoff term in momentum space assumes the form:⁴

$$\Delta S_k[\varphi] = \frac{1}{2} \int \frac{d^d q}{(2\pi)^d} \varphi(-q) R_k(q^2) \varphi(q). \quad (1.11)$$

One should think of the regulator $R_k(q^2)$ as a scale-dependent mass term. To make this idea more precise, let us have a look at the propagator that results from the introduction of this regulator term:

$$G_k(q^2) = \frac{1}{q^2 + R_k(q^2)}. \quad (1.12)$$

It shows clearly, that we indeed introduced an infrared cutoff. To follow the strategy outlined above, all high momentum modes should be left unchanged and thus should acquire a mass $m_k = R_k(q^2) \approx 0$ whenever $|q| > k$. Furthermore, we may want to make sure that the limit $R_k \rightarrow 0$ happens sufficiently fast (e.g. exponentially). The low momentum modes on the other hand should obtain a mass $m_k = R_k(q^2) \approx k$, for all $|q| < k$, such that their energy always remains below the mass gap. It is often beneficial to choose the transition between these two regimes to be smooth. This is because when dealing with the vertex expansion approximation scheme of the renormalisation group equation or with anomalous dimensions, there are often times derivatives acting on the cutoff operator. However, one of the most popular choices of the cutoff operator, the optimised cutoff, is merely continuous.

⁴Here again we denote Fourier transforms, including the fields themselves, with the same symbols as the original variable.

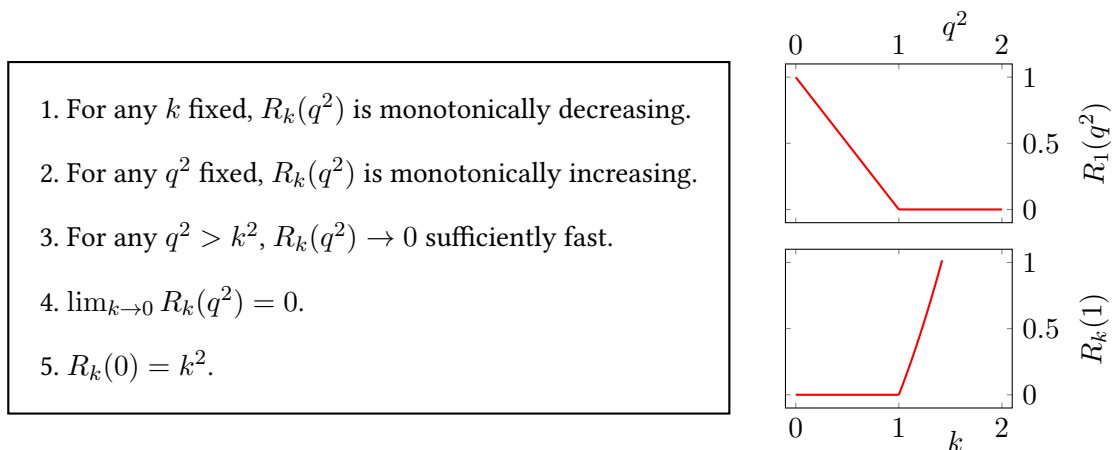


Figure 1.1: (Left) Formal requirements on a (standard) cutoff operator. (Right) Graphical illustration of the first two requirements, using the optimised cutoff as an example. The upper panel shows $R_k(q^2)$ with $k = 1$ fixed, and in the lower panel $q^2 = 1$ is fixed. Note that the last three requirements are also satisfied.

We summarise the requirements on the cutoff operator⁵ in Fig. 1.1. Requirements 1–3 have been explained above⁶ and simply implement our cutoff strategy. Requirement 4 is self-evident, as it guarantees to match the standard case when the cutoff is switched off. The last requirement will turn out to guarantee that we recover the universal one-loop beta functions for dimensionless variables. It may be viewed as a normalisation condition.

After this technical motivation, let us now list some examples of cutoff operators used in actual calculations. Assigning canonical dimensions to all fields, we can factor out the dimensional dependence in the cutoff operator and write

$$R_k(q^2) = k^2 r(y), \quad (1.13)$$

where $y = q^2/k^2$ is the dimensionless momentum of the modes which get integrated over in the path integral in units of the squared scale k^2 , and $r(y)$ is a dimensionless function, usually called the (cutoff) profile function. Some popular choices of profile functions include:

$$r(y) = \frac{y}{e^y - 1}, \quad (1.14)$$

$$r(y) = \frac{y^2}{e^{y^2} - 1}, \quad (1.15)$$

$$r(y) = (1 - y) \theta(1 - y). \quad (1.16)$$

The last profile function, the optimised cutoff, cf. Refs. [15, 16], is by far the most widely used. We display the shapes of these three profiles and the propagator that result in Fig. 1.2.

⁵The requirements listed here characterise a so-called standard cutoff. We will not be dealing with non-standard cutoffs in this thesis.

⁶It might be easier to understand requirement 2, by realising that for decreasing k the mass gap should reduce for all momentum modes q^2 simultaneously.

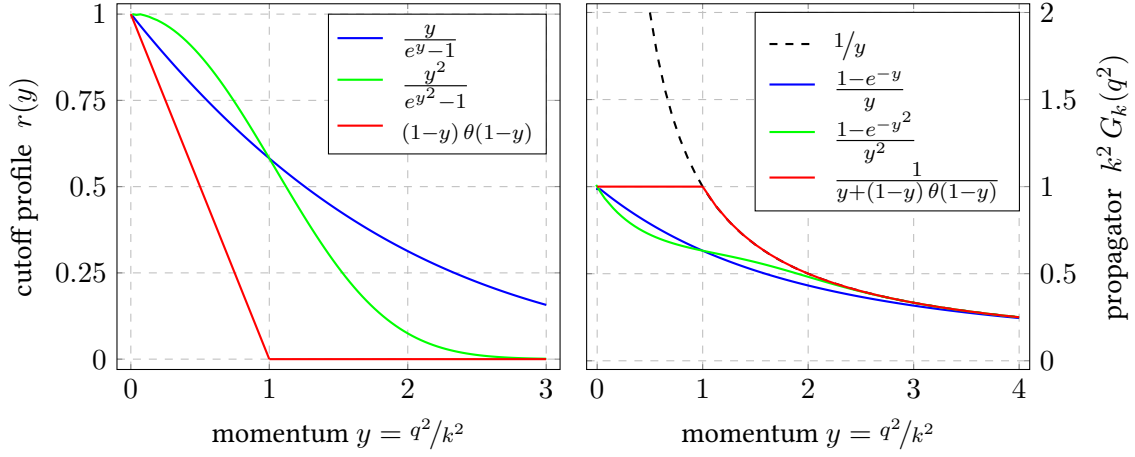


Figure 1.2: (Left) Standard profile functions and (right) their resulting propagators in units of the squared cutoff scale k^2 . The free propagator is added here as reference.

Let us now introduce a cutoff classification that has been developed in Ref. [17]. It is of practical importance and relies on the observation that the Hessian of the effective average action, which appears in the functional renormalisation group equation, as we will see shortly, is generically proportional to a differential operator

$$-\nabla^2 + \mathbb{E}, \quad (1.17)$$

where ∇ is the covariant derivative with respect to the gauge connection(s), including gravity as well as internal symmetries, and \mathbb{E} is an endomorphism which may include mass terms or curvature invariants. Since the cutoff term will be added to this Hessian, it will turn out computationally handy to choose the operator Δ , of which the cutoff kernel is a functional, to include parts of $-\nabla^2 + \mathbb{E}$. To express the classification, we have to split the endomorphism $\mathbb{E} = \mathbb{E}_1 + \mathbb{E}_2$ into a part \mathbb{E}_1 which has no scale-dependent couplings and a part \mathbb{E}_2 which contains renormalisation group dependent couplings only. Then the following three types of cutoff operators are defined:

- type I: $\Delta = -\nabla^2$
- type II: $\Delta = -\nabla^2 + \mathbb{E}_1$
- type III: $\Delta = -\nabla^2 + \mathbb{E}_1 + \mathbb{E}_2$

Note that when using a type III cutoff, the spectrum of the operator Δ will change along the renormalisation group flow.

To conclude this subsection let us now comment on the case of having several (possibly multi-component) fields. The cutoff term is then expressed through a matrix relation

$$\Delta S_k[\Phi_{\mathcal{A}}] = \int d^d x \Phi_{\mathcal{A}} R_k^{AB} \Phi_{\mathcal{B}} \quad (1.18)$$

where \mathcal{A} and \mathcal{B} run over the number of fields as well as their space-time and possibly internal indices. Although one could in principle mix different fields with the same symmetry structure in

this way, R_k^{AB} is usually chosen to be diagonal in field space. Also note that this introduces the additional freedom of choosing the tensor structure of the cutoff. In practise however, one usually uses the tensor structure found in the respective Hessian.

1.1.3 Effective average action and its exact flow

Having defined a scale-dependent cutoff operator for the classical action, we can now proceed and define a scale dependent generating functional via⁷

$$e^{W_k[J]} = \int \mathcal{D}\tilde{\varphi} e^{-S[\tilde{\varphi}] - \Delta S_k[\tilde{\varphi}] + \int d^d x J(x) \tilde{\varphi}(x)}. \quad (1.19)$$

It will turn out to be more convenient to pass to the functional Legendre transform of $W_k[J]$ which is defined by

$$\hat{\Gamma}_k[\varphi] = -W_k[J] + \int d^d x J(x) \varphi(x). \quad (1.20)$$

Here we have introduced a new variable φ as the functional derivative of the old functional W_k with respect to the old variable J :⁸

$$\frac{\delta W_k}{\delta J(x)} = \langle \tilde{\varphi}(x) \rangle \equiv \varphi(x). \quad (1.21)$$

The first equality holds by definition of the generating functional W_k and the new variable is called the classical field, since it is exactly this expectation value that appears in the classical action. The last relation must be invertible such that the old variable may be expressed in terms of the new one, $J = J[\phi]$. We can then take the functional derivative of the new function $\hat{\Gamma}_k$ with respect to the new variable ϕ in order to discover that

$$\frac{\delta \hat{\Gamma}_k}{\delta \varphi(x)} = - \int d^d y \frac{\delta W_k}{\delta J(y)} \frac{\delta J(y)}{\delta \varphi(x)} + \int d^d y \frac{\delta J(y)}{\delta \varphi(x)} \varphi(y) + \int d^d y J(y) \delta(x-y) = J(x), \quad (1.22)$$

where we made use of the definition of the new variable φ . With this observation, we can write the exponential of the negative Legendre transform as

$$e^{-\hat{\Gamma}_k[\varphi]} = \int \mathcal{D}\tilde{\varphi} e^{-S[\tilde{\varphi}] - \Delta S_k[\tilde{\varphi}] + \int d^d x \frac{\delta \hat{\Gamma}_k}{\delta \varphi(x)} (\tilde{\varphi}(x) - \varphi(x))}. \quad (1.23)$$

We can now perform a change of the integration variable to $\tilde{\chi} = \tilde{\varphi} - \varphi$, to obtain (assuming invariance of the integration measure under constant shifts):

$$e^{-\hat{\Gamma}_k[\varphi]} = \int \mathcal{D}\tilde{\chi} e^{-S[\tilde{\chi} + \varphi] - \Delta S_k[\tilde{\chi} + \varphi] + \int d^d x \frac{\delta \hat{\Gamma}_k}{\delta \varphi(x)} \tilde{\chi}(x)}. \quad (1.24)$$

⁷From now on, we will add a tilde above fields which get integrated over in the path integral in order to be able to use the same letter for said field to denote its classical equivalent, cf. below.

⁸Having a finite source function $J(x)$ we can define a functional expectation value via

$$\langle \mathcal{O}[\Phi] \rangle_J \equiv \frac{1}{Z[J]} \int \mathcal{D}\Phi \mathcal{O}[\Phi] e^{-S[\Phi] + \int d^d x J(x) \Phi(x)},$$

for any field operator $\mathcal{O}[\Phi]$. This generalises Eqn. (1.2) using the modified partition function Eqn. (1.3). Since we do not directly want to evaluate partition functions, we can always assume J to be non-zero and drop the explicit index.

We will now shift the Legendre transform by the cutoff action in order to obtain a more beautiful final expression:

$$\Gamma_k \equiv \hat{\Gamma}_k - \Delta S_k. \quad (1.25)$$

The resulting functional Γ_k is called the effective average action. Observing that due to the bilinear form of the cutoff action we have

$$-\Delta S_k[\tilde{\chi} + \varphi] + \Delta S_k[\varphi] + \int d^d x \frac{\delta \Delta S_k}{\delta \varphi(x)} \tilde{\chi}(x) = -\Delta S_k[\tilde{\chi}], \quad (1.26)$$

we finally arrive at the following expression:

$$e^{-\Gamma_k[\varphi]} = \int \mathcal{D}\tilde{\chi} e^{-S[\tilde{\chi} + \varphi] - \Delta S_k[\tilde{\chi}] + \int d^d x \frac{\delta \Gamma_k}{\delta \varphi(x)} \tilde{\chi}(x)}. \quad (1.27)$$

From the last identity, one can show using the formal requirements on a standard cutoff that

$$\lim_{k \rightarrow 0} \Gamma_k = \Gamma \quad \text{and} \quad \lim_{k \rightarrow \infty} \Gamma_k = S, \quad (1.28)$$

where Γ is the usual effective action define without the cutoff action ΔS_k .

We are now ready to derive the exact renormalisation group equation. To this end we define a renormalisation group time

$$t \equiv \log \left(\frac{k}{\mu} \right), \quad (1.29)$$

where μ is an arbitrary energy scale. Then from the definition of the effective average action we have

$$\frac{d\Gamma_k}{dt} = -\frac{dW_k}{dt} - \frac{d\Delta S_k}{dt}. \quad (1.30)$$

The first term can be re-expressed by observing that

$$\frac{de^{W_k}}{dt} = \dot{W}_k e^{W_k} = \int \mathcal{D}\tilde{\varphi} \left(-\Delta \dot{S}_k \right) e^{-S[\tilde{\varphi}] - \Delta S_k[\tilde{\varphi}] + \int d^d x J(x) \tilde{\varphi}(x)} = \langle -\Delta \dot{S}_k \rangle e^{W_k}, \quad (1.31)$$

where we used dots to denote derivatives with respect to time t . This expression implies

$$\dot{W}_k = \langle -\Delta \dot{S}_k \rangle = -\frac{1}{2} \left\langle \int d^d x \tilde{\varphi}(x) \dot{R}_k \tilde{\varphi}(x) \right\rangle. \quad (1.32)$$

Using the fact that the cutoff operator R_k is independent of the field $\tilde{\varphi}$ we can write the time derivative of the effective average action as

$$\frac{d\Gamma_k}{dt} = \frac{1}{2} \text{Tr} \left[\left(\langle \tilde{\varphi} \tilde{\varphi} \rangle - \langle \tilde{\varphi} \rangle^2 \right) \dot{R}_k \right], \quad (1.33)$$

where the trace operator Tr indicates integration over space-time and momentum, as well as summation over space-time and internal indices, as appropriate. To make further progress, we first note that the definition of W_k implies

$$\frac{\delta^2 W_k}{\delta J(x) \delta J(y)} = \langle \tilde{\varphi}(x) \tilde{\varphi}(y) \rangle - \langle \tilde{\varphi}(x) \rangle \langle \tilde{\varphi}(y) \rangle, \quad (1.34)$$

and that we can furthermore re-express the second derivative acting on W_k as

$$\frac{\delta^2 W_k}{\delta J \delta J} = \frac{\delta \varphi}{\delta J} = \left(\frac{\delta J}{\delta \varphi} \right)^{-1} = \left(\frac{\delta^2 \hat{\Gamma}_k}{\delta \varphi \delta \varphi} \right)^{-1}. \quad (1.35)$$

Here, the first equality follows from the definition of the classical field, and the last equality from the definition of the Legendre transform.⁹ This finally enables us to write

$$\langle \tilde{\varphi}(x) \tilde{\varphi}(x) \rangle - \langle \tilde{\varphi}(x) \rangle \langle \tilde{\varphi}(x) \rangle = \left(\frac{\delta^2 \hat{\Gamma}_k}{\delta \varphi(x) \delta \varphi(x)} \right)^{-1}. \quad (1.36)$$

Substituting the definition of Γ_k into the last expression, we can obtain the exact or functional renormalisation group equation, also called Wetterich or simply flow equation, as follows

$$\frac{d\Gamma_k}{dt} = \frac{1}{2} \text{Tr} \left[\left(\frac{\delta^2 \Gamma_k}{\delta \varphi \delta \varphi} + R_k \right)^{-1} \dot{R}_k \right]. \quad (1.37)$$

Having formalised Wilson's idea of a functional renormalisation group, and arrived at a rigorous equivalent to Eqn. (1.7), some comments are in order. Let us in particular reappraise the features which we considered advantageous of an renormalisation group approach:

- *The renormalisation group is conceptually simple and physically intuitive.* In particular, it is generic and may be applied to any quantum field theory, may it be fundamental or effective.
- *The renormalisation group is non-perturbative.* This is true, since no approximation is made on the way of deriving the equation, hence the name "exact".
- *The renormalisation group equation has a simple one-loop form.* In particular, it contains a closed loop on its right hand side, composed of a full (regularised) propagator and an insertion of the running cutoff operator \dot{R}_k . The full propagator, obtained from the quantum effective action contains all the non-perturbative information. The origin of the one-loop form is manifestly due to the bilinear cutoff operator. If one would choose to include higher order terms, higher order vertices would appear in the renormalisation group equation.
- *The resulting beta function is finite.* This is due to the fact that $\dot{R}_k(q^2)$ goes to zero sufficiently fast whenever $q^2 > k^2$, thus guaranteeing convergence of the momentum integrals in the ultraviolet. The cutoff operator R_k additionally imparts an infrared regularisation by introducing a mass gap whenever $k \neq 0$.

Moreover, given an effective action at some scale k_0 the effective average action can be defined at any other scale k via the function renormalisation group equation. This allows in particular, as we already anticipated, to calculate the quantum effective action Γ at $k = 0$, given that Γ_k has been fixed at some scale k . Lastly note, that no reference to ultraviolet physics is made anywhere in the exact renormalisation group equation, *i.e.* all quantities involved only depend on some intermediate scale k .

⁹Note that W_k is a functional of J only.

1.1.4 Approximation schemes

Now that we have derived an exact renormalisation group equation, we can discuss strategies how to search for solutions of said equation. To this end, after having specialised the field content, as well as all global and/or local (gauge) symmetries, one has to search for solutions in the space of all quantum field theories with the given properties. Namely, the effective average action assumes the form

$$\Gamma_k[\Phi] = \sum_{i \in \mathcal{I}} g_i(k) \mathcal{O}_i[\Phi], \quad (1.38)$$

which is an infinite sum over a countable index set \mathcal{I} . Here, the $\mathcal{O}_i[\Phi]$ represent all monomial operators which can be build through integration over space-time of powers of the given fields Φ and their covariant derivatives, in such a way that they are scalars under all specified symmetry groups. The coefficients $g_i(k)$ are hereby scale-dependent coupling constants which in their entirety reflect the renormalisation group running of the effective average action. Plugging this expression back into the flow equation yields an equivalent description in terms of infinitely many coupled equations in terms of the infinitely many coefficients $g_i(k)$ and their first derivatives $\dot{g}_i(k)$ with respect to the renormalisation group time.

Clearly there is not much hope to find an exact solution to the exact equation even for the simplest possible choice of field content and symmetry structure. This is why one has to rely on approximation schemes to find only approximate solutions to the exact equation. In this subsection we will introduce the two schemes which are the most relevant for practical computations and which will be used throughout this thesis. But before going into the details of these schemes, let us add some general remarks how to approximate the effective average action in most cases.

Since we are dealing with a non-perturbative formulation of quantum field theories, in the most general case there is no (obvious) expansion parameter available that could reliably be used for the full energy range from the ultraviolet to the infrared. This is why one often decides to solve only a finite subset of the infinitely many equation in full theory space. This approach is called truncation, and effectively shrinks the index set \mathcal{I} to some finite, or infinite, proper subset $\bar{\mathcal{I}}$. In the latter case one usually assumes some functional form for the operators, such as in the case of $f(R)$ gravity. The choice of the operators involved in this approximation is arbitrary, but in practise one often chooses to use the lowest (mass) dimensional operators—as one would do also in perturbation theory.

Truncations are hard to justify *a priori*, as the renormalisation group equation couples all operators to every other, at least indirectly. That is, even setting some running coupling to zero at some scale would therefore likely imply that it is non-zero at other scales. Hence a truncation restricts the dynamics possible in the solution quantum field theory. The common strategy to circumvent this issue is to subsequently enlarge the truncated space and include higher dimensional operators. Stability in the behaviour of couplings which were already been included in previously studied approximations, can then be interpreted as apparent convergence of the approximate solution. In the framework of asymptotic safety this procedure can indeed be used to recover well-know critical behaviour in scalar field theories.

Both of the approximation schemes we want to introduce here make use of truncations of theory space. The first one, the vertex expansion, is based on rewriting the sum over all possible

operators as a functional Taylor expansion around some given field configuration $\bar{\varphi}(x)$:¹⁰

$$\Gamma_k[\varphi] = \sum_{n=0}^{\infty} \frac{1}{n!} \int d^d x_1 \int d^d x_2 \dots \int d^d x_n \Gamma_{x_1 x_2 \dots x_n}^{(n)} \prod_{i=1}^n (\varphi(x_i) - \bar{\varphi}(x_i)) \quad (1.39)$$

where we introduced the scale-dependent interaction vertices via

$$\Gamma_{x_1 x_2 \dots x_n}^{(n)}[\varphi] \equiv \frac{\delta^n \Gamma_k}{\delta \varphi(x_1) \delta \varphi(x_2) \dots \delta \varphi(x_n)}, \quad (1.40)$$

which are functional derivatives of the full effective average action. These vertices give their name to the approximation scheme. When plugging the Taylor expansion back into the renormalisation group equation, we will obtain a hierarchy of flow equations for each vertex. As we will explicitly see shortly, these equations are coupled and in particular will the flow of the n -point vertex depend on itself, as well as the $n + 1$ and the $n + 2$ vertex. That is, to make the scheme useful (and indeed approximate) we will truncate the resulting system of equations by setting $\dot{\Gamma}^{(n)} = 0$ for all $n > N_{\text{trunc}}$ and some initial choice of N_{trunc} . Assuming that for any given scale k all vertices $\Gamma^{(n)}$ give contributions of the same order to the functional traces in the flow equations, due to the combinatorial factor $1/n!$ in the Taylor expansion, one might indeed be confident that this approximation scheme is useful. However, this has to be verified by increasing N_{trunc} iteratively and investigating the stability of the obtained results.

To explicitly obtain the flow of some n -point vertex, one has to take n functional derivatives of the renormalisation group equation with respect to the field variable $\varphi(x)$. To do this for the first few vertices let us introduce a shorthand for the regularised full quantum propagator:

$$\Delta_{xy}[\varphi] \equiv \left[\frac{\delta^2 \Gamma_k}{\delta \varphi(x) \delta \varphi(y)} + R_k(x, y) \right]^{-1}. \quad (1.41)$$

Taking one and two functional derivatives, we may then express the running one- and two-point function in a very compact manner:

$$\partial_t \Gamma_x^{(1)} = -\frac{1}{2} \text{Tr} \left[\Delta_{ab} \Gamma_{bcx}^{(3)} \Delta_{cd} \partial_t R_{k,da} \right], \quad (1.42)$$

$$\partial_t \Gamma_{xy}^{(2)} = \text{Tr} \left[\Delta_{ab} \Gamma_{bcx}^{(3)} \Delta_{cd} \Gamma_{dey}^{(3)} \Delta_{ef} \partial_t R_{k,fa} \right] - \frac{1}{2} \text{Tr} \left[\Delta_{ab} \Gamma_{bcxy}^{(4)} \Delta_{cd} \partial_t R_{k,da} \right]. \quad (1.43)$$

It is in many ways very instructive to re-express the right hand sides of these equation in terms of Feynman diagrams. Denoting propagators as solid lines, the functional traces as closed loops and the regulator insertion $\partial_t R_k$ with the symbol \otimes , we can iconographically express the functional renormalisation group equation as

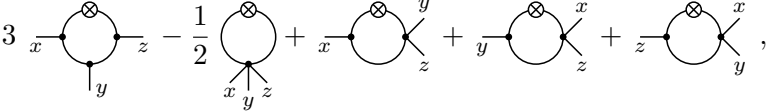
$$\partial_t \Gamma_k = \frac{1}{2} \text{Tr} \left(\text{Loop} \otimes \right). \quad (1.44)$$

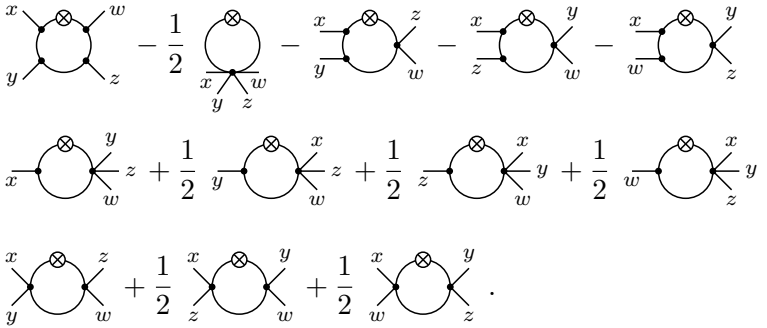
¹⁰For simplicity of notation, we will once more return to the case of a single scalar field.

Similarly, we can express the running of the first four n -point functions as follows:

$$\partial_t \Gamma_x^{(1)} = -\frac{1}{2} \text{Diagram}, \quad (1.45)$$


$$\partial_t \Gamma_{xy}^{(2)} = \text{Diagram} - \frac{1}{2} \text{Diagram}, \quad (1.46)$$


$$\partial_t \Gamma_{xyz}^{(3)} = -3 \text{Diagram} - \frac{1}{2} \text{Diagram} + \text{Diagram} + \text{Diagram} + \text{Diagram}, \quad (1.47)$$


$$\begin{aligned} \partial_t \Gamma_{xyzw}^{(4)} = & 3 \text{Diagram} - \frac{1}{2} \text{Diagram} - \text{Diagram} - \text{Diagram} - \text{Diagram} \\ & + \frac{1}{2} \text{Diagram} + \frac{1}{2} \text{Diagram} + \frac{1}{2} \text{Diagram} + \frac{1}{2} \text{Diagram} \\ & + \frac{1}{2} \text{Diagram} + \frac{1}{2} \text{Diagram} + \frac{1}{2} \text{Diagram}. \end{aligned} \quad (1.48)$$


We will use the vertex expansion later on in chapters 4 and 5, and in particular make use of the diagrammatic representation in terms of Feynman diagrams.

Let us now turn to the second approximation scheme, the derivative expansion. As the name already suggests, in this approximation scheme one expands the effective average into functions of fixed order of the (covariant) derivative. This is in particular useful in flat space-time, where this is essentially an expansion in powers of the running momentum scale squared, k^2 . It has the advantage, that an operator of fixed power (and index structure) in the derivatives is allowed to be an arbitrary function of constant field configurations $\bar{\varphi}$, and not only a polynomial in the latter. In this way, one can study non-analytic truncations of the effective average action, and in particular truncations with infinitely many monomial operators. The functional renormalisation group equation then becomes a system of coupled partial differential equations for the scale-dependent functions of the fields.

To illustrate this scheme, let us consider the example of a single scalar quantum field theory with a \mathbb{Z}_2 symmetry, *i.e.* with an action that is invariant under the transformation $\varphi \mapsto -\varphi$. The most general effective average action to $\mathcal{O}(\partial^4)$ in the derivative expansion then reads:

$$\Gamma_k[\varphi] = \int d^d x \left[V_k(\varphi) + \frac{1}{2} Z_k(\varphi) (\partial_\mu \varphi \partial^\mu \varphi) + \frac{1}{2} W_k^{(1)}(\varphi) (\square \varphi \square \varphi) \right. \quad (1.49)$$

$$\left. + \frac{1}{2} W_k^{(2)}(\varphi) (\partial_\mu \varphi \partial^\mu \varphi \varphi \square \varphi) + \frac{1}{4} W_k^{(3)}(\varphi) (\partial_\mu \varphi \partial^\mu \varphi \partial_\nu \varphi \partial^\nu \varphi) + \mathcal{O}(\partial^6) \right], \quad (1.50)$$

where we defined $\square \equiv \partial_\mu \partial^\mu$. Here the effective potential V_k , the wave-function renormalisation Z_k and the three fourth order functions $W_k^{(i)}$ are all arbitrary functions of φ . To extract their renormalisation group running, one has to obtain the flow of the n -point function of the effective average action first, and then evaluate the resulting expression on constant field configurations

$\bar{\varphi}$. The number n is hereby given by the power of φ that is ‘outside’ the function in the term of the action, respectively. So to extract the running of V_k one would consider the running of the zero-point function, while for Z_k and $W_k^{(1)}$ one would consider the running of the two-point function. At second order in the derivatives, this would yield a system of the following form

$$\partial_t V_k(\bar{\varphi}) = \mathfrak{F}_V[V_k'', Z_k], \quad (1.51)$$

$$\partial_t Z_k(\bar{\varphi}) = \mathfrak{F}_Z[V_k'', V_k''', Z_k, Z_k', Z_k''], \quad (1.52)$$

where \mathfrak{F}_V and \mathfrak{F}_Z are functionals of V_k and Z_k , and primes denote derivatives with respect to the (constant) field variable $\bar{\varphi}$. The derivative expansion to zeroth order, where only a function V_k is kept, is commonly referred to as the local potential approximation.

We will review the very example of a \mathbb{Z}_2 invariant scalar field theory soon, when we will study critical behaviour and non-trivial fixed points in the next part of this chapter. We will also use this approximation schemes in chapters 2 and 3.

1.2 Asymptotic safety

In this section we will finally present the idea of asymptotic safety using the language of the renormalisation group developed in the last section. We will start with a general classification of quantum field theories and their relation to the renormalisation group, introducing the concepts of fixed points and conformal field theories along the way. After that we will give an introduction on how to use these ideas for practical calculations, studying the case example of a scalar field theory. In particular, we will make use of the local potential approximation and investigate scaling solutions such as the Wilson-Fisher fixed point. For general reviews of asymptotic safety, *cf.* [18–25].

1.2.1 Fixed points and fundamental quantum field theories

As we have mentioned in Sec. 1.1.3, the effective average action flows under the exact renormalisation group equation towards the bare action in the ultraviolet, $\lim_{k \rightarrow \infty} \Gamma_k = S$. Similarly, in the infrared the effective average action approaches the full quantum effective action, which contains all the information of the quantum field theory, $\lim_{k \rightarrow 0} \Gamma_k = \Gamma$. As we have already said, this latter property allows us in principle to solve any quantum field theory by integrating a well-defined differential equation instead of calculating the ill-defined path integral. To do this, we fix the effective average action in theory space at some initial scale k_0 and integrate the flow towards the infrared.

However, the first of the above properties provides us with another tool to investigate quantum field theories. Namely, integrating the exact flow equation towards the ultraviolet, we can study the high-energy behaviour of a quantum field theory in terms of the convergence or divergence of its coupling constants.

Generically, one would assume that at least one of the infinitely many couplings $g_i(k)$ in the expansion of Eqn. (1.38) tends to infinity when taking the limit $k \rightarrow \infty$. This happens indeed for instance in quantum electrodynamics where the divergent coupling is said to have a Landau pole. An equivalent behaviour restricts the (renormalised) quartic coupling in φ^4 -theory to be zero, which is known as quantum triviality. These kind of theories are called effective, since historically they were thought to arise from fundamental theories in which some (high-energy) degrees of freedom got “integrated out”. In the language of the exact renormalisation group, they simply do not admit a well-defined ultraviolet limit, $k \rightarrow \infty$. They may, however, still perfectly well be used

to make independent predictions in their range of validity after matching only a finite number of (relevant) couplings at some (infrared) energy scale. In this sense, the standard model is also an effective field theory, since it does not seem to be well-defined beyond the Planck scale. Nonetheless, after determining its 19 free parameters by experiments, it has great predictive power in its range of validity.

The other possible behaviour a quantum field theory may exhibit when flowing towards the ultraviolet, is the one for which none of the couplings of the theory diverges. This may be interpreted geometrically in such a way, that the trajectory of the effective average action under the exact renormalisation group flow is restricted to a finite subset of theory space. The simplest possibility of such a scenario is the existence of a so-called fixed point of the beta functions of all couplings of the theory. This means that there exists a value for each coupling in the theory which will not change under the renormalisation group flow. We will see this in more detail shortly. Quantum field theories that exhibit such a well-defined ultraviolet limit under the exact renormalisation group flow—in one way or another—are called fundamental, because one can make sense of them mathematically at any energy scale.

Historically the most important case of such a fundamental quantum field theory is quantum chromodynamics. More generally, the same behaviour manifests itself for Yang-Mills theories as long as the number of fermions is smaller than some symmetry group-dependent upper limit. In the latter case the theory becomes free in the ultraviolet, which was quite suggestively named *asymptotic freedom*. We will see that in the renormalisation group language, asymptotic freedom corresponds to a fixed point of the effective average action under the exact renormalisation group flow, for which all couplings vanish. This fixed point is also known as the Gaussian fixed point. However, there may also exist non-trivial fixed points which have non-zero values for (at least some of) the couplings. In this case the theory is said to be *asymptotically safe*. This scenario was discovered and called “asymptotic safety” by Steven Weinberg in 1979, *cf.* Ref. [5].

This classification of quantum field theories according to their renormalisation group behaviour in the ultraviolet opens up another powerful application of the exact renormalisation group. That is, instead of solving a given quantum field theory by integrating its flow equation towards the infrared, one can also study all trajectories of a given theory space, and choose a trajectory that is ultraviolet-finite in order to define a fundamental quantum field theory with some given field content and symmetries. A particular strategy to do so, is to first search for ultraviolet fixed points in theory space and then to find a renormalisation group trajectory that emanates from one of these very fixed points and flows towards the infrared in such a way that it matches the known values of the physical couplings in the infrared. This strategy may in particular be used to try to construct a quantum field theory of gravity. A corresponding program has been initiated by Martin Reuter in 1996, *cf.* Ref. [6], and is the main motivation underlying this thesis.

Before investigating fixed points and renormalisation group properties in a more quantitative manner, some remarks about the rescaling and essentiality of couplings of the effective average action are in order. One may naïvely think that theory space is spanned by all couplings $g_i(k)$ for the expansion of Eqn. (1.38). However integrating from a scale k towards a scale $k + \delta k$ results in a change of physical length and energy scales. Consequently, all dimensionful quantities (such as the couplings and the fields themselves) would need to be rescaled accordingly. This issue is most easily circumvented if one works with dimensionless couplings only. They can be defined via

$$\bar{g}_i(k) = k^{-d_i} g_i(k), \quad (1.53)$$

where d_i is the (classical) mass dimension of the coupling g_i . In the same way one also introduces a

‘coupling’ $Z_k^{(\varphi)}$, the so-called wave-function renormalisation, as a prefactor to the canonical kinetic term to avoid the need to rescale the field variables. For a scalar field, for instance, we may write

$$\frac{1}{2} Z_k^{(\varphi)} (\partial\varphi)^2 = \frac{1}{2} Z_k^{(\varphi)} k^{-2d_\varphi} (\partial\bar{\varphi})^2, \quad (1.54)$$

where $d_\varphi = d/2 - 1$ is the classical dimension of a scalar field. Instead of rescaling the fields, such that they are canonically normalised for every value of k , one absorbs this dependence into the coupling Z_k itself. We will often use the anomalous dimension η_φ instead of the wave-function renormalisation in the following, which are related via

$$\eta_\varphi \equiv -\frac{d \log Z_k^{(\varphi)}}{d \log k}. \quad (1.55)$$

The definition is such that at a fixed point $\partial_t \log Z_k^{(\varphi)} = -\eta_\varphi^*$ we have

$$\frac{1}{2} Z_k^{(\varphi)} k^{-2d_\varphi} (\partial\bar{\varphi})^2 = \frac{1}{2} k^{-2d_\varphi - \eta_\varphi^*} (\partial\bar{\varphi})^2, \quad (1.56)$$

that is, η_φ indeed measures the anomaly of the dimension of the field φ with respect to its classical value. Note that we still could have absorbed $Z_k^{(\varphi)}$ by a redefinition of the field variables and according redefinitions of the other couplings. This would however introduce an additional term in the beta functions of the dimensionless couplings \bar{g}_i , as we will see shortly.

The latter remark however applies quite generally. In particular, one calls a coupling inessential if it can be removed from the Lagrangian by a (local) field redefinition. Couplings for which this is not possible are called essential. Putting these two things together we see that the actual physical theory space is parametrised by the essential, dimensionless couplings $\bar{g}_i(k)$ only. In most of this thesis, for simplicity, we will work with the stronger requirement that the beta functions of *all* dimensionless couplings vanish at a fixed point.

Let us now discuss how to precisely extract the scale-dependence of the coordinates of theory space from the exact renormalisation group equation. Taking the scale-derivative ∂_t of the expansion Eqn. (1.38), and using the exact flow equation we find

$$\sum_{i \in \mathcal{I}} \partial_t g_i(k) \mathcal{O}_i[\Phi] = \partial_t \Gamma_k[\Phi] = \frac{1}{2} \text{Tr} \left[\left(\frac{\delta^2 \Gamma_k}{\delta\varphi \delta\varphi} + R_k \right)^{-1} \dot{R}_k \right] = \sum_{i \in \mathcal{I}} \beta_i(g_j, k) \mathcal{O}_i[\Phi], \quad (1.57)$$

where we assumed that the result of performing the functional trace can again be expanded in monomials of the field operators and covariant derivatives. The prefactors β_i in this expansion are called the beta functions of the couplings g_i and will in general depend on all other couplings g_j as well as on the scale k , explicitly. Passing to dimensionless variables and equating the running coupling $\partial_t g_i$ with its respective beta function, we find the following infinite system¹¹ of coupled flow equations for the dimensionless couplings of the theory

$$\partial_t \bar{g}_i = -d_i \bar{g}_i + \beta_i(k^{-d_j} g_j, k=1) \equiv \bar{\beta}_i(\bar{g}_j). \quad (1.58)$$

The first term of the dimensionless beta function $\bar{\beta}_i$ is the classical contribution, which is proportional to the classical mass dimension of the coupling. However, as we will see shortly, it is the second

¹¹In practical computations, this system may be reduced to a finite one, using one of the approximation schemes discussed in the last section.

term, the quantum contribution, which will be responsible for whether asymptotic safety occurs or not, and how predictive the resulting theory may be.

As we have hinted already above, the easiest way to guarantee that all couplings of the theory remain finite in the ultraviolet limit is to demand that each of them is scale-invariant, *i.e.* does not change its value along the flow, $\partial_t \bar{g}_i = 0$, $\forall i \in \mathcal{I}$. A solution vector $\{\bar{g}_i^*\}_{i \in \mathcal{I}}$ to this system of equations is called a fixed point,¹² and may be found as a root to the system of coupled algebraic equations that results from setting the dimensionless beta functions to zero

$$\bar{\beta}_i(\bar{g}_j) = 0, \quad \forall i \in \mathcal{I}. \quad (1.59)$$

In the following we will call this system the fixed point equations.

Assuming a solution vector to this system exists, the first thing we will be interested in, is whether this fixed point is reached in the ultraviolet or in the infrared. To decide which one is the case, we need to define a notion of subsets in theory space, that are attracted by the fixed point. This is done via so-called critical surfaces:

- The *infrared critical surface* is the set of all points which flow towards the fixed point in the limit $k \rightarrow 0$
- The *ultraviolet critical surface* is the set of all points which flow towards the fixed point in the limit $k \rightarrow \infty$

Note that a generic fixed point may well have both a non-empty infrared as well as a non-empty ultraviolet critical surface. This fixed point will then attract some couplings in the ultraviolet limit and others in the infrared limit. The notion of an infrared or ultraviolet fixed point, thus only has meaning, if there is single coupling.¹³

To obtain the dimension of the critical surfaces, we can linearise the flow equations about the fixed point. Introducing new variables

$$\hat{g}_i = \bar{g}_i - \bar{g}_i^*, \quad (1.60)$$

due to the vanishing of the beta functions at the fixed point, the flow reduces to

$$\partial_t \hat{g}_i = \left. \frac{\partial \bar{\beta}_i}{\partial \bar{g}_j} \right|_{\bar{g}_k = \bar{g}_k^*} \hat{g}_j + \mathcal{O}(\hat{g}^2). \quad (1.61)$$

Diagonalising the Jacobian $\partial \bar{\beta}_i / \partial \bar{g}_j = S_{ia} \delta_{ab} \lambda_b S_{bj}^{-1}$ at the fixed point—which is also known as the stability matrix—it is straightforward to see that the linearised flow equations for the eigenvectors $g_i^{(d)}$ assume the form¹⁴

$$\partial_t \hat{g}_i^{(d)} = \lambda_i \hat{g}_i^{(d)} + \mathcal{O}(\hat{g}_i^{(d)2}), \quad (1.62)$$

¹²A fixed point is in fact a stationary point for the couplings themselves, $\partial_t \bar{g}_i = 0$, a zero of the beta functions $\beta_i(\bar{g}_j^*) = 0$, and a fixed point in the usual mathematical sense, *i.e.* $T_k(\bar{g}_i^*) = \bar{g}_i^*$, for the map $T_k : \mathcal{T} \rightarrow \mathcal{T}$ that maps a point at scale k in theory space to another point at scale $k + \delta k$ in theory space.

¹³In the literature, however, fixed points are often referred to as ultraviolet if their ultraviolet critical surfaces is non-empty.

¹⁴There is no summation over the index i on the right hand side.

where λ_i are the eigenvalues of the Jacobian. In particular, using the definition of the renormalisation group time t , we can integrate the system to obtain the *linear* perturbations around the fixed point:

$$\hat{g}_i^{(d)} \propto \left(\frac{k}{\mu}\right)^{\lambda_i}. \quad (1.63)$$

This gives us all the information we need to determine the dimension of the critical surfaces of the fixed point. Namely, we have to distinguish three cases:

1. $\lambda_i < 0$: [relevant]	$\hat{g}_i^{(d)}$ diverges in the infrared \Leftrightarrow repelled by fixed point $\hat{g}_i^{(d)}$ vanishes in the ultraviolet \Leftrightarrow attracted by fixed point
2. $\lambda_i = 0$: [marginal]	$\hat{g}_i^{(d)}$ remains at fixed point \Leftrightarrow attraction/repulsion beyond linear analysis
3. $\lambda_i > 0$: [irrelevant]	$\hat{g}_i^{(d)}$ vanishes in the infrared \Leftrightarrow attracted by fixed point $\hat{g}_i^{(d)}$ diverges in the ultraviolet \Leftrightarrow repelled by fixed point

Directions $\hat{g}_i^{(d)}$ of the first category flow towards the fixed point in the ultraviolet limit, and are called relevant. The irrelevant directions on the other hand, that correspond to positive eigenvalues $\lambda_i > 0$, flow towards the fixed point in the infrared limit. Marginal directions finally, may be either (marginally) relevant or irrelevant—this has to be decided through the behaviour of the quadratic or higher perturbations around the fixed point.

To adhere to conventions coming from the theory of critical phenomena, we will often use the so-called *scaling* or *critical exponents* θ_i instead of the eigenvalues λ_i , which are simply defined by:

$$\theta_i \equiv -\lambda_i. \quad (1.64)$$

The above analysis shows that the directions (*i.e.* the eigenvectors) corresponding to the *negative* eigenvalues of the Jacobian of the beta functions span the tangent space to the ultraviolet critical surface at the fixed point. In particular, the number of negative eigenvalues is equal to the dimension of the ultraviolet critical surface.¹⁵

In order for a fixed point to be an ultraviolet attractor, there must hence be at least one negative eigenvalue of the Jacobian of the beta functions. Moreover, to be able to define a predictive fundamental quantum field theory through this fixed point, we also have to demand that the number of relevant directions is finite. This may be understood looking at the three-dimensional cartoon in Fig. 1.3: Since we want to define a fundamental quantum field theory, we have to choose a renormalisation group trajectory that lies within the ultraviolet critical surface. To do so, we thus need to fix n parameters for the n relevant directions \hat{g}_i , for instance in the deep infrared through n independent experiments. All the irrelevant critical exponents will then automatically be fixed by the requirement for the trajectory to lie in the ultraviolet critical surface, *i.e.* they are predicted by the theory. That is, the fewer relevant direction an asymptotically safe theory has, the more predictive it is. In particular, having infinitely many relevant direction would require to fix infinitely many couplings in the infrared, and thus make the usefulness of the theory dubious. The above also shows the origin of the terminology ‘relevant’ and ‘irrelevant’, since the respective couplings have to be either measure or are predicted.

¹⁵Such statements are always understood modulo the behaviour of the marginal directions.

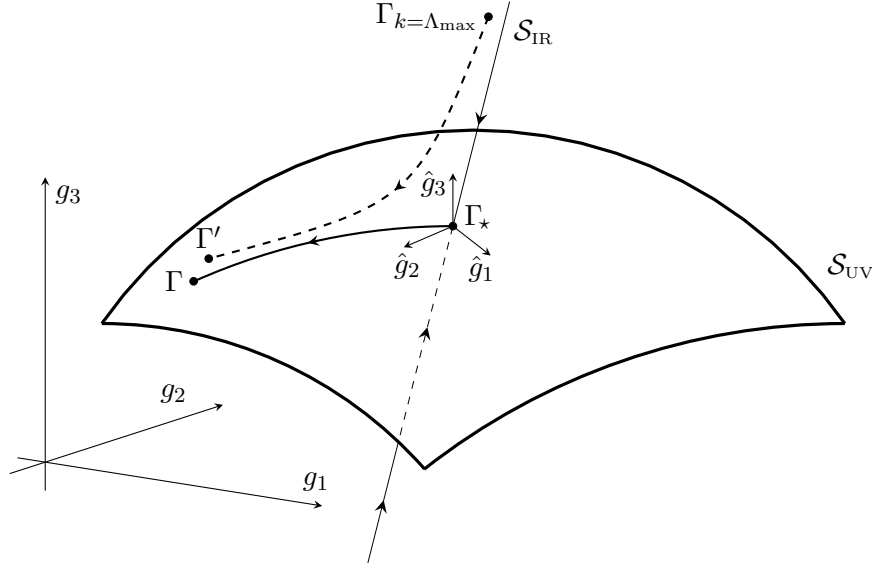


Figure 1.3: Three-dimensional cartoon of a two-dimensional ultraviolet critical surface \mathcal{S}_{UV} in theory space. There are two relevant directions \hat{g}_1 and \hat{g}_2 , as well as one irrelevant direction \hat{g}_3 . Arrows point in the direction of decreasing energy. Points Γ that lie on the ultraviolet critical surface flow towards the fixed point Γ_* in the ultraviolet limit and their trajectories represent fundamental quantum field theories. Points Γ' outside the critical surface flow away from the fixed point in the ultraviolet, although their trajectory might approach the ultraviolet critical surface at some point along the flow. The trajectories of these theories represent effective field theories with some cutoff Λ_{\max} .

Now that we have established how to find the basins of attraction of a fixed point in the ultraviolet and the infrared, and how to quantitatively determine the predictivity of the theory defined by such a fixed point, we can study the existence of fixed points in a general context. Let us first have a look at the free (massless) theory, for which all (essential) couplings are zero.¹⁶ Clearly this theory is scale-invariant, and thus has vanishing beta functions. The respective fixed point $\{\bar{g}_i^* = 0\}_{i \in \mathcal{I}}$ is called the Gaussian fixed point. To study its properties we may expand the dimensionless beta functions as follows¹⁷

$$\bar{\beta}_i = -d_i \bar{g}_i + \alpha_{ij} \bar{g}_j + \alpha_{ijk} \bar{g}_j \bar{g}_k + \mathcal{O}(\bar{g}^3). \quad (1.65)$$

This expansion cannot have a constant term, for it would spoil $\bar{\beta}_i(\bar{g}_j^*) = 0$ with $\bar{g}_j^* = 0$. Furthermore, we have $\alpha_{ij} \neq 0$, only for $j > i$, which can be verified considering which Feynman diagrams may enter the beta functions. It has the immediate consequence that the Jacobian

$$\left. \frac{\partial \bar{\beta}_i}{\partial \bar{g}_j} \right|_{\bar{g}_k=0} = -d_i \delta_{ij} + \alpha_{ij}, \quad (1.66)$$

has eigenvalues given by $-d_i$. But this in turn implies that the relevant directions, which determine the dimensionality of the ultraviolet critical surface, are given by monomial operators of positive

¹⁶In this case, the rescaling of the couplings in order to achieve $Z = 1$ does not have any consequence, since $\bar{g}_i = 0$.

¹⁷See footnote 14.

classical mass dimension, $d_i > 0$. This is nothing but the property of perturbative power-counting renormalisability.

What is more, since for any fixed space-time dimension d , there are only finitely many such (local) operators, the ultraviolet critical surface is finite-dimensional. That is, if such a fixed point exists, the resulting theory predicts that all (infinitely many) power-counting non-renormalisable couplings vanish in the ultraviolet. This is precisely the case of asymptotic freedom, and the origin of the immense predictivity of a theory defined via an ultraviolet Gaussian fixed point. We can now also understand, that perturbation theory covers the part of theory space around the Gaussian fixed point for which all couplings remain small, $\bar{g}_i < 1$.

However, note that power-counting renormalisability is only a necessary but not a sufficient condition for the existence of such an ultraviolet fixed point. This may be illustrated using the case of a single coupling. Passing back to dimensionful variables, the above expansion reads:

$$\partial_t g = \beta(g) = \alpha g^2 + \mathcal{O}(g^3), \quad (1.67)$$

which can easily be integrated to yield

$$g(k) = \frac{g(\mu)}{1 - \alpha g(\mu) \log\left(\frac{k}{\mu}\right)}. \quad (1.68)$$

Since for the ultraviolet regime, $k > \mu$, the logarithm is positive, we have to choose α negative in order to guarantee that the denominator never vanishes. Then we have indeed

$$\lim_{k \rightarrow \infty} g(k) = \lim_{k \rightarrow \infty} \left[\frac{1}{|\alpha| \log\left(\frac{k}{\mu}\right)} + \mathcal{O}(k^{-1}) \right] = 0, \quad (1.69)$$

the behaviour of an asymptotically free coupling. That is, in this simple case the sign of the second derivative of the beta function determines whether the Gaussian fixed point is an infrared or an ultraviolet fixed point, *cf.* also Fig. 1.4.

For the case of a non-trivial, also called an *interacting* or *non-Gaussian fixed point*, one can say much less in general. The cartoon Fig. 1.4 which covers the case of a single coupling, illustrates how such a fixed point may arise. Note in particular that the value of the couplings at the interacting fixed point is not restricted by any means, and may very well be $\bar{g}_i^* \gg 1$, which would disallow for a perturbative treatment. More severely yet, the quantum contributions, which may induce non-trivial solutions to the fixed point equations

$$\bar{\beta}_i(\bar{g}_j) = -d_i \bar{g}_i + \text{quantum corrections}, \quad (1.70)$$

in the first place, may also alter the signs of the eigenvalues of the Jacobian of the beta functions at the fixed point:

$$\lambda_i = -d_i + \text{quantum corrections}' . \quad (1.71)$$

In this way, an alleged ultraviolet critical surface may become infinite-dimensional, which would in turn spoil the predictivity of theory, as we would have to fix an infinite number of independent parameters through experiments. However, as long as these quantum corrections remain smaller than the classical contributions, in particular if the fixed point lies close to the Gaussian one, we would expect the ultraviolet critical surface to be finite dimensional.

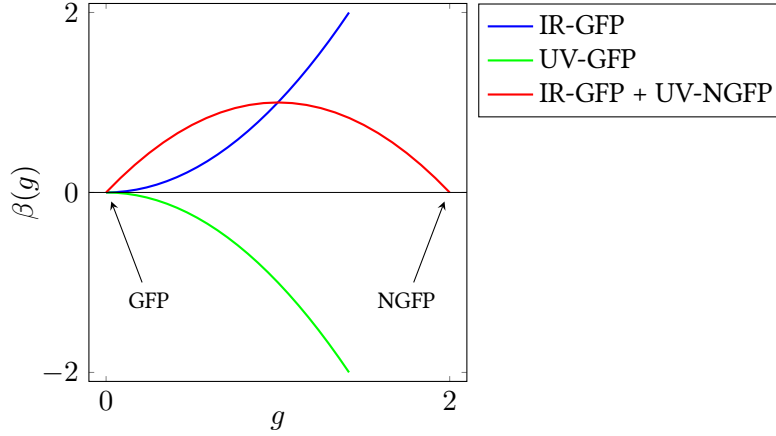


Figure 1.4: Cartoon of the possible shapes of a quadratic beta function in a 1+1 dimensional theory space with non-negative value of the coupling at the fixed point. The blue curve develops an infrared (IR) Gaussian fixed point (GFP) as in the case of QED. The red curve features an ultraviolet (UV) Gaussian fixed point with $\alpha = -1$, cf. Eqn. (1.67), as it appears in Yang-Mills theories such as QCD. The red curve finally, $\beta(g) = 2g - g^2$, develops both an infrared Gaussian fixed point, as well as an ultraviolet non-Gaussian fixed point (NGFP), as in perturbative Einstein gravity.

The scale-invariant quantum field theory defined by the fixed point is often a conformal field theory. In particular, expanding the flow equations to second order around the fixed point in the diagonal directions

$$\partial_t \hat{g}_i^{(d)} = \lambda_i \hat{g}_i^{(d)} + \left(S_{ia}^{-1} \frac{\partial^2 \bar{\beta}_a}{\partial \bar{g}_b \partial \bar{g}_c} \Big|_{\bar{g}_d = \bar{g}_d^*} S_{bj} S_{ck} \right) \hat{g}_j^{(d)} \hat{g}_k^{(d)} + \mathcal{O}(\hat{g}^{(d)3}), \quad (1.72)$$

we can match it with the expansion of conformal perturbation theory

$$\partial_t \hat{g}_i^{(d)} = -2(1 - \Delta_i) \hat{g}_i^{(d)} + \pi c_{ijk} \hat{g}_j^{(d)} \hat{g}_k^{(d)} + \mathcal{O}(\hat{g}^{(d)3}), \quad (1.73)$$

where Δ_i are the scaling dimensions and c_{ijk} are the structure constants. Together they specify the dynamics of the conformal field theory completely. We can thus reconstruct the conformal field theory at the fixed point by setting

$$\Delta_i = \frac{\lambda_i + 2}{2}, \quad (1.74)$$

$$c_{ijk} = \frac{1}{\pi} \left(S_{ia}^{-1} \frac{\partial^2 \bar{\beta}_a}{\partial \bar{g}_b \partial \bar{g}_c} \Big|_{\bar{g}_d = \bar{g}_d^*} S_{bj} S_{ck} \right). \quad (1.75)$$

To summarise this subsection, we draw a sketch of theory space in Fig. 1.5. We have seen, that in order to define a fundamental quantum field theory, we can integrate the functional renormalisation group equation from an ultraviolet fixed point, characterised by a conformal field theory $\Gamma_\infty = S_{UV}$ towards the infrared, fixing the relevant critical exponents at some intermediate scale k_0 . This allows (in principle) to solve the quantum field theory and obtain an effective action Γ . We have

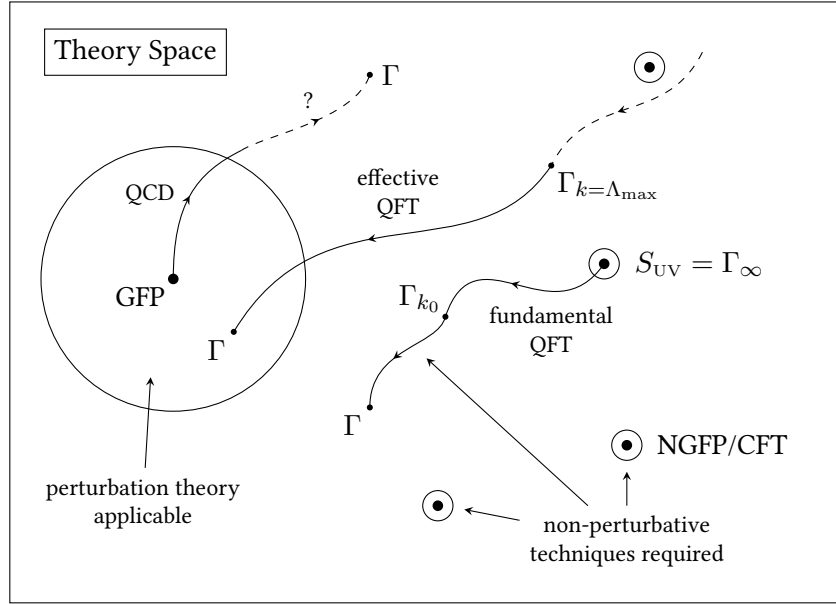


Figure 1.5: A cartoon of theory space. The Gaussian (GFP) and non-Gaussian (NGFP) fixed points are represented with big dots. Other points in theory space are denoted with small dots. Trajectories in theory space represent quantum field theories, and arrows point in the direction for decreasing energy scale k .

also seen that such a fixed point may be a trivial Gaussian fixed point, describing a free theory, or a non-trivial non-Gaussian fixed point, describing an interacting quantum field theory. The former case is known as asymptotic freedom, whilst the latter case is called asymptotic safety. The theory space containing the Gaussian fixed point, where the dimensionless essential couplings remain small is accessible through perturbation theory. Finally, effective field theories may be understood as trajectories in theory space which do not lie on any ultraviolet critical surface. Consequently at least one of the couplings in the theory will diverge at some finite value of the running scale k . However, the theory is still well-defined up to some finite ultraviolet cutoff scale $k = \Lambda_{\max}$.

1.2.2 Case study: scalar field theory

In the last section of this chapter we want to use the techniques and ideas introduced so far to study quantum field theories with a single scalar field which possesses a \mathbb{Z}_2 symmetry, such that the action is invariant under the transformation $\varphi \mapsto -\varphi$.

In particular, we will use the functional renormalisation group, first to study a very crude φ^4 -approximation, and second to investigate the local potential approximation of the derivative expansion. The former gives a first hint of the existence of a non-trivial infrared fixed point in $d = 3$, the Wilson-Fisher fixed point. In the latter we will use polynomial approximations, as well as the method of shooting, to study the existence of scaling solutions.

φ^4 -theory

The simplest possible approximation of the full \mathbb{Z}_2 scalar field theory one can study is to assume the following ansatz of the effective average action

$$\Gamma_k[\varphi] = \int d^d x \left[\frac{1}{2} \partial^\mu \varphi \partial_\mu \varphi + \frac{1}{2} m_k^2 \varphi^2 + \frac{1}{4!} \lambda_k \varphi^4 \right]. \quad (1.76)$$

Here the squared mass m_k^2 and the φ^4 -coupling λ_k are the two scale-dependent couplings of the theory. Note that this ansatz is much more restrictive than to assume the same form for the bare or ultraviolet action of the theory. This is because in the latter case the effective average action (and the infrared effective action in particular) would contain all operators allowed by the \mathbb{Z}_2 symmetry, which appear through the procedure of integrating out the scalar field in the path integral. Here instead, the effective average action is restricted to contain only three terms at *any* energy scale.

To extract the running of the couplings in this approximation, we can use the derivative expansion which we studied in Sec. 1.1.4. Using Eqns. (1.46) and (1.48) and evaluating the two- and four-point function at vanishing external momenta, we find

$$\partial_t \Gamma_k^{(2)}(0, 0) = \partial_t m_k^2 = -\frac{1}{2} \lambda_k \int \frac{d^d q}{(2\pi)^d} G_k(q^2) \partial_t R_k(q^2) G_k(q^2), \quad (1.77)$$

$$\partial_t \Gamma_k^{(4)}(0, 0, 0, 0) = \partial_t \lambda_k = 3 \lambda_k^2 \int \frac{d^d q}{(2\pi)^d} G_k(q^2) \partial_t R_k(q^2) G_k^2(q^2), \quad (1.78)$$

where the full regulated propagator in momentum space reads

$$G_k(q^2) = \frac{1}{q^2 + m_k^2 + R_k(q^2)}. \quad (1.79)$$

If we choose to use the optimised cutoff, we can evaluate the integrals on the right hand sides explicitly. Using $\partial_t R_k(q^2) = 2 k^2 \theta(k^2 - q^2)$ the dimensionful beta functions become:

$$\partial_t m_k^2 = -c_d k^{d-2} \frac{\lambda_k}{[1 + m_k^2/k^2]^2}, \quad (1.80)$$

$$\partial_t \lambda_k = 6 c_d k^{d-4} \frac{\lambda_k}{[1 + m_k^2/k^2]^3}, \quad (1.81)$$

where for later convenience we introduce the d -dimensional volume coefficient

$$c_d = \frac{1}{(4\pi)^{d/2} \Gamma(d/2 + 1)}. \quad (1.82)$$

Before searching for fixed points we now have to pass to dimensionless variables $\bar{m}_k^2 = m_k^2/k^2$ and $\bar{\lambda}_k = \lambda_k/k^{4-d}$, as we have explained above. In this variables the flow equations assume the form

$$\bar{\beta}_{\bar{m}_k^2} = \partial_t \bar{m}_k^2 = -2 \bar{m}_k^2 - \frac{c_d \bar{\lambda}_k}{[1 + \bar{m}_k^2]^2}, \quad (1.83)$$

$$\bar{\beta}_{\bar{\lambda}_k} = \partial_t \bar{\lambda}_k = (d-4) \bar{\lambda}_k + \frac{6 c_d \bar{\lambda}_k}{[1 + \bar{m}_k^2]^3}. \quad (1.84)$$

If we now set the beta functions to zero we find the following solutions to the fixed point equations:

$$\text{G: } \bar{m}_k^{2*} = 0, \quad \bar{\lambda}^* = 0, \quad (1.85)$$

$$\text{WF: } \bar{m}_k^{2*} = \frac{d-4}{16-d}, \quad \bar{\lambda}^* = \frac{288}{c_d} \frac{d-4}{(d-16)^3}. \quad (1.86)$$

The first solution is the familiar Gaussian fixed point (G). The second one however, is a non-trivial fixed point, known as the Wilson-Fisher fixed point (WF), which has first been discovered in $d = 3$

and belongs to the Ising (bi-critical) universality class. Note that the second one coincides with the first one in $d = 4$ where only the Gaussian fixed point exists.

We can now also linearise the flow about the fixed points to obtain critical exponents. To this end, we first calculate the stability matrices:

$$M_G = \begin{pmatrix} -2 & 0 \\ -c_d & d-4 \end{pmatrix}, \quad (1.87)$$

$$M_{WF} = \begin{pmatrix} -\frac{d+2}{3} & -\frac{72}{c_d} \frac{(d-4)^2}{(d-16)^2} \\ -c_d \frac{(d-16)^2}{144} & 4-d \end{pmatrix}. \quad (1.88)$$

The critical exponents can then be found as the negative of the eigenvalues:

$$\text{G:} \quad \theta_1 = 2, \quad \theta_2 = 4 - d, \quad (1.89)$$

$$\text{WF:} \quad \theta_{1,2} = -\frac{1}{6} \left(10 - 4d \pm \sqrt{484 - 200d + 22d^2} \right). \quad (1.90)$$

The local potential approximation

After having used the exact renormalisation group equation to extract the scale-dependence of two perturbatively renormalisable couplings, we now want to study truly functional approximations of the effective average action, where we study the behaviour of a large number or possibly even infinitely many couplings at the same time.

As we have seen in Sec. 1.1.4, one of the approximation schemes available to do this is the derivative expansion. In particular, because of Lorentz symmetry, we can write the effective average action in this approximation as a series in even powers of the space-time derivative ∂_μ

$$\Gamma_k = \Gamma_{0,k} + \Gamma_{2,k} + \Gamma_{4,k} + \mathcal{O}(\partial^6), \quad (1.91)$$

where each of these terms has to be invariant under the transformation $\varphi \mapsto -\varphi$ by itself. We will here study the local potential approximation (LPA)

$$\Gamma_k[\varphi] = \int d^d x \left[\frac{1}{2} \partial^\mu \varphi \partial_\mu \varphi + V_k(\varphi) \right], \quad (1.92)$$

which corresponds to the zeroth order of the derivative expansion with the addition of a canonical kinetic term, so that the scalar field can propagate. The effective potential V_k is allowed to be a function of φ and carries implicitly infinitely many monomials and couplings of the scalar field.

In the second order of the derivative expansion we would introduce a function $Z_k(\varphi)$ as a prefactor to the kinetic term. Sometimes an intermediate approximation where Z_k is a scale-depend number only, is used. In this way one can study the running of the anomalous dimension of the scalar field.

To extract the renormalisation group dependence of the effective potential V_k , we first have to calculate the regulated inverse propagator in our approximation:

$$\Gamma_k^{(2)} + R_k = -\partial^2 + R_k(-\partial^2) + V_k'', \quad (1.93)$$

where primes denote derivatives with respect to the field φ . In the following chapters we will sometimes abbreviate the combination $P_k(-\partial^2) = -\partial^2 + R_k(-\partial^2)$. We can now write the flow equation as

$$\partial_t \Gamma_k = \frac{1}{2} \text{Tr} \left[\frac{\partial_t R_k}{-\partial^2 + R_k + V_k''} \right], \quad (1.94)$$

where as before the traces includes an integration over space-time and momenta. It can be evaluate with the following strategy: For some general function $W(-\partial^2)$ we can rewrite the trace as an integral over its Fourier-transform and integrate explicitly over the angular dependence

$$\text{Tr } W(-\partial^2) = \int d^d x \int \frac{d^d q}{(2\pi)^d} \tilde{W}(q^2) = \frac{\text{vol}(\mathbb{S}^{d-1})}{(2\pi)^d} \int d^d x \int_0^\infty dq q^{d-1} \tilde{W}(q^2), \quad (1.95)$$

where $\text{vol}(\mathbb{S}^{d-1}) = \frac{2\pi^{d/2}}{\Gamma(d/2)}$ is the surface of the d dimensional sphere. It is also often times convenient to pass to momentum squared as the integration variable $z \equiv q^2$, such that the integration measure becomes

$$dq q^{d-1} = \frac{1}{2} dz z^{d/2-1}. \quad (1.96)$$

Finally, we define the so-called Q -functionals as

$$Q_n[W] \equiv \frac{1}{\Gamma(n)} \int_0^\infty dz z^{n-1} \tilde{W}(z), \quad (1.97)$$

such that the trace can be evaluated as

$$\text{Tr } W(-\partial^2) = \frac{1}{(4\pi)^{d/2}} \int d^d x Q_{d/2}[W]. \quad (1.98)$$

Now we are able to evaluate the left hand side of the exact renormalisation group equation. Note that the right hand side contains already the scale-derivative of the effective potential we are looking for, albeit integrate over space-time. To make further progress we can choose to set the field configuration constant, which truly makes the potential a function of the variable φ , rather than a functional of the space-time function $\varphi(x)$. Then the space-time volume factor cancels on both sides of the flow equation, and we obtain for the dimensionful beta function of the effective potential

$$\partial_t V_k(\varphi) = \frac{1}{2(4\pi)^{d/2}} Q_{d/2} \left[\frac{\partial_t R_k}{-\partial^2 + R_k + V_k''} \right]. \quad (1.99)$$

Note that the value of the Q -functional on the right hand side depends on the choice of the cutoff. In general it is good practise to test values of fixed points and critical exponents against changes of the cutoff profile. This will give a measure of the robustness and convergence of the results. Here, however, for illustrative purposes, we will only use the optimised cutoff, since it allows the integrals to be evaluated analytically.

In particular, for any $n, l > 0$ and any function $A_k \in \mathcal{O}(\partial^0)$, we have for the optimised cutoff

$$\begin{aligned} Q_n \left[\frac{\partial_t R_k}{-\partial^2 + R_k + A_k} \right] &= \frac{1}{\Gamma(n)} \int_0^\infty dz z^{n-1} \frac{2k^2 \theta(k^2 - z) + 2k^2(k^2 - z) \delta(k^2 - z)}{\left[z + (k^2 - z) \theta(k^2 - z) + A_k \right]^l} \\ &= \frac{1}{\Gamma(n)} \int_0^\infty dz z^{n-1} \frac{2k^2}{\left[k^2 + A_k \right]^l} \\ &= \frac{2}{\Gamma(n+1)} \frac{k^{2(n-l+1)}}{\left[1 + \bar{A}_k \right]^l}, \end{aligned} \quad (1.100)$$

where $\bar{A}_k = A_k/k^2$ is the dimensionless function. Using this result, the dimensionful beta function of the effective potential assumes the simple form

$$\partial_t V_k(\varphi) = \frac{c_d k^{d+2}}{k^2 + V''}. \quad (1.101)$$

We now have to introduce dimensionless fields $\bar{\varphi} = k^{-\frac{d-2}{2}} \varphi$, so that we can write the dimensionless potential as $\bar{V}(\bar{\varphi}) = k^{-d} V(\bar{\varphi} k^{\frac{d-2}{2}})$, and the dimensionless beta function becomes

$$\partial_t \bar{V}_k(\bar{\varphi}) = -d \bar{V} + \frac{d-2}{2} \bar{\varphi} \bar{V}' + \frac{c_d}{1 + \bar{V}''}. \quad (1.102)$$

Polynomial truncations

Before attempting to solve the fixed point equation resulting from this flow equation in full generality, let us study a simple polynomial approximation. For this we may write the dimensionful effective potential, respecting the \mathbb{Z}_2 symmetry, as

$$V(\varphi^2) = \sum_{n=0}^N \frac{\lambda_{2n}}{(2n)!} \varphi^{2n}. \quad (1.103)$$

In this way, we can extract the beta functions for the couplings λ_{2n} by taking derivatives of the beta function of the potential with respect to the field and setting it to zero subsequently

$$\beta_{2n} = \frac{\partial^{2n}}{\partial \varphi^{2n}} \partial_t V_k \Big|_{\varphi=0}. \quad (1.104)$$

We can then pass once again to dimensionless variables $\bar{\lambda}_{2n} \equiv k^{d(n-1)-2n} \lambda_{2n}$, such that the dimensionless beta functions read

$$\bar{\beta}_{2n} = [d(n-1) - 2n] \bar{\lambda}_{2n} + k^{d(n-1)-2n} \beta_{2n}. \quad (1.105)$$

Using the result Eqn. (1.100) and the dimensionful beta function of the potential we obtain the following first five beta functions for the couplings

$$\bar{\beta}_0 = -d \bar{\lambda}_0 + \frac{c_d}{1 + \bar{\lambda}_2}, \quad (1.106)$$

$$\bar{\beta}_2 = -2 \bar{\lambda}_2 - \frac{c_d \bar{\lambda}_4}{(1 + \bar{\lambda}_2)^2}, \quad (1.107)$$

$$\bar{\beta}_4 = (d-4) \bar{\lambda}_4 - \frac{c_d \bar{\lambda}_6}{(1 + \bar{\lambda}_2)^2} + \frac{6 c_d \bar{\lambda}_4^2}{(1 + \bar{\lambda}_2)^3}, \quad (1.108)$$

$$\bar{\beta}_6 = (2d-6) \bar{\lambda}_6 - \frac{c_d \bar{\lambda}_8}{(1 + \bar{\lambda}_2)^2} + \frac{30 c_d \bar{\lambda}_4 \bar{\lambda}_6}{(1 + \bar{\lambda}_2)^3} - \frac{90 c_d \bar{\lambda}_4^3}{(1 + \bar{\lambda}_2)^4}, \quad (1.109)$$

$$\bar{\beta}_8 = (3d-8) \bar{\lambda}_8 - \frac{c_d \bar{\lambda}_{10}}{(1 + \bar{\lambda}_2)^2} + \frac{56 c_d \bar{\lambda}_4 \bar{\lambda}_8}{(1 + \bar{\lambda}_2)^3} + \frac{70 c_d \bar{\lambda}_6^2}{(1 + \bar{\lambda}_2)^3} - \frac{1260 c_d \bar{\lambda}_4^2 \bar{\lambda}_6}{(1 + \bar{\lambda}_2)^4} + \frac{2520 c_d \bar{\lambda}_4^4}{(1 + \bar{\lambda}_2)^5}. \quad (1.110)$$

These equations can now in particular be used to study the Wilson-Fisher fixed point in $d = 3$ in some more detail. Starting from the simplest truncation for which $N = 2$,

$$\bar{\beta}_2 = -2\bar{\lambda}_2 - \frac{1}{6\pi^2} \frac{\bar{\lambda}_4}{(1 + \bar{\lambda}_2)^2}, \quad (1.111)$$

$$\bar{\beta}_4 = -\bar{\lambda}_4 + \frac{1}{\pi^2} \frac{\bar{\lambda}_4^2}{(1 + \bar{\lambda}_2)^3}, \quad (1.112)$$

one set the beta functions to zero and finds a non-trivial fixed point at

$$\bar{\lambda}_2^* = -\frac{1}{13} \approx -0.0769, \quad \bar{\lambda}_4^* = \frac{1728\pi^2}{2197} \approx 7.76. \quad (1.113)$$

Again, one may linearise the flow around this fixed point to extract the critical exponents using the eigenvalues of the stability matrix. These yields the two critical exponents

$$\theta_1 = 1.843, \quad \theta_2 = -1.176, \quad (1.114)$$

precisely the same that we found in the “perturbative” φ^4 -analysis, *cf.* Eqn.(1.90). However, we may now enlarge the system including the dimensionless coupling $\lambda_6 = \bar{\lambda}_6$. Then the system becomes

$$\bar{\beta}_2 = -2\bar{\lambda}_2 - \frac{1}{6\pi^2} \frac{\bar{\lambda}_4}{(1 + \bar{\lambda}_2)^2}, \quad (1.115)$$

$$\bar{\beta}_4 = -\bar{\lambda}_4 - \frac{1}{6\pi^2} \frac{\bar{\lambda}_6}{(1 + \bar{\lambda}_2)^2} + \frac{1}{\pi^2} \frac{\bar{\lambda}_4^2}{(1 + \bar{\lambda}_2)^3}, \quad (1.116)$$

$$\bar{\beta}_6 = \frac{5}{\pi^2} \frac{\bar{\lambda}_4 \bar{\lambda}_6}{(1 + \bar{\lambda}_2)^3} - \frac{15}{\pi^2} \frac{\bar{\lambda}_4^3}{(1 + \bar{\lambda}_2)^4}. \quad (1.117)$$

Again, we find a single non-Gaussian fixed point with the following fixed point values and critical exponents:

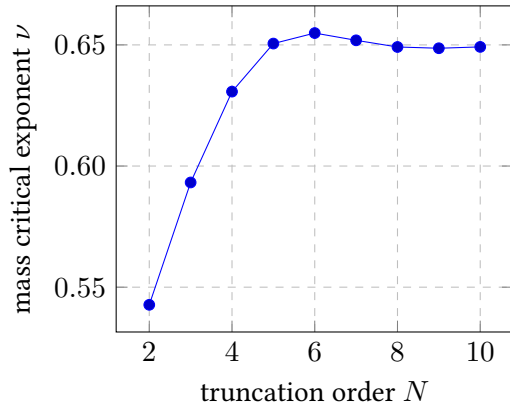
$$\bar{\lambda}_2^* = -\frac{1}{7} \approx -0.1429, \quad \bar{\lambda}_4^* = \frac{432\pi^2}{343} \approx 12.43, \quad \bar{\lambda}_6^* = \frac{93312\pi^4}{16807} \approx 540.8, \quad (1.118)$$

$$\theta_1 = 1.686, \quad \theta_2 = -1.133, \quad \theta_3 = -12.22. \quad (1.119)$$

Note that the first two critical exponents are fairly close to the previous values and that there is now an additional irrelevant direction, which is very different from its perturbative value zero. One can now continue with this procedure by including the running of the perturbatively non-renormalisable coupling λ_8 . However, starting at this order, one finds an additional, second non-trivial solution to the system of fixed point equations.

Solely within the polynomial truncation one cannot decide which one of these fixed points, or if possibly both of them are physical. However, it is always possible to identify one of the solutions as the continuation of a previously encountered fixed point. Unsurprisingly, the number of solutions grows with the order of the polynomial, since this approximation provides a system of N equations for N unknowns.

Polynomial truncations are very useful to quantify solutions numerically and extract critical exponents. As an example, we show the convergence of the first few critical exponents, as well as the mass critical exponent $\nu = 1/\theta_1$ for polynomial truncations up to $N = 10$ in Fig. 1.6. However, using these truncations we can neither prove that a true solution for the whole effective potential exists, nor that the additional fixed point solutions are artefacts of the approximation.



N	ν	$\theta_{1,2,3}$
2	0.54272	1.8426, -1.1759
3	0.59322	1.6857, -1.1328, -12.220
4	0.63071	1.5855, -0.9565, -8.8239
5	0.65055	1.5372, -0.7805, -6.5218
6	0.65488	1.5270, -0.6614, -4.8441
7	0.65189	1.5340, -0.6191, -3.7419
8	0.64914	1.5405, -0.6331, -3.1637
9	0.64862	1.5417, -0.6581, -2.9859
10	0.64917	1.5404, -0.6667, -3.0531

Figure 1.6: Convergence behaviour of the mass critical exponent $\nu = 1/\theta_1$, as well as the first three critical exponents θ_i using polynomial truncations up to order $N = 10$.

Scaling solutions

To address this issue, one has to study the full behaviour of the fixed point equation for the effective potential

$$0 = -d\bar{V}^* + \frac{d-2}{2}\bar{\varphi}\bar{V}^{*\prime} + \frac{c_d}{1+\bar{V}^{*\prime\prime}}. \quad (1.120)$$

Since this is a second order ordinary differential equation, each of its solutions—called scaling solutions—can be parametrised in terms of two boundary conditions. Since the potential contains only even powers of the field variable, its first derivatives has to vanish at the origin, $\bar{V}^{*\prime}(0) = 0$. If we furthermore fix the value of the second derivative at zero $\bar{V}^{*\prime\prime}(0) = \sigma$, the two conditions read

$$\bar{V}^{*\prime}(0) = 0 \quad \text{and} \quad \bar{V}^{*\prime\prime}(0) = \sigma \iff \bar{V}^*(0) = \frac{c_d}{d(1+\sigma)}. \quad (1.121)$$

Since the fixed point equation is non-linear, one has to use numerical methods to solve it. In doing so, one observes that for almost all values of σ the solution ends up in a singularity at a finite value of the field variable $\bar{\varphi}$. To find a value for σ , for which a solution is defined for all real numbers \mathbb{R} instead, one proceeds as follows. First one defines a function $\Phi(d, \sigma)$, which maps the (continuous) dimension d and the parameter σ to the maximal value of the field variable $\bar{\varphi}$, for which a solution to Eqn. (1.120) with boundary conditions (1.121) can be found. Since we are interested in solutions which are defined for any value of $\bar{\varphi}$, we have to look for divergences in $\Phi(d, \sigma)$. To this end one may numerically calculate $\Phi(d, \sigma)$ and look for ‘spikes’ in the plot of Φ as a functions of σ , cf. Ref. [26]. This procedure is also called shooting method. Extracting a critical value for σ in this way, one is then able to integrate the fixed point equation to find a scaling solution for the effective potential.

We illustrate this approach in Fig.1.7. Although this procedure may be applied to continuous, fractal dimensions, we focus on the cases $d = 4$ and $d = 3$ here. Note that the spike at $\sigma = -1$ is due to the pole in the denominator of the last term in the fixed point equation and does not correspond to a true solution of the system. For values $\sigma < -1$ the effective potential is unbounded from below and thus physically irrelevant.

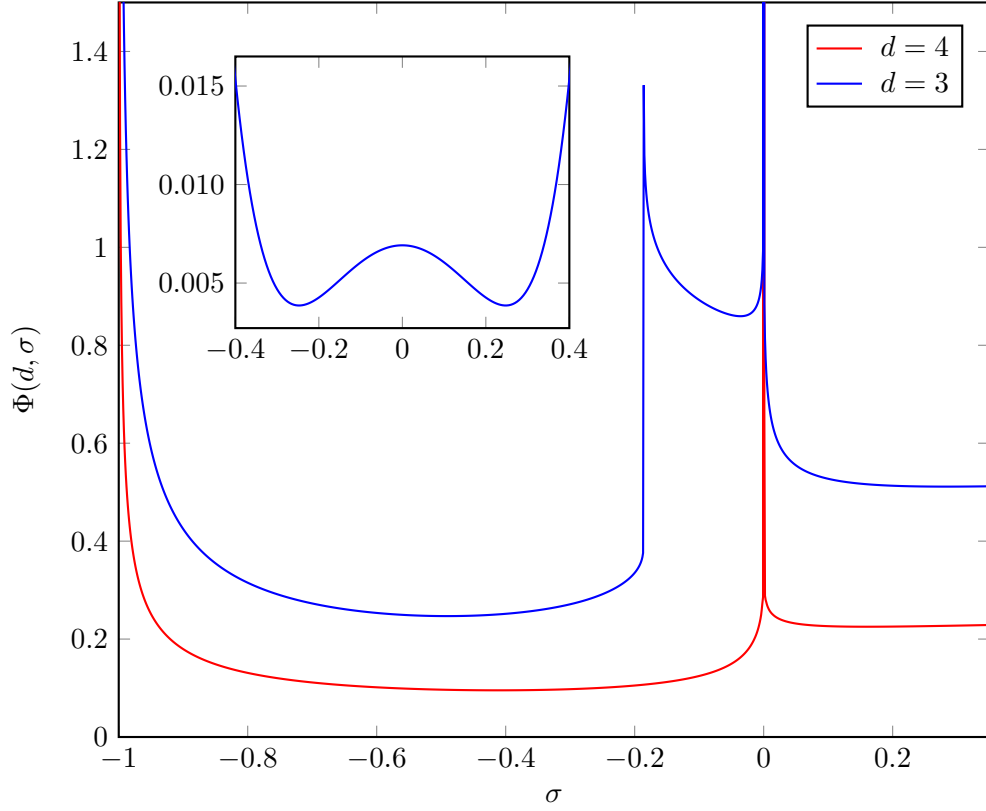


Figure 1.7: The peaks in the spike plots reveal at which parameter value σ a global scaling solution exists. In $d = 4$ there is only the Gaussian fixed point, whereas in $d = 3$ there also exists the non-trivial Wilson-Fisher fixed point for $\sigma_* = -0.186064$. The resulting effective potential as a function of $\bar{\varphi}$ is displayed in the inset.

As we have seen before, in $d = 4$ there is only one fixed point, the trivial Gaussian fixed point at $\sigma = 0$, where the potential remains constant

$$\bar{V}^* = \frac{1}{128\pi^2}. \quad (1.122)$$

In $d = 3$, there is however an additional spike for $\sigma_* = -0.186064$, which corresponds to the Wilson-Fisher fixed point and belongs to the bi-critical Ising universality class. The resulting potential has two minima and is shown in the inset in Fig. 1.7.

2. Background Independence in Quantum Gravity

Following Ref. [6], non-perturbative renormalization group flows for quantum gravity have been formulated by utilising the technical device of splitting the metric in terms of a background metric and a fluctuation field—the background field formalism.

Physical results must however be independent of this arbitrary split, in other words should be background independent. The background metric however is in particular used to define the effective cutoff scale k (via the background Laplacian). This breaks background independence at intermediate scales k but such that background independence can be recovered in the limit $k \rightarrow 0$ providing certain modified split Ward identities (msWIs) are imposed [12, 27–36]. RG properties on the other hand are defined at intermediate scales k . There is therefore the potential for conflict in this formulation between RG notions such as fixed points, and the requirement of background independence.

In this chapter we want to expand on the results of Ref. [35], and study a truncated formulation of conformally reduced gravity. In this theory, the explicit dependence on the background field displays itself only in the cutoff operator, and not in the gauge fixing and ghost sector, as it would be for the full theory of quantum gravity. This simplifies the investigation considerably.

An unsettling conclusion from the research reported in Ref. [35] is that the requirement of background independence in a theory of quantum gravity may actually *be* in conflict with renormalization group properties in flows formulated as above: fixed points under changes in the effective cutoff scale k , can be forbidden by the msWIs that are enforcing background independence.

In the conformally truncated gravity model investigated in Ref. [35], this happens generically when the anomalous dimension η is non-vanishing. It can however be avoided by a careful choice of parametrisation. On the other hand it was shown in Ref. [35] that the situation is saved in all cases, at least in the conformally reduced gravity model, by the existence of an alternative background-independent description. This involves in particular a background-independent notion of scale, \hat{k} . This background independent description exists at a deeper underlying level since in

terms of these background-independent variables, the RG fixed points and corresponding flows always exist, and are manifestly independent of the choice of parametrisation.

After approximating the exact RG flow equations and msWIs to second order in the derivative expansion, the crucial technical insight was to notice that, just as in the scalar field theory model [28], the msWIs and RG flow equations can be combined into linear partial differential equations. It is the solution of the latter equations that uncovers the background independent variables. And it is by comparing the description in these variables with the equivalent description in the original variables, that we see that fixed points in the original variables are in general forbidden by background independence.

However in order to facilitate combining the RG flow equations and msWIs when the anomalous dimension $\eta \neq 0$, the authors of Ref. [35] were led to a particular form of cutoff profile R_k , namely a power-law cutoff profile. We will show in this chapter that in fact this cutoff profile plays a rôle that is much deeper than the convenience of this mathematical trick. To this end, we will introduce the notion of compatibility and investigate under which assumptions flow equation and msWIs are in fact compatible up to $\mathcal{O}(\partial^2)$ in the derivative expansion. We will see that $\eta = 0$ is sufficient to allow the derivative expansions of the exact RG and msWI equations to be compatible, and we will investigate the implications of background independence to the solutions of the combined system.

But even if the msWIs are not compatible with the flow equations, it does not immediately follow that there are no simultaneous solution to the system of equations. However, as we argue in sec. 2.2.4 and verify by example in sec. 2.3.2, if the msWIs are not compatible, the equations are overconstrained and it is for this reason that it is hopeless to expect any solutions.

To investigate the combined system of the LPA flow and msWI equations, we will both use the trick of combining these equations into a linear partial differential equation, as well as studying polynomial truncations, since it seems likely that the latter is the only way we could investigate system using the exact non-perturbative flow equations. Viewed from this perspective, we will see that the problem is that if the RG fixed point equations and msWI equations are truly independent, then they will overconstrain the solutions if carried to sufficiently high order truncation.

Our analysis suggests therefore that the full non-perturbative Ward identities would lead to important constraints on RG properties. Unfortunately it seems very challenging to investigate this, since we will see that the number of equations only exceeds the number of vertices for the first time at the six-point level. We discuss potential conflict for the exact non-perturbative flow equations further in the conclusions.

2.1 Conformally reduced gravity at order derivative-squared

In this section we give a quick resumé of the results we need and their context, from Ref. [35]. We arrive at conformally reduced gravity (in Euclidean signature) by writing:

$$\tilde{g}_{\mu\nu} = f(\tilde{\phi}) \hat{g}_{\mu\nu} = f(\chi + \tilde{\varphi}) \hat{g}_{\mu\nu} \quad \text{and} \quad \bar{g}_{\mu\nu} = f(\chi) \hat{g}_{\mu\nu}. \quad (2.1)$$

Here $\tilde{g}_{\mu\nu}$ is the metric that is integrated over in the partition function. It is restricted to an overall conformal factor $f(\tilde{\phi})$ times a fiducial metric which in fact we set to flat: $\hat{g}_{\mu\nu} = \delta_{\mu\nu}$.

Examples of parametrisations used previously in the literature include $f(\phi) = \exp(2\phi)$ [37] and $f(\phi) = \phi^2$ [32, 38]. However we leave the choice of parametrisation f unspecified. It is important to note however that f cannot depend on k since it is introduced at the bare level and has no relation to the infrared cutoff. Later we will change to dimensionless variables using k and in these variables it can be forced to depend on k (see especially secs. 2.2.5 and 2.3.1).

We split the total conformal factor field $\tilde{\phi}(x)$ into a background conformal factor field $\chi(x)$ and fluctuation conformal factor field $\tilde{\varphi}(x)$. It is then the latter that is integrated over in the path integral. This will yield the classical fluctuation field $\varphi = \langle \tilde{\varphi} \rangle$ and the total classical field $\phi = \langle \tilde{\phi} \rangle = \chi + \varphi$, respectively. Also as shown, we similarly parametrise the background metric $\bar{g}_{\mu\nu}$ in terms of the background conformal factor field χ .

Precisely as in the last chapter, we will introduce a cutoff operator R_k which is responsible for suppressing momentum modes below the infrared cutoff scale k , in order to derive the non-perturbative flow equation. The crucial observation is that in the context of the background field method in quantum gravity the cutoff operator itself depends on the background field χ . The reason for this is that the cutoff operator is a function of the covariant Laplacian of the background metric $R_k(-\bar{\nabla}^2)$, as it is with respect to the spectrum of $-\bar{\nabla}^2$ that modes are integrated out or suppressed in the path integral, *cf.* [39, 40].

A remnant diffeomorphism invariance enforces this χ dependence in the approximation chosen in Ref. [35]. By specialising to a background metric $\bar{g}_{\mu\nu}$ that is slowly varying, so that space-time derivatives of this can be neglected, we effectively terminate at the level of the LPA for the background conformal factor χ . For the classical fluctuating conformal factor φ however, $\mathcal{O}(\partial^2)$ in the derivative expansion approximation is fully implemented, making no other approximation. The effective action thus takes its most general form at this level of truncation:

$$\Gamma_k[\varphi, \chi] = \int d^d x \sqrt{\bar{g}} \left[-\frac{1}{2} K(\varphi, \chi) \bar{g}^{\mu\nu} \partial_\mu \varphi \partial_\nu \varphi + V(\varphi, \chi) \right]. \quad (2.2)$$

The modified split Ward identity encodes the extent to which the effective action violates *split symmetry*:

$$\tilde{\varphi}(x) \mapsto \tilde{\varphi}(x) + \varepsilon(x), \quad \chi(x) \mapsto \chi(x) - \varepsilon(x). \quad (2.3)$$

Due to the special rôle played by χ , the infrared cutoff operator breaks this symmetry, leading to the msWI:

$$\frac{1}{\sqrt{\bar{g}}} \left(\frac{\delta \Gamma_k}{\delta \chi} - \frac{\delta \Gamma_k}{\delta \varphi} \right) = \frac{1}{2} \text{Tr} \left[\frac{1}{\sqrt{\bar{g}} \sqrt{\bar{g}}} \frac{\delta^2 \Gamma_k}{\delta \varphi \delta \varphi} + R_k[\chi] \right]^{-1} \frac{1}{\sqrt{\bar{g}}} \left[\frac{\delta R_k[\chi]}{\delta \chi} + \frac{d}{2} \partial_\chi \log f R_k[\chi] \right]. \quad (2.4)$$

Exact background independence would be realised if the right hand side of the msWI was zero, implying that the effective action is only a functional of the total field $\phi = \chi + \varphi$. The presence of the cutoff operator however causes the right hand side to be non-vanishing in general. It is only in the limit $k \rightarrow 0$ (holding physical, *i.e.* unscaled, momenta and fields fixed) that the cutoff operator drops out and background independence can be restored exactly. We note therefore that imposing the msWI in addition to the flow equation automatically ensures exact background independence in the limit $k \rightarrow 0$. The observation we further explore in this chapter is that restricting flows to satisfy the msWI then has consequences for the RG properties, in particular fixed point behaviour.

Computing the flow equation and msWI in the derivative expansion (2.2), as done in Ref. [35], results in flow equations and modified split Ward identities¹, for the potential V :

$$\partial_t V(\varphi, \chi) = f(\chi)^{-\frac{d}{2}} \int dp p^{d-1} Q_p \dot{R}_p, \quad (2.5)$$

$$\partial_\chi V - \partial_\varphi V + \frac{d}{2} \partial_\chi \log f V = f(\chi)^{-\frac{d}{2}} \int dp p^{d-1} Q_p \left[\partial_\chi R_p + \frac{d}{2} \partial_\chi \log f R_p \right], \quad (2.6)$$

¹Although we always mean these modified identities, we will sometimes refer to them simply as Ward identities.

and for the kinetic function K :

$$f^{-1} \partial_t K(\varphi, \chi) = 2f^{-\frac{d}{2}} \int dp p^{d-1} P_p(\varphi, \chi) \dot{R}_p, \quad (2.7)$$

$$f^{-1} \left[\partial_\chi K - \partial_\varphi K + \frac{d-2}{2} \partial_\chi \log f K \right] = 2f^{-\frac{d}{2}} \int dp p^{d-1} P_p(\varphi, \chi) \left[\partial_\chi R_p + \frac{d}{2} \partial_\chi \log f R_p \right]. \quad (2.8)$$

The p subscripts denote the momentum dependence of Q_p, P_p and the cutoff R_p and as usual RG time derivatives are denoted also by a dot on top. Q_p is defined as

$$Q_p = \left(\partial_\varphi^2 V - p^2 \frac{K}{f} + R_p \right)^{-1}, \quad (2.9)$$

and P_p is given by

$$\begin{aligned} P_p = & -\frac{1}{2} \frac{\partial_\varphi K}{f} Q_p^2 + \frac{\partial_\varphi K}{f} \left(2\partial_\varphi^3 V - \frac{2d+1}{d} \frac{\partial_\varphi K}{f} p^2 \right) Q_p^3 \\ & - \left[\left(\frac{4+d}{d} \frac{\partial_\varphi K}{f} p^2 - \partial_\varphi^3 V \right) \left(\partial_{p^2} R_p - \frac{K}{f} \right) + \frac{2}{d} p^2 \partial_{p^2}^2 R_p \left(\frac{\partial_\varphi K}{f} - \partial_\varphi^3 V \right) \right] \\ & \times \left(\partial_\varphi^3 V - \frac{\partial_\varphi K}{f} p^2 \right) Q_p^4 - \frac{4}{d} p^2 \left(\partial_{p^2} R_p - \frac{K}{f} \right)^2 \left(\partial_\varphi^3 V - \frac{\partial_\varphi K}{f} p^2 \right)^2 Q_p^5. \end{aligned} \quad (2.10)$$

2.2 Compatibility of the msWI with the flow equation

Compatibility of the msWI with the flow equation means the following. Write the msWI in the form $\mathcal{W} = 0$ and assume that this holds at some scale k . Computing $\dot{\mathcal{W}}$ by using the flow equation, we say that the msWI is compatible if $\dot{\mathcal{W}} = 0$ then follows at scale k without further constraints.

In the first part of this section we briefly outline the necessary steps to derive the flow equation and msWI for conformally reduced gravity. This derivation will be organised in a slightly different way from Ref. [35] and the last chapter so as to make the steps that will follow more transparent. We then prove that they are compatible with one another. So far, this is naturally to be expected since both are derived from the same partition function. For completeness we include it here in order to fully understand the issues once we consider derivative expansions. (For a proof of the exact case in a more general context see Ref. [36].) In the second part we study the notion of compatibility for conformally reduced gravity in the truncation (2.2). Asking for compatibility in the derivative expansion is actually non-trivial. We derive the requirements necessary to achieve it.

2.2.1 Compatibility at the exact level

The proof of compatibility of the un-truncated system consists of demonstrating that the RG time derivative of the msWI is proportional to the msWI itself [41, 42]. In analogy with references [41, 42], we expect to find that this RG time derivative is, more specifically, proportional to a second functional derivative with respect to φ acting on the msWI and it is with this in mind that we proceed (see also Ref. [36]).

We begin by considering the following Euclidean functional integral over the fluctuation field $\tilde{\varphi}$

$$e^{W_k} = \int \mathcal{D}\tilde{\varphi} e^{-S[\chi+\tilde{\varphi}] - \Delta S_k[\tilde{\varphi}, \bar{g}] + S_{\text{src}}[\tilde{\varphi}, \bar{g}]}. \quad (2.11)$$

This integral is regulated in the UV (as it must be), however we leave this regularisation implicit in what follows. Compatibility can be shown most easily by presenting both the flow equation and the msWI as matrix expressions. Thus we begin by rewriting the source term using matrix notation like so

$$S_{\text{src}}[\tilde{\varphi}, \bar{g}] = \int d^d x \sqrt{\bar{g}(x)} \tilde{\varphi}(x) J(x) \equiv \tilde{\varphi}_x T_{xy} J_y \equiv \tilde{\varphi} \cdot T \cdot J, \quad (2.12)$$

where $T_{xy} \equiv T(x, y) \equiv \sqrt{\bar{g}(x)} \delta(x - y)$. We will use a generalised Einstein summation convention where repeated indices or equivalently the dot notation represent integration over position space. Similarly, we write the cutoff action as

$$\Delta S_k[\tilde{\varphi}, \bar{g}] = \frac{1}{2} \int d^d x \sqrt{\bar{g}(x)} \tilde{\varphi}(x) R_k[\bar{g}] \tilde{\varphi}(x) \equiv \frac{1}{2} \tilde{\varphi}_x r_{xy} \tilde{\varphi}_y \equiv \frac{1}{2} \tilde{\varphi} \cdot r \cdot \tilde{\varphi}, \quad (2.13)$$

where

$$r_{xy} \equiv r(x, y) \equiv \sqrt{\bar{g}(x)} \sqrt{\bar{g}(y)} R_k(x, y), \quad (2.14)$$

and where the cutoff operator and its kernel are related according to

$$R_k(x, y) = R_k[\bar{g}(x)] \frac{\delta(x - y)}{\sqrt{\bar{g}(y)}}. \quad (2.15)$$

We refrain from putting a k subscript on r_{xy} to avoid clutter with indices, but note that it still has k -dependence. Also note that now the factors of $\sqrt{\bar{g}}$ are no longer part of the integration; this is to enable all χ -dependent quantities to be easily accounted for when acting with $\delta/\delta\chi$ later on. With these definitions in place, we may as before take the Legendre transform $\tilde{\Gamma}_k$ of W_k and from this define the effective average action $\Gamma_k[\varphi, \bar{g}] = \tilde{\Gamma}_k[\varphi, \bar{g}] - \Delta S_k[\varphi, \bar{g}]$. Using similar steps as in the last chapter, we quickly arrive at the flow equation for the latter, which now reads

$$\dot{\Gamma}_k = \frac{1}{2} \text{Tr}[\Delta \dot{r}], \quad \text{where} \quad \Delta_{xy} \equiv \left[\frac{\delta^2 \Gamma_k}{\delta \varphi_x \delta \varphi_y} + r_{xy} \right]^{-1}. \quad (2.16)$$

The msWI on the other hand is derived by applying the split symmetry transformations (2.3), with infinitesimal $\varepsilon(x)$, to the functional integral (2.11). The bare action is invariant under this shift, however the source term and cutoff action are not. It is the breaking of this symmetry that indicates background independence has been lost. Applying these shifts to (2.11) we obtain

$$-\frac{\delta W_k}{\delta \chi} \cdot \varepsilon = \left\langle \varepsilon \cdot T \cdot J - \tilde{\varphi} \cdot \left(\frac{\delta T}{\delta \chi} \cdot \varepsilon \right) \cdot J - \varepsilon \cdot r \cdot \tilde{\varphi} + \frac{1}{2} \tilde{\varphi} \cdot \left(\frac{\delta r}{\delta \chi} \cdot \varepsilon \right) \cdot \tilde{\varphi} \right\rangle. \quad (2.17)$$

Under these same shifts, the Legendre transformation of W_k gives

$$\frac{\delta W_k}{\delta \chi} \cdot \varepsilon = J \cdot \left(\frac{\delta T}{\delta \chi} \cdot \varepsilon \right) \cdot \varphi - \frac{\delta \tilde{\Gamma}_k}{\delta \chi} \cdot \varepsilon. \quad (2.18)$$

Substituting this relation into (2.17) together with $\Gamma_k = \tilde{\Gamma}_k - \Delta S_k$, we obtain the msWI

$$\frac{\delta \Gamma_k}{\delta \chi_\omega} - \frac{\delta \Gamma_k}{\delta \varphi_\omega} = \frac{1}{2} \Delta_{xy} \frac{\delta r_{yx}}{\delta \chi_\omega}, \quad (2.19)$$

where we have used the fact that the identity must hold for arbitrary $\varepsilon(\omega)$. Note that in deriving the msWI the contribution of the source term to the separate background field dependence of $\Gamma_k[\varphi, \chi]$ drops out.

The msWI and flow equation just derived appear at first sight to be in conflict with results from the last chapter. In particular factors of \sqrt{g} seem to be missing. This is because these factors are absorbed in a different definition of the inverse kernel. Indeed the inverse kernel in (2.16) now satisfies

$$\left[\frac{\delta^2 \Gamma_k}{\delta \varphi_x \delta \varphi_y} + r_{xy} \right] \Delta_{yz} = \delta_{xz} \quad (2.20)$$

without a $\sqrt{g}(y)$ included in the integration over y .

Now that we have derived the flow equation and msWI written in a convenient notation, we are ready to prove that they are compatible. We begin by defining

$$\mathcal{W}_\omega \equiv \frac{\delta \Gamma_k}{\delta \chi_\omega} - \frac{\delta \Gamma_k}{\delta \varphi_\omega} - \frac{1}{2} \Delta_{xy} \frac{\delta r_{yx}}{\delta \chi_\omega} = 0. \quad (2.21)$$

Taking the RG time derivative of \mathcal{W}_ω then gives

$$\dot{\mathcal{W}}_\omega = \frac{\delta \dot{\Gamma}_k}{\delta \chi_\omega} - \frac{\delta \dot{\Gamma}_k}{\delta \varphi_\omega} + \frac{1}{2} \left[\Delta \left(\frac{\delta^2 \dot{\Gamma}_k}{\delta \varphi \delta \varphi} + \dot{r} \right) \Delta \right]_{xy} \frac{\delta r_{yx}}{\delta \chi_\omega} - \frac{1}{2} \Delta_{xy} \frac{\delta \dot{r}_{yx}}{\delta \chi_\omega} \quad (2.22)$$

and upon substituting the flow equation (2.16) into the right hand side, we have

$$\begin{aligned} \dot{\mathcal{W}}_\omega &= -\frac{1}{2} \Delta_{xz} \frac{\delta^3 \Gamma_k}{\delta \varphi_z \delta \varphi_{z'} \delta \chi_\omega} \Delta_{z'y} \dot{r}_{yx} + \frac{1}{2} \Delta_{xz} \frac{\delta^3 \Gamma_k}{\delta \varphi_z \varphi_{z'} \varphi_\omega} \Delta_{z'y} \dot{r}_{yx} \\ &\quad + \frac{1}{4} \Delta_{xz} \left(\frac{\delta^2}{\delta \varphi_z \delta \varphi_{z'}} \Delta_{uu'} \right) \dot{r}_{u'u} \Delta_{z'y} \frac{\delta r_{yx}}{\delta \chi_\omega} \\ &= -\frac{1}{2} (\Delta \dot{r} \Delta)_{zz'} \frac{\delta^2}{\delta \varphi_{z'} \delta \varphi_z} \left(\frac{\delta \Gamma}{\delta \chi_\omega} - \frac{\delta \Gamma}{\delta \varphi_\omega} \right) + \frac{1}{4} \left(\frac{\delta^2}{\delta \varphi_z \delta \varphi_{z'}} \Delta_{uu'} \right) \dot{r}_{u'u} \Delta_{z'y} \frac{\delta r_{yx}}{\delta \chi_\omega} \Delta_{xz}. \end{aligned} \quad (2.23)$$

The first term in the last equality is in the form we want: a differential operator acting on (part of) \mathcal{W}_ω . We now expand out the second term with the aim of also putting it into the desired form. For the sake of neatness let us define

$$\Gamma_{x_1 \dots x_n}^{(n)} \equiv \frac{\delta^n \Gamma_k}{\delta \varphi_{x_1} \dots \delta \varphi_{x_n}}. \quad (2.24)$$

Expanding out the second term then gives

$$\begin{aligned} \left(\frac{\delta^2}{\delta \varphi_z \delta \varphi_{z'}} \Delta_{uu'} \right) \dot{r}_{u'u} \Delta_{z'y} \frac{\delta r_{yx}}{\delta \chi_\omega} \Delta_{xz} &= \Delta_{xz} \left(\Delta_{uv} \Gamma_{zvs}^{(3)} \Delta_{sv'} \Gamma_{z'v's'}^{(3)} \Delta_{s'u'} \right. \\ &\quad \left. + \Delta_{uv'} \Gamma_{v's'z'}^{(3)} \Delta_{s'v} \Gamma_{zvs}^{(3)} \Delta_{su'} - \Delta_{uv'} \Gamma_{v's'zz'}^{(4)} \Delta_{s'u'} \right) \dot{r}_{u'u} \Delta_{z'y} \frac{\delta r_{yx}}{\delta \chi_\omega}. \end{aligned} \quad (2.25)$$

Upon exchanging factors of Δ and relabelling indices, we find

$$\left(\frac{\delta^2}{\delta \varphi_z \delta \varphi_{z'}} \Delta_{uu'} \right) \dot{r}_{u'u} \left(\Delta_{z'y} \frac{\delta r_{yx}}{\delta \chi_\omega} \Delta_{xz} \right) = (\Delta \dot{r} \Delta)_{s'v'} \frac{\delta^2}{\delta \varphi_{v'} \delta \varphi_{s'}} \Delta_{xy} \frac{\delta r_{yx}}{\delta \chi_\omega}, \quad (2.26)$$

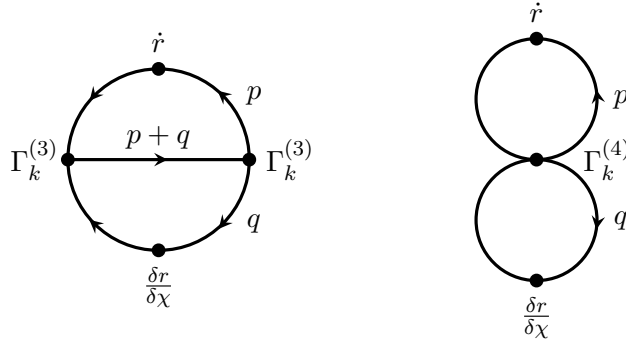


Figure 2.1: The two-loop diagrams in (2.25). Their symmetry immediately implies the identity (2.26). Momentum flow is indicated in the case where the fluctuation field φ is then set to zero.

which now has the structure we require. Thus we have shown that the RG time derivative of the msWI can be written as

$$\dot{\mathcal{W}}_\omega = -\frac{1}{2} \text{Tr} \left[\Delta \dot{r} \Delta \frac{\delta^2}{\delta\varphi\delta\varphi} \right] \mathcal{W}_\omega, \quad (2.27)$$

i.e. that it is proportional to the msWI itself. If Γ_k satisfies \mathcal{W}_ω at some initial scale k_0 , and satisfies the flow equation there, it thus follows without further restriction that $\dot{\mathcal{W}}_\omega|_{k_0} = 0$ since it is proportional to \mathcal{W}_ω . Thus the msWI is compatible with the flow equation. If Γ_k continues to evolve according to the flow equation, it then follows that \mathcal{W}_ω and thus $\dot{\mathcal{W}}_\omega$ will be zero for all k .

2.2.2 Compatibility versus derivative expansion

Recalling that Δ is an infrared regulated full propagator, we see from (2.25) that the identity (2.26) can be understood diagrammatically in terms of two-loop diagrams as sketched in Fig. 2.1. The symmetry of these diagrams means that nothing changes if we exchange $\dot{r} \leftrightarrow \delta r / \delta\chi$. This exchange immediately leads to the identity (2.26).

This identity breaks down in general in the derivative expansion. If the Ward identity is approximated by a derivative expansion, the full propagator in the one-loop term in (2.21) is also expanded in a derivative expansion. This full propagator has loop momentum q say, and is then expanded in powers of momenta carried by the external fluctuation field $\varphi(p)$, *i.e.* by the external legs. The RG time derivative of the Ward identity yields the RG time derivative of such vertices, as can be seen from the $\delta^2 \dot{\Gamma}_k / \delta\varphi^2$ term in (2.22). This latter term has two internal legs given by the explicit functional derivatives, carrying the loop momentum q and joining full internal propagators Δ , and any number of external legs contained in the vertices of $\dot{\Gamma}_k$. Substituting the flow equation (2.16) then gives in particular the last term in Eqn. (2.23) in which two of these external legs are now joined to form a loop connected via \dot{r} . However it is momenta external to *this new loop* which are Taylor expanded in the derivative expansion of the flow equation (see also [43, 44]). This is illustrated in the diagram displayed in Fig. 2.1. In particular when the remaining external fluctuation field dependence is removed by setting $\varphi = 0$, we have exactly the momentum dependence displayed in the figure. We see that a derivative expansion of the Ward identity involves Taylor expanding in small p , while integrating over q . However a derivative expansion of the flow equation involves

Taylor expanding in small q , and integrating over p instead. Thus the symmetry between the two loops is broken and the identity (2.26) no longer follows.

On the other hand we see that if \dot{r} and $\delta r/\delta\chi$ have the same momentum dependence then the identity (2.26) is restored because it is no longer possible to distinguish the two loops. Returning the placement of \sqrt{g} from (2.14) to the integration measure, this in fact would give us relation (2.45) which, as we will see, is necessary and sufficient for compatibility of the Ward identities within the derivative expansion, and which we will now derive directly within the derivative expansion.

2.2.3 Compatibility at order derivative-squared

We now proceed to calculate the flow of the msWI for the system truncated at $\mathcal{O}(\partial^2)$ as described in sec. 2.1, and investigate directly under what circumstances it vanishes. Let us start by writing the flow equations and msWIs for both V and K in the following form so that we can study both cases simultaneously:

$$\dot{A}(\varphi, \chi) = \int_p B_p \dot{R}_p, \quad (2.28)$$

$$\mathcal{W}^{(A)} = \bar{\partial}A - \gamma A + \int_p B_p (\partial_\chi R_p + \gamma R_p) = 0, \quad (2.29)$$

where A is either V or K/f such that B_p is either Q_p or $2P_p$ respectively. Here we have also introduced the shorthand notation

$$\int_p \equiv f(\chi)^{-\frac{d}{2}} \int dp p^{d-1}, \quad \gamma \equiv \frac{d}{2} \partial_\chi \log f, \quad \text{and} \quad \bar{\partial} \equiv \partial_\varphi - \partial_\chi. \quad (2.30)$$

It will also be useful to have to hand the following relations:

$$(\bar{\partial} + \partial_t - \gamma) V = \mathcal{W}^{(V)} + \int_q Q_q (\dot{R}_q - \partial_\chi R_q - \gamma R_q), \quad (2.31)$$

$$(\bar{\partial} + \partial_t - \gamma) \frac{K}{f} = \mathcal{W}^{(K)} + 2 \int_q P_q (\dot{R}_q - \partial_\chi R_q - \gamma R_q), \quad (2.32)$$

$$\begin{aligned} (\bar{\partial} + \partial_t + n\gamma) Q_p^n &= -n Q_p^{n+1} \int_q (\partial_\varphi^2 Q_q - 2p^2 P_q) (\dot{R}_q - \partial_\chi R_q - \gamma R_q) \\ &\quad - n Q_p^{n+1} (\dot{R}_p - \partial_\chi R_p - \gamma R_p) - n Q_p^{n+1} (\partial_\varphi^2 \mathcal{W}^{(V)} - p^2 \mathcal{W}^{(K)}). \end{aligned} \quad (2.33)$$

The first two relations are derived by subtracting the msWI from the flow equation for V and K/f respectively. The last relation is then derived by using the first two relations above together with the definition of Q_p given in (2.9).

We begin by taking the RG time derivative of (2.29). Substituting in the flow equation for \dot{A} , and remembering the power of $f(\chi)$ hidden in the integral over p , this gives

$$\dot{\mathcal{W}}^{(A)} = \int_p \dot{R}_p (\bar{\partial} + \partial_t + \gamma) B_p - \int_p \dot{B}_p (\dot{R}_p - \partial_\chi R_p - \gamma R_p). \quad (2.34)$$

In order to proceed we have to assume a particular form of B_p so that we can compute the result of the linear operators under the integral acting on it. A general term in P_p takes the form

$$\tilde{B}_p = (\partial_\varphi^i V)^a \left(\partial_\varphi^j \frac{K}{f} \right)^b \left(\partial_{p^2}^k R_p \right)^c (p^2)^l Q_p^e, \quad (2.35)$$

where a, b, c, e, i, j, k (not to be confused with the cutoff scale), and l are non-negative integers. From the structure of the terms in P_p one can read off the following sum rule for the exponents:

$$a + b + c = e - 1. \quad (2.36)$$

Notice that the case $B_p = Q_p$ for the potential is also included, since $a = b = c = l = 0$ and $e = 1$ also satisfies the sum rule. Taking the term under the first integral of (2.34), we find

$$\begin{aligned} (\bar{\partial} + \partial_t + \gamma)\tilde{B}_p &= \left[a (\partial_\varphi^i V)^{-1} \partial_\varphi^i (\bar{\partial} + \partial_t) V + b \left(\partial_\varphi^j \frac{K}{f} \right)^{-1} \partial_\varphi^j (\bar{\partial} + \partial_t) \frac{K}{f} \right. \\ &\quad \left. + c \left(\partial_{p^2}^k R_p \right)^{-1} \partial_{p^2}^k (-\partial_\chi + \partial_t) R_p + e Q_p^{-1} (\bar{\partial} + \partial_t) Q_p + \gamma \right] \tilde{B}_p. \end{aligned} \quad (2.37)$$

Substituting equations (2.31)–(2.33) into the above expression and using the sum rule, we obtain

$$\begin{aligned} (\bar{\partial} + \partial_t + \gamma)\tilde{B}_p &= \left[a (\partial_\varphi^i V)^{-1} \partial_\varphi^i \left(\mathcal{W}^{(V)} + \int_q Q_q \bar{R}_q \right) \right. \\ &\quad + b \left(\partial_\varphi^j \frac{K}{f} \right)^{-1} \partial_\varphi^j \left(\mathcal{W}^{(K)} + 2 \int_q P_q \bar{R}_q \right) + c \left(\partial_{p^2}^k R_p \right)^{-1} \partial_{p^2}^k \bar{R}_p \\ &\quad \left. - e Q_p \int_q (\partial_\varphi^2 Q_q - 2p^2 P_q) \bar{R}_q - e Q_p \bar{R}_p - e Q_p \left(\partial_\varphi^2 \mathcal{W}^{(V)} - p^2 \mathcal{W}^{(K)} \right) \bar{R}_q \right] \tilde{B}_p. \end{aligned} \quad (2.38)$$

where we have introduced the shorthand notation

$$\bar{R}_p = \dot{R}_p - \partial_\chi R_p - \gamma R_p. \quad (2.39)$$

Turning our attention now to the second integral of (2.34) we take the RG time derivative of \tilde{B}_p and again substitute in the flow equations for V and K/f . This gives

$$\begin{aligned} \dot{\tilde{B}}_p &= \left[a (\partial_\varphi^i V)^{-1} \partial_\varphi^i \int_q Q_q \dot{R}_q + b \left(\partial_\varphi^j \frac{K}{f} \right)^{-1} \partial_\varphi^j \int_q 2P_q \dot{R}_q \right. \\ &\quad \left. + c \left(\partial_{p^2}^k R_p \right)^{-1} \partial_{p^2}^k \dot{R}_p - e Q_p \int_q (\partial_\varphi^2 Q_q - 2p^2 P_q) \dot{R}_q - e Q_p \dot{R}_q \right] \tilde{B}_p. \end{aligned} \quad (2.40)$$

Inserting (2.38) and (2.40) into (2.34) we obtain

$$\begin{aligned} \dot{\mathcal{W}}^{(A)} &= \sum_{\tilde{B}_p} \left\{ a \int_{p,q} \tilde{B}_p (\partial_\varphi^i V)^{-1} \partial_\varphi^i \left(\dot{R}_p \mathcal{W}^{(V)} + Q_q [\dot{R}, \partial_\chi R + \gamma R]_{qp} \right) \right. \\ &\quad + b \int_{p,q} \tilde{B}_p \left(\partial_\varphi^j \frac{K}{f} \right)^{-1} \partial_\varphi^j \left(\dot{R}_p \mathcal{W}^{(K)} + 2P_q [\dot{R}, \partial_\chi R + \gamma R]_{qp} \right) \\ &\quad + c \int_p \tilde{B}_p \left(\partial_{p^2}^k R_p \right)^{-1} \left((\partial_\chi R_p + \gamma R_p) \partial_{p^2}^k \dot{R}_p - \dot{R}_p \partial_{p^2}^k (\partial_\chi R_p + \gamma R_p) \right) \\ &\quad \left. - e \int_p \tilde{B}_p Q_p \dot{R}_p \left(\partial_\varphi^2 \mathcal{W}^{(V)} - p^2 \mathcal{W}^{(K)} \right) - e \int_{p,q} \tilde{B}_p Q_p \left(\partial_\varphi^2 Q_q - 2p^2 P_q \right) [\dot{R}, \partial_\chi R + \gamma R]_{qp} \right\}, \end{aligned} \quad (2.41)$$

where we have introduced the commutator-like construct $[A, B]_{qp} = A_q B_p - B_q A_p$.

When $A = V$ the above expression simplifies considerably to

$$\dot{\mathcal{W}}^{(V)} = - \int_p Q_p^2 \dot{R}_p \left(\partial_\varphi^2 \mathcal{W}^{(V)} - p^2 \mathcal{W}^{(K)} \right) - \int_{p,q} Q_p^2 \left(\partial_\varphi^2 Q_q - 2p^2 P_q \right) [\dot{R}, \partial_\chi R + \gamma R]_{qp}, \quad (2.42)$$

which we see contains only terms that contain either the Ward identities or the ‘commutator’ $[\dot{R}, \partial_\chi R + \gamma R]_{qp}$. On the other hand for the flow of the K/f msWI, the terms do not collect, so that it remains separately dependent on the individual \dot{R}_p . However each term either contains the Ward identities themselves, the ‘commutator’ $[\dot{R}, \partial_\chi R + \gamma R]_{qp}$, or the additional commutator-like structures:

$$(\partial_\chi R_p + \gamma R_p) \partial_{p^2}^k \dot{R}_p - \dot{R}_p \partial_{p^2}^k (\partial_\chi R_p + \gamma R_p). \quad (2.43)$$

These appear in the third line of (2.41), and the integer k takes values 1 and 2. For a general cutoff R_p , these two additional commutator terms neither vanish nor combine with other terms of the flow.

If $[\dot{R}, \partial_\chi R + \gamma R]_{qp}$ vanishes, the flow (2.42) of the V msWI is automatically satisfied providing that both the K and V msWI are also satisfied. In this case we have by rearrangement that

$$(\partial_\chi R_p + \gamma R_p) / \dot{R}_p = (\partial_\chi R_q + \gamma R_q) / \dot{R}_q, \quad (2.44)$$

which means that the ratio is independent of momentum. Equivalently

$$\partial_\chi R_p + \gamma R_p = F(\chi, t) \dot{R}_p, \quad (2.45)$$

where F can be a function of χ and t but not of p . However it is straightforward to see that (2.45) also forces the additional commutators (2.43) to vanish.

We have therefore shown that all the commutator-like terms vanish if and only if \dot{R}_p and $\partial_\chi R_p + \gamma R_p$ have the same dependence on p , with the consequence that both the $\dot{\mathcal{W}}^{(A)}$ vanish, if the Ward identities $\mathcal{W}^{(A)}$ themselves vanish. Since for general choices of the functions, the vanishing of the ‘commutators’ is surely necessary to achieve $\dot{\mathcal{W}}^{(A)} = 0$ without further restriction, we have thus shown that the condition (2.45) is necessary and sufficient to ensure compatibility, as defined at the beginning of this section.

2.2.4 Incompatibility implies no solutions

However even if the commutators do not vanish, and thus the Ward identities are incompatible with the flow equations, *a priori* there could still be a non-empty restricted set of solutions that both satisfy the flow equations and Ward identities. In this case the equations are satisfied not by the vanishing of the commutators themselves, but by the fact that for the given solutions the sum of all these terms vanish after performing the integration over momenta. Therefore, as well as obeying the flow equations and the msWIs $\mathcal{W}^{(A)} = 0$, the solutions must also separately obey two further conditions, namely the vanishing of the right hand sides of (2.41). In the language of Dirac’s classification of constraints [45, 46], the $\mathcal{W}^{(A)} = 0$ provide the primary constraints. We have shown that if the ‘commutators’ do not vanish, then the solutions are subject also to non-trivial secondary constraints $\dot{\mathcal{W}}^{(A)} = 0$. Given the involved form of $\dot{\mathcal{W}}^{(K)}$ in particular, we can be sure that the procedure does not close and that actually there is then an infinite tower of secondary constraints,

$\partial_t^n \mathcal{W}^{(A)} = 0$, $\forall n > 0$, all of which must be satisfied. It would therefore seem inevitable that there are in fact no non-trivial solutions in this case. We will confirm this by example in sec. 2.3.2. We conclude that *the vanishing of the ‘commutators’, and hence condition (2.45), is both necessary and sufficient for there to be any solutions to the flows and Ward identities in the derivative expansion approximation outlined in sec. 2.1.*

The condition (2.45) was already used in Ref. [35], where however it was introduced as a mathematical trick to help solve the coupled system of flow equations and msWI. As we recall below, it implies either that $\eta = 0$ or R_p is of power-law form. We now see that the requirement for \dot{R}_p and $\partial_\chi R_p + \gamma R_p$ to have the same dependence on p , goes much deeper: the flow equations (2.5) and (2.7), and the Ward identities (2.6) and (2.8), are incompatible without this constraint, and incompatibility forces there to be no solutions to the combined system.

2.2.5 Required form of the cutoff profile

Note that R_p must take a form that respects the scaling dimensions. Introducing dimensionless variables for use in the next section and later, we can make these scaling dimensions explicit by employing the RG scale k . We denote the new dimensionless quantities with a bar. We have

$$\begin{aligned} \varphi &= k^{\eta/2} \bar{\varphi}, & \chi &= k^{\eta/2} \bar{\chi}, & f(\chi) &= k^{d_f} \bar{f}(\chi), \\ V(\varphi, \chi) &= k^{d_V} \bar{V}(\bar{\varphi}, \bar{\chi}), & K(\varphi, \chi) &= k^{d_R - 2 + d_f} \bar{K}(\bar{\varphi}, \bar{\chi}), \end{aligned} \quad (2.46)$$

where

$$d_V = d(1 - d_f/2) \quad \text{and} \quad d_R = d_V - \eta, \quad (2.47)$$

and thus from (2.13) and (2.1), we have by dimensions that R_p must take the form

$$R(p^2/f) = -k^{d_R} r\left(\frac{p^2}{k^{2-d_f} f}\right) = -k^{d_R} r(\hat{p}^2), \quad (2.48)$$

where r is a dimensionless cutoff profile of a dimensionless argument,² and we have introduced the dimensionless momentum magnitude $\hat{p} = p\sqrt{k^{d_f-2}/f}$.

If \dot{R}_p and $\partial_\chi R_p + \gamma R_p$ have the same dependence on p , i.e. satisfy (2.45), then either $\eta = 0$ or R_p is of power-law form [35]. To see this, note that from (2.48) and (2.30) we have

$$\gamma \dot{R}_p = d_V [\partial_\chi R_p + \gamma R_p] - \eta \gamma R_p. \quad (2.49)$$

Thus (choosing $F = \gamma/d_V$) we see that (2.45) is satisfied if $\eta = 0$, without further restriction on R . However if $\eta \neq 0$, then (2.49) together with (2.45) implies

$$f \frac{\partial R_p}{\partial f} = \frac{d}{2} \left(\frac{\eta F}{d_V F - \gamma} - 1 \right) R_p, \quad (2.50)$$

and thus from (2.48)

$$\hat{p} \frac{d}{d\hat{p}} r(\hat{p}^2) = -d \left(\frac{\eta F}{d_V F - \gamma} - 1 \right) r(\hat{p}^2). \quad (2.51)$$

²The minus sign in (2.48) is necessary to work with the wrong sign kinetic term in (2.2) [35].

Since the term in brackets does not depend on p , we see that this is only possible if in fact the term in brackets is a constant. Setting this constant to be $2n/d$ for some constant n , we thus also deduce that $r \propto \hat{p}^{-2n}$.

An example of a cutoff that does not satisfy (2.45) if $\eta \neq 0$, and thus leads to incompatible msWIs in this case, is the optimised cutoff [15, 47]:

$$r(\hat{p}^2) = (1 - \hat{p}^2) \theta(1 - \hat{p}^2). \quad (2.52)$$

It is straight-forward to confirm that this does not satisfy (2.45) if $\eta \neq 0$. Using (2.48) and (2.49) we find

$$\dot{R}_p \propto d_V \left[\frac{2}{d} \theta(1 - \hat{p}^2) + (1 - \hat{p}^2) \theta(1 - \hat{p}^2) \right] - \eta (1 - \hat{p}^2) \theta(1 - \hat{p}^2). \quad (2.53)$$

In order for (2.52) to satisfy (2.45), the right hand side must be proportional to $\partial_\chi R_p + \gamma R_p$ *i.e.* to the term in square brackets. This is only true if $\eta = 0$.

2.3 LPA equations

We will now use the Local Potential Approximation to further investigate the restriction imposed by the msWI on the RG flow equation, in terms of general solutions and also on the existence of k -fixed points (*i.e.* RG fixed points with respect to variations in k). We start with a very clear example where the msWI forbids the existence of k -fixed points.

Then using the concrete example of the optimised cutoff we show explicitly that compatibility forces $\eta = 0$ for non-power-law cutoffs. Setting $\eta = 0$ we will see that background independent variables exist, in other words they exist whenever the msWI is compatible with the flow. We will also see that such \hat{k} -fixed points coincide with the k -fixed points. The background independent variables allow us to solve for the fixed points explicitly, uncovering a line of fixed points, consistent with the findings for power-law cutoff [48].

2.3.1 Demonstration of background independence forbidding fixed points in general

We use the change to dimensionless variables (2.46) and (2.48). In the LPA we discard the flow and Ward identity for K , and set $\bar{K} = 1$. The result, for general cutoff profile $r(\hat{p}^2)$, is:

$$\partial_t \bar{V} + d_V \bar{V} - \frac{\eta}{2} \bar{\varphi} \frac{\partial \bar{V}}{\partial \bar{\varphi}} - \frac{\eta}{2} \bar{\chi} \frac{\partial \bar{V}}{\partial \bar{\chi}} = \int_0^\infty d\hat{p} \hat{p}^{d-1} \frac{d_R r - \frac{d_V}{d} \hat{p} r'}{\hat{p}^2 + r - \partial_{\bar{\varphi}}^2 \bar{V}}, \quad (2.54)$$

$$\frac{\partial \bar{V}}{\partial \bar{\chi}} - \frac{\partial \bar{V}}{\partial \bar{\varphi}} + \bar{\gamma} \bar{V} = \bar{\gamma} \int_0^\infty d\hat{p} \hat{p}^{d-1} \frac{r - \frac{1}{d} \hat{p} r'}{\hat{p}^2 + r - \partial_{\bar{\varphi}}^2 \bar{V}}, \quad (2.55)$$

where r' means $dr/d\hat{p}$ and from the change to dimensionless variables we find:

$$\bar{\gamma} = \frac{d}{2} \frac{\partial}{\partial \bar{\chi}} \log \left[\bar{f} \left(e^{\eta t/2} \mu^{\eta/2} \bar{\chi} \right) \right]. \quad (2.56)$$

Note that since f cannot depend on t (see the discussion in sec. 2.1), once we go to dimensionless (*i.e.* scaled) variables, \bar{f} is in general forced to depend on t if χ has non-vanishing scaling dimension η . At the (k -)fixed point we must have $\partial_t \bar{V} = 0$. We see at once why fixed points are generically forbidden by the msWI: the fixed point potential \bar{V} would have to be independent of t , but through (2.55) and

(2.56) this is impossible in general since \bar{V} is forced to be dependent on explicit t -dependence in \bar{f} through the Ward identity. This is true even in the case of power-law cutoff profile³ which as we have seen allows (2.55) to be compatible with the flow (2.54).

At first sight an escape from this problem is simply to set f to be power-law. Indeed setting $f \propto \chi^\rho$ for some constant ρ , (2.56) implies

$$\bar{\gamma} = \frac{d}{2} \frac{\rho}{\bar{\chi}}, \quad (2.57)$$

and thus (2.55) no longer has explicit t dependence. Recall that for power-law cutoff profiles r , it was indeed found that k -fixed points for \bar{V} are allowed if f is chosen of power-law form [35].⁴ However we have seen in sec. 2.2.5 that any other cutoff profile does not allow the Ward identity to be compatible with the flow unless $\eta = 0$. We argued in sec. 2.2.4 that incompatibility overconstrains the equations leading to no solutions. In the next subsection, sec. 2.3.2, we will confirm this explicitly, choosing as a concrete example the optimised cutoff profile and space-time dimension $d = 4$.

On the other hand, if we set $\eta = 0$ then the msWI (2.55) is compatible with the flow (2.54), for any parametrisation f . Apparently k -fixed points are also now allowed without further restriction, since again (2.56) loses its explicit t dependence. Opting once more for optimised cutoff profile and $d = 4$, we will see in sec. 2.3.3 that indeed they are allowed and furthermore they coincide with fixed points in a background independent description that we also uncover.

2.3.2 Confirmation of no solutions if the msWI is incompatible with the flow

Specialising to optimised cutoff and (for simplicity) the most interesting case of spacetime dimension $d = 4$, the equations read

$$\partial_t \bar{V} + d_V \bar{V} - \frac{\eta}{2} \bar{\varphi} \partial_{\bar{\varphi}} \bar{V} - \frac{\eta}{2} \bar{\chi} \partial_{\bar{\chi}} \bar{V} = \left(\frac{d_R}{6} + \frac{\eta}{12} \right) \frac{1}{1 - \partial_{\bar{\varphi}}^2 \bar{V}}, \quad (2.58)$$

$$\partial_{\bar{\chi}} \bar{V} - \partial_{\bar{\varphi}} \bar{V} + \bar{\gamma} \bar{V} = \frac{\bar{\gamma}}{6} \frac{1}{1 - \partial_{\bar{\varphi}}^2 \bar{V}}. \quad (2.59)$$

Choosing power-law f and thus (2.57) there is no explicit t dependence and apparently these equations can work together. Combining them by eliminating their right hand sides, we get

$$2\partial_t \bar{V} + \eta \bar{V} - (\eta \bar{\varphi} - \alpha \bar{\chi}) \partial_{\bar{\varphi}} \bar{V} - (\eta + \alpha) \bar{\chi} \partial_{\bar{\chi}} \bar{V} = 0, \quad (2.60)$$

where we have introduced the constant $\alpha = (d_R + \eta/2)/\rho$. This equation can be solved by the method of characteristics (see *e.g.* the appendix in Ref. [35]). Parametrising the characteristic curves with t , they are generated by the following equations:

$$\frac{d\bar{V}}{dt} = -\frac{\eta}{2} \bar{V}, \quad \frac{d\bar{\chi}}{dt} = -\frac{\alpha + \eta}{2} \bar{\chi}, \quad \frac{d\bar{\varphi}}{dt} = \frac{\alpha \bar{\chi} - \eta \bar{\varphi}}{2}. \quad (2.61)$$

Solving the second equation before the third, it is straightforward to find the curves:

$$\bar{V} = \hat{V} e^{-\eta t/2}, \quad \bar{\chi} = \hat{\chi} e^{-(\eta + \alpha)t/2}, \quad \bar{\varphi} + \bar{\chi} = \hat{\varphi} e^{-\eta t/2}, \quad (2.62)$$

³And indeed this issue was highlighted, but in a different way in Ref. [35].

⁴This is true also for \bar{K} . However if the dimensions of f and χ do not match up, these fixed points do not agree with the background independent \hat{k} -fixed points and furthermore the effective action Γ_k still runs with k [35].

in terms of initial data $\hat{V}, \hat{\phi}, \hat{\chi}$. Thus the solution to (2.60) can be written as

$$\bar{V} = e^{-\eta t/2} \hat{V}(\hat{\phi}, \hat{\chi}) = e^{-\eta t/2} \hat{V} \left(e^{\eta t/2} [\bar{\varphi} + \bar{\chi}], e^{(\eta+\alpha)t/2} \bar{\chi} \right), \quad (2.63)$$

as can be verified directly. Plugging this into either (2.58) or (2.59) gives the same equation, which in terms of the hatted variables reads

$$\hat{\chi} \partial_{\hat{\chi}} \hat{V} + 2\rho \hat{V} = \frac{\rho}{3} \frac{1}{e^{-\frac{\eta}{2}t} - \partial_{\hat{\phi}}^2 \hat{V}}. \quad (2.64)$$

Since $\hat{V}(\hat{\phi}, \hat{\chi})$ is independent of t , we see there are no solutions unless $\eta = 0$. We saw in sec. 2.2.5 that this was also the necessary and sufficient condition for compatibility in this case.

2.3.3 Background independence at vanishing anomalous dimension

We now set $\eta = 0$. As recalled in sec. 2.2.5, the msWI is now compatible with the flow, and furthermore from (2.56) the explicit t dependence has dropped out. For power-law cutoff profiles we found that k -fixed points exist and coincide with background independent \hat{k} -fixed points for any form of f with any dimension d_f [35]. We will see that for non-power law cutoff that the same is true. (Again we choose optimised cutoff and $d = 4$ as an explicit example.) We will uncover consistent background independent variables for which the full line of fixed points is visible [48].

Since $\eta = 0$, in the equations (2.58) and (2.59), we also have $d_R = d_V = 2(2 - d_f)$ and $\bar{\gamma} = 2\partial_{\bar{\chi}} \log \bar{f}(\bar{\chi})$. Note that from (2.48), $d_f = 2$ is excluded otherwise the IR cutoff no longer depends on k . Also note that since $\eta = 0$ we can drop the bars on χ and φ . Combining the equations into a linear partial differential equation we get

$$\partial_t \bar{V} + \frac{2 - d_f}{\partial_{\chi} \log f} (\partial_{\varphi} \bar{V} - \partial_{\chi} \bar{V}) = 0, \quad (2.65)$$

whose characteristic curves satisfy

$$\frac{d\chi}{dt} = \frac{d_f - 2}{\partial_{\chi} \log f}, \quad \frac{d\varphi}{dt} = \frac{2 - d_f}{\partial_{\chi} \log f}, \quad \frac{d\bar{V}}{dt} = 0. \quad (2.66)$$

Solving the first equation gives:

$$\hat{t} = t + \frac{\log \bar{f}}{2 - d_f}, \quad (2.67)$$

where the integration constant \hat{t} is thus the background independent definition of RG time (see the appendix to Ref. [35]). Exponentiating,

$$\hat{k} = k [f(\chi)]^{\frac{1}{2-d_f}} = k^{\frac{2(1-d_f)}{2-d_f}} [f(\chi)]^{\frac{1}{2-d_f}}, \quad (2.68)$$

where the second equality follows from (2.46). The sum of the first two equations in (2.66) tells us that $\phi = \varphi + \chi$ is an integration constant for the characteristics, and finally the last equation says that \bar{V} is also constant for characteristics. Thus we learn that the change to background independent variables is achieved by writing

$$\bar{V} = \hat{V}(\phi, \hat{t}). \quad (2.69)$$

It is straightforward to verify that this solves (2.65). Substituting into either (2.58) or (2.59) gives the same flow equation:

$$\partial_t \hat{V} + d_V \hat{V} = \frac{d_V}{6} \frac{1}{1 - \partial_\phi^2 \hat{V}}, \quad (2.70)$$

which is indeed now background independent, *i.e.* independent of χ , and indeed independent of parametrisation f . There remains a dependence on the dimension of f through $d_V = 2(2 - d_f)$ although this disappears for \hat{k} -fixed points, and can be removed entirely by a rescaling $\hat{t} \mapsto \hat{t} d_V$ which however changes the dimension of \hat{k} to d_V .

We also see from (2.67) and (2.69) that

$$\partial_t \bar{V} = \partial_t \hat{V}, \quad (2.71)$$

and thus fixed points in k coincide with the background independent fixed points.

Finally, the fixed points are readily found from (2.70) similarly to Refs. [48, 49] by recognising that

$$\frac{d^2 \hat{V}}{d\phi^2} = 1 - \frac{1}{6\hat{V}} \quad (2.72)$$

is equivalent to Newton's equation for acceleration with respect to 'time' ϕ of a particle of unit mass at 'position' \hat{V} in a potential $U = -\hat{V} + (\log \hat{V})/6$. In this way it can be verified that there is a line of fixed points ending at the Gaussian fixed point, which is here $\hat{V} = 1/6$, in agreement with the findings for power-law cutoff in [48].

2.4 Polynomial truncations

The analysis so far has used properties of conformally truncated gravity and the derivative expansion approximation method. In order to gain insight about what might happen at the non-perturbative level, and in full quantum gravity, we will consider how the issues would become visible in polynomial truncations.

The generic case treated in sec. 2.3.1 will be just as clear in the sense that truncations of the Ward identity will still force the effective potential (effective action in general) to be t dependent if the dimensionless parametrisation (2.56) is similarly forced to be t dependent. In general therefore, if the way the metric is parametrised forces the parametrisation to become t dependent, we can expect that background independence excludes the possibility of fixed points, at least with respect to t .

Consider next the situation treated in sec. 2.3.2. Expanding the dimensionless potential and the equations in a double power series in the fluctuation and the background field, we write:

$$\bar{V}(\bar{\varphi}, \bar{\chi}) = \sum_{n, m=0}^{\infty} a_{nm} \bar{\varphi}^n \bar{\chi}^m. \quad (2.73)$$

Substituting expression (2.57) for $\bar{\gamma}$ into the msWI (2.59) and multiplying through by $\bar{\chi}$, we can read off from this and the flow (2.58) the zeroth level equations:

$$d_V a_{00} = \left(\frac{d_R}{6} + \frac{\eta}{12} \right) \frac{1}{1 - 2a_{20}}, \quad (2.74)$$

$$2\rho a_{00} = \frac{\rho}{3} \frac{1}{1 - 2a_{20}}. \quad (2.75)$$

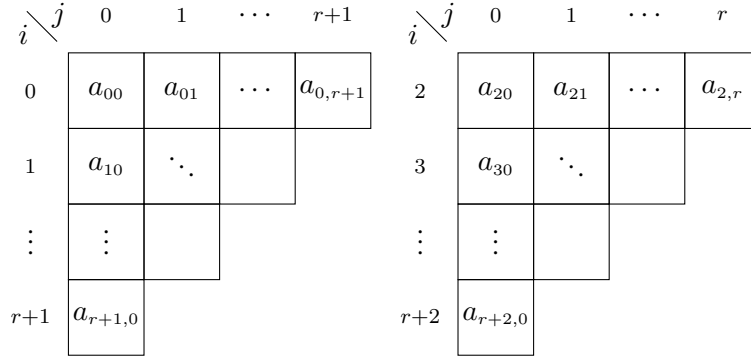


Figure 2.2: Coefficients of the potential appearing on the left sides of the equations (left diagram) and in the expansion of the propagator (right diagram).

Since ρ cannot vanish and a_{20} cannot diverge, combining these equations gives $d_V = d_R + \eta/2$ which from (2.47) implies $\eta = 0$. Thus we recover already from the zeroth order level that fixed points are excluded unless $\eta = 0$. (Of course the real reason, namely that the equations are incompatible, and the full consequence that there are no t -dependent solutions either, is maybe not so easy to see this way.)

2.4.1 Counting argument

We already argued in the introduction, that generically the coefficients become overconstrained if we consider a sufficiently high truncation. We now proceed to make a careful count and estimate the level at which this happens.

We concentrate on fixed point solutions to the LPA system (2.54), (2.55) and (2.56) where either $\eta = 0$ or we choose power-law f , so that explicit t dependence does not already rule out such solutions. We introduce the short-hand notation $\bar{V}^{(n,m)} = \partial_{\bar{\varphi}}^n \partial_{\bar{\chi}}^m \bar{V}(\bar{\varphi}, \bar{\chi})$. To obtain the system at order r we have to plug the expansion of the potential (2.73) into both the fixed point equation and msWI, act on them with operators $\frac{\partial^{i+j}}{\partial \bar{\varphi}^i \partial \bar{\chi}^j}$ such that $i + j = r$, before finally setting the fields to zero. In particular, for any fixed value r_* we have $2(r_* + 1)$ equations and hence up to order r there are

$$n_{\text{eqn}}(r) = \sum_{i=0}^r 2(i+1) = r^2 + 3r + 2 \quad (2.76)$$

equations. To count the coefficients appearing in these $n_{\text{eqn}}(r)$ equations let us start with the left hand sides. First note that

$$\bar{V}^{(i,j)} \Big|_{\bar{\varphi}=\bar{\chi}=0} \propto a_{ij}. \quad (2.77)$$

That is, for any fixed pair (i, j) the left hand side of (2.55) will contain the coefficients $a_{ij}, a_{i+1,j}$ and $a_{i,j+1}$, whereas the left hand side of (2.54) will only contain a_{ij} . Up to some fixed order r there will be thus coefficients a_{ij} where i and j run from 0 to $r+1$ and $i+j \leq r+1$

$$\left\{ a_{00}, a_{01}, \dots, a_{0,r+1}, a_{10}, \dots, a_{1,r}, \dots, a_{2,r-1}, \dots, a_{r+1,0} \right\}, \quad (2.78)$$

cf. Fig. 2.2. This adds up to the following number of coefficients

$$n_{\text{lhs}}(r) = \sum_{i=1}^{r+2} i = \frac{1}{2} r^2 + \frac{5}{2} r + 3. \quad (2.79)$$

Including the coefficients of the right hand side, we have to be careful not to double count any coefficients that have already been taken account of on the left hand sides. Let us suppose we have fixed the cutoff and let us assume that for the moment $\bar{\gamma} = \text{const}$. Then all additional coefficients on the right hand side come from the expansion of the propagator

$$\left. \frac{\partial^{i+j}}{\partial \bar{\varphi}^i \partial \bar{\chi}^j} \left(\frac{1}{1 - \bar{V}^{(2,0)}} \right) \right|_{\bar{\varphi}=\bar{\chi}=0} = \left. \frac{\partial^j}{\partial \bar{\chi}^j} \left[\frac{\partial^{i-1}}{\partial \bar{\varphi}^{i-1}} \left(\frac{\bar{V}^{(3,0)}}{(1 - \bar{V}^{(2,0)})^2} \right) \right] \right|_{\bar{\varphi}=\bar{\chi}=0}. \quad (2.80)$$

Since we can always arrange the $\bar{\varphi}$ -derivatives to act first, the expression in the square brackets will involve terms $\bar{V}^{(2,0)} \dots \bar{V}^{(i+2,0)}$. Using Eqn. (2.77), we see that the expression given in Eqn. (2.80) will then include the following terms

$$\left\{ a_{20}, a_{21}, \dots, a_{2i}, a_{30}, \dots, a_{3i}, \dots, a_{i+2,0}, \dots, a_{i+2,j} \right\}. \quad (2.81)$$

Up to any fixed order r , i and j can take values between 0 and r such that $i + j = r$, and in total we will have the following coefficients on the right hand sides

$$\left\{ a_{20}, \dots, a_{2,r}, a_{30}, \dots, a_{3,r-1}, \dots, a_{4,r-2}, \dots, a_{r+2,0} \right\}, \quad (2.82)$$

cf. again Fig. 2.2. Most of these coefficients have however already been accounted for on the left hand sides and the only ones not counted yet are

$$\left\{ a_{2,r}, a_{3,r-1}, a_{4,r-2}, \dots, a_{r+2,0} \right\}. \quad (2.83)$$

This is displayed graphically in Fig. 2.3. They precisely add up to a further $r + 1$ coefficients. We also must include another two coefficients, namely η and d_f . Finally, since γ is in general some function of χ it is easy to see that

$$\frac{d^r}{d\bar{\chi}^r} \bar{\gamma} \propto \frac{d^r}{d\bar{\chi}^r} \left(\frac{f'}{f} \right) \subseteq \left\{ f, f', \dots, f^{(r+1)} \right\}, \quad (2.84)$$

which gives us an additional $(r + 2)$ coefficients from the Taylor expansion of f . The total number of coefficients is then given by

$$n_{\text{coeff}}(r) = n_{\text{lhs}} + (r + 1) + (r + 2) + 2 = \frac{1}{2} r^2 + \frac{9}{2} r + 8. \quad (2.85)$$

From (2.76) we see that for large r the number of equations $\sim r^2$, while from (2.85) the number of coefficients only goes for large r as $\sim r^2/2$. There are therefore asymptotically twice as many equations as coefficients, as already discussed in the Introduction. Equating the number of equations and coefficients yields the positive solution

$$r = 5.3. \quad (2.86)$$

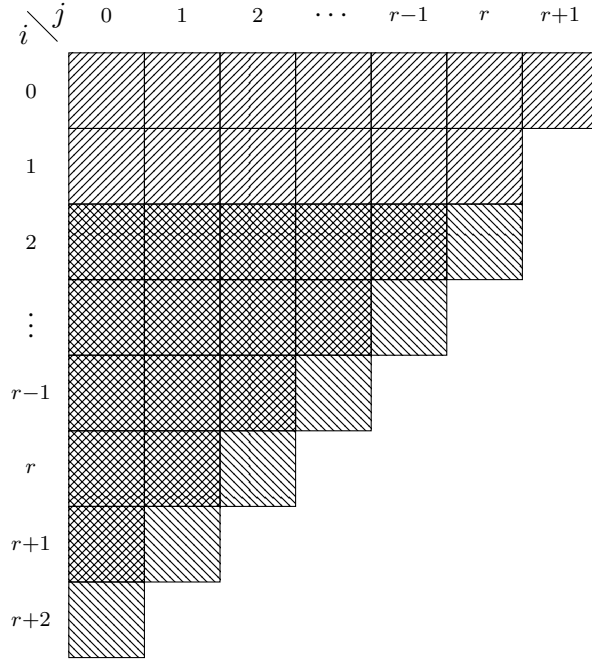


Figure 2.3: All the coefficients of the potential appearing on both sides of the equations.

Therefore the number of equations exceeds the number of coefficients for the first time at order $r = 6$. If there is to be a conflict between the existence of (k -)fixed points and background independence generically we would expect this to become evident at about this level. Equally, if there is no conflict between background independence and the existence of (k -)fixed points then from this level onwards some equations become redundant (*i.e.* they provide constraints that are automatically satisfied once the other equations are obeyed). In the limit $r \rightarrow \infty$ fully half of the equations must become redundant if (k -)fixed points are to be consistent with background independence.

For the convenience of the reader we summarise our findings of this chapter, together with those of Ref. [35], in table 2.1.⁵

2.5 Towards background independence in full quantum gravity

First attempts to go beyond conformally truncated gravity and study background independence in theories of the full metric field using similar ideas as the ones of this chapter have been made in Refs. [50, 51]. For alternative approaches also see Refs. [32–34, 52–55].

In the case of full quantum gravity split symmetry takes the much more general form

$$\bar{g}_{\mu\nu}(x) \mapsto \bar{g}_{\mu\nu}(x) + \varepsilon_{\mu\nu}(x), \quad h_{\mu\nu}(x) \mapsto h_{\mu\nu}(x) - \varepsilon_{\mu\nu}(x), \quad (2.87)$$

which is a $d(d+1)/2$ parameter set of space-time dependent transformations.

⁵For power-law cutoff $r(z) = z^{-n}$, $d_f = 2 - \eta/(n+2)$ is excluded [35], and from sec. 2.2.5 when $\eta = 0$, $d_f = 2$ is excluded for any cutoff profile: in these cases the cutoff term is independent of k .

anomalous dimension	parametrisation f			cutoff profile r	
	type	d_f	runs	power-law	not power-law
$\eta \neq 0$	not power-law	any	yes	FP , $\widehat{\text{FP}}$	incompatible
	power-law	$\neq \rho\eta/2$	yes	$\text{FP} \neq \widehat{\text{FP}}$	incompatible
	($f = \chi^\rho$)	$= \rho\eta/2$	no	$\text{FP} = \widehat{\text{FP}}$	incompatible
$\eta = 0$	any	$\neq 0$	yes		$\text{FP} = \widehat{\text{FP}}$
		$= 0$	no		

Table 2.1: RG properties of the derivative expansion for conformally truncated gravity with the msWI satisfied. $\widehat{\text{FP}}$ indicates that a background-independent description exists, while (~~FP~~) FP indicates that k -fixed points are (not) allowed; the (in)equality shows how these relate to the \hat{k} -fixed points.

In addition to the cutoff operator, in theories of the full metric field, there is another source of split symmetry breaking. Namely, since gravity is a gauge theory, when integrating over the fluctuation field in the path integral a gauge has to be fixed in order to remove spurious gauge configurations. This will generate a functional determinant in the path integral which can be rewritten via the Faddeev-Popov procedure through the introduction of a number of auxiliary fields, the so-called ghosts. Since gauge fixing should remove spurious gauge configurations the gauge condition has to be implied on the fluctuation field $h_{\mu\nu}$ using covariant derivatives of the background metric, in such a way, that one necessarily has to introduce an asymmetry between these two fields. This is then an additional (potential) source of split symmetry breaking.

In Ref. [50], this issue has been addressed for the first time using a linear split for background and fluctuation field, and restricting the set of split symmetry transformations to background scale transformations, also called background Weyl transformations⁶

$$\bar{g}_{\mu\nu}(x) \mapsto (1 + 2\varepsilon) \bar{g}_{\mu\nu}(x), \quad (2.88)$$

where ε is a space-time constant. Using a linear parametrisation of the metric, background and fluctuation field thus transform as

$$\delta_\varepsilon \bar{g}_{\mu\nu} = +2\varepsilon \bar{g}_{\mu\nu}, \quad (2.89)$$

$$\delta_\varepsilon h_{\mu\nu} = -2\varepsilon h_{\mu\nu}. \quad (2.90)$$

If we additionally use the York decomposition of the fluctuation field (cf. App. A) and further decompose the trace part as⁷

$$h(x) = \bar{h} + h^\perp(x) \quad (2.91)$$

⁶Here and in the following, we always adhere to the transformation conventions of Ref. [51]. The results of Ref. [50] may then be obtained via $\varepsilon \mapsto -\varepsilon$ (and setting $\varepsilon = 1$).

⁷In the following we assume the background to be a compact manifold (such that the volume is finite). Then \bar{h} is the zero mode of the background Laplacian $-\bar{\nabla}^2$.

where \bar{h} and $h^\perp(x)$ are orthogonal to each other, in such a way that $\langle \bar{h}, h^\perp \rangle \equiv \bar{h} \int d^d x h^\perp = 0$, one can derive the following transformation laws:

$$\delta_\varepsilon h^\perp = -2\varepsilon h^\perp, \quad (2.92)$$

$$\delta_\varepsilon \bar{h} = -2\varepsilon (\bar{h} + d), \quad (2.93)$$

$$\delta_\varepsilon h_{\mu\nu}^T = 0. \quad (2.94)$$

From this it is easy to see that the following field combinations are invariant under background rescaling:

$$h_{\mu\nu}^T, \bar{g}_{\mu\nu}, \left(1 + \frac{\bar{h}}{d}\right) \bar{g}_{\mu\nu}. \quad (2.95)$$

Having established the transformation laws of the background and the fluctuation fields, one next has to establish the transformation properties of the full quantum effective action, which will be derived from a partition function that now reads

$$e^{W_k} = \int \mathcal{D}\tilde{h}_{\mu\nu} e^{-S[g_{\mu\nu}] - \Delta S_k[\bar{g}_{\mu\nu}, \tilde{h}_{\mu\nu}] + S_{\text{gf}}[\bar{g}_{\mu\nu}, \tilde{h}_{\mu\nu}] + S_{\text{ghost}}[\bar{g}_{\mu\nu}, \tilde{h}_{\mu\nu}] + S_{\text{aux}}[\bar{g}_{\mu\nu}, \tilde{h}_{\mu\nu}] + S_{\text{src}}[\bar{g}_{\mu\nu}, \tilde{h}_{\mu\nu}]}. \quad (2.96)$$

It includes the classical gravitational action, the cutoff operator, the gauge fixing term, the resulting ghost action, the action of auxiliary fields, introduced through changes of variables, as well as the usual source terms. The strategy of Ref. [50] was to derive the flow equation as well as the (modified) Ward identity of background scaling, and again try to combine and solve those two equations to uncover a background (scale) independent description of the renormalisation group. Using the linear parametrisation of the fluctuation field, this was possible if and only if the space-time dimension takes the value $d = 6$.

The first term in the action we shall look at is the gauge fixing. In Ref. [50], a conventional gauge fixing was assumed

$$S_{\text{gf}} = \frac{1}{2\alpha} \int d^d x \sqrt{\bar{g}} \bar{g}^{\mu\nu} F_\mu F_\nu, \quad (2.97)$$

where the gauge fixing condition F_μ is linear in $h_{\mu\nu}$ and only contains terms with covariant derivatives

$$F_\mu = \bar{\nabla}_\rho h^\rho{}_\mu - \frac{\beta + 1}{d} \bar{\nabla}_\mu h = \bar{\nabla}_\rho h^{\rho\mu} - \frac{\beta}{d} \bar{\nabla}_\mu h. \quad (2.98)$$

One can then show that the gauge condition transforms homogeneously

$$\delta_\varepsilon F_\mu = 2\varepsilon F_\mu, \quad (2.99)$$

and at least in Landau-DeWitt gauge ($\alpha = 0, \beta = 1$), the gauge fixing is manifestly invariant under background rescaling:

$$\delta_\varepsilon S_{\text{gf}} = 0. \quad (2.100)$$

Furthermore, because of the particular form of the gauge fixing, the ghost action will always be bilinear in the fluctuation fields and only depend on the transformation properties of the background.

The same is true for the auxiliary action, since it arises from functional Jacobians of fluctuations around the background. Consequently, we can always arrange the transformations (or equivalently the mass dimensions) of the ghost and auxiliary fields to make their respective actions invariant under background rescaling

$$\delta_\varepsilon S_{\text{ghost}} = \delta_\varepsilon S_{\text{aux}} = 0. \quad (2.101)$$

The last part of the action to consider is the cutoff action

$$\Delta S_k = \sum_u \int d^d x \sqrt{\bar{g}} u R_u u, \quad (2.102)$$

where we sum over all fluctuation fields u and define the cutoff operators by

$$R_u = \Gamma_k^{(2u)}(P_k) - \Gamma_k^{(2u)}(\bar{\Delta}), \quad (2.103)$$

in such a way, that we effectively replace

$$\bar{\Delta} \mapsto P_k(\bar{\Delta}) \equiv \bar{\Delta} + k^2 r(\bar{\Delta}/k^2) \quad (2.104)$$

in the Hessian $\Gamma_k^{(2)}$. Here, $r(y)$ is a dimensionless cutoff profile, and $\bar{\Delta} = -\bar{\nabla}^2 + \bar{E}$ is a second order differential operator with endomorphism E . With this definitions and the transformation properties of the various fluctuation fields one can show that

$$\delta_\varepsilon(\Delta S_k) = 2d \int d^d x \sqrt{\bar{g}} R_h h - \frac{1}{2} \int d^d x \sqrt{\bar{g}} \sum_u u \dot{R}_u u - \frac{d-6}{2} \int d^d x \sqrt{\bar{g}} \sum_{u=h_{\mu\nu}^T, h} u R_u u. \quad (2.105)$$

The first two terms in this transformation will generate an anomaly in the modified Ward identity that is proportional to the renormalisation group flow, and it will be this contribution that enables one to combine the Ward identity and the flow equation. The third term however, is an additional anomaly that only vanishes in $d = 6$. Moreover, one can show, that using the background field method⁸ $d = 6$ is a necessary and sufficient condition for compatibility of the Ward identity and the flow equation. In the compatible case, one can combine the two equations as

$$\delta_\varepsilon \Gamma_k = \sum_u \frac{\delta \Gamma_k}{\delta u} \delta_\varepsilon u = \varepsilon \dot{\Gamma}_k, \quad (2.106)$$

and we see that the only anomaly of background scale symmetry is given by the beta function of the effective average action itself. It is then possible, by means of the method of characteristics, to obtain solutions to the last equation of the form

$$\Gamma_k[\bar{g}_{\mu\nu}](\bar{h}) = \hat{\Gamma}_{\hat{k}}[\hat{g}_{\mu\nu}], \quad (2.107)$$

⁸In this approximation scheme, also called single-metric approximation, one replaces derivatives w.r.t. the fluctuation field with derivatives w.r.t. background field and then sets the former to zero. This scheme was and is very popular to do actual calculations and we will use it in the next chapter.

such that the (dynamical) dependence of the fluctuation field \bar{h} gets incorporated into new variables

$$\hat{k} = \frac{k}{\sqrt{1 + \bar{h}/d}}, \quad \text{and} \quad \hat{g}_{\mu\nu} = \sqrt{1 + \frac{\bar{h}}{d}} \bar{g}_{\mu\nu}, \quad (2.108)$$

and the new action $\hat{\Gamma}$ obeys a formally equivalent flow equation as the old single-metric approximated action. That is, solutions to the flow equations in the latter approximation scheme respect background scale invariance, albeit the interpretation of the renormalisation group procedure completely changed under the light of this investigation.

The rather unsatisfactory condition of $d = 6$ has subsequently been weakened in Ref. [51]. There it was shown that using the exponential parametrisation of the metric fluctuation field (*cf.* App. A) all terms proportional to $(d - 6)$ in the transformation laws of the cutoff action disappear. In addition, it was necessary to guarantee that no dimensionful parameters enter neither the gauge fixing term nor the cutoff operator (the latter is known as a ‘pure’ cutoff, *cf.* Sec. 3.6). The former could then be made invariant by itself, as in the case of the linear parametrisation, by using a higher derivative gauge fixing action

$$S_{\text{gf}} = \frac{1}{2\alpha} \int d^d x \sqrt{\bar{g}} \bar{g}^{\mu\nu} F_\mu \bar{\Delta}^{\frac{d}{2}-1} F_\nu, \quad (2.109)$$

with the gauge condition given above (for any values of the parameters α and β), or using the unimodular gauge (*cf.* again App. A).

3. Non-minimally Scalar-Tensor Theory

After investigating issues of more technical nature which arose due to the use of the background field method in non-perturbative RG flows of quantum gravity, we are now ready to begin our study of the inclusion of matter fields in an asymptotic safe gravitational quantum field theory. In this first chapter, we will investigate a scalar-tensor theory with N_S scalar fields which are non-minimally coupled to the gravitational sector. We will thereby treat the metric field in a background approximation, where we set the fluctuation field to zero, and use a derivative expansion up to terms linear in the background Ricci scalar \bar{R} . We will then fix the background to be a d -dimensional sphere \mathbb{S}^d and derive the flow equation using heat kernel techniques. We can then look for scaling solutions of our particular truncation and study their critical behaviour.

In the following chapters 4 and 5 we will study a similar setup, but in a truly dynamic treatment, using a fluctuation field calculation. This will however force us to restrict ourselves to a minimally-coupled theory on a flat background \mathbb{R}^4 . In chapter 5 we will additionally use the msWIs in combination with the flow equations to investigate further the rôle of the cutoff operator in the dynamics of the background.

In Ref. [56] fixed-functional solutions in a scalar-tensor theory with an action containing a potential $V(\varphi)$ and a generic non-minimal interaction $-F(\varphi)\bar{R}$ for a single scalar field were already discussed. It was found that in generic dimension d the flow equations for the dimensionless functions $\bar{V}(\bar{\varphi}) = k^{-d}V(\varphi)$ and $\bar{F}(\bar{\varphi}) = k^{2-d}F(\varphi)$ of the dimensionless field $\bar{\varphi} = k^{1-d/2}\varphi$ admit some simple exact solutions where $\bar{V} = \bar{V}_0$ is constant and $\bar{F} = \bar{F}_0 + \bar{F}_2\bar{\varphi}^2$ is a quadratic polynomial. These solutions can have interesting applications to cosmology in $d = 4$, [57]. Unfortunately it seems that one of these solutions, with \bar{F}_0 and \bar{F}_2 both non-zero, does not survive, at least with the same mathematical structure, when one applies the ‘renormalisation group improvement’, in which one keeps renormalisation time-derivatives of the dimensionful variables on the right hand side of the flow equation. Another solution, which remains unchanged under this improvement, has $\bar{F}_0 = 0$ but $\bar{F}_2 < 0$, making its physical relevance questionable.

In this chapter we will consider the case of N_S scalar fields with an $O(N_S)$ -invariant action of the general form

$$\Gamma_k[g_{\mu\nu}, \varphi^i] = \int d^d x \sqrt{g} \left[-F(\varphi) R + \frac{1}{2} \sum_{i=1}^{N_S} (\nabla \varphi^i)^2 + V(\varphi) \right], \quad (3.1)$$

where V and F are functions of the radial degree¹ scalar field $\varphi = \sqrt{\sum_i \varphi^i \varphi^i}$. The remaining $N_S - 1$ angular degrees of freedom will be referred to as the Goldstone bosons. One of the main results of this chapter will be to show that in the case $N_S > 1$ there exists a previously unobserved solution with $\bar{F}_0 = 0$ and $\bar{F}_2 > 0$.

The other main result will be the confirmation of the existence of an upper bound on the number of scalar fields, if a fixed point with positive \bar{F} is to be observed. Such bounds have been discussed earlier in Ref. [7], but only for minimally coupled fields. We will see that the existence of a potential and non-minimal interactions do not change this picture substantially.

For $d = 3$, we will also discuss the existence of a non-trivial gravitationally dressed Wilson-Fisher fixed point and give a specific solution for $N_S = 2$. Finally we will employ an alternative coarse-graining scheme in order to test the scheme-dependence of the analytical scaling solutions.

3.1 Flow equations

For the construction of the flow equations we follow the same steps as in Ref. [56], which we will briefly recall. The calculation is based on the background field method, but instead of the usual linear classical-background-plus-quantum-fluctuation split we use an exponential parametrisation for the metric of the form $g_{\mu\nu} = \bar{g}_{\mu\rho}(e^h)^\rho{}_\nu$. This has some concrete practical advantages that will be mentioned later, but the original theoretical motivation is that it respects the non-linear nature of the metric. The fluctuation field is further York decomposed into its irreducible spin-two, spin-one and spin-zero components $h_{\mu\nu}^{\text{TT}}$, ξ_μ , σ and h . Then one calculates the second variation of the action with respect to the fields, which appears as a central ingredient in the flow equation. In order to have a diagonal Hessian we define new scalar fields that involve a mixture of σ and ϕ . We then choose a very simple “unimodular physical gauge” which amounts simply to suppressing the fields ξ_μ and h . We describe the steps involved in the York decomposition, the gauge fixing and the resulting Faddeev–Popov ghost sector in app. A. Further details concerning the derivation of the Hessian and the flow equations may be found in app. B. We will use a type-I cutoff, which is introduced by replacing all occurrences of $-\bar{\nabla}^2$ with $-\bar{\nabla}^2 + R_k(-\bar{\nabla}^2)$, [17]. In particular, we will use the optimised cutoff $R_k(z) = (k^2 - z) \theta(k^2 - z)$, [16]. Note that this cutoff is “spectrally adjusted”, in the sense that it depends on some running couplings, and also depends explicitly on the background scalar field, in addition to the background metric. Later we shall consider other types of cutoffs as well.

On a sphere \mathbb{S}^d in general dimension d and for any number of scalars N_S , we find the following

¹Later on, it will sometimes prove more convenient to treat V and F as functions of the variable $\rho = \varphi^2/2$ instead.

flow equations in dimensionless variables

$$\begin{aligned}
\dot{\bar{V}} = & -d\bar{V} + \frac{1}{2}(d-2)\bar{\varphi}\bar{V}' + c_d \frac{(d-1)(d^2-d-3)}{d+2} + c_d \frac{(d-2)(d+1)[2\dot{\bar{F}} - (d-2)\bar{\varphi}\bar{F}']}{4(d+2)\bar{F}} \\
& + c_d \frac{2(d^2-4)\bar{F} + (d-2)(1+\bar{V}'') [2\dot{\bar{F}} - 6\bar{F} - (d-2)\bar{\varphi}\bar{F}']}{2(d+2)[2(d-1)(\bar{F}')^2 + (d-2)\bar{F}(1+\bar{V}'')]} \\
& + c_d \frac{4(d-1)\bar{F}' [2\dot{\bar{F}}' + (d-1)\bar{F}' - (d-2)\bar{\varphi}\bar{F}''']}{2(d+2)[2(d-1)\bar{F}'^2 + (d-2)\bar{F}(1+\bar{V}'')]} + c_d \frac{(N_s-1)\bar{\varphi}}{\bar{\varphi} + \bar{V}'}, \tag{3.2}
\end{aligned}$$

$$\begin{aligned}
\dot{\bar{F}} = & (2-d)\bar{F} + \frac{1}{2}(d-2)\bar{\varphi}\bar{F}' - c_d \frac{d^6 - 2d^5 - 15d^4 - 46d^3 + 38d^2 + 96d - 24}{12(d+2)(d-1)d} \\
& - c_d \frac{(d^5 - 17d^3 - 60d^2 + 4d + 48) [2\dot{\bar{F}} - (d-2)\bar{\varphi}\bar{F}']}{48(d-1)d(d+2)\bar{F}} \\
& - c_d \frac{(d-2)\bar{F}\bar{F}'' + 2\bar{F}'^2}{(d+2)\bar{F} [2(d-1)(\bar{F}')^2 + (d-2)\bar{F}(\bar{V}'' + 1)]^2} \times \left\{ (d-2)(d+2)\bar{F}^2 \right. \\
& \left. + (d-1)\bar{F}'^2 [(d-2)\bar{\varphi}\bar{F}' - 2\dot{\bar{F}}] + 2(d-1)\bar{F}\bar{F}' [(2-d)\bar{\varphi}\bar{F}'' + (d+2)\bar{F}' + 2\dot{\bar{F}}'] \right\} \\
& + c_d \frac{1}{24 [2(d-1)(\bar{F}')^2 + (d-2)\bar{F}(\bar{V}'' + 1)]} \times \left\{ \bar{F}' [(d-2)\bar{\varphi}(4(d-1)\bar{F}'' \right. \\
& \left. + (d-2)(\bar{V}'' + 1)) - 8(d-1)\dot{\bar{F}}'] + 2(d-2) [d\bar{F}\bar{V}'' - \dot{\bar{F}}(\bar{V}'' + 1)] \right\} \\
& - c_d \frac{d(N_s-1)\bar{\varphi}}{12(\bar{\varphi} + \bar{V}')} - c_d \frac{(N_s-1)\bar{\varphi}\bar{F}'(\bar{\varphi})}{\bar{\varphi} + \bar{V}'^2}, \tag{3.3}
\end{aligned}$$

where we recall that the d -dimensional volume coefficient c_d was given by

$$c_d = \frac{1}{(4\pi)^{d/2} \Gamma(d/2 + 1)}.$$

The only difference between the case $N_s = 1$ discussed in Ref. [56] and the case of general N_s , is the additional contribution of the Goldstone modes, which can easily be identified by the factor $N_s - 1$. The ‘RG-unimproved’ or ‘one-loop’ flow equations, where one sets the RG-time derivatives to zero on the right hand sides, can be recovered by carrying out the replacement

$$\dot{\bar{F}} \mapsto -(d-2)\bar{F} + \frac{d-2}{2}\bar{\varphi}\bar{F}', \quad \dot{\bar{F}}' \mapsto -\frac{d-2}{2}\bar{F}' + \frac{d-2}{2}\bar{\varphi}\bar{F}''.$$

3.2 Scaling solutions

In this section we list some simple analytic solutions which exist in any and every dimension d . Assuming an ansatz where both \bar{V} and \bar{F} are constant reveals a fixed point *FP1*. Using the simple, unimproved equations, it has the following coordinates:

$$\bar{V}_\star = c_d \left[\frac{(d-1)(d-2)}{2d} + \frac{N_s - 1}{d} \right], \quad (3.4)$$

$$\bar{F}_\star = -c_d \frac{d^5 - 4d^4 - 7d^3 - 50d^2 + 60d + 24}{24d(d-1)(d-2)} - c_d \frac{(N_s - 1)d}{12(d-2)}. \quad (3.5)$$

We note that the first fraction in \bar{F}_\star is positive for $d < 6.17$. Thus for $N_s = 1$ this is an upper bound on the dimension dictated by positivity of Newton's constant. Having additional scalars lowers this bound. The bound becomes lower than four between $N_s = 11$ and $N_s = 12$. Thus, the fixed point has negative Newton's constant when there are more than 11 scalar fields, a result that is in rough agreement with previous calculations [7], where a similar cutoff has been used.

If we include the RG improvement the coordinates of *FP1* change to:

$$\bar{V}_\star = c_d \left[\frac{(d^2 - 1)(d - 2)}{d(d + 2)} + \frac{N_s - 1}{d} \right], \quad (3.6)$$

$$\bar{F}_\star = -c_d \frac{d^6 - 2d^5 - 15d^4 - 46d^3 + 38d^2 + 96d - 24}{12d(d-1)(d^2-4)} - c_d \frac{(N_s - 1)d}{12(d-2)}. \quad (3.7)$$

Now, for $N_s = 1$ positivity of Newton's constant requires $d < 5.73$, and the bound becomes lower than four between $N_s = 14$ and $N_s = 15$. Thus, the fixed point has negative Newton's constant when there are more than 14 scalar fields.

If we make an ansatz where \bar{V} is constant and \bar{F} is of the form $\bar{F}_0 + \bar{F}_2 \bar{\varphi}^2$, there is a solution *FP2* for the unimproved fixed point equations which reads

$$\bar{V}_\star = c_d \left[\frac{(d-1)(d-2)}{2d} + \frac{N_s - 1}{d} \right], \quad (3.8)$$

$$\bar{F}_\star(\bar{\varphi}) = c_d \left[\frac{d^5 - 4d^4 - 7d^3 - 50d^2 + 84d + 24}{24d(d-1)(d-2)} - \frac{(N_s - 1)(d^2 - d + 12)}{12(d-1)(d-2)} \right] + \frac{\bar{\varphi}^2}{2(d-1)}. \quad (3.9)$$

We observe that while \bar{F}_2 is always positive, \bar{F}_0 becomes negative when either d or N_s become too large. For example for fixed $N_s = 2$ this happens at $d \approx 5.8$ and for fixed $d = 4$ this happens for $N_s \approx 5.6$. The solution is probably unphysical in these cases.

The same ansatz does not yield a solution for the improved equations. We suspect that there may be a solution with very similar properties but different functional form. The search of such generalization is beyond the scope of this chapter however.

If we make the ansatz that \bar{V} is constant and \bar{F} is proportional to $\bar{\varphi}^2$ (i.e. that $\bar{F}_0 = 0$), the fixed point equation is quadratic and admits two real solutions *FP3* and *FP4*. They are the same for the improved and unimproved flow equations. The expressions for arbitrary d are quite long, so we will only give here the formulae for $d = 3$

$$\bar{V}_\star = \frac{N_s}{18\pi^2}, \quad \bar{F}_\star = -\frac{9N - 80 \pm \sqrt{9N_s^2 - 264N_s + 5296}}{96(N_s - 1)} \bar{\varphi}^2, \quad (3.10)$$

and $d = 4$

$$\bar{V}_\star = \frac{2 + N_s}{128\pi^2}, \quad \bar{F}_\star = -\frac{6N - 41 \pm \sqrt{4N_s^2 - 100N_s + 1321}}{48(N_s - 1)} \bar{\varphi}^2, \quad (3.11)$$

where the upper sign corresponds to *FP3* and the lower sign corresponds to *FP4*. We note that *FP3* has a finite $N_s \rightarrow 1$ limit, while in the case of *FP4* there is a divergence. In fact, in the case of $N_s = 1$ the fixed point *FP3* had already been seen in Ref. [56], but *FP4* does not exist in that case. Imposing that $\bar{F} > 0$ we find that *FP3* is always unphysical while *FP4* is acceptable for $0 < N_s < 15.33$ in $d = 3$ and $1 < N_s < 11.25$ in $d = 4$.

3.3 Large N_s limit

All solutions described in the previous section have the property that the function \bar{F}_\star becomes negative if the number of scalar fields exceeds a certain limit. In order to confirm that this behaviour indeed persists for larger N_s as well, we will now consider the large- N_s limit of the flow. Here, it is convenient to use the variable $\bar{\rho} = \bar{\varphi}^2/2$ as the argument of the functions \bar{V} and \bar{F} instead of $\bar{\varphi}$. It is easy to see that in the large- N_s limit \bar{V} , \bar{F} as well as $\bar{\rho}$ scale linearly in N_s . In this limit the flow equations—in terms of already rescaled quantities—simply read

$$\dot{\bar{V}} = -d\bar{V} + (d-2)\bar{\rho}\bar{V}' + \frac{c_d}{1 + \bar{V}'}, \quad (3.12)$$

$$\dot{\bar{F}} = -(d-2)\bar{F} + \left[(d-2)\bar{\rho} - \frac{c_d}{(1 + \bar{V}')^2} \right] \bar{F}' - \frac{d}{12} \frac{c_d}{1 + \bar{V}'}. \quad (3.13)$$

The fixed point equation for the scalar potential \bar{V} is the same as in flat spacetime. It has two analytically known solutions, *cf.* Ref. [58], one of which is constant and one of which is not. In the case of a constant potential the combined fixed point equations have the following solution:

$$\bar{V}_\star = \frac{c_d}{d}, \quad (3.14)$$

$$\bar{F}_\star(\bar{\rho}) = -\left(\frac{d}{12(d-2)} c_d + 2a \right) + 2a \frac{d-2}{c_d} \bar{\rho}, \quad (3.15)$$

where a is an arbitrary constant of integration. For $d > 2$, any point on this line of solutions may be considered unphysical, since either the linear or the constant term in \bar{F} will become negative.

In order to deal with the second, non-trivial solution for \bar{V} , the equation is best rewritten in its implicit form

$$\bar{\rho} = \frac{d c_d}{4} {}_2F_1\left(2, 1 - \frac{d}{2}; 2 - \frac{d}{2}; -w(\bar{\rho})\right), \quad (3.16)$$

where d is now an odd integer and $w(\bar{\rho}) = \bar{V}'(\bar{\rho})$. The Gaussian or ordinary hypergeometric function is thereby defined as:

$${}_2F_1(a, b; c; z) = \sum_{n=0}^{\infty} \frac{(a)_n (b)_n}{(c)_n} \frac{z^n}{n!}. \quad (3.17)$$

The scalar sector therefore admits a Wilson-Fisher type global scaling solution as long as $2 < d < 4$. The fixed point equation for \bar{F} can also be simplified by rewriting it in terms of w

$$0 = -(d-2)g + 2wg' - \frac{d}{12} \frac{c_d}{1+w}, \quad (3.18)$$

where we defined a new function $g(w(\bar{\rho})) = \bar{F}(\bar{\rho})$. This equation can be solved analytically and its solution is implicitly given by

$$\bar{F}(\bar{\rho}) = -\frac{dc_d}{12(d-2)} {}_2F_1\left(1, 1 - \frac{d}{2}; 2 - \frac{d}{2}; -w(\bar{\rho})\right), \quad (3.19)$$

which is always negative for $d > 2$. For $2 < d < 4$, such a fixed point therefore appears to lead to a negative gravitational interactions in the large N_s limit. We also note that in the asymptotic region one has

$$\lim_{\bar{\rho} \rightarrow \infty} \bar{F}(\bar{\rho}) = -\frac{2}{3d(d-2)} \bar{\rho}. \quad (3.20)$$

3.4 Stability analysis

In this section we discuss the linearisation of the flow in $d = 4$ around the fixed point *FP1*, for which we will write $\bar{V} = \bar{V}_* + \delta\bar{V}$ and $\bar{F} = \bar{F}_* + \delta\bar{F}$. We begin with the simpler RG-unimproved case, which yields the following linearised equations:

$$0 = -(\lambda + 4)\delta\bar{V} + \left[\bar{\varphi} - \frac{N_s - 1}{32\pi^2 \bar{\varphi}}\right] \delta\bar{V}' - \frac{1}{32\pi^2} \delta\bar{V}'' , \quad (3.21)$$

$$0 = -(\lambda + 2)\delta\bar{F} + \left[\bar{\varphi} - \frac{N_s - 1}{32\pi^2 \bar{\varphi}}\right] \delta\bar{F}' + \frac{N_s - 1}{96\pi^2 \bar{\varphi}} \delta\bar{V}' + \frac{1}{96\pi^2} \delta\bar{V}'' - \frac{1}{32\pi^2} \delta\bar{F}' . \quad (3.22)$$

In this case the critical exponents are equal to their classical values:

$$\begin{aligned} \theta_1 &= 4, & w_1^t &= (\delta\bar{V}, \delta\bar{F})_1 = (1, 0), \\ \theta_3 &= 2, & w_3^t &= (\delta\bar{V}, \delta\bar{F})_3 = (0, 1), \\ \theta_5 &= 0, & w_5^t &= (\delta\bar{V}, \delta\bar{F})_5 = \left(0, -\frac{N_s}{32\pi^2} + \bar{\varphi}^2\right). \end{aligned} \quad (3.23)$$

The solution *FP1* for the full fixed point equations in $d = 4$ has coordinates

$$\bar{V}_* = \frac{N_s + 4}{128\pi^2}, \quad \bar{F}_* = \frac{169 - 12N_s}{2304\pi^2}. \quad (3.24)$$

Linearising the full flow equations around this solution we get the eigenvalue equations for the eigenperturbations:

$$0 = -(\lambda + 4)\delta\bar{V} + \frac{72\lambda}{169 - 12N_s} \delta\bar{F} + \left[\bar{\varphi} - \frac{N_s - 1}{32\pi^2 \bar{\varphi}}\right] \delta\bar{V}' + \frac{72\bar{\varphi}}{12N_s - 169} \delta\bar{F}' - \frac{1}{32\pi^2} \delta\bar{V}'' , \quad (3.25)$$

$$\begin{aligned} 0 = & \left[\frac{3\lambda(45 - 4N_s)}{12N_s - 169} - 2\right] \delta\bar{F} + \left[\frac{3(4N_s - 45)\bar{\varphi}}{12N_s - 169} - \frac{N_s - 1}{32\pi^2 \bar{\varphi}}\right] \delta\bar{F}' - \frac{1}{32\pi^2} \delta\bar{F}'' \\ & + \frac{N_s - 1}{96\pi^2 \bar{\varphi}} \delta\bar{V}' + \frac{1}{96\pi^2} \delta\bar{V}'' . \end{aligned} \quad (3.26)$$

We can study the spectrum of the leading eigenvalues analytically. We find four relevant and one marginal direction for $N_s < \frac{45}{4}$, while for $\frac{45}{4} < N_s < \frac{169}{12}$ there are only two relevant and one marginal directions, since θ_2 and θ_4 become negative. In particular

$$\begin{aligned}
\theta_1 &= 4, & (\overline{\delta V}, \overline{\delta F})_1 &= (1, 0), \\
\theta_2 &= 2 + \frac{68}{3(45 - 4N_s)}, & (\overline{\delta V}, \overline{\delta F})_2 &= \left(\frac{72}{12N_s - 101}, 1 \right), \\
\theta_3 &= 2, & (\overline{\delta V}, \overline{\delta F})_3 &= \left(-\frac{29N_s}{544\pi^2} + \overline{\varphi}^2, \frac{N_s(169 - 12N_s)}{3264\pi^2} \right), \\
\theta_4 &= \frac{68}{3(45 - 4N_s)}, & (\overline{\delta V}, \overline{\delta F})_4 &= \left(-\frac{3N_s(48N_s(3N_s - 76) + 22475)}{16\pi^2(4N_s - 45)(6N_s - 59)(12N_s - 101)} \right. \\
& & & \left. + \frac{72}{12N_s - 101} \overline{\varphi}^2, -\frac{N_s(12N_s - 169)(12N_s - 125)}{96\pi^2(4N_s - 45)(12N_s - 101)} + \overline{\varphi}^2 \right), \\
\theta_5 &= 0, & (\overline{\delta V}, \overline{\delta F})_5 &= \left(\frac{29N_s(N_s + 2)}{17408\pi^4} - \frac{29(N_s + 2)}{272\pi^2} \overline{\varphi}^2 + \overline{\varphi}^4, \right. \\
& & & \left. \frac{N_s(N_s + 2)(12N_s - 227)}{224\pi^4} - \frac{(N_s + 2)(12N_s - 169)}{1632\pi^2} \overline{\varphi}^2 \right).
\end{aligned} \tag{3.27}$$

We note that the eigenvalues come in groups within which they are shifted by two. This behaviour had already been observed and explained in Ref. [59].

3.5 Gravitationally dressed Wilson-Fisher fixed point

In Ref. [56], scaling solutions in $d = 3$ with a potential \overline{V} resembling that of the Wilson-Fisher fixed point were searched for. There, the unimproved equations were used and a solution for sufficiently small $\overline{\varphi}$ whose potential is almost indistinguishable from the Wilson-Fisher potential was found. For this solution the function \overline{F} starts out positive at $\overline{\varphi} = 0$, but has negative second derivative such that it crosses zero at some critical value $\overline{\varphi} \approx 0.92$. It was therefore not possible to establish the global existence of that solution. More importantly still, the Hessian becomes ill-defined at the critical point, so that the equations themselves become unreliable. A little later, using more powerful numerical techniques, a global solution was found for the improved RG equation in Ref. [60]. The fixed point potential for this solution is again very similar to the Wilson-Fisher potential, but the function \overline{F} now has positive second derivative and is positive everywhere, avoiding the issues mentioned above. With hindsight, this solution can also be found with simpler techniques, such as the ones used in Ref. [56], *e.g.* Taylor expansion and the shooting method. Near the origin it has the expansion

$$\lim_{\overline{\varphi} \rightarrow 0} \overline{V}_*(\overline{\varphi}) = 0.009355 - 0.029266 \overline{\varphi}^2 + 0.003591 \overline{\varphi}^4 + 1.14530 \overline{\varphi}^6 + \dots, \tag{3.28}$$

$$\lim_{\overline{\varphi} \rightarrow 0} \overline{F}_*(\overline{\varphi}) = 0.068604 + 0.172245 \overline{\varphi}^2 - 0.132631 \overline{\varphi}^4 + 0.39032 \overline{\varphi}^6 + \dots. \tag{3.29}$$

We have looked for generalizations of this solution for $N_s > 1$. Treating N_s as a continuous variable, candidate scaling solutions can be found with the shooting method. We show, as an example, in Fig. 3.1 the cases $N_s = 1$ and $N_s = 2$. A spiralling structure appears close to the fixed point which is characterized by a very sharp relative peak.

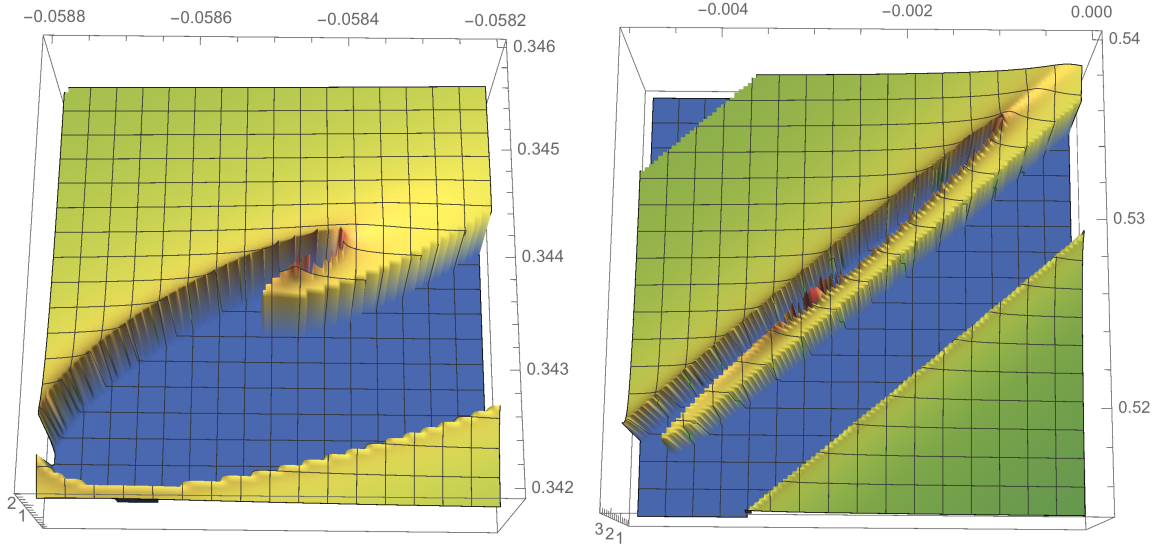


Figure 3.1: The maximal value of the field reached in the numerical evolution before encountering a singularity, as a function of the initial conditions $\bar{V}''(\bar{\varphi} = 0)$ and $\bar{F}''(\bar{\varphi} = 0)$, for the case $d = 3$ and $N_s = 1$ (left panel) and $N_s = 2$ (right panel). A clear spike can be seen in the centre of each figure.

For $N_s = 2$ the solution can be approximated near the origin by

$$\lim_{\bar{\varphi} \rightarrow 0} \bar{V}_*(\bar{\varphi}) = 0.014669 - 0.001482 \bar{\varphi}^2 - 0.438516 \bar{\varphi}^4 + 4.35302 \bar{\varphi}^6 + \dots, \quad (3.30)$$

$$\lim_{\bar{\varphi} \rightarrow 0} \bar{F}_*(\bar{\varphi}) = 0.053294 + 0.263370 \bar{\varphi}^2 - 0.570919 \bar{\varphi}^4 + 1.43572 \bar{\varphi}^6 + \dots \quad (3.31)$$

The shape of the potential \bar{V} shows that this scaling solution characterises a broken phase. The asymptotic behaviour of the solution for large $\bar{\varphi}$ is

$$\lim_{\bar{\varphi} \rightarrow \infty} \bar{V}_*(\bar{\varphi}) = A\bar{\varphi}^6 + \frac{23}{1440\pi^4 B\bar{\varphi}^2} + \frac{240\pi^4 B^2(16B + 5N_s - 4) - 1357A}{216000\pi^6 AB^2\bar{\varphi}^4} + \dots, \quad (3.32)$$

$$\lim_{\bar{\varphi} \rightarrow \infty} \bar{F}_*(\bar{\varphi}) = B\bar{\varphi}^2 + \frac{23}{36\pi^2} + \frac{1219}{25920\pi^4 B\bar{\varphi}^2} - \frac{71921A + 2160\pi^4 B^2(16B + 5N_s - 4)}{4665600\pi^6 AB^2\bar{\varphi}^4} + \dots \quad (3.33)$$

For the case $N_s = 2$, we were able to establish a very good match between the numerical solution obtained via shooting methods about the origin and the asymptotic behaviour given above (setting $A \simeq 5.149$ and $B \simeq 0.273$) about $\bar{\varphi} \simeq 0.65$. We consider this a good candidate for a global scaling solution of the gravitationally dressed $O(2)$ scalar model.

3.6 Scalar-free cutoff

So far we have only considered type-I cutoffs which in the gravitational sector has the general form $F(\chi^i)R_k(-\bar{\nabla}^2)$, where again we denote the background scalar fields with χ^i . The presence of the prefactor F is useful because the effect of adding the cutoff results simply in the replacement of $-\bar{\nabla}^2$ with $P_k(\bar{\nabla}^2) = -\bar{\nabla}^2 + R_k(-\bar{\nabla}^2)$ in the Hessians. However, this advantage comes at a

price: through F the cutoff will depend on running couplings and there is now an explicit breaking of the scalar split symmetries $\chi^i \mapsto \chi^i - \epsilon^i$, $\bar{\varphi}^i \mapsto \bar{\varphi}^i + \epsilon^i$, $i = 1, \dots, N_s$, which we discussed in the last chapter. As shown in Ref. [28], even in pure scalar theory the presence of the scalar background field in the cutoff action can lead to unphysical results. This argument casts doubts on the use of these cutoffs, and it is therefore important to study cutoffs without such a prefactor F , as well. In the Einstein-Hilbert truncation, where $F = 1/16\pi G_N$, such cutoffs were called “pure”, [61]. Here we shall call them “scalar-free”. It is important to keep in mind that any such cutoff will still depend on the background metric, as we discussed in the last chapter. Here we only get rid of the χ^i -dependences due to the (matter) scalar fields and have the scalar msWIs automatically fulfilled. In particular we shall add in the diagonal entries for $h_{\mu\nu}^{\text{TT}}$ and σ'' of the Hessian given in Eqn. (B.17) a cutoff $\bar{\gamma} k^{d-2} (k^2 - z) \theta(k^2 - z)$, with the same sign of the Laplacian term, to implement the coarse-graining procedure. For all the other terms we shall use the more common $(k^2 - z) \theta(k^2 - z)$.

We will not report the form of the flow equations in arbitrary dimensions—which contain hypergeometric functions—but rather focus on the case $d = 4$ here only:

$$\begin{aligned} \dot{\bar{V}} = & -4\bar{V} + \bar{\varphi} \bar{V}' - \frac{1}{8\pi^2} - \frac{\bar{F} \left[\bar{F}(\bar{V}'' + 1) \log \left(\frac{3\bar{F}'^2}{\bar{F}(\bar{V}'' + 1)} + 1 \right) - 3\bar{F}'^2 \right]}{144\pi^2 \bar{F}'^4} \\ & + \frac{3\bar{\gamma} \left[-\bar{\gamma}^2 + 4\bar{\gamma}\bar{F} - 2\bar{\gamma}(\bar{\gamma} - 2\bar{F}) \log \left(\frac{\bar{F}}{\bar{\gamma}} \right) - 3\bar{F}^2 \right]}{16\pi^2 (\bar{\gamma} - \bar{F})^3} + \frac{(N_s - 1)\bar{\varphi}}{32\pi^2 (\bar{V}' + \bar{\varphi})}, \end{aligned} \quad (3.34)$$

$$\begin{aligned} \dot{\bar{F}} = & -2\bar{F} + \bar{\varphi} \bar{F}' + \frac{19}{384\pi^2} + \frac{\bar{F} \left[\frac{6\bar{F}'^2 (\bar{F}\bar{F}'' + \bar{F}'^2)}{3\bar{F}'^2 + \bar{F}(\bar{V}'' + 1)} - (2\bar{F}\bar{F}'' + 3\bar{F}'^2) \log \left(\frac{3\bar{F}'^2}{\bar{F}(\bar{V}'' + 1)} + 1 \right) \right]}{288\pi^2 \bar{F}'^4} \\ & + \frac{10\bar{\gamma}(\bar{\gamma} - 2\bar{F})(\bar{\gamma} - \bar{F}) - 5\bar{\gamma}(\bar{\gamma}^2 - 3\bar{\gamma}\bar{F} + 4\bar{F}^2) \log \left(\frac{\bar{F}}{\bar{\gamma}} \right)}{96\pi^2 (\bar{\gamma} - \bar{F})^3} \\ & + \frac{\bar{\gamma} \left[-\bar{\gamma} + (\bar{\gamma} - 2\bar{F}) \log \left(\frac{\bar{F}}{\bar{\gamma}} \right) + \bar{F} \right]}{96\pi^2 (\bar{\gamma} - \bar{F})^2} - \frac{(N_s - 1)\bar{\varphi} (3\bar{F}' + \bar{V}'(\bar{\varphi}) + \bar{\varphi})}{96\pi^2 (\bar{V}' + \bar{\varphi})^2}. \end{aligned} \quad (3.35)$$

Unlike (3.2) and (3.3), these equations are transcendental and cannot be solved analytically. For comparison, we will discuss scaling solution $FP1$ only which was defined via $\bar{V}(\bar{\varphi}) = \bar{V}_0$ and $\bar{F}(\bar{\varphi}) = \bar{F}_0$. With this ansatz, the fixed point condition reduces to a set of algebraic equations which can be solved numerically. The linearisation of the flow equation around $FP1$ yields the

following equations:

$$0 = -(\lambda + 4) \delta \bar{V} - \left[\frac{3\bar{\gamma} (3\bar{F}_0^2 + 5\bar{\gamma}\bar{F}_0 - 2\bar{\gamma}^2)}{16\pi^2 \bar{F}_0 (\bar{F}_0 - \bar{\gamma})^3} + \frac{3\bar{\gamma}^2 (\bar{\gamma} - 4\bar{F}_0)}{8\pi^2 (\bar{F}_0 - \bar{\gamma})^4} \log \left(\frac{\bar{F}_0}{\bar{\gamma}} \right) \right] \delta \bar{F} \\ + \left(\bar{\varphi} - \frac{N_s - 1}{32\pi^2 \bar{\varphi}} \right) \delta \bar{V}' - \frac{1}{32\pi^2} \delta \bar{V}'' \quad (3.36)$$

$$0 = -(\lambda + 2) \delta \bar{F} + \left[\frac{\bar{\gamma} (37\bar{F}_0^2 - 11\bar{\gamma}\bar{F}_0 + 4\bar{\gamma}^2)}{96\pi^2 \bar{F}_0 (\bar{F}_0 - \bar{\gamma})^3} - \frac{\bar{\gamma}\bar{F}_0 (2\bar{\gamma} + 3\bar{F}_0)}{16\pi^2 (\bar{F}_0 - \bar{\gamma})^4} \log \left(\frac{\bar{F}_0}{\bar{\gamma}} \right) \right] \delta \bar{F} \\ + \left(\bar{\varphi} - \frac{N_s - 1}{32\pi^2 \bar{\varphi}} \right) \delta \bar{F}' + \frac{N_s - 1}{96\pi^2 \bar{\varphi}} \delta \bar{V}' + \frac{1}{96\pi^2} \delta \bar{V}'' - \frac{1}{32\pi^2} \delta \bar{F}'' \quad (3.37)$$

For $N_s = 1$ and $\bar{\gamma} = 1$ we have $\bar{V}_{0\star} = 0.03314$ and $\bar{F}_{0\star} = 0.01552$. The relevant eigenperturbations around this solution may be found numerically and the corresponding eigenvalues are given by $-4, -2.272, -2, -0.272, 0$. Therefore, there are four relevant and one marginal coupling. For $\bar{\gamma} = 0.006$ we have $\bar{V}_{0\star} = 0.00353$ and $\bar{F}_{0\star} = 0.00670$, which are very close to the values found with the other cutoff in Ref. [56]. The relevant eigenperturbations around this solution have eigenvalues $-4, -2.542, -2, -0.542, 0$, which are also closer to the other cutoff.

For $N_s = 4$ and $\bar{\gamma} = 1$ the fixed point values are given by $\bar{V}_{0\star} = 0.03635$ and $\bar{F}_{0\star} = 0.01413$. The perturbative analysis around the fixed point gives the following eigenvalues: $-4, -2.299, -2, -0.299, 0$. If instead we were to choose $\bar{\gamma} = 0.006$, we had $\bar{V}_{0\star} = 0.00669$ and $\bar{F}_{0\star} = 0.00549$, and the eigenvalues were $-4, -2.682, -2, -0.682, 0$.

Using the scalar-free cutoff scheme, it is interesting to study solutions to the fixed point equations for FP_1 in the large- N_s limit as well. It is easy to see that in this limit they assume the following values:

$$\bar{V}_{0\star} \approx \frac{16N_s - 205}{512\pi^2}, \quad \bar{F}_{0\star} \approx \bar{\gamma} \exp \frac{55 - 4N_s}{16}. \quad (3.38)$$

We see that this behaviour is very different from the one obtained previously: in particular $\bar{F}_{0\star}$ becomes exponentially small but never changes sign. Thus there is apparently no upper bound in N_s from the requirement of having a positive $\bar{F}_{0\star}$. This behaviour is induced by the interplay between the logarithmic singularity in $\bar{F}_{0\star}$ and the linear dependence in N_s in the equations. This result is probably not physically correct for the following reason: in the functional renormalisation group one should use the Hessian defined as the second derivative of the effective average action with respect to the quantum field. Instead in order to close the flow equation, we are using the second derivative of the effective average action with respect to the background field. Even though the function F does not appear in the cutoff, it does appear in the denominator, where the coefficient of $-\bar{\nabla}^2$ is $(\bar{F} - \bar{\gamma})k^{d-2}$. This term is absent with the type-I cutoff and it is its presence with the scalar-free cutoff that gives rise to the logarithmic terms in the flow equation. In a proper bi-metric calculation the coefficient of $-\bar{\nabla}^2$ in the denominator of the functional renormalisation group equation would be $Z_h - \bar{\gamma}k^{d-2}$, where Z_h is the graviton wave-function renormalisation. The argument of the logarithmic term would then be $Z_h/\bar{\gamma}$ and the beta function of \bar{F} would probably be regular for $\bar{F} = 0$.

4. Dynamics of Gravity-Matter Vertices

The effective average action of a gravitational quantum field theory at a finite energy scale k depends on both the background as well as the fluctuation field metric, *i.e.* $\Gamma_k = \Gamma_k[\bar{g}_{\mu\nu}, h_{\mu\nu}]$, as we have already seen in Ch. 2. This dependence is such that one cannot recombine $\bar{g}_{\mu\nu}$ and $h_{\mu\nu}$ to give the full metric field, and modified split Ward identities have to be imposed additionally to recover split symmetry. This symmetry breaking is due to two sources: the gauge fixing term, which gauge-fixes the fluctuations with respect to the background, as well as the cutoff term, as we have seen already in the case of conformally reduced gravity in Ch. 2.

As a consequence, couplings of background field operators do not share the same beta function as the couplings of the fluctuation field operators. For instance, one could define a Newton coupling from the prefactor of the Einstein-Hilbert term in the effective action, from the momentum-squared part of the graviton three-point function or from a graviton-matter vertex. All of these three definitions of the Newton coupling obey a different renormalisation group running. Modified Ward-identities govern the background-field dependence of the results, and have to be imposed on the RG flow, but using them in practical calculations is still work in its infancy. We will have a glimpse on how to potentially subtract the background dependence due to the cutoff term by using these Ward identities in the next chapter.

In the literature on asymptotically safe gravity, many results are obtained within a single-metric approximation, where the difference between background couplings and fluctuation couplings is ignored. There, one finds an interacting fixed point with a finite number of relevant couplings, *i.e.* free parameters, *cf.* Refs. [6, 17, 62–86].

First explorations of the bi-metric structure in asymptotically safe quantum gravity have indicated that the evidence for asymptotic safety from the single-metric approximation is still present when resolving this approximation, *cf.* Refs. [32–34, 53–55, 87, 88]. One should note that at this stage only a few couplings have been considered in a bi-metric setting, and higher-order truncations could yield different results. As discussed in Ref. [28] using the example of a scalar

field, a single-metric approximation can result in spurious fixed points, and a treatment of the full bi-metric structure is crucial. Within gravity-matter systems, a first step in this direction has been done in Refs. [7, 89], where the anomalous dimension of the graviton and matter fields was evaluated in addition to the beta functions of the gravitational background couplings. In Refs. [55, 88], renormalisation group flows formulated in terms of fluctuation field gravitational couplings have been investigated and lend quantitative support to the results for the pure-gravity case in the single-metric approximation. The system has been extended to include the effect of matter fluctuations on pure-gravity-couplings in Ref. [90].

In this chapter, we will make a step towards disentangling the running of the fluctuation field and background field couplings, focusing on the matter-gravity sector. In the context of asymptotic safety, this implies that a viable fixed point for the running of the effective average action must not only exist for the gravitational interactions, but also for matter-gravity interactions and the matter self-interactions. As the standard model by itself is most likely not asymptotically safe, the effect of gravity would have to induce a combined fixed point, as conjectured in Ref. [91], *cf.* for instance Refs. [92–97] for evidence in this direction.

As a step towards showing that this could indeed be the case, we investigate the flow of a gravity-scalar-vertex, with one external spin-2 gravitational mode and two matter scalar fields, and show that it admits an interacting ultraviolet fixed point. We emphasize that the flow of this coupling is independent from the flow of the usual Newton coupling, defined with respect to gravitational vertices only. Our result therefore constitutes non-trivial evidence for the potential viability of asymptotic safety for a joint description of gravity and matter in our universe.

4.1 Matter-gravity flow setup

In this section we will summaries our setup to study the non-perturbative renormalisation group flow of the 1-graviton-2-scalar coupling.

4.1.1 Truncation

Our truncation consist of the usual Einstein-Hilbert term for the gravitational sector minimally coupled to N_S massless scalar fields in the matter sector. To set it up, we start from an auxiliary action $\hat{\Gamma}_k$ given in terms of the full metric $g_{\mu\nu}$, which reads

$$\hat{\Gamma}_k[\bar{g}_{\mu\nu}, h_{\mu\nu}, \varphi] = \int d^4x \sqrt{\bar{g}} \left[-\frac{R}{16\pi G_N} + \frac{1}{2} \sum_{i=1}^{N_S} (\nabla\varphi^i)^2 \right]. \quad (4.1)$$

Note, that this is the same effective average action for $d = 4$ as in the previous chapter with $F = 1/16\pi G_N$ and $V = 0$. We drop a possible volume term in our calculation, as its fluctuations do not enter the RG flow in our choice of gauge.

As before, we will use the exponential parametrisation of the metric field, employ a York decomposition for the fluctuation field and use the unimodular physical gauge. We will specialise our calculation to a flat background \mathbb{R}^4 in four dimensions. Details of all the involved steps may be found in app. A. Since fluctuations of ξ_μ and h are gauged to zero, we are left with contributions of $h_{\mu\nu}^{\text{TT}}$ and σ to the running couplings.

To calculate the flow, we define a truncation in the following way: Starting from the action $\hat{\Gamma}_k$ we expand in powers of $h_{\mu\nu}$ up to fourth order, and then redefine $h_{\mu\nu} \mapsto \sqrt{32\pi G_N} h_{\mu\nu}$. In the non-perturbative renormalisation group setting, the running of the couplings of operators at

different orders in $h_{\mu\nu}$ may very well differ. This is why we introduce several different “avatars” of the Newton coupling which we denote by G_3, G_4, g_3, g_4 and g_5 , and define our truncation to be

$$\Gamma_k^{\text{rhs}} = \sqrt{\frac{G_3}{G_N}} \hat{\Gamma}_k^{(3,0)} + \frac{G_4}{G_N} \hat{\Gamma}_k^{(4,0)} + \sqrt{\frac{g_3}{G_N}} \hat{\Gamma}_k^{(1,2)} + \frac{g_4}{G_N} \hat{\Gamma}_k^{(2,2)} + \left(\frac{g_5}{G_N}\right)^{3/2} \hat{\Gamma}_k^{(3,2)} + \text{quadratic terms} . \quad (4.2)$$

Here $\hat{\Gamma}_k^{(n,m)}$ stands for the terms of n -th order in the fluctuation field $h_{\mu\nu}$ and m -th order in the scalar field. Note that the action that contains the scalar fields is quadratic, so we only have terms with $m = 0, 2$. Our redefinition of all separate prefactors of the different vertices allows us to explicitly distinguish these avatars of the Newton coupling, instead of approximating them all by G_N . One should not expect a universal definition of the Newton coupling to exist in the non-perturbative quantum gravity regime, similarly to what has been found in the perturbative regime in Ref. [98]. As replicas of Newton’s coupling, G_3, G_4, g_3, g_4 and g_5 all have dimensionality $2 - d$. This justifies the different powers with which they appear in the various terms in our truncation.

In detail, the different terms on a flat background, where we have $\bar{g}_{\mu\nu} = \delta_{\mu\nu}$, are given by:

$$\hat{\Gamma}_k^{(3,0)} = -\frac{2\sqrt{32\pi G_N}}{3!} \int d^4x \left[\frac{3}{2} h_{\mu\nu} (\partial_\mu h_{\kappa\lambda}) \partial_\nu h_{\kappa\lambda} - 3 h_{\kappa\lambda} (\partial_\lambda h_{\mu\nu}) \partial_\mu h_{\nu\kappa} \right], \quad (4.3)$$

$$\begin{aligned} \hat{\Gamma}_k^{(4,0)} = & -\frac{64\pi G_N}{4!} \int d^4x \left[3 h_{\mu\nu} h_{\kappa\lambda} (\partial_\mu h_{\kappa\rho}) \partial_\lambda h_{\rho\nu} - 2 h_{\mu\nu} h_{\kappa\lambda} (\partial_\lambda h_{\nu\rho}) \partial_\rho h_{\mu\kappa} \right. \\ & - 3 h_{\mu\nu} h_{\nu\kappa} (\partial_\kappa h_{\rho\sigma}) \partial_\mu h_{\rho\sigma} + 4 h_{\mu\nu} h_{\nu\kappa} (\partial_\mu h_{\rho\sigma}) \partial_\sigma h_{\rho\kappa} + h_{\nu\kappa} h_{\kappa\rho} (\partial_\sigma h_{\mu\nu}) \partial_\mu h_{\rho\sigma} \\ & \left. + h_{\mu\nu} h_{\kappa\lambda} (\partial_\rho h_{\mu\kappa}) \partial_\rho h_{\nu\lambda} - h_{\mu\nu} h_{\nu\kappa} (\partial_\rho h_{\mu\sigma}) \partial_\rho h_{\kappa\sigma} \right], \quad (4.4) \end{aligned}$$

$$\hat{\Gamma}_k^{(1,2)} = -\frac{\sqrt{32\pi G_N}}{2} \int d^4x h^{\mu\nu} \sum_{i=1}^{N_S} \partial_\mu \varphi^i \partial_\nu \varphi^i, \quad (4.5)$$

$$\hat{\Gamma}_k^{(2,2)} = \frac{32\pi G_N}{2} \int d^4x h^{\mu\rho} h_\rho^\nu \sum_{i=1}^{N_S} \partial_\mu \varphi^i \partial_\nu \varphi^i, \quad (4.6)$$

$$\hat{\Gamma}_k^{(3,2)} = -\frac{(32\pi G_N)^{3/2}}{2} \int d^4x h^{\mu\rho} h_\rho^\lambda h_\lambda^\nu \sum_{i=1}^{N_S} \partial_\mu \varphi^i \partial_\nu \varphi^i, \quad (4.7)$$

where appropriate symmetrizations are understood implicitly, as $h_{\mu\nu} = h_{\nu\mu}$. Here, we have already imposed the gauge $h = \text{const}$, and thus the trace of the fluctuation field can be dropped from the vertices. This simplifies the vertices considerably. More details of the derivations of these vertices in the exponential parametrisation may be found in app. C.

In a slight abuse of notation, we will not distinguish between dimensionful and dimensionless couplings in this chapter, as all our beta functions will always be expressed in terms of the dimensionless couplings only, whereas all couplings in Eqns. (4.3)–(4.7) are still dimensionful.

By the superscript rhs in (4.2) we indicate that this action is used to define the vertices and propagators that enter the functional renormalisation group equation. In other words, these are the fluctuation-field structures that *induce* the renormalization group flow. In this paper we will

not calculate the running of all these couplings, but only the beta function of g_3 , and the wave-function renormalisations Z_Ψ , where $\Psi = \{\text{TT}, \sigma, \text{S}\}$. The wave-function renormalisations Z_Ψ nevertheless couple into the beta-functions of the essential couplings in a non-trivial way via the anomalous dimensions

$$\eta_\Psi = -\partial_t \log Z_\Psi. \quad (4.8)$$

The running of G_3 has been calculated in Ref. [90] using a linear parametrisation of the metric and a more conventional gauge. We find that the simpler structure of the gravity-matter vertex avoids some of the issues that are encountered with multi-graviton vertices, and in any case it is of interest to compare the results of different procedures.

The coupled nature of the functional renormalisation group equation clearly prevents us from defining a closed truncation, in which we can extract the flow of all couplings that we have included on the right-hand side; thus approximations are necessary in which some couplings contribute to the running of others, but their running is not calculated. The remaining couplings in (4.2) can accordingly be treated in various ways. Since they enter in the flow equation for g_3 , it is better to avoid a truncation where they are set to zero. Instead, they can be set equal to g_3 , or treated as free parameters. We will discuss different possible approximations with respect to these higher-order couplings below. It is important to realize that if we were to restrict our truncation to g_3 , and set all other couplings to zero, all but diagrams 4 and 5 in Fig. 4.2 would vanish. On the other hand, the original action is diffeomorphism invariant, and accordingly a 1-graviton-2-scalar-vertex is necessarily accompanied by a 2-graviton-2-scalar vertex etc.

To close the system of couplings, we clearly have to choose an approximation, and we will mostly opt for the choice $g_3 = g_4 = g_5$ in the following (which is dictated by dimensionality). To check how useful this approximation is, we will keep track of all couplings separately; however, we will not evaluate the flows of higher-order couplings.

Note an interesting difference of β_{g_3} to the running of the background Newton coupling: As there is no closed scalar loop contributing to β_{g_3} , its only dependence on N_s arises through the anomalous dimension η_{TT} .

4.1.2 Projection rules

We use the transverse traceless mode $h_{\mu\nu}^{\text{TT}}$ to define the matter-gravity coupling g_3 . Then the running of g_3 can be extracted unambiguously on a flat background. To do this, we employ a projection rule as follows:

$$\partial_t \sqrt{g_3} = \frac{8}{3} \frac{1}{\sqrt{32\pi}} \left(p_{1\mu} p_{2\nu} \frac{\delta}{\delta h_{\mu\nu}^{\text{TT}}(p_3)} \frac{\delta}{\delta \varphi(p_1)} \frac{\delta}{\delta \varphi(p_2)} \partial_t \hat{\Gamma}_k \right) \Big|_{(p^2)^2}, \quad (4.9)$$

where we use the symmetric configuration for the three momenta, such that an angle of $2\pi/3$ lies between them, and their absolute value is $|p_1| = |p_2| = |p_3| = p$. Note that the functional derivative with respect to the TT mode generates the projector

$$\mathcal{P}_{\mu\nu\kappa\lambda}^{\text{TT}} = \frac{1}{2} (T_{\mu\kappa} T_{\nu\lambda} + T_{\mu\lambda} T_{\nu\kappa}) - \frac{1}{d-1} T_{\mu\nu} T_{\kappa\lambda}, \quad (4.10)$$

where $T_{\mu\nu} = \delta_{\mu\nu} - p_\mu p_\nu / p^2$. As we are using the transverse traceless component of the graviton for the projection, there is no mixing with non-minimal couplings that arise from the diffeomorphism-invariant operator $\varphi^2 R$, since the first variation of R does not have a transverse traceless component

on a flat background. Furthermore, working with a transverse traceless external graviton mode also excludes an admixture of non-diffeomorphism invariant operators at the same order of momenta, which might be generated by the flow and which depend on the momenta of the graviton.

Any given vertex contains a large number of different tensor structures, and these are not necessarily all featuring the same running coupling. In particular, transverse traceless structures and scalar structures could be expected to exhibit prominent differences in their running. As a first step into this direction, we distinguish the wave-function renormalization for the TT mode and the σ mode, Z_{TT} and Z_σ . On the other hand, we do not distinguish the couplings in the same fashion.

To extract the flow of the wave-function renormalisations, we define projection rules as follows:

$$\partial_t Z_S = \frac{\partial}{\partial p^2} \frac{\delta}{\delta \varphi(-p)} \frac{\delta}{\delta \varphi(p)} \partial_t \hat{\Gamma}_k, \quad (4.11)$$

$$\partial_t Z_{\text{TT}} = \frac{\partial}{\partial p^2} \frac{\mathcal{P}_{\mu\nu\kappa\lambda}^{\text{TT}}(p)}{5} \frac{\delta^2}{\delta h_{\mu\nu}^{\text{TT}}(p) \delta h_{\kappa\lambda}^{\text{TT}}(-p)} \partial_t \hat{\Gamma}_k, \quad (4.12)$$

$$\partial_t Z_\sigma = -\frac{8}{3} \frac{\partial}{\partial p^2} \frac{\delta}{\delta \sigma(-p)} \frac{\delta}{\delta \sigma(p)} \partial_t \hat{\Gamma}_k, \quad (4.13)$$

where the right-hand sides are evaluated at $p = 0$, and at vanishing external fields $h_{\mu\nu}^{\text{TT}}$, σ and φ .

4.2 Results for beta functions and anomalous dimensions

For our explicit results, we will employ a regulator shape function of the form

$$R_{\Psi k}(p^2) = Z_{\Psi k}(p^2 - k^2) \theta(k^2 - p^2),$$

with the appropriate wave-function renormalization for all modes, *cf.* Ref. [16].

4.2.1 Anomalous dimensions

To extract the running of the anomalous dimensions, we had to evaluate 18 diagrams, 7 for each of the gravitational modes and 4 for the matter scalar. We display the types of diagrams arising for the TT mode and for φ on the next page in Fig. 4.1. Actually, each diagram displayed there is the sum of n different terms, where each summand is the same diagram, except that it carries an additional regulator, inserted in exactly one of the n propagators. We also present the analytic results for each of these diagrams on the same page in Tab. 4.1.

Summing all contributions given in the table, we obtain the following results:

$$\eta_{\text{TT}} = \frac{N_S g_3}{24\pi} - \frac{G_3}{1728\pi} (2928 - 455\eta_{\text{TT}} + 35\eta_\sigma) + \frac{29 G_4}{648\pi} (18 - 5\eta_{\text{TT}} + 2\eta_\sigma), \quad (4.14)$$

$$\eta_\sigma = \frac{N_S g_3}{48\pi} (8 - 3\eta_S) + \frac{G_3}{108\pi} (24 - 25\eta_{\text{TT}} - 5\eta_\sigma) + \frac{11 G_4}{648\pi} (18 - 5\eta_{\text{TT}} + 2\eta_\sigma), \quad (4.15)$$

$$\eta_S = \frac{g_3}{16\pi} (16 - \eta_\sigma - \eta_S) + \frac{g_4}{24\pi} (18 - 5\eta_{\text{TT}} + 2\eta_\sigma). \quad (4.16)$$

Note that the sign of the matter contribution agrees for η_{TT} and η_σ and is the opposite one from that in the linear parametrisation and de Donder gauge, *cf.* Ref. [7]. Since the exponential parametrisation and the linear parametrisation can be understood as underlying two distinct definitions of the configuration space for asymptotically safe quantum gravity, such a difference could possibly persist

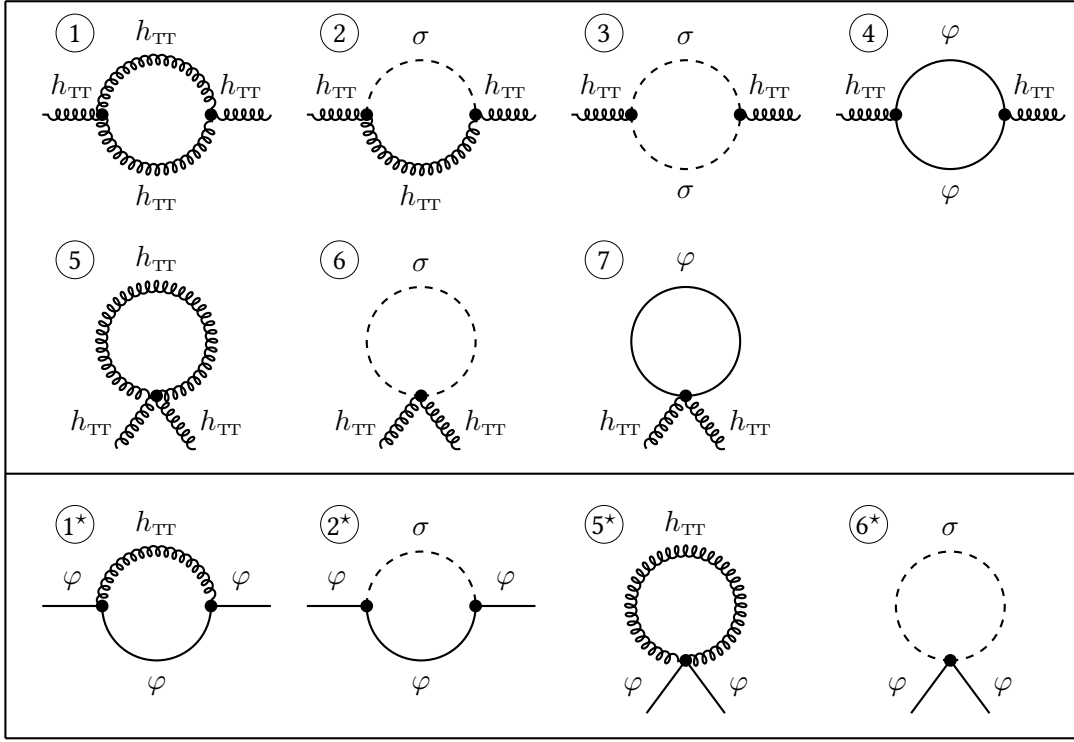


Figure 4.1: Diagrams which contribute to the running of the anomalous dimensions η_{TT} (first two rows) and η_{S} (third row). Diagrams similar to the ones in the first two rows, but with external σ legs, contribute to the running of the anomalous dimension η_{σ} .

diagram	η_{TT}	η_{σ}	η_{S}
1 / 1*	$-\frac{5 G_3}{864\pi} (388 - 53\eta_{\text{TT}})$	$\frac{5 G_3}{432\pi} (40 - 23\eta_{\text{TT}})$	0
2 / 2*	$\frac{25 G_3}{576\pi} (16 - \eta_{\text{TT}} - \eta_{\sigma})$	$-\frac{5 G_3}{144\pi} (16 - \eta_{\text{TT}} - \eta_{\sigma})$	$\frac{g_3}{16\pi} (16 - \eta_{\sigma} - \eta_{\text{S}})$
3	$-\frac{G_3}{216\pi} (31 - 5\eta_{\sigma})$	$\frac{G_3}{432\pi} (136 - 35\eta_{\sigma})$	—
4	$\frac{N_{\text{S}} g_3}{24\pi}$	$\frac{N_{\text{S}} g_3}{48\pi} (8 - 3\eta_{\text{S}})$	—
5 / 5*	$\frac{145 G_4}{648\pi} (6 - \eta_{\text{TT}})$	$\frac{55 G_4}{648\pi} (6 - \eta_{\text{TT}})$	$\frac{5 g_4}{24\pi} (6 - \eta_{\text{TT}})$
6 / 6*	$-\frac{29 G_4}{324\pi} (6 - \eta_{\sigma})$	$-\frac{11 G_4}{324\pi} (6 - \eta_{\sigma})$	$-\frac{g_4}{12\pi} (6 - \eta_{\sigma})$
7	0	0	—

Table 4.1: All individual contributions to the anomalous dimensions η_{TT} , η_{σ} and η_{S} contributing due to the diagrams displayed in Fig. 4.1 above.

in extended truncations, and points towards a difference in the number of relevant directions in the two settings, *cf.* also Ref. [99].

The two-vertex diagrams (first row in Fig. 4.1) enter with opposite signs in η_{TT} as compared to η_σ . This will imply that the two anomalous dimensions will typically have values of similar magnitude but opposite sign. Thus, setting $\eta_\sigma = \eta_{\text{TT}}$ does not seem to be a good approximation, if indeed this trend persists beyond our truncation. Moreover, this could suggest that even in calculations without a York decomposition, it might be necessary to disentangle the tensor structures of the graviton, and work with projection tensors. Comparing the anomalous dimension η_h for the graviton (without York decomposition) in the linear parametrisation to η_{TT} obtained here, we observe that it has a leading order contribution of opposite sign, *cf.* Eqn. (24) in Ref. [7].

There are only four diagrams contributing to the flow of η_s , two tadpole diagrams and two two-vertex diagrams, *cf.* the third row in Fig. 4.1. Overall, η_s is positive at leading order, when $g_3 > 0, g_4 > 0$. This is the opposite behaviour as that observed in the linear parametrisation and the de Donder gauge, *cf.* Ref. [7].

4.2.2 Flow of the graviton-matter coupling

There are 12 diagrams contributing to the flow of the 1-graviton-2-scalar-vertex which together with their analytical values can be found on the next page in Fig. 4.2 and Tab. 4.2, respectively.

The flow of $\sqrt{g_3}$ is driven by three types of diagrams. First of all, there are three-vertex diagrams in which all vertices are proportional to $\sqrt{g_3}$ themselves, namely diagrams 4 and 5. We do not distinguish between the coupling of two scalars and one σ mode and the coupling of two scalars and the TT mode, although we use only the latter to read off the running of g_3 . Note that diagrams 4 and 5 do not get contributions from the TT mode; the transverse traceless mode contributes to the running of the 1-graviton-2-scalar-vertex only at a higher order in the momenta, when our projection prescription (4.9) is used. The leading-order contribution to the beta function coming from these diagrams has a positive sign.

The other two types of diagrams are the tadpole diagrams 11 and 12 and the two-vertex diagrams 6–10. They contain the couplings g_4 and $g_5^{3/2}$ and some of them (diagrams 9–12) exclusively arise from the kinetic term of the scalar. The two tadpole diagrams contribute at $\mathcal{O}(g_5^{3/2})$ to the flow of g_3 . The two-vertex diagrams 9 and 10 contain only gravity-matter vertices and contribute at $\mathcal{O}(\sqrt{g_3}g_4)$ to the flow of $\sqrt{g_3}$. Finally, there are two- and three-vertex diagrams (diagrams 1–3 and 6–8) which contain the vertex $\sqrt{G_3}$, arising from the Einstein-Hilbert action.

4.2.3 Beta function for the graviton-matter coupling

By summing all the contributions in Tab. 4.2 we obtain the beta function for $\sqrt{g_3}$, from which we can derive the beta function of the dimensionless coupling g_3 :

$$\begin{aligned}
\beta_{g_3} = & (2 + \eta_{\text{TT}} + 2\eta_s) g_3 + \frac{3}{4\pi} g_3^2 + \frac{3}{4\pi} g_3^{3/2} \sqrt{G_3} - \frac{20}{9\pi} g_3 g_4 \\
& - \frac{2}{3\pi} \sqrt{g_3} \sqrt{G_3} g_4 - \frac{19}{18\pi} g_5^{3/2} \sqrt{g_3} + \left(\frac{5}{108\pi} g_4 \sqrt{G_3} + \frac{95}{324\pi} g_5^{3/2} \right) \sqrt{g_3} \eta_{\text{TT}} \\
& + \left(-\frac{1}{40\pi} g_3^{3/2} - \frac{1}{20\pi} g_3 \sqrt{G_3} + \frac{5}{36\pi} \sqrt{g_3} g_4 + \frac{1}{27\pi} g_4 \sqrt{G_3} - \frac{19}{162\pi} g_5^{3/2} \right) \sqrt{g_3} \eta_\sigma \\
& + \left(-\frac{1}{20\pi} g_3^{3/2} - \frac{1}{40\pi} g_3 \sqrt{G_3} + \frac{5}{36\pi} \sqrt{g_3} g_4 \right) \sqrt{g_3} \eta_s .
\end{aligned} \tag{4.17}$$

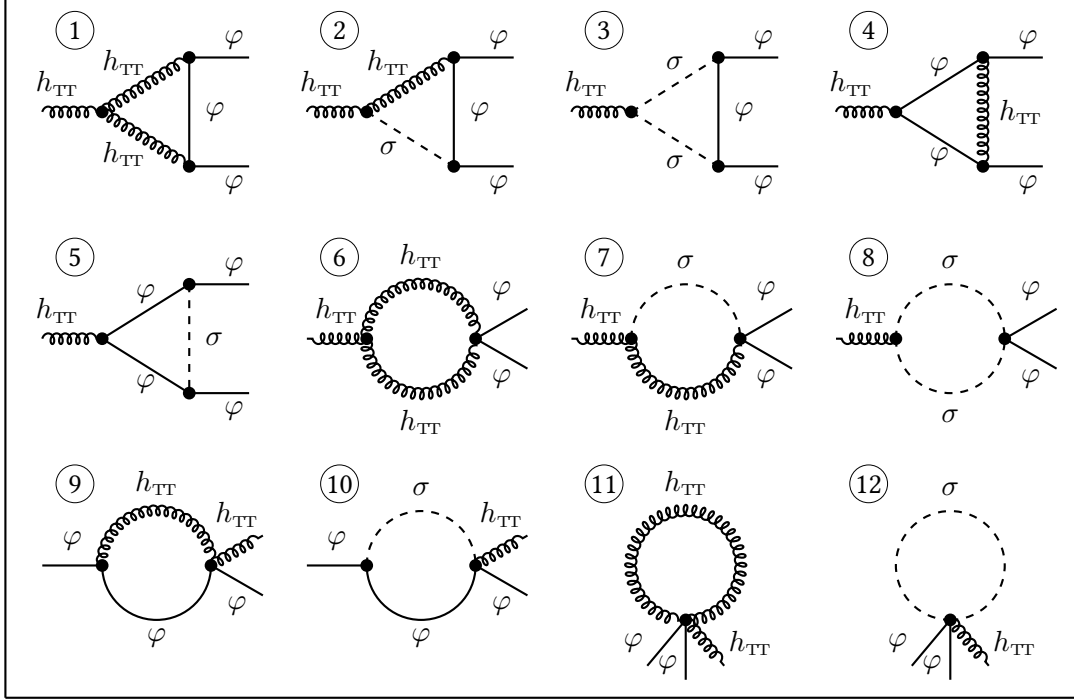


Figure 4.2: Diagrams which contribute to the beta function of the gravity-matter coupling $\sqrt{g_3}$.

diagram	$\beta_{\sqrt{g_3}}$	diagram	$\beta_{\sqrt{g_3}}$
1	0	7	0
2	0	8	$\frac{\sqrt{g_4 G_3}}{54\pi} (8 - \eta_\sigma)$
3	$\frac{\sqrt{g_3^2 G_3}}{80\pi} (30 - 2\eta_\sigma - \eta_s)$	9	0
4	0	10	$-\frac{5\sqrt{g_3 g_4^2}}{72\pi} (16 - \eta_\sigma - \eta_s)$
5	$\frac{\sqrt{g_3^3}}{80\pi} (30 - \eta_\sigma - 2\eta_s)$	11	$-\frac{95\sqrt{g_5^3}}{648\pi} (6 - \eta_{TT})$
6	$-\frac{5\sqrt{g_4^2 G_3}}{216\pi} (8 - \eta_{TT})$	12	$\frac{19\sqrt{g_5^3}}{324\pi} (6 - \eta_\sigma)$

Table 4.2: All individual contributions to the beta function of $\sqrt{g_3}$, coming from the diagrams displayed in Fig. 4.2 above.

Herein, the factors $\eta_{\text{TT}} g_3$ and $2 \eta_s g_3$ appear if the kinetic terms of both fields are redefined with a canonical prefactor, and the corresponding factors of the wave-function renormalization are absorbed in the coupling g_3 .

There is a significant difference to other possible definitions of a running Newton coupling: the beta function of g_3 depends only implicitly on N_s , since only η_{TT} and η_σ contain an N_s dependence. There is no pure matter-loop contributing to the beta function of g_3 , though, as there is for some other definitions of a running Newton coupling, *e.g.* for the background Newton coupling in Ref. [7], or for the pure-gravity coupling G_3 in Ref. [90].

4.3 Results for the pure gravity case

Let us now analyse the fixed-point structure within various approximations. If we consider the scalar as an external field, and only integrate out metric fluctuations, we can still consider g_3 as our definition of the running Newton coupling. In that case, the beta function of g_3 is determined by the tadpole diagrams 11 and 12, and the two-vertex diagrams 6–8 in Fig. 4.2. The anomalous dimensions instead will only receive contributions from those diagrams in Fig. 4.1 that do not contain matter fields in the loops. Their values may be obtained from the general formulas simply by putting $N_s = 0$. Here we further put the anomalous dimension η_s to zero. If we then employ the approximation $g_5 = g_4 = g_3$, $G_3 = G_4 = g_3$, we obtain:

$$\beta_{g_3} = (2 + \eta_{\text{TT}})g_3 - \frac{31}{18\pi} g_3^2 + \frac{55}{162\pi} g_3^2 \eta_{\text{TT}} - \frac{13}{162\pi} g_3^2 \eta_\sigma, \quad (4.18)$$

where

$$\eta_{\text{TT}} = \frac{2g_3(1591g_3 - 55296\pi)}{2665g_3^2 - 3384\pi g_3 + 124416\pi^2}, \quad (4.19)$$

$$\eta_\sigma = \frac{2g_3(16195g_3 + 32832\pi)}{2665g_3^2 - 3384\pi g_3 + 124416\pi^2}. \quad (4.20)$$

We define the semi-perturbative approximation by setting $\eta_{\text{TT}} = \eta_\sigma = \eta_s = 0$ on the right-hand sides of all diagrams contributing to the flow of the anomalous dimensions. Then η_{TT} and η_s still appear on the right-hand side of β_{g_3} . This semi-perturbative approximation removes potential poles from β_{g_3} that are due to the non-perturbative structure of the anomalous dimensions, and which could induce artificial zeros. In this approximation

$$\beta_{g_3} = 2g_3 - \frac{47}{18\pi} g_3^2 - \frac{223}{648\pi} g_3^3. \quad (4.21)$$

This structure—in particular the negative sign in front of the term proportional to g_3^2 —is similar to that found for other definitions of the Newton coupling.

The interplay between the classical scaling $2g_3$ and the leading order term from quantum fluctuations $-g_3^2$ induces one real interacting fixed point as given in Tab. 4.3. The semi-perturbative approximation features another real fixed point, which we discard as a truncation artefact, as it is not present in the full beta function. Moreover, the perturbative approximation, in which we set all anomalous dimensions to zero everywhere, yields a similar result, where the critical exponent is of course set exactly by the negative dimensionality of the coupling.

The real part of the critical exponent is remarkably close to values in previous approximations, both in the single- and bi-metric case. We emphasize that this is a rather non-trivial result. In our

approximation	$g_{3\star}$	θ	η_{TT}	η_σ
full	2.204	2.17	-0.62	0.50
semi-perturbative	2.203	2.17	-0.62	0.37
perturbative	3.65	2	-	-

Table 4.3: Coordinates and critical exponents at an interacting fixed point for vanishing scalar fluctuations. In the perturbative approximation we have set $\eta_{\text{TT}} = \eta_\sigma = 0$.

approximation	$g_{3\star}$	θ	η_{TT}
full	2.20	2.19	-0.67
semi-perturbative	2.26	2.12	-0.64

Table 4.4: Coordinates and critical exponents of an interacting fixed point with the approximation $\eta_\sigma = \eta_{\text{TT}}$.

case, we define a coupling g_3 , which is related to a gravity-scalar interaction vertex, in contrast to previous pure-gravity definitions. Accordingly, the diagrams entering the beta function have a fairly different structure, as does the beta function. It is rather reassuring to note that different ways of defining a Newton coupling and projecting the RG flow onto it, result in similar universal properties.

The relatively large fixed-point value for g_3 is clearly responsible for the large absolute values of the anomalous dimensions, as they are proportional to $g_{3\star}$: For instance, if we would set $g_{3\star} = 1$ by hand, we would obtain $\eta_{\text{TT}} = -0.28$ and $\eta_\sigma = 0.20$. It has been observed previously that the exponential parametrisation features a large fixed-point value for the Newton coupling in the single-metric approximation, *cf.* Ref. [56], and our definition of the fluctuation-field coupling exhibits similar behaviour.

The large negative value for the TT anomalous dimension suggests a propagator that decays with a higher power of the momentum in the UV, potentially suppressing the effect of TT quantum fluctuations in the UV. On the other hand, the positive value for the scalar anomalous dimension implies that the σ mode is actually enhanced in the UV. In particular, this could have very interesting consequences for gravity-operators at the UV fixed point. Operators of more “scalar character” would be shifted towards relevance by the positive anomalous dimension η_σ , while operators with a larger contribution to the transverse traceless sector would be shifted towards irrelevance, even if the canonical dimension of both operators agrees. In particular, this could suggest that more complicated tensor structures, such as, *e.g.* powers of the Ricci tensor or Riemann tensor could be less relevant than their Ricci scalar counterparts. (This concurs with an observation made in Ref. [70].)

Interestingly, the sign of η_{TT} is opposite to results in the linear parametrisation, *cf.* Refs. [7, 55, 87]. If we identify $\eta_\sigma = \eta_{\text{TT}}$ we obtain a fixed point with the properties listed in Tab. 4.4. We observe a comparable value for the critical exponent θ with respect to the previous case. The anomalous dimension for the TT mode remains essentially the same. We see that the assumption $\eta_\sigma = \eta_{\text{TT}}$ gives the wrong sign for η_σ . Since the anomalous dimensions contribute to the scaling dimensions of operators, this is of course a serious shortcoming.

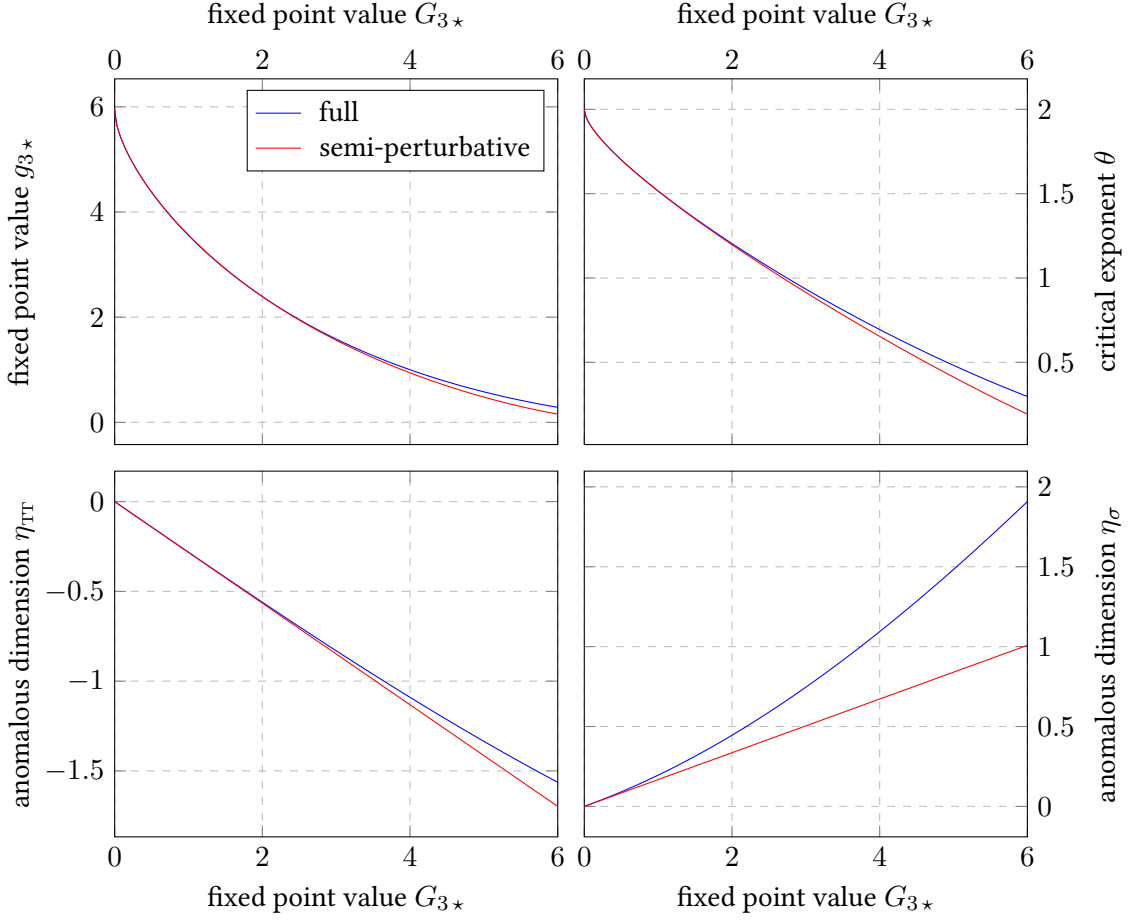


Figure 4.3: Results for the pure gravity case $N_s = 0$, $g_3 = g_4 = g_5$ and $G_3 = G_4$: fixed point value for g_3 , critical exponent θ , and the anomalous dimensions η_{TT} and η_σ as a function of the value G_{3*} at the fixed point.

To test the stability of our results with respect to extended truncations which would include separate beta functions for G_3 etc., we consider an approximation where $g_3 = g_4 = g_5$. We treat the pure-gravity coupling $G_3 = G_4$ as an external parameter, and test whether a viable fixed point exists for values of these couplings between 0 and 6. For this case, we display the semi-perturbative result, as it allows a clear understanding of the terms:

$$\beta_{g_3} = 2g_3 - \frac{8}{9\pi} g_3 G_3 - \frac{19}{18\pi} g_3^2 - \frac{209}{648\pi^2} g_3^2 G_3 - \frac{2}{3\pi} g_3^{3/2} \sqrt{G_3} - \frac{7}{324\pi^2} g_3^{3/2} G_3^{3/2}. \quad (4.22)$$

When G_3 increases, the fixed point for g_3 decreases, *cf.* Fig. 4.3. We see that the fixed point that we have observed in the approximation $G_3 = g_3$, persists for a large range of values of G_3 . We interpret this as a sign of stability.

Fig. 4.3 also shows the anomalous dimensions at the fixed point as functions of G_3 . Note that they vanish for $G_3 = 0$, since, in the absence of matter self interactions, they are generated only by diagrams proportional to G_3 . Note that to obtain this result, the identification $g_5 = g_3$, suggested by diffeomorphism invariance, is crucial, as it gives rise to the above structure of the beta function.

The critical exponent θ in this approximation is not equal to the result of Tab. 4.3 at $G_3 = g_3$, since $\partial\beta_{g_3}/\partial G_3|_{G_3=g_3}$ contributes to the critical exponent quoted in that table. When we distinguish g_3 and G_3 , then $\partial\beta_{g_3}/\partial G_3|_{G_3=g_3}$ yields an *off-diagonal* contribution to the stability matrix, which can contribute to the critical exponents if operators mix at the non-Gaussian fixed point. As we only evaluate the diagonal entry of the stability matrix in our approximation, where G_3 is treated as an external parameter, this contribution is absent.

We now supplement our beta functions with a beta function for the background Newton coupling \bar{G} , as obtained in Ref. [56], where

$$\beta_{\bar{G}} = 2\bar{G} - \frac{\bar{G}^2}{\pi} \left(\frac{15}{8} - \frac{5\eta_{\text{TT}}}{18} + \frac{\eta_{\sigma}}{24} \right). \quad (4.23)$$

We observe that η_{TT} and η_{σ} enter with opposite signs. At the fluctuation-field fixed point, $\eta_{\text{TT}} < 0$ and $\eta_{\sigma} > 0$. This sign combination strengthens the gravitational fluctuation effects that induce a fixed point, lending further support to the observation that all modes of the graviton act towards asymptotic safety, *cf.* Refs. [39, 100].

Plugging in the fluctuation field fixed point-values—which are of course independent of \bar{G} , as they should—we obtain $\bar{G}_{\star} = 3.04$ and $\theta = 2$.

4.4 Results for the interacting matter-gravity system

In the following section, we will switch on the scalar fluctuations as well, which add several diagrams to the flow of g_3 and additional contributions to β_{g_3} , η_{TT} and η_{σ} . Our main goal is to find out whether the pure-gravity results discussed above can be extended to $N_{\text{S}} > 0$ in a stable way, or whether scalars have a significant effect on the fixed point in our approximation. First, we will set $\eta_{\text{S}} = 0$ by hand, while keeping the other anomalous dimensions η_{TT} and η_{σ} non-zero. The reason for this unequal treatment of fluctuation fields will become clear below.

4.4.1 Fixed-point results without scalar anomalous dimension

As a first approximation, we set $G_3 = G_4 = g_3 = g_5 = g_5$ to search for an extension of the pure-gravity fixed point with $N_{\text{S}} > 0$. Unlike the beta functions for the background Newton coupling and the pure-gravity couplings G_3 and G_4 , β_{g_3} receives no correction from diagrams containing a scalar loop in our approximation. Consequently, β_{g_3} does not depend on N_{S} explicitly, if we set all anomalous dimensions to zero. It only depends on N_{S} if we include the anomalous dimensions η_{TT} and η_{σ} . This gives rise to a beta function of the form

$$\beta_{g_3} = 2g_3 - \frac{1}{3\pi} g_3^2 \left(10 - \frac{N_{\text{S}}}{8} \right) + \mathcal{O}(g_3^3). \quad (4.24)$$

Herein, the factor $10/3\pi$ differs from the factor $47/18\pi$ in Eqn. (4.21) since it includes contributions from scalar fluctuations which do not scale with N_{S} . In our determination of fixed points we also take into account all higher-order terms, but the main effect of scalars is clear from the $\mathcal{O}(g_3^2)$ term: As the contribution of scalars, that scales with N_{S} explicitly, comes with the opposite sign from the asymptotic safety-inducing term which enters with $-10g_3^2/3\pi$, scalars push the fixed-point of g_3 towards larger values. This is the same effect that was already observed for the background-system in Ref. [7]. Interestingly, the contribution of scalars to the running of the three-graviton coupling features the opposite sign in the approximation used in Ref. [90]. On the other hand, the overall

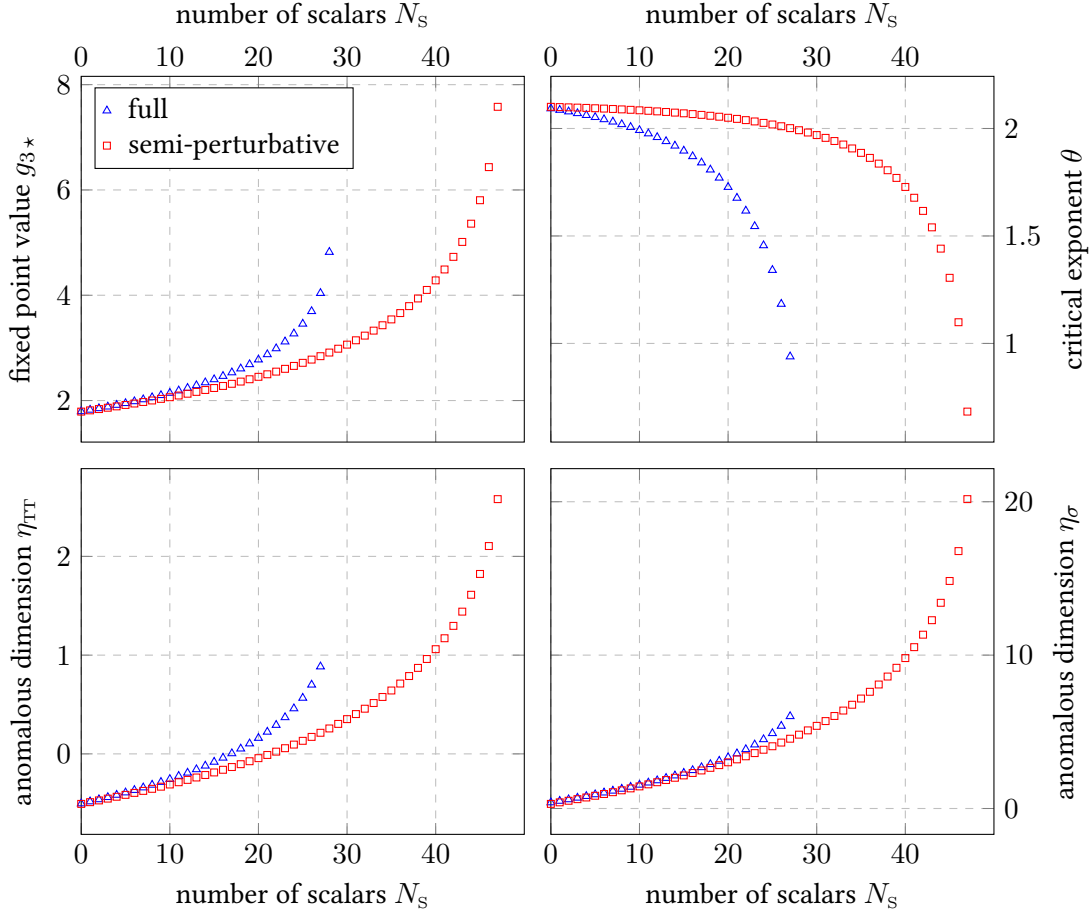


Figure 4.4: Results for $\eta_S = 0$ and $g_3 = g_4 = g_5 = G_3 = G_4$: fixed point value for g_3 , critical exponent θ , and the anomalous dimensions η_{TT} and η_σ as a function of the number of scalars N_S for both the full result and in the semi-perturbative approximation.

fixed-point dynamics in Ref. [90] are similar, as G_{3*} is also pushed towards larger values. The destabilising effects of scalars show up in the momentum-independent part of the graviton two- and three-point functions.

In our approximation, the fixed point merges with another, non-physical fixed point at $N_S \approx 28$, where the fixed point disappears into the complex plane, *cf.* Fig. 4.4. While this could indicate the existence of a bound on N_S in asymptotically safe gravity, we note that $\eta_\sigma > 2$ already at $N_S = 14$, indicating that a larger truncation is required to investigate that regime in more detail, *cf.* Ref. [90] as well. In the semi-perturbative approximation, the anomalous dimensions are slightly smaller, and the fixed-point collision accordingly occurs at larger N_S .

To investigate the stability of our results, we again distinguish the pure-gravity couplings from the gravity-matter couplings. We treat $G_3 = G_4$ as an external parameter, and investigate the fixed point in g_3 as a function of G_3 and N_S . In particular, at smaller G_3 , the value of η_σ at small N_S remains smaller. We observe that larger values of G_3 lead to a slower increase in the fixed-point value for g_3 , and increase the value N_S , at which the fixed-point annihilation occurs,

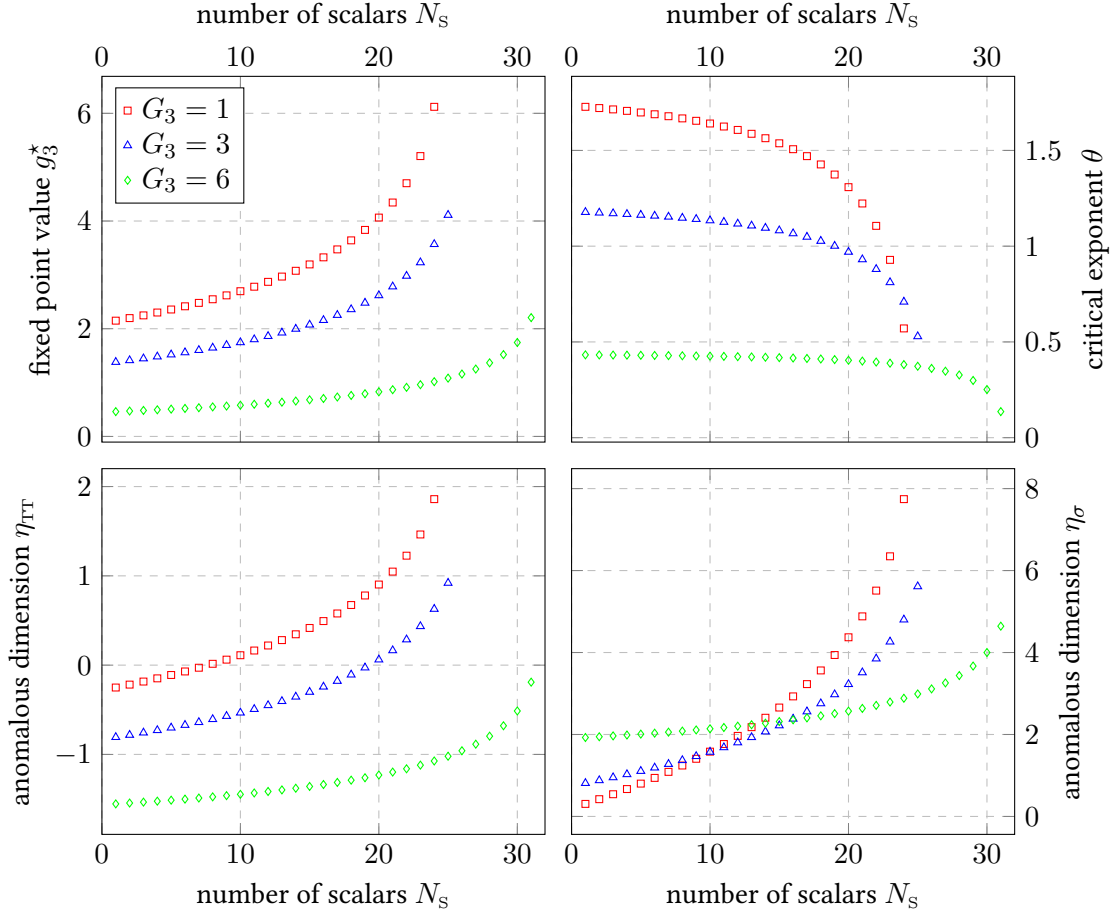


Figure 4.5: Results for $\eta_s = 0$, $g_3 = g_4 = g_5$ and $G_3 = G_4$: fixed point value for g_3 , critical exponent θ , and the anomalous dimensions η_{TT} and η_σ as a function of the number of scalars N_s .

cf. Fig. 4.5. While quantitative details change, the overall effect of increasing N_s is similar to the previous approximation, cf. Fig. 4.5. This suggests that our results will be qualitatively stable under extensions of the truncation including the running of the gravity-couplings as in Ref. [90]. On the other hand, a non-trivial interplay between the gravity-matter couplings and the pure-gravity couplings at large N_s is not excluded, as the effect of varying g_3 on $G_{3\star}$ remains to be studied.

4.4.2 Fixed-point results including scalar anomalous dimension

We now set all gravitational couplings and gravity-scalar couplings equal to the Newton coupling as defined from the gravity-matter interaction and include the anomalous dimension η_s for the scalar. This yields a new contribution to β_{g_3} , which now reads

$$\beta_{g_3} = 2g_3 + 2g_3\eta_s - \frac{1}{6\pi} g_3^2 \left(20 - \frac{N_s}{4} + \frac{23}{60} \eta_s \right) + \mathcal{O}(g_3^3). \quad (4.25)$$

fixed point	approximation	$g_{3\star}$	θ	η_{TT}	η_σ	η_s
<i>FP1</i>	full	-13.9	3.85	3.27	-0.31	-6.50
<i>FP1</i>	semi-perturbative	-8.67	3.42	2.34	-1.92	-4.83
<i>FP2</i>	full	53.4	11.7	-5.21	10.8	25.2
<i>FP2</i>	semi-perturbative	12.2	4.81	-3.28	2.69	6.78

Table 4.5: Coordinates and critical exponents of the interacting fixed points at $N_s = 1$, both in semi-perturbative and full approximations.

Using $\eta_s = \frac{7}{4\pi} g_3 + \mathcal{O}(g_3^2)$, Eqn. (4.24) gets replaced by

$$\beta_{g_3} = 2g_3 + \frac{4 + N_s}{24\pi} g_3^2 + \mathcal{O}(g_3^3). \quad (4.26)$$

Therefore, in this simplified form, the terms of $\mathcal{O}(g_3^2)$ in the beta function are always positive, and by themselves would not produce a fixed point. Fixed points appear when we consider higher non-linearities, but their properties are not very stable.

For small numbers of scalars, both in the semi-perturbative approximation and using the full equations, we have, in addition to the Gaussian fixed point, also two non-trivial fixed points. The first, which we call *FP1*, has negative g_3 and the second, which we call *FP2*, has positive g_3 . The fixed point *FP1* cannot be immediately discarded on the basis of having a negative g_3 . While a negative value of the Newton coupling in the infrared is of course incompatible with observations, a negative ultra-violet fixed-point value is viable, as long as the RG flow can cross to $g_3 > 0$ towards the infrared. As the full beta function contains terms proportional to g_5 etc., which imply $\beta_{g_3} \neq 0$ at $g_3 = 0$, this situation is realized here.

In the semi-perturbative approximation the solutions of the fixed point equation can be written explicitly as

$$g_{3\star} = \frac{9\pi \left(60 + 15N_s \pm \sqrt{41904 - 2008N_s + 45N_s^2} \right)}{1287 - 74N_s}. \quad (4.27)$$

The solution *FP2* (which corresponds to the positive sign in front of the square root) is a growing function of N_s , which has a simple pole between $N_s = 17$ and $N_s = 18$, and asymptotes to $-135\pi/37$ for large N_s . The solution *FP1* is a negative, smooth, monotonically increasing function of N_s that asymptotes to zero.

The solutions of the full equations are more complicated to display in closed form and are best studied numerically. Let us start from the case $N_s = 1$. The properties of the fixed points in the two approximations are listed in Tab. 4.5. In the full approximation, *FP2* has very large critical exponent and anomalous dimensions, that put it far beyond the regime where our approximation is reliable. In fact, the dependence on N_s is quite different in the two approximations. In the full calculation, the fixed point value $g_{3\star}$ for *FP2* is initially decreasing as a function of N_s , has a minimum near $N_s = 30$ and then increases again. The fixed point ceases to exist for $N_s > 95$. It switches from UV attractive to repulsive near $N_s = 47$, and there is no value of N_s for which the critical exponents have reasonably small values. This is very different from its behaviour in the semi-perturbative approximation.

Also *FP1* in the full calculation behaves very differently from the semi-perturbative approximation: instead of increasing steadily to zero, it decreases monotonically and diverges to $-\infty$ for N_s just above 46. Some of the anomalous dimensions have more reasonable values but there is no N_s for which they are all small. Thus *FP1* has slightly better chances of being a true fixed point, but in the present approximations it cannot be reliably assessed.

We observe that already in the case $N_s = 1$ the anomalous dimensions of the graviton modes have opposite signs compared to the case when we neglected η_s , and become rather large, as a consequence of a rather large absolute value of g_3 . The critical exponent also differs considerably from the pure-gravity case. As a consequence, it becomes hard to identify either of the fixed points with the one that we found for $N_s = 0$, when we do not set η_s to zero.

These results could lead to different conclusions: the approximation $G_3 = g_3$ might not be particularly reliable beyond small N_s , or, more likely, our current estimate for the scalar anomalous dimension needs improvement, and the results for $\eta_s = 0$ might be closer to the correct result.

The significant changes in the fixed-point properties compared with the pure-gravity case arises from the scalar anomalous dimension. Accordingly, the perturbative approximation, where $\eta_{\text{TT}} = \eta_\sigma = \eta_s = 0$ features a fixed point at $g_3 = 2.57$ with $\theta = 2$ for all values of N_s . As η_s has such a significant effect on the existence and properties of fixed points, it is important to understand whether our truncation already captures all major operators that determine η_s . Recall that metric fluctuations induce non-vanishing momentum-dependent matter self-interactions, e.g. of the form $(g^{\mu\nu} \partial_\mu \varphi \partial_\nu \varphi)^2$, cf. Ref. [96]. As soon as these couplings are non-zero, they yield a non-vanishing contribution to η_s . Our current truncation does not include these effects. We therefore conjecture that the results could improve once these further operators are included. By a simple count of modes, $N_s = 1$ should not dramatically change the results, and the case $N_s = 1$ should still feature a fixed point with properties similar to the pure-gravity one, just as exhibited by the approximation $\eta_s = 0$. We tentatively suggest that the calculation with $\eta_s = 0$, which shows a destabilising effect setting in at $N_s \gg 1$, might capture the full dynamics more accurately than our current estimate with $\eta_s \neq 0$.

4.4.3 Background beta functions

The background couplings can only appear on the right-hand side of beta functions through a trivial scaling, for instance proportional to \bar{G}^2 , since the prefactor of the curvature term in the Einstein-Hilbert action is $1/16\pi\bar{G}$. All couplings that appear on the right-hand side from either propagators or vertices are always fluctuation field couplings. Accordingly, η_{TT} , η_σ and η_s , which will appear on the right-hand side of the beta function of \bar{G} , depend on the fluctuation-field couplings g_3, g_4, g_5, G_3, G_4 only. Thus we obtain the following matter contribution to the beta function for the background Newton coupling:

$$\beta_{\bar{G}} \Big|_{\text{scalar}} = \frac{\bar{G}^2}{24\pi} N_s (4 - \eta_s). \quad (4.28)$$

Following Ref. [56], we therefore find the following background beta function:

$$\beta_{\bar{G}} = 2\bar{G} - \frac{\bar{G}^2}{\pi} \left(\frac{15}{8} - \frac{5\eta_{\text{TT}}}{18} + \frac{\eta_\sigma}{24} - \frac{N_s}{24} (4 - \eta_s) \right). \quad (4.29)$$

If we set $\eta_{\text{TT}} = \eta_\sigma = \eta_s = 0$, we obtain $N_s = 45$ as the maximal number of scalars before the fixed point in \bar{G} diverges.

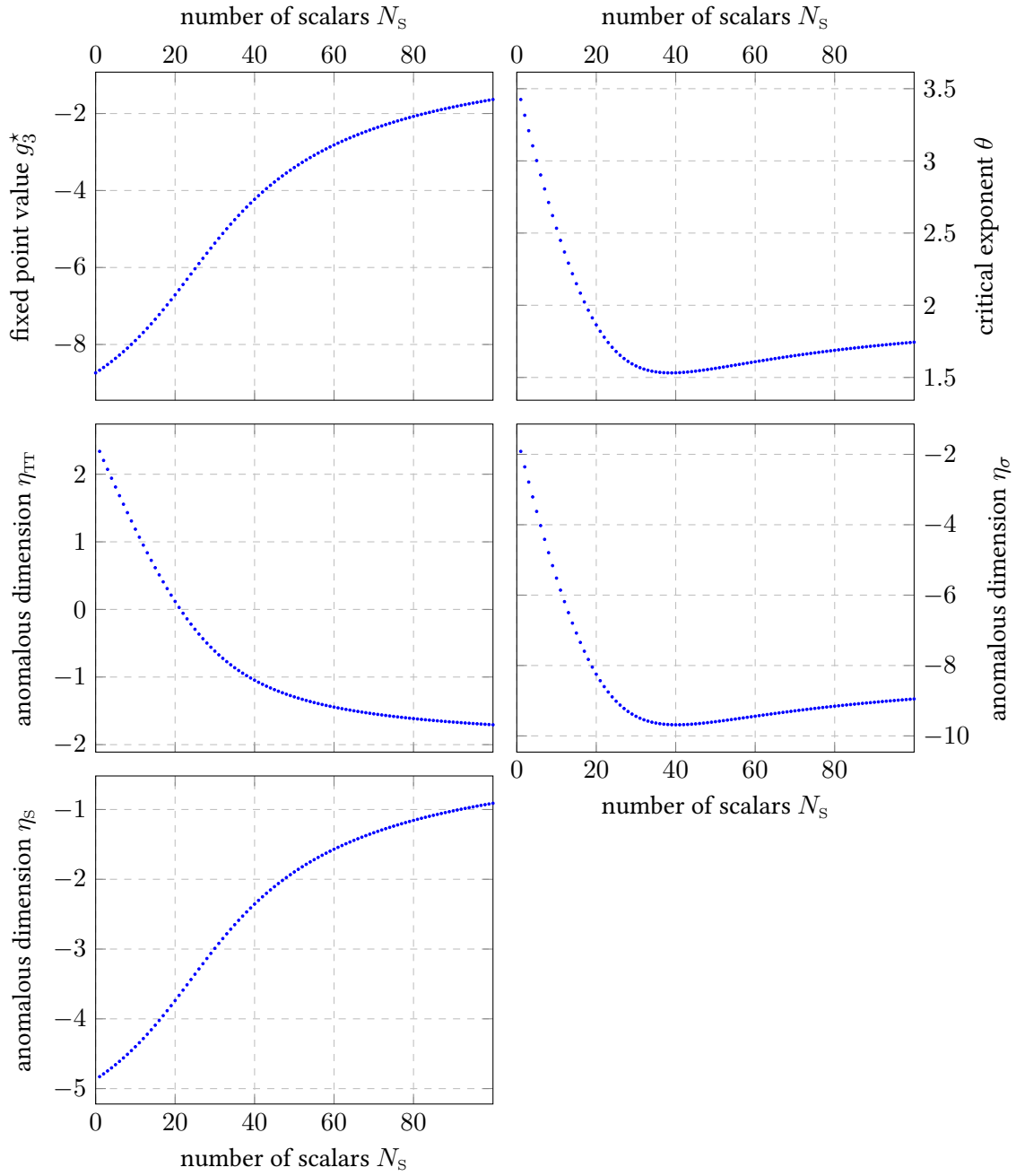


Figure 4.6: Results for $\eta_s \neq 0$ and $g_3 = g_4 = g_5 = G_3 = G_4$ in the semi-perturbative approximation: fixed point value for g_3 , critical exponent θ , and the anomalous dimensions η_{TT} , η_σ and η_S as a function of the number of scalars N_s .

If we now use the approximation of equating all fluctuation couplings in the expressions for the anomalous dimensions, as in Sec. 4.4.2, we obtain a fixed point at $\bar{G}_* = 12.14$, with critical exponent $\theta = 2$, for $N_S = 1$ at the fixed point $g_* = -13.9$. The location of a possible bound depends on the assumptions for the couplings g_4, g_5, G_3, G_4 . For the case $g_4 = g_5 = 0, G_3 = G_4 = 0$, the continuation of the pure-gravity fixed point in the background coupling ceases to exist beyond $N_S = 9$. For the approximation where we set $\eta_S = 0$, we obtain a bound at $N_S = 12$, which is close to the bound from the fluctuation coupling, at $N_S = 14$.

Note that fixed-point values for the background couplings are affected by a strong regulator dependence: As the background metric enters the regulator function, there are contributions to all beta functions of background couplings that are due to the regularisation only, and are unphysical in that sense, see also Refs. [27, 28, 31, 101]. Thus, even divergences in background couplings might turn out to be compatible with a model that is asymptotically safe in a physical sense, *i.e.* where all physical quantities have a well-behaved UV limit. To understand on which couplings a fixed-point requirement must be imposed, and which couplings may even diverge, one must investigate physical observables. As this is clearly beyond the scope of the work presented here, we conclude that the most conservative assumption is that *all* couplings must feature fixed points, and therefore divergences in the background couplings are not acceptable, even if the fluctuation couplings are well-behaved. Interpreted along these lines, the one-loop approximation, where we set all anomalous dimensions to zero everywhere, and only the background Newton coupling depends on N_S , would suggest that there could be an upper limit of scalars that is compatible with a viable fixed point.

5. Effective Universality in Quantum Gravity

In the last chapter, we have begun to disentangle the different renormalisation group flows of gravity-matter vertices on the level of fluctuating fields. Specifically, in these systems, scattering with gravitons is described by scale-dependent couplings

$$G_{\mathbf{n}}, \quad \text{where } \mathbf{n} = (n_h, n_\varphi, n_\psi, n_{A_\mu}, n_c \dots). \quad (5.1)$$

With n_Ψ we denote the number of fields Ψ involved in the process (*cf.* notation of Ref. [102]). We have referred to these couplings as ‘avatars’ of Newton’s constant G_N . As before, we want to limit ourselves here to gravity-scalar systems, and focus on pure-graviton and graviton-scalar couplings. Suppressing the number of ghost fields n_c for the sake of clarity, this leaves us with couplings carrying two indices

$$G_{(n_h, n_\varphi)}. \quad (5.2)$$

At the classical level, Einstein gravity is diffeomorphism invariant, and all these couplings are of course equal to each other. However, in the functional renormalisation group approach to quantum gravity, we expand the effective average action in terms of diffeomorphism-invariant terms and diffeomorphism-variant corrections that depend on the gauge fixing as well as the infrared regularisation (the cutoff operator). If the latter terms were missing, the different couplings $G_{(n_h, n_\varphi)}$ would be identical and a unique Newton coupling G_N would be present. This property indeed holds for the diffeomorphism-invariant effective action

$$\Gamma[g_{\mu\nu}] = \Gamma[\bar{g}_{\mu\nu} + h_{\mu\nu}]. \quad (5.3)$$

In renormalisable theories, dimensionless couplings have a two-loop universality, *i.e.* the first two non-vanishing coefficients of the β functions are universal in mass-independent renormalisation schemes. This also relates the momentum-dependence of vertices to each other.

In gravity, however, couplings are not dimensionless and universality is missing (except for the R^2 -coupling). But yet, in a diffeomorphism-invariant action the couplings would agree with each other, which again would restricts the momentum-dependence of vertices. Supplementing the flow equation with the modified split Ward identities, as outlined in Ch. 2, one may thus ask if it is possible to uncover some notion of ‘effective universality’ based on the underlying diffeomorphism invariance.

In this chapter we want to investigate this question. Our motivation will be two-fold. First, in the last chapter we have noticed, that contributions to the anomalous dimensions coming from the scalar fields had different signs with respect to an older calculation done in Ref. [7], cf. Secs. 4.2 and 4.3. This might be either due to the use of the exponential parametrisation of the metric field, or due to the use of the background approximation in Ref. [7] compared to the fluctuation field calculation we have done in the last chapter. This is why we want to re-do the latter calculation in the linear parametrisation, using a different gauge fixing procedure at the same time. This will also test the robustness on the scheme-dependence of the results obtained so far. Secondly, we want to use the msWI derived in a background field approximation together with the background flow equation to investigate whether the artificial background field contributions of the cutoff operator can be removed and the effective behaviour of the fluctuation field couplings can be recovered.

5.1 Matter-gravity flow setup

In this chapter we will again compare two versions of the Newton coupling. The first is defined through the three-graviton vertex, as in Refs. [88, 90], and we will call its dimensionless version $G_{(3,0)}$ (this corresponds to G_3 in the last chapter). The second coupling is defined through the one-graviton-two-scalar vertex (g_3 in the last chapter), and here we will denote its dimensionless version with $G_{(1,2)}$.

Differently from the last chapter, we will use the linear parametrisation

$$g_{\mu\nu} = \bar{g}_{\mu\nu} + h_{\mu\nu}. \quad (5.4)$$

for the metric fluctuations and we will not York-decompose the respective spin modes. Additionally, we rescale the fluctuation field $h_{\mu\nu}$ by a dimensionful constant of mass-dimension -1 , such that $h_{\mu\nu}$ has a canonical dimension 1 for the bosonic fluctuation field $h_{\mu\nu}$. If we derive all pure-graviton and graviton-matter vertices from a diffeomorphism invariant action containing an Einstein-Hilbert term with Newton coupling G_N , then that dimensionful constant should be $\sqrt{G_N}$. In a second step, we then reabsorb the corresponding power of G_N in the fluctuation field vertices.

Furthermore, we will again use a symmetric momentum configuration, and for the analytical results we will project onto $p = 0$. For the numerical results, we will employ a bi-local projection instead, as in Refs. [88, 90]. We also compare our results with the background Newton coupling, \bar{G} . Throughout this chapter, we use a conventional gauge fixing procedure where we set the gauge parameters to $\alpha = 0$ and $\beta = 1$.

We will define our truncation in a very similar manner as in the last chapter: Starting from an auxiliary effective average action composed out of the Einstein-Hilbert action (including a cosmological constant, and augmented by a gauge fixing and ghost term) and a kinetic term for the minimally coupled N_S scalar fields

$$\hat{\Gamma}_k[\bar{g}_{\mu\nu}, h_{\mu\nu}, \varphi] = \int d^4x \sqrt{g} \left[-\frac{R - 2\Lambda}{16\pi G_N} + \frac{1}{2} \sum_{i=1}^{N_S} (\nabla\varphi^i)^2 \right], \quad (5.5)$$

we insert the linear parametrisation Eqn. (5.4). We then expand the Einstein-Hilbert term to fifth order and the kinetic term for the scalar fields to third order in $h_{\mu\nu}$.

Once again, due to the breaking of background independence, the running of the three-graviton vertex will differ from the one of the four- and five-graviton vertex, as well as the different graviton-scalar vertices. Accordingly, we again introduce separate couplings, denoted by $G_{(n_h, n_\varphi)}$ in front of these vertices. Similarly, we will have to distinguish the different avatars of the cosmological constant by introducing the graviton mass parameter μ associated to -2Λ and the momentum-independent part of the n -graviton vertex, λ_n . Thus, the effective average action of our truncation schematically reads

$$\Gamma_k = Z_h \int d^4x h_{\mu\nu} \left(\hat{\Gamma}_{G_N}^{(2,0)} \right)^{\mu\nu\kappa\lambda} h_{\kappa\lambda} + Z_h \mu \int d^4x h_{\mu\nu} \left(\hat{\Gamma}_\Lambda^{(2,0)} \right)^{\mu\nu\kappa\lambda} h_{\kappa\lambda} + \dots \quad (5.6)$$

As we have pointed out before, the beta function of $G_{(4,0)}$ depends on $G_{(6,0)}$, and the one of $G_{(5,0)}$ on $G_{(6,0)}$ and $G_{(7,0)}$, which we have excluded from our truncation. To close the system of beta functions, we will use a similar strategy as in the last chapter, and leave $G_{(4,0)}$, $G_{(5,0)}$, $G_{(2,2)}$, $G_{(3,2)}$ as well as λ_4 , λ_5 as free parameters. These free parameters will then appear in the beta functions of $G_{(3,0)}$ and $G_{(2,1)}$. Later, we will have the choice of either equating them to one of the lower-order couplings, or setting them to some fixed value.

5.2 Effective universality for the scalar contribution to the Newton coupling

We first focus on the beta functions for three avatars of the Newton coupling, namely the three-graviton coupling $G_{(3,0)}$, the graviton-scalar coupling $G_{(1,2)}$ and the background Newton coupling \bar{G} . The beta functions for the first two depend on higher n -point functions, such as the four-graviton coupling $G_{(4,0)}$. In the following, all pure-graviton couplings will be set equal to $G_{(3,0)}$, *i.e.* $G_{(n,0)} = G_{(3,0)}$, and all graviton-matter couplings will be set equal to $G_{(1,2)}$, *i.e.* $G_{(n,m)} = G_{(1,2)}$ for $m > 0$. We then obtain

$$\beta_{G_{(3,0)}} = (2 + 3\eta_h) G_{(3,0)} + \beta_{G_{(3,0)}} \Big|_{\text{grav}} - G_{(3,0)}^{1/2} G_{(1,2)}^{3/2} N_s \frac{86 + \eta_s}{1140\pi}, \quad (5.7)$$

$$\beta_{G_{(1,2)}} = (2 + \eta_h + 2\eta_s) G_{(1,2)} - \frac{2G_{(1,2)}^2}{3\pi} (6 - \eta_h) + \frac{2\sqrt{G_{(3,0)}} G_{(1,2)}^{3/2}}{\pi} (24 - 3\eta_h), \quad (5.8)$$

$$3\beta_{\bar{G}} = 2\bar{G} - \frac{79}{24\pi} \bar{G}^2 + \bar{G}^2 \frac{N_s}{24\pi} (4 - \eta_s). \quad (5.9)$$

The matter contribution to the background Newton coupling is the same as in Ref. [7] since the contribution from the scalar loop is independent of the gauge. Let us first comment on the case of vanishing anomalous dimensions and $N_s = 1$. In that case,

$$\beta_{G_{(3,0)}} \Big|_{\text{grav}} = -\frac{833}{285\pi} G_{(3,0)}^2. \quad (5.10)$$

We then obtain a fixed point at

$$G_{(1,2)}^* = 2.04, \quad G_{(3,0)}^* = 3.30, \quad \bar{G}^* = 2.01. \quad (5.11)$$

The set of critical exponents, defined as the eigenvalues of the stability matrix multiplied by an additional sign, read

$$\theta_1 = 2.95, \quad \theta_2 = 2, \quad \theta_3 = 2. \quad (5.12)$$

This simple approximation yields a fixed point at positive values of the Newton couplings and with critical exponents of approximately the expected size. The agreement between θ_2 and θ_3 is a simple consequence of the structure of the quadratic equations, which result in a critical exponent being equal to the negative canonical dimension.

Our focus is now on the N_s -dependent part in Eqns. (5.7)- (5.9). If we neglect that η_h can have an N_s dependence, we obtain a picture that suggests very strong violations of diffeomorphism invariance. For simplicity we equate $G_{(3,0)} = G_{(1,2)} = G$, and obtain an N_s dependence in $\beta_{G_{(3,0)}}$ that is proportional to $-G^2$. On the other hand there is no N_s dependence in $\beta_{G_{(1,2)}}$, as there is no closed scalar loop that contributes. Finally, the N_s dependence in $\beta_{\bar{G}}$ comes with $+\bar{G}^2$. Thus, in this approximation the three avatars of the Newton coupling exhibit all three possible dependences on N_s , *i.e.* either no N_s -dependence in $\beta_{G_{(1,2)}}$, a positive N_s dependence in $\beta_{G_{(3,0)}}$, or a negative one in $\beta_{\bar{G}}$.

Let us now add the graviton anomalous dimension, for which

$$\eta_h = \eta_h \Big|_{\text{grav}} + G_{(1,2)} \frac{N_s}{24\pi}. \quad (5.13)$$

If we insert this relation into Eqns. (5.7) and (5.8), we obtain the following contribution linear in N_s

$$\begin{aligned} \beta_{G_{(3,0)}} \Big|_{N_s} &= 3 G_{(3,0)} G_{(1,2)} \frac{N_s}{24\pi} - G_{(3,0)}^{1/2} G_{(1,2)}^{3/2} N_s \frac{86 + \eta_s}{1140\pi} \\ &= G^2 N_s \frac{113}{2280\pi} \approx 0.016 G^2 N_s, \end{aligned} \quad (5.14)$$

$$\begin{aligned} \beta_{G_{(1,2)}} \Big|_{N_s} &= G_{(1,2)}^2 \frac{N_s}{24\pi} \\ &\approx 0.013 G^2 N_s, \end{aligned} \quad (5.15)$$

where we have set $G_{(1,2)} = G_{(3,0)} = G$ in the second lines of both equations. These two results agree within a 16% deviation with each other. That is, allowing for a non-trivial graviton anomalous dimension forces the two couplings to behave very similarly, as (classical) diffeomorphism invariance would have suggested in the first place. Furthermore, we observe that the contribution to $\beta_{G_{(1,2)}}$ comes with the same sign as in the exponential parametrisation and using the physical gauge, *cf.* Eqns. (4.24) and (4.26) in the last chapter.

For the background coupling, the N_s coefficient is larger by a factor of four. Nevertheless, all three definitions of the coupling share the same qualitative behaviour, and their values at the fixed point grow as a function of N_s . The running of the Newton coupling thus features an effective universality, *i.e.* different definitions of the coupling lead to qualitatively similar behaviour in their scale-dependence.

The agreement between the scalar contribution to different versions of the fluctuation coupling and the background result relies on the dominance of the graviton anomalous dimension in the case of the fluctuation results, which yields an opposite sign for the N_s -dependence of the flow of the coupling $G_{(3,0)}$ as compared to that of the vertex, which does not include η_h , *cf.* Eqn. (5.7) for $\eta_h = 0$. In the case of the coupling $G_{(1,2)}$ there is no N_s dependence at all in the running of the vertex itself. The observation, that even for dimensionless couplings an important contribution to the universal one-loop running is carried by the anomalous dimension and not the running of the vertex, together with the potentially even higher importance of the anomalous dimension in

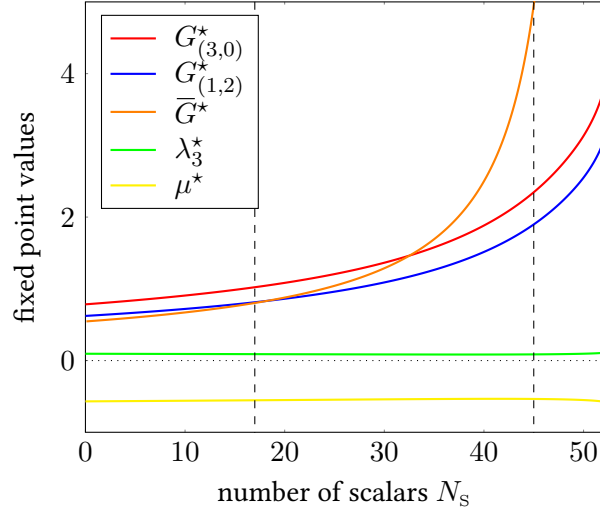


Figure 5.1: Comparison of the numerical results of the fixed point values for the three avatars of Newton’s constant and the cosmological constants. In this and the following plots, the dashed line at $N_s = 17$ shows where $\eta_h(0)$ exceeds 2, whereas the one at $N_s = 45$ shows where $\eta_h(k^2)$ exceeds 2. The latter should be viewed as an indicator of where the range of validity of the approximation is lost.

models with momentum-dependent interactions, highlights the need to include the anomalous dimension of the fluctuation field to obtain (close-to) universal results.

Let us remark that the effective universality is simply a fact of the beta functions that we observe, but no mechanism for it is apparent at present. In particular, the sign of the scalar contribution to η_h is not fixed by physical arguments, and the relative size of the contribution of scalars to η_h and to the running of the three-point vertices is also unrestricted. Thus we do not find an explanation for the emergence of effective universality. Therefore it remains to be clarified whether it persists under extensions of our truncation or whether it might be a mere accident at the present level of the truncation. We speculate that there is a mechanism underlying the emergence of effective universality that still remains to be discovered.

5.3 Threshold effects

Until now, we have only considered the N_s dependence of the beta functions for different avatars of the Newton coupling. However, ultimately we are interested in modelling the graviton propagator, which includes a non-trivial denominator. Thus, we include threshold effects as well as full anomalous dimensions in the beta functions and will now consider the full beta functions and evaluate fixed points. Specifically, in our truncation these are limited to the background cosmological constant $\bar{\lambda}$ in the background approximation versus the graviton mass parameter μ for the fluctuation field approximation. All fluctuation field propagators appear with a dependence on μ , *i.e.* unlike for the Newton coupling, this coupling has no analogue that is defined from a matter-gravity interaction term.

To capture the momentum-dependence of the flow, we will use a bi-local projection for the fluctuation Newton couplings, and will include the anomalous dimension projected at k . Our

projection prescriptions are

$$\begin{aligned} \beta_{G_{(3,0)}} &= 2 G_{(3,0)} + 3 \eta_h(k^2) G_{(3,0)} - \frac{24}{19} \left[\eta_h(k^2) - \eta_h(0) \right] \lambda_3 G_{(1,2)} \\ &+ \frac{64}{171} \frac{(32\pi)^2 \sqrt{G_{(3,0)}}}{k} \left[\text{Flow}_{\text{TT},G_{(3,0)}}^{(hhh)}(k^2) - \text{Flow}_{\text{TT},G_{(3,0)}}^{(hhh)}(0) \right], \end{aligned} \quad (5.16)$$

$$\begin{aligned} \beta_{G_{(1,2)}} &= 2 G_{(1,2)} + \eta_h(k^2) G_{(1,2)} + 2 \eta_s(k^2) G_{(1,2)} \\ &+ \frac{32\pi \sqrt{G_{(1,2)}}}{8} \frac{8}{3} \text{Flow}_{\text{TT},G_{(1,2)}}^{(h\varphi\varphi)}(k^2). \end{aligned} \quad (5.17)$$

Here, the subscripts $\text{TT},G_{(3,0)}$ and $\text{TT},G_{(1,2)}$ indicate that a projection onto the corresponding coupling is carried out on the right hand side of the exact renormalisation group equation, *cf.* the procedure of Refs. [7, 90]. $\text{Flow}_{\text{TT},G_{(3,0)}}^{(hhh)}(0)$ is the right hand side of the renormalisation group equation, projected onto contributions with three external gravitons and evaluated at vanishing momentum.

Here, we observe a markedly different behaviour in the background approximation from the fluctuation results. Whereas the fixed point for the background Newton coupling grows as a function of N_s , if threshold effects are neglected, it decreases if threshold effects are included. This is in contrast to the behaviour of $G_{(3,0)}^*$, $G_{(1,2)}^*$, both of which still increase as a function of N_s if threshold effects are taken into account, *cf.* Fig. 5.1.

Within a hybrid calculation with background couplings and a fluctuation anomalous dimension in Ref. [7], a behaviour qualitatively closer to that of the fluctuation system was observed. This can be traced back to a growth of the anomalous dimension, *cf.* Fig. 5.2. For anomalous dimensions exceeding the bound $\eta = 2$ (for bosonic fields), the UV behaviour of the regulator is altered [90]. This is a result of our choice of regulator, $R_k \sim Z_h$. As $Z_h \sim k^{-\eta_h}$ in the fixed-point regime, $\eta_h > 2$ destroys the UV behaviour of the regulator that should suppress all modes in the limit $k \rightarrow \infty$. For $\eta_h > 4$, signs of diagrams in the beta function for the Newton coupling start to flip. The type-I-regulator does not exhibit the same behaviour, as it features higher powers of $(1 - 2\lambda)$ in the denominator, Although the case $\eta_h > 4$ necessitates a re-examination with a regulator that is independent of Z_h , it is nevertheless intriguing to observe that the hybrid background-fluctuation system, where threshold effects destroy the similarity to the fluctuation system, attempts to restore this similarity through a very large η_h .

5.4 Effective universality

Going beyond the background field approximation results in the appearance of μ instead of $\bar{\lambda}$ on the right hand side of the flow equation. In contrast, the background couplings do not appear on the right hand side of the flow equation. Therefore the full system can be solved by first finding a fixed point solution for the fluctuation system. Inserting the fixed point values for the μ into the background flow then provides fixed points for the background system.

Once we only use fluctuation quantities on the right hand side, the fixed point in the Newton coupling exhibits an effective universality, *cf.* Fig. 5.1. Both fluctuation couplings as well as the background coupling take very similar values as a function of N_s and increase as a function of N_s . In particular, all three Newton couplings are driven to larger fixed-point values when N_s is increased. Remarkably, the quantitative deviations between the three different couplings are

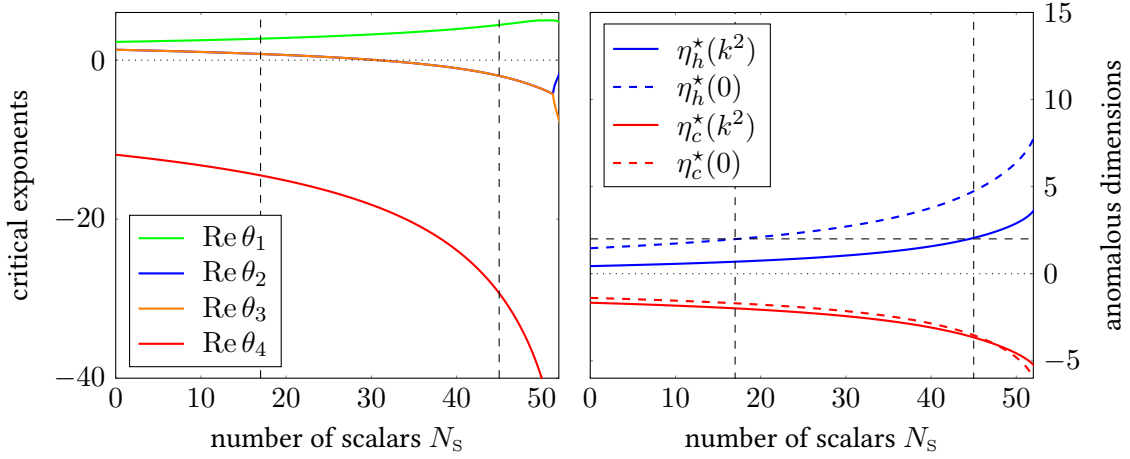


Figure 5.2: Numerical results for (real parts of) critical exponents, and anomalous dimensions as a function of N_s .

not even particularly large. Moreover, the behaviour is in agreement with that of g_3 in the last chapter, where we used a different choice of parametrisation, gauge, and projection. This robustness with respect to (unphysical) variations of the scheme is encouraging. As the fluctuation Newton couplings enter the graviton anomalous dimension, η_h increases as a function of N_s , cf. Fig. 5.1. This implies that the bounds on η_h , discussed in [90], are violated at large N_s . At the level of the cosmological constant, there is no such property.

5.4.1 Effective gravitational coupling

Ultimately, we are interested in the strength of the metric propagator, as this appears to be the decisive quantity to determine the quantum gravity effects on matter [103, 104].

The fluctuation field of the metric $h_{\mu\nu}$ enters the Feynman diagrams either via a pure propagator, or via a propagator that is dressed with a cutoff insertion $\partial_t R_k$. Accordingly, for any combination (n, m) , we can define two effective gravitational couplings through

$$g_1^{\text{eff}} \equiv \frac{G_{(n,m)}}{1 + \mu} \quad \text{and} \quad g_2^{\text{eff}} \equiv \frac{G_{(n,m)}}{(1 + \mu)^2}. \quad (5.18)$$

For diagrams contributing to the flow of vertices composed out of matter and gravitons, these are the only two combinations of $G_{(n,m)}$ and μ that may appear. In the case of pure gravity, however, diagrams feature additional factors of $G_{(n,0)}$ associated with the number of external gravitons n coming from the vertices of the Feynman diagrams. Hence, the beta functions for the purely gravitational couplings contain different powers of $1/1+\mu$ than powers of $G_{(3,0)}$. However, each internal graviton line is still associated with either of the two above effective couplings. Since μ stays approximately constant as N_s increases, while $G_{(3,0)}$ increases with N_s , $g_{\text{eff}, 1/2}$ increase as well, cf. Fig. 5.3.

5.4.2 Large N_s limit

In the limit of large N_s , all closed loops which do not feature a propagating scalar field are suppressed by a factor of $1/N_s$. We will assume here, that this suppression is not counteracted by an implicit

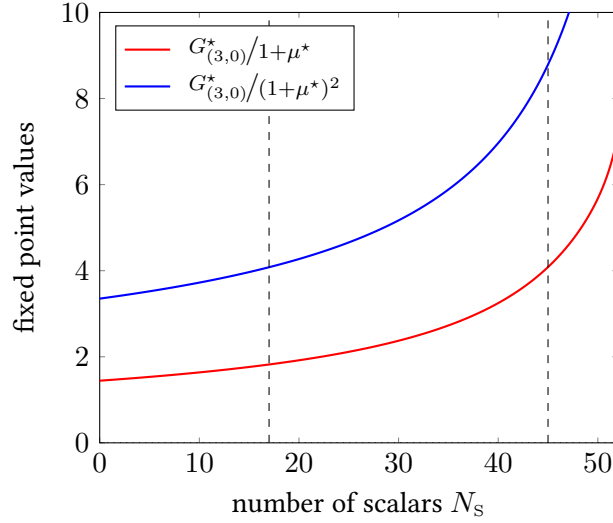


Figure 5.3: Numerical results for the fixed point values of the effective gravitational couplings as a function of N_s .

scaling with N_s of the couplings. With this assumption, we obtain the following large N_s limit within our truncation:

$$\beta_{G_{(3,0)}} = 2 G_{(3,0)} + 3 G_{(3,0)} \eta_h - \sqrt{G_{(3,0)}} G_{(1,2)}^{3/2} \frac{86 N_s}{1140\pi}, \quad (5.19)$$

$$\beta_{G_{(1,2)}} = 2 G_{(1,2)} + G_{(1,2)} \eta_h, \quad (5.20)$$

$$\eta_h = G_{(1,2)} \frac{N_s}{24\pi}, \quad (5.21)$$

$$\eta_s = 0. \quad (5.22)$$

As the system is only driven by scalar fluctuations, the increase of η_h does not pose a problem for the choice of regulator. The system admits three fixed points

$$G_{3\star} = 0, \quad g_{3\star} = 0, \quad \theta_{1,2} = -2, \quad (5.23)$$

$$G_{3\star} = -\frac{355008\pi}{9025N_s}, \quad g_{3\star} = -\frac{48\pi}{N_s}, \quad \theta_{1,2} = 2, \quad (5.24)$$

$$G_{3\star} = 0, \quad g_{3\star} = -\frac{48\pi}{N_s}, \quad \theta_1 = 2, \quad \theta_2 \rightarrow -i\infty. \quad (5.25)$$

Due to the presence of the Gaussian fixed point, the fixed point with negative values of $G_{(3,0)}$ and $G_{(1,2)}$ cannot be connected to positive values of the Newton couplings in the infrared. It must thus be regarded as unphysical.

5.5 Level-1 improvement

It is highly desirable to find a simple approximation of the system that ideally does not require the calculation of background flows and fluctuation flows. Therefore, we study whether the background

approximation can qualitatively or even quantitatively reproduce the behaviour of the full system. Such an approximate agreement appears to arise at the level of pure gravity, where fixed point results are quantitatively similar—although the structure of the threshold effects in the flow equations is different. These differences become more pronounced as scalar matter is taken into account.

We caution that the disagreement between background flows and fluctuation flows might conceivably be resolved by extended truncations that take into account higher-order operators.

In this section we want to study how to use the msWI, which we have already seen in Ch. 2, to improve upon the background field approximation. Related derivations and applications in a similar context can be found in Refs. [12, 27, 31, 52, 105–107].

5.5.1 Background field approximation and Ward identities

As we have outlined already in Sec. 2.5, in the case of full quantum gravity the msWI receives contributions from both the cutoff action as well as the gauge sector, which includes the gauge fixing term and the resulting ghost action. In our present application to the gravity-matter system we will ignore the background-dependence of the scalar fields, since we are dealing with a free theory here and only keep track of the background dependence of the metric field. The msWI for the latter then reads

$$\frac{\delta\Gamma_k}{\delta\bar{g}_{\mu\nu}} - \frac{\delta\Gamma_k}{\delta h_{\mu\nu}} = \frac{1}{2} \frac{1}{\sqrt{\bar{g}}} \text{Tr} \frac{\delta\sqrt{\bar{g}}R_k[\bar{g}]}{\delta\bar{g}_{\mu\nu}} G_k[\bar{g}, h] + \left\langle \frac{\delta S_{\text{gauge}}[\bar{g}, h]}{\delta\bar{g}_{\mu\nu}} - \frac{\delta S_{\text{gauge}}[\bar{g}, h]}{\delta h_{\mu\nu}} \right\rangle, \quad (5.26)$$

where $S_{\text{gauge}} = S_{\text{gf}} + S_{\text{ghost}}$ encodes both the gauge fixing as well as the ghost sector. In this chapter we want to work within the approximation

$$\lim_{k \rightarrow \infty} \left(\frac{\delta\Gamma_k}{\delta\bar{g}_{\mu\nu}} - \frac{\delta\Gamma_k}{\delta h_{\mu\nu}} \right) \simeq \frac{1}{2} \text{Tr} \frac{1}{\sqrt{\bar{g}}} \frac{\delta\sqrt{\bar{g}}R_k[\bar{g}]}{\delta\bar{g}_{\mu\nu}} G_k[\bar{g}, h], \quad (5.27)$$

dropping the background-dependence due to the gauge sector. The latter accounts for the difference of the wave function renormalisation of the fluctuation and the background graviton propagator. That is, we only want to improve the background field approximation by removing the background-dependence introduced through the regulator. Note however that comparing the contributions of the cutoff term and the gauge fixing sector to the ultraviolet flow, combinatorial arguments suggest that the cutoff term will contribute dominantly. This is because it couples to all fluctuation modes of the graviton, whilst the contributions of the gauge sector directly couple only to the longitudinal modes. Strictly speaking, however, this argument applies only to quantities which are invariant under the renormalisation group such as the Newton's constant G_N if and only if

$$\mu \frac{d}{d\mu} G_N = 0, \quad (5.28)$$

where μ is the renormalisation group scale of the underlying theory.

By taking a derivative with respect to the fluctuation field $h_{\mu\nu}$ of Eqn. (5.27), we can thus derive a modified background field approximation for the graviton two-point function. Namely, applying the operator $\delta_{\bar{g}} + \delta_h$ to Eqn. (5.27) and dropping mixed derivatives will result in

$$\frac{\delta^2\Gamma_k}{\delta h_{\mu\nu} \delta h_{\rho\sigma}} \simeq \frac{\delta^2\Gamma_k}{\delta\bar{g}_{\mu\nu} \delta\bar{g}_{\rho\sigma}} - \frac{1}{2} \left(\frac{\delta}{\delta\bar{g}_{\rho\sigma}} + \frac{\delta}{\delta h_{\rho\sigma}} \right) \text{Tr} \left[\frac{1}{\sqrt{\bar{g}}} \frac{\delta\sqrt{\bar{g}}R_k[\bar{g}]}{\delta\bar{g}_{\mu\nu}} G_k[\bar{g}, h] \right]. \quad (5.29)$$

In App. D we have studied a similar approximation in Yang-Mills theory, in order to derive the universal one-loop beta function of the Yang-Mills coupling. There we have shown in particular, that the equivalent of the fluctuation field derivative of the term in the square brackets on the right hand side of (5.29) gives only sub-leading contributions. In analogy, we will assume that the same feature holds true for gravity, and with that we arrive at the final approximation for the two-point function of the metric fluctuation field:

$$\frac{\delta^2 \Gamma_k}{\delta h_{\mu\nu} \delta h_{\rho\sigma}} \approx \frac{\delta^2 \Gamma_k}{\delta \bar{g}_{\mu\nu} \delta \bar{g}_{\rho\sigma}} - \frac{1}{2} \frac{\delta}{\delta \bar{g}_{\rho\sigma}} \int \frac{1}{\sqrt{\bar{g}}} \frac{\delta \sqrt{\bar{g}} R_k}{\delta \bar{g}_{\mu\nu}} \frac{\delta \Gamma_k}{\delta R_k}. \quad (5.30)$$

This approximation has been used in gravity *e.g.* in Refs. [52, 107]. Apart from the standard two-point function of the background field it contains a second, purely regulator induced term. The flow of this term is given by

$$F_{\text{RG}}(x) = \int_{x_0}^x dx' \frac{\partial R_k(x')}{\partial x'} G_k(x', \bar{R} = 0), \quad (5.31)$$

cf. also the definition Eqn. (D.8) for the Yang-Mills case. Here we have to restrict ourselves to infrared-finite regulators. Note that F_{RG} seem to depend on the parameter x_0 . However, this dependence will drop out later, as we take a functional derivative with respect to $\bar{g}_{\mu\nu}$. For simplicity, we will set $x_0 = 0$ from now on.

The corrections to the background approximation Eqn. (5.31) can be computed with heat-kernel techniques. Details of this derivation may be found in App. E. Similarly to our Yang-Mills example of App. D we have for infrared-finite regulators

$$\frac{1}{2} \text{Tr} \left[\frac{1}{\sqrt{\bar{g}}} \frac{\delta \sqrt{\bar{g}} R_k(\bar{\Delta})}{\delta \bar{g}_{\mu\nu}} G_k(\bar{\Delta}, \bar{R}) \right] = \frac{1}{2} \text{Tr} \frac{\delta}{\delta \bar{g}_{\mu\nu}} F_{\text{RG}}(\bar{\Delta}) + \frac{1}{2} \text{Tr} \frac{1}{\sqrt{\bar{g}}} \frac{\delta \sqrt{\bar{g}}}{\delta \bar{g}_{\mu\nu}} R_k(\bar{\Delta}) G_k(\bar{\Delta}, \bar{R}). \quad (5.32)$$

We further note that

$$\frac{\delta}{\delta \bar{g}_{\mu\nu}} F_{\text{RG}}(\bar{\Delta}) = \frac{\delta}{\delta \bar{g}_{\mu\nu}} \int_0^{\bar{\Delta}} dx' \frac{\partial R_k(x')}{\partial x'} G_k(x', \bar{R} = 0) = \frac{\delta R_k(\bar{\Delta})}{\delta \bar{g}_{\mu\nu}} G_k(\bar{\Delta}, \bar{R} = 0). \quad (5.33)$$

In gravity the luxury of using a background field to ensure gauge invariance turns into the necessity of using a background metric in the gauge fixing sector (if one insists on linear gauge fixing in the fluctuation field h). In ultraviolet flows, the cutoff operator with respect to this background metric however gives leading contributions to field operators such as two-, three-, and four-point functions. In terms of diffeomorphism invariant objects, this influences the running of the cosmological constant Λ , the curvature scalar R and the curvature scalar squared R^2 , which is the presumably minimal set of relevant operators in asymptotically safe quantum gravity.

In [34] the so-called bi-metric approach to quantum gravity was put forward, aiming at a distinction of the fluctuating and the background part of the metric. For computational reasons the following approximation was considered,

$$\Gamma_k[\bar{g}, h] = \Gamma_{\text{EH},k}[g] + \bar{\Gamma}_{\text{EH},k}[\bar{g}] + M_k \int d^4x \sqrt{\bar{g}} \left(\frac{\sqrt{\bar{g}}}{\sqrt{g}} \right)^n, \quad (5.34)$$

where $\Gamma_{\text{EH},k}, \bar{\Gamma}_{\text{EH},k}$ is the Einstein-Hilbert actions with cutoff-dependent parameters. In later extended computations [53], the last term has been dropped, $M_k = 0$. Evidently, this approximation violates the approximated msWI (5.29) and only holds if

$$\frac{\delta}{\delta h_{\rho\sigma}} \text{Tr} \left[\frac{1}{\sqrt{\bar{g}}} \frac{\delta \sqrt{\bar{g}} R_k[\bar{g}]}{\delta \bar{g}_{\mu\nu}} G_k[\bar{g}, h] \right] \approx 0, \quad (5.35)$$

at least at vanishing fluctuation field $h_{\mu\nu} = 0$.

5.5.2 Background flow equations

In this subsection we have a look at the flow equations of the background couplings. First of all, they are necessary to be able to directly compare results of the background field approximation with the fluctuation field results. Furthermore, we will use them to express the flow of the level one fluctuation couplings with the flow of the background quantities and the modified split Ward identities. Once again, we use a type I optimised cutoff and fix the gauge parameters to be $\alpha = \beta = 0$. We also specialise the background to a sphere in four dimensions.

We then obtain the following flow equations for the background couplings

$$\partial_t \bar{G} = (2 + \eta_s) \bar{G}, \quad (5.36)$$

$$\partial_t \bar{\Lambda} = -4 \bar{\Lambda} + \frac{\bar{\Lambda}}{\bar{G}} \partial_t \bar{G} + 8\pi \bar{G} \text{Flow}_{\bar{\Gamma}} \Big|_{\mathcal{O}(\bar{R}^0)}, \quad (5.37)$$

$$\eta_s = 16\pi \bar{G} \text{Flow}_{\bar{\Gamma}} \Big|_{\mathcal{O}(\bar{R}^1)}, \quad (5.38)$$

where

$$\begin{aligned} \text{Flow}_{\bar{\Gamma}} = & \frac{\sqrt{\bar{g}}}{32\pi^2} \left\{ \left[\frac{5 - \frac{5}{6}\eta_h}{1 - 2\lambda} + \frac{1 - \frac{1}{6}\eta_h}{1 - \frac{4}{3}\lambda} - 4 - \frac{2}{3}\eta_h + \frac{4}{3}\eta_c + N_s \right] k^4 \right. \\ & + \left[-\frac{10}{3} \frac{1 - \frac{1}{6}\eta_h}{(1 - 2\lambda)^2} - \frac{5}{3} \frac{1 - \frac{1}{4}\eta_h}{1 - 2\lambda} + \frac{1}{3} \frac{1 - \frac{1}{4}\eta_h}{1 - \frac{4}{3}\lambda} - \frac{23}{12} - \frac{7}{18}\eta_h + \frac{14}{18}\eta_c + \frac{1}{3}N_s \right] k^2 \bar{R} \\ & \left. + \left[\frac{20}{9} \frac{1}{(1 - 2\lambda)^3} + \frac{10}{9} \frac{1}{(1 - 2\lambda)^2} - \frac{1}{216} \frac{1}{1 - 2\lambda} + \frac{29}{1080} \frac{1}{1 - \frac{4}{3}\lambda} - \frac{149}{270} + \frac{29}{1080} N_s \right] \bar{R}^2 \right\} \\ & + \mathcal{O}(\bar{R}^3). \end{aligned} \quad (5.39)$$

Our result for the gravity part of the background flows agrees with Ref. [85], and the scalar part agrees with Ref. [7]. Details of the derivation may be found in App. E.

Note that the quantities in $\text{Flow}_{\bar{\Gamma}}$ should be taken from the fluctuation two-point function. In this case the background couplings are non-dynamical spectators. We obtain the usual background field approximation by setting $\lambda = \bar{\Lambda}$ and $\eta_h = \eta_s = \eta_c = 0$.

5.5.3 Fluctuation couplings via Ward identities

We can now analyse whether the level-1 improvement leads to a closed system that reproduces the fluctuation results more closely than the background approximation does. To that end, we

compare the N_S -dependence of the fixed points at each level of the approximation, *i.e.* we use the background couplings on the right hand side of the exact renormalisation group equation for the background approximation. Similarly, we use level-1 couplings on the right hand side to obtain the level-1 approximation. Finally, the fluctuation system is evaluated with the fluctuation couplings on the right hand side.

It turns out that the level-1 approximation tracks the background approximation in its qualitative dependence on N_S . On the other hand, the quantitative difference between the fixed point results for the fluctuation field and that in the level-1 approximation is smaller than the quantitative difference of the fluctuation results and the background results, *cf.* Fig. 5.4. Thus, the level-1 approximation might be considered a slight improvement over the background approximation. However, given its failure to capture the fluctuation results, a level-1 approximation seems hardly justified in view of the significantly increased computational effort—at least based on the results in our truncation. Details of the computation may be found in App. E.

Finally, we observe that the level-1 approximation even appears to break the effective universality that was observed for the Newton coupling. When evaluated with the fluctuation couplings on the right hand side of the flow equation, the qualitative and quantitative dependence of $G_{(1,0)}^*$ on N_S does not match that of the other couplings, *cf.* Fig. 5.5. For the ‘cosmological constants’, we make the opposite observation: whilst the background cosmological constant deviates strongly from the N_S dependence of the graviton mass parameter, the level-1 cosmological constant approaches it towards larger N_S . For the canonically most relevant coupling in the truncation, the step from the background coupling to the level-1 coupling is therefore a significant step towards effective universality.

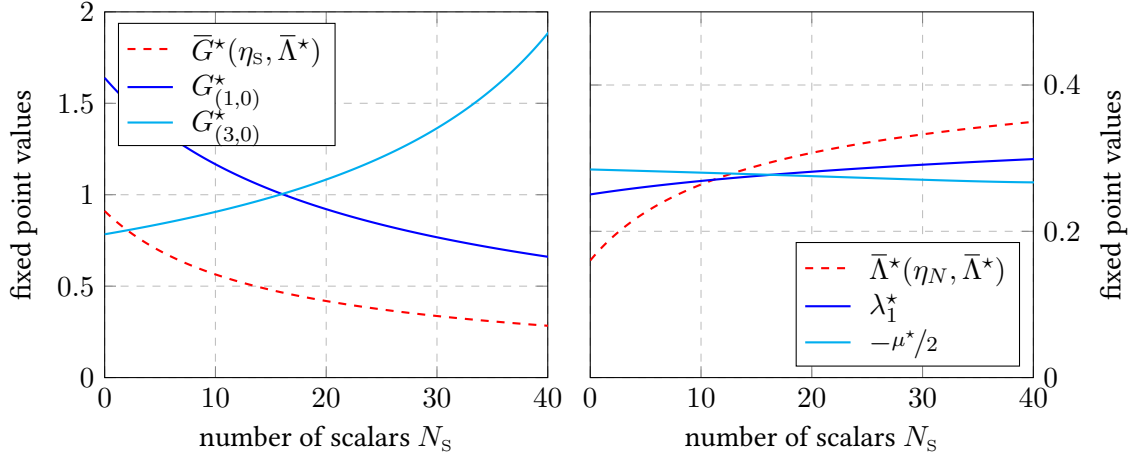


Figure 5.4: We show the fixed-point values as a function of N_S in the background approximation (red dashed), in the level-1 approximation (dark blue) and for the fluctuation system (light blue).

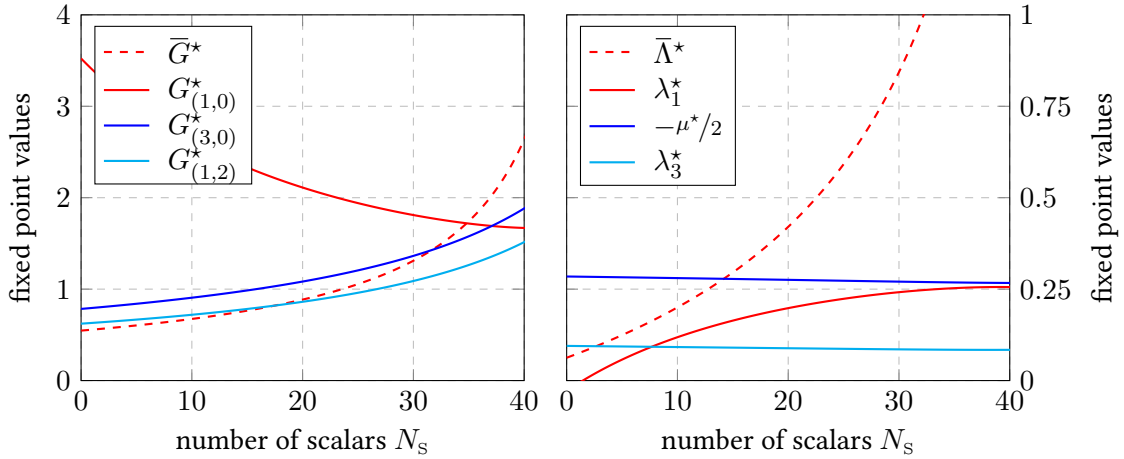


Figure 5.5: Comparison of different level- n gravitational couplings (left) and 'cosmological constants' (right). All couplings were evaluated with the input of the full fluctuation system on the right hand side. While the gravitational couplings behave qualitatively similar, the level- n 'cosmological constants' display significant differences in their behaviour.

This page intentionally left blank.

Conclusions

In this thesis we investigated the scenario of asymptotic safety in quantum gravity which may allow for the construction a fundamental quantum field theory of the gravitational interactions through the existence of an ultraviolet fixed point.

We were in particular interested in the inclusion of matter fields and their influence on the stability of gravitationally induced fixed points. This is important in order to investigate the viability of the asymptotic safety scenario for gravity together with the standard model of particle physics.

Chapter 1

In the first chapter we reviewed the technical device of the functional renormalisation group equation which was then used throughout this thesis. In particular, after inspection of Wilson's original idea of the renormalisation group and the introduction of smooth scale-dependent cutoff operators in the path integral, we derived said renormalisation group equation and studied some approximation schemes which are used in practical computations.

Using the language of the renormalisation group, we then gave an introduction to the asymptotic safety scenario, including the notion of fixed points as well as critical behaviour. To illustrate the tools and ideas introduced in this chapter, we concluded with the study of a \mathbb{Z}_2 invariant scalar field theory. This included the investigation of the Gaussian and Wilson-Fisher fixed point in $d = 4$ and $d = 3$ in a φ^4 -approximation, as well as the local potential approximation of the derivative expansion. We calculated the mass critical exponent ν using a polynomial truncation and studied scaling solutions using shooting methods.

Chapter 2

In the second chapter we studied the issue of background field independence in quantum gravity. It occurs when constructing the functional renormalisation group equation for gravity by introducing

a cutoff operator defined through a background metric. In this case, independence from the artificial metric can only be achieved if the appropriate modified split Ward identity is obeyed. However even if it is obeyed, background independence is guaranteed only in the infrared limit $k \rightarrow 0$. Renormalisation group properties on the other hand are defined at intermediate scales k . There is therefore the potential for conflict in this formulation between renormalisation group notions such as fixed points, and the requirement of background independence.

In this chapter we have continued an investigation of these issues in the setup of conformally truncated gravity, which was initiated in Ref. [35]. The first question that needs to be addressed is whether the Ward identity is compatible with the exact renormalisation group equation. At the exact level, compatibility is guaranteed since both identities are derived from the same partition function. Within the approximation of the derivative expansion, we have shown that compatibility holds if and only if either the anomalous dimension vanishes or the cutoff profile is power-law. We have also shown why precisely the derivative expansion breaks compatibility in general and why the special cases above restore it. Moreover, we argued that if the equations are incompatible they are overconstrained since then there is an infinite number of secondary constraints, and thus not even scale-dependent solutions can exist. We confirmed this latter conclusion by an example. Using a counting argument, we also saw that the fixed point equations and Ward identities together generically overconstrain the system when expanded in terms of vertices beyond the six-point level.

However, even if the equations are compatible, the Ward identity can still forbid fixed points. We have seen this explicitly in the local potential approximation. For example, we have seen that fixed points with respect to k are forbidden for the exponential parametrisation if the field grows a non-zero anomalous dimension. It is clear that the reasons for this conflict are general and not tied to the derivative expansion of the conformally truncated model *per se*.

For full quantum gravity, such conflicts between k -fixed points and background independence may also show up clearly in a vertex expansion, but generically it may not become visible until the six-point level. However for full quantum gravity, if we are to follow the standard procedure, we must also fix the gauge. The original Ward identity, which formally expresses background independence before gauge fixing, will no longer be compatible with the flow equation. Instead we must use the appropriate version which has contributions from the background dependence of the gauge fixing and ghost terms as well as from cutoff terms for the ghost action itself. These issues have been addressed in Refs. [50, 51], which we have reviewed here as well.

Chapter 3

In this third chapter we extended earlier investigations of scalar-tensor theories of gravity [56], where we used the exponential parametrisation of the metric. The *a priori* motivation of this parametrisation is that it respects the non-linear structure of the space of Riemannian metrics. It appears *a posteriori* that it leads to better behaved flows: there are no infrared singularities [56, 83] and the equations can be made gauge-independent even off-shell [83].

Moreover, quite generally, the use of the exponential parametrisation in conjunction with the physical gauge leads to simpler equations. In the theory considered here, they are sufficiently simple so that analytic scaling solutions can be found. We have given these solutions in arbitrary space-time dimensions and for any number of scalar fields. Relative to the earlier work Ref. [56], the advantage of having more than one scalar field is that there exists now an additional scaling solution for which the gravitational interactions remain attractive everywhere.

One interesting by-product of our analysis is the confirmation of several upper bounds for the

number of scalar fields, which is dictated by the requirement of having attractive gravitational interactions at the fixed point. These results are not confirmed when one uses a scalar-free cutoff, but we have argued that this is probably not physically correct.

We have also studied the large N -limit, for which we could construct exact analytic solutions. We have shown that they are unphysical in the type-I cutoff scheme which has been used.

Moreover, we have investigated the existence of the gravitationally dressed Wilson-Fisher scaling solution in $d = 3$ for various values of N . In particular, we have shown that physically acceptable solution do exist for small N , and we have given details for the case $N = 2$.

Chapter 4

In this chapter, we discussed how setting up the renormalisation group flow of a gravity-matter system, necessitates the distinction between couplings of matter to the background metric and couplings to fluctuations of the metric. We took a first step in disentangling the scale-dependence of the different couplings by studying the running of a vertex composed out of two scalar fields and one metric fluctuation field. From this vertex we defined an avatar of the Newton coupling, g_3 . We observed that the so-defined Newton coupling features an interacting fixed point when $N_S = 0$ where only metric fluctuations contribute to the renormalisation group flow. The universal critical exponent at this fixed point is close to that of other approximations and definitions. We consider this rather strong evidence for the asymptotic safety scenario in the pure-gravity case, that complements previous results. We emphasize that this is the first evidence for asymptotic safety in gravity-matter interactions, as all previous results are related to a Newton coupling which was defined from either background or fluctuation field gravitational interactions.

We also investigate the anomalous dimensions for different components of the graviton, and find a large negative anomalous dimension η_{TT} for the transverse, traceless mode which is not too far from the single-metric approximation $\eta = -2$. Such a large negative anomalous dimension implies that propagator is strongly suppressed in the ultraviolet, $p^{-2+\eta_{\text{TT}}}$. The corresponding position space propagator is reminiscent of a lower-dimensional setting. Thus our result is in line with other indications for some form of dynamical dimensional reduction in asymptotically safe gravity [64, 108–111], however see also Ref. [112].

On the other hand, the σ -anomalous dimension has the opposite sign. This suggests that different tensor structures in gravity exhibit different running—reminiscent of the difference between the transverse and longitudinal gluons in the infrared regime in Yang-Mills theory in Landau gauge. This result is an indication that one should also disentangle the flow of different tensor structures at the level of the vertices. We moreover observe a difference with respect to results obtained in the linear parametrisation, where the anomalous dimensions are typically smaller in absolute value.

Within functional renormalisation group flows, it is never possible to find a finite-dimensional closed truncation, as higher-order couplings always couple back into the flow of lower-order ones. This makes it necessary to choose a particular approximation to close the system of flow equations. Typical choices in the literature include setting higher-order couplings to zero, or equating them to lower order ones. In our results, we explicitly keep the dependence on all couplings that enter the flow of g_3 , enabling us to study the reliability of different approximations: We observe that the choice of approximation for those couplings for which no beta function is determined explicitly, quantitatively alters the properties of the fixed point. By treating, *e.g.* the pure-gravity couplings G_3 and G_4 as external parameters, we observe that the fixed point in g_3 persists for all values of these couplings that we have investigated, but, *e.g.* anomalous dimensions and the critical exponent

change. It is reassuring that the existence of a fixed point does not depend on making specific choices for couplings for which no beta function is determined, as of course all results in the literature make specific choices for these couplings. On the other hand, our investigation of the dependence of fixed-point properties on these choices highlights that quantitatively more precise results require more elaborate truncation schemes which disentangle some of these couplings.

In the case where we include scalar fluctuations, we observe that they have a significant impact on the dynamics. We first worked in the approximation, where we set the anomalous dimension for the scalar matter field to zero. There we observe that matter fluctuations have a destabilising effect on the gravitational fixed point, and move it toward larger values. This observation is in accordance with the general scenario discussed at the level of the background couplings in Refs. [7, 89], where it is argued that the inclusion of dynamical matter degrees of freedom will impact the microscopic dynamics for gravity, and an increasing number of scalars leads to a growth of the fixed point value for the Newton coupling. In Ref. [90] a similar behaviour is found for the fluctuation coupling G_3 . The increasing fixed-point value leads to an increase in the anomalous dimension for the graviton. As our regularisation scheme requires $\eta < 2$ for all anomalous dimensions, the region of $N_s \geq 14$ requires a re-investigation with a different regularisation scheme and/or significantly larger truncations. We should therefore take care when interpreting our present results. Keeping in mind this word of caution, we observe that scalar matter seems to have a significant effect on an interacting fixed point and could potentially destabilize it. However, it is reassuring to observe that $N_s = 4$, which corresponds to the number of scalar fields in the Standard Model, admits a gravitational fixed point in our setting, again in line with the results of Refs. [7, 89, 90].

Including a scalar anomalous dimension η_s leads to a very significant change already for $N_s = 1$ of the fixed-point properties. Based on a mode-counting argument, we expect that this strong effect of a single scalar field only arises within our truncation, and such significant effects of matter should not be expected for small N_s . We also identify a mechanism through which an extension of our truncation would potentially lead to significant changes of the anomalous dimension of the scalars: Quantum-gravity effects induce non-vanishing momentum-dependent self-interactions for scalars [96] which will couple back into η_s . If we take quantum-gravity induced matter self-interactions into account, not only η_s will change. Amongst the diagrams contributing to the flow of g_3 , there will also be one that features a closed scalar loop, and thus yields a contribution that scales with N_s . Within our present approximation, there is no such explicit contribution, and the N_s dependence only arises through the anomalous dimensions.

Chapter 5

In the last chapter we continued the study of a gravity-matter system with N_s minimally coupled scalar fields from the previous chapter. In particular we used again the vertex expansion and the fluctuation field approximation, but this time employing the linear parametrisation of the metric field and a conventional gauge fixing. This was done in order to establish the origin of the sign difference of the scalar contributions to the gravitational coupling $G_{(1,2)}$, which has been observed with respect to the computation done in Ref. [7].

We mostly used an approximation where we set all scalar-gravity couplings to $G_{(1,2)}$ and all pure gravity couplings to $G_{(3,0)}$. If we further neglect anomalous dimensions and restrict ourselves to one scalar field $N_s = 1$, we find a fixed point at positive values of the couplings and three relevant directions. Furthermore, we studied the N_s dependence of the three different avatars of Newton's coupling in our truncation in order to establish whether quantum gravity shows

effective universality, *i.e.* the different versions of the couplings behave similarly. To do so, we investigated two approximations. First we set the scalar contributions to the anomalous dimension of the graviton to zero $\eta_h = \eta_h|_{\text{grav}}$, for which we observed a strong violation of diffeomorphism invariance. Allowing η_h to have a non-trivial N_S -dependence on the other hand, forced the different versions of the gravitational coupling to behave quantitatively very similar up to large numbers of scalar fields. The physical origin of this effective universality, as well as the connection to the particular approximations studied here, is however not yet fully understood, and will require additional research.

To conclude the chapter, we tried to find a simple approximation of the gravity-matter system, for which the correct fluctuation field behaviour could be obtained within a background field approximation. Such a procedure could be of great practical benefit to study larger truncations. To this end, we accompanied the background flow equations with modified split Ward identities derived from an approximation where we tracked only the background dependence of the cutoff operator and dropped the gauge sector dependence. We can then compare the N_S -dependence of the level-1 couplings that result from the above procedure with the true fluctuation field couplings and the background approximation couplings. We find that the level-1 Newton coupling behaves qualitatively very similar to the one from the background approximation, although the numerical difference of the fixed point values decreases with respect to the fluctuation field calculation. In the case of the cosmological constant, however, the level-1 approximation seems to track the qualitative behaviour of the graviton mass parameter of the fluctuation field calculation much better than the background field approximation did in the first place. Judging from the truncation studied here, the practical value of this procedure remains somewhat unclear.

This page intentionally left blank.

Bibliography

- [1] Peter Labus, Roberto Percacci, and Gian Paolo Vacca. Asymptotic safety in $O(N)$ scalar models coupled to gravity. *Phys. Lett.*, B753:274–281, 2016, arXiv:1505.05393 [hep-th].
- [2] Pietro Donà, Astrid Eichhorn, Peter Labus, and Roberto Percacci. Asymptotic safety in an interacting system of gravity and scalar matter. *Phys. Rev.*, D93(4):044049, 2016, arXiv:1512.01589 [gr-qc]. [Erratum: *Phys. Rev.*, D93(12):129904, 2016].
- [3] Peter Labus, Tim R. Morris, and Zoë H. Slade. Background independence in a background dependent renormalization group. *Phys. Rev.*, D94(2):024007, 2016, arXiv:1603.04772 [hep-th].
- [4] Astrid Eichhorn, Peter Labus, Jan M. Pawłowski, and Manuel Reichert. Effective universality in gravity-matter flows. 2017. *In preparation*.
- [5] Steven Weinberg, SW Hawking, and W Israel. General Relativity: An Einstein Centenary Survey. *Cambridge University Press, Cambridge*, 1979.
- [6] Martin Reuter. Nonperturbative evolution equation for quantum gravity. *Phys. Rev.*, D57:971–985, 1998, arXiv:hep-th/9605030 [hep-th].
- [7] Pietro Donà, Astrid Eichhorn, and Roberto Percacci. Matter matters in asymptotically safe quantum gravity. *Phys. Rev.*, D89(8):084035, 2014, arXiv:1311.2898 [hep-th].
- [8] Roberto Percacci. A Short introduction to asymptotic safety. In *Time and Matter: Proceedings, 3rd International Conference, TAM2010, Budva, Montenegro, 4-8 October, 2010*, pages 123–142, 2011, arXiv:1110.6389 [hep-th].
- [9] Roberto Percacci. *An Introduction to Covariant Quantum Gravity and Asymptotic Safety*. 100 Years of General Relativity. 2017.

- [10] Juergen Berges, Nikolaos Tetradis, and Christof Wetterich. Nonperturbative renormalization flow in quantum field theory and statistical physics. *Phys. Rept.*, 363:223–386, 2002, arXiv:hep-ph/0005122 [hep-ph].
- [11] K. Aoki. Introduction to the nonperturbative renormalization group and its recent applications. *Int. J. Mod. Phys.*, B14:1249–1326, 2000.
- [12] Jan M. Pawłowski. Aspects of the functional renormalisation group. *Annals Phys.*, 322:2831–2915, 2007, arXiv:hep-th/0512261 [hep-th].
- [13] Holger Gies. Introduction to the functional RG and applications to gauge theories. *Lect. Notes Phys.*, 852:287–348, 2012, arXiv:hep-ph/0611146 [hep-ph].
- [14] Oliver J. Rosten. Fundamentals of the Exact Renormalization Group. *Phys. Rept.*, 511:177–272, 2012, arXiv:1003.1366 [hep-th].
- [15] Daniel F. Litim. Optimization of the exact renormalization group. *Phys. Lett.*, B486:92–99, 2000, arXiv:hep-th/0005245 [hep-th].
- [16] Daniel F. Litim. Optimized renormalization group flows. *Phys. Rev.*, D64:105007, 2001, arXiv:hep-th/0103195 [hep-th].
- [17] Alessandro Codello, Roberto Percacci, and Christoph Rahmede. Investigating the Ultraviolet Properties of Gravity with a Wilsonian Renormalization Group Equation. *Annals Phys.*, 324:414–469, 2009, arXiv:0805.2909 [hep-th].
- [18] Max Niedermaier and Martin Reuter. The Asymptotic Safety Scenario in Quantum Gravity. *Living Rev. Rel.*, 9:5–173, 2006.
- [19] M. Niedermaier. The Asymptotic safety scenario in quantum gravity: An Introduction. *Class. Quant. Grav.*, 24:R171–230, 2007, arXiv:gr-qc/0610018 [gr-qc].
- [20] Daniel F. Litim. Fixed Points of Quantum Gravity and the Renormalisation Group. 2008, arXiv:0810.3675 [hep-th]. [PoSQG-Ph,024(2007)].
- [21] Daniel F. Litim. Renormalisation group and the Planck scale. *Phil. Trans. Roy. Soc. Lond.*, A369:2759–2778, 2011, arXiv:1102.4624 [hep-th].
- [22] Roberto Percacci. Asymptotic Safety. 2007, arXiv:0709.3851 [hep-th].
- [23] Martin Reuter and Frank Saueressig. Quantum Einstein Gravity. *New J. Phys.*, 14:055022, 2012, arXiv:1202.2274 [hep-th].
- [24] Martin Reuter and Frank Saueressig. Asymptotic Safety, Fractals, and Cosmology. *Lect. Notes Phys.*, 863:185–223, 2013, arXiv:1205.5431 [hep-th].
- [25] Sandor Nagy. Lectures on renormalization and asymptotic safety. *Annals Phys.*, 350:310–346, 2014, arXiv:1211.4151 [hep-th].
- [26] Tim R. Morris. On truncations of the exact renormalization group. *Phys. Lett.*, B334:355–362, 1994, arXiv:hep-th/9405190 [hep-th].

- [27] Daniel F. Litim and Jan M. Pawłowski. Wilsonian flows and background fields. *Phys. Lett.*, B546:279–286, 2002, arXiv:hep-th/0208216 [hep-th].
- [28] I. Hamzaan Bridle, Juergen A. Dietz, and Tim R. Morris. The local potential approximation in the background field formalism. *JHEP*, 03:093, 2014, arXiv:1312.2846 [hep-th].
- [29] Martin Reuter and Christof Wetterich. Gluon condensation in nonperturbative flow equations. *Phys. Rev.*, D56:7893–7916, 1997, arXiv:hep-th/9708051 [hep-th].
- [30] Daniel F. Litim and Jan M. Pawłowski. On gauge invariant Wilsonian flows. In *The exact renormalization group. Proceedings, Workshop, Faro, Portugal, September 10-12, 1998*, pages 168–185, 1998, arXiv:hep-th/9901063 [hep-th].
- [31] Daniel F. Litim and Jan M. Pawłowski. Renormalization group flows for gauge theories in axial gauges. *JHEP*, 09:049, 2002, arXiv:hep-th/0203005 [hep-th].
- [32] Elisa Manrique and Martin Reuter. Bimetric Truncations for Quantum Einstein Gravity and Asymptotic Safety. *Annals Phys.*, 325:785–815, 2010, arXiv:0907.2617 [gr-qc].
- [33] Elisa Manrique, Martin Reuter, and Frank Saueressig. Matter Induced Bimetric Actions for Gravity. *Annals Phys.*, 326:440–462, 2011, arXiv:1003.5129 [hep-th].
- [34] Elisa Manrique, Martin Reuter, and Frank Saueressig. Bimetric Renormalization Group Flows in Quantum Einstein Gravity. *Annals Phys.*, 326:463–485, 2011, arXiv:1006.0099 [hep-th].
- [35] Juergen A. Dietz and Tim R. Morris. Background independent exact renormalization group for conformally reduced gravity. *JHEP*, 04:118, 2015, arXiv:1502.07396 [hep-th].
- [36] Mahmoud Safari. Splitting Ward identity. *Eur. Phys. J.*, C76(4):201, 2016, arXiv:1508.06244 [hep-th].
- [37] Pedro F. Machado and R. Percacci. Conformally reduced quantum gravity revisited. *Phys. Rev.*, D80:024020, 2009, arXiv:0904.2510 [hep-th].
- [38] Alfio Bonanno and Filippo Guarnieri. Universality and Symmetry Breaking in Conformally Reduced Quantum Gravity. *Phys. Rev.*, D86:105027, 2012, arXiv:1206.6531 [hep-th].
- [39] Martin Reuter and Holger Weyer. Background Independence and Asymptotic Safety in Conformally Reduced Gravity. *Phys. Rev.*, D79:105005, 2009, arXiv:0801.3287 [hep-th].
- [40] Martin Reuter and Holger Weyer. The Role of Background Independence for Asymptotic Safety in Quantum Einstein Gravity. *Gen. Rel. Grav.*, 41:983–1011, 2009, arXiv:0903.2971 [hep-th].
- [41] Daniel F. Litim and Jan M. Pawłowski. Flow equations for Yang-Mills theories in general axial gauges. *Phys. Lett.*, B435:181–188, 1998, arXiv:hep-th/9802064 [hep-th].
- [42] Daniel F. Litim and Jan M. Pawłowski. On gauge invariance and Ward identities for the Wilsonian renormalization group. *Nucl. Phys. Proc. Suppl.*, 74:325–328, 1999, arXiv:hep-th/9809020 [hep-th].

- [43] Tim R. Morris and John F. Tighe. Convergence of derivative expansions of the renormalization group. *JHEP*, 08:007, 1999, arXiv:hep-th/9906166 [hep-th].
- [44] Tim R. Morris and John F. Tighe. Convergence of derivative expansions in scalar field theory. *Int. J. Mod. Phys.*, A16:2095–2100, 2001, arXiv:hep-th/0102027 [hep-th].
- [45] Paul Adrien Maurice Dirac. *Lectures on Quantum Mechanics*, volume 2. Courier Corporation, 2001.
- [46] Paul A. M. Dirac. Generalized Hamiltonian dynamics. *Can. J. Math.*, 2:129–148, 1950.
- [47] Daniel F. Litim. Mind the gap. *Int. J. Mod. Phys.*, A16:2081–2088, 2001, arXiv:hep-th/0104221 [hep-th].
- [48] Juergen A. Dietz, Tim R. Morris, and Zoe H. Slade. Fixed point structure of the conformal factor field in quantum gravity. *Phys. Rev.*, D94(12):124014, 2016, arXiv:1605.07636 [hep-th].
- [49] Tim R. Morris. The Renormalization group and two-dimensional multicritical effective scalar field theory. *Phys. Lett.*, B345:139–148, 1995, arXiv:hep-th/9410141 [hep-th].
- [50] Tim R. Morris. Large curvature and background scale independence in single-metric approximations to asymptotic safety. *JHEP*, 11:160, 2016, arXiv:1610.03081 [hep-th].
- [51] Roberto Percacci and Gian Paolo Vacca. The background scale Ward identity in quantum gravity. *Eur. Phys. J.*, C77(1):52, 2017, arXiv:1611.07005 [hep-th].
- [52] Ivan Donkin and Jan M. Pawłowski. The phase diagram of quantum gravity from diffeomorphism-invariant RG-flows. 2012, arXiv:1203.4207 [hep-th].
- [53] Daniel Becker and Martin Reuter. En route to Background Independence: Broken split-symmetry, and how to restore it with bi-metric average actions. *Annals Phys.*, 350:225–301, 2014, arXiv:1404.4537 [hep-th].
- [54] Nicolai Christiansen, Daniel F. Litim, Jan M. Pawłowski, and Andreas Rodigast. Fixed points and infrared completion of quantum gravity. *Phys. Lett.*, B728:114–117, 2014, arXiv:1209.4038 [hep-th].
- [55] Nicolai Christiansen, Benjamin Knorr, Jan M. Pawłowski, and Andreas Rodigast. Global Flows in Quantum Gravity. *Phys. Rev.*, D93(4):044036, 2016, arXiv:1403.1232 [hep-th].
- [56] Roberto Percacci and Gian Paolo Vacca. Search of scaling solutions in scalar-tensor gravity. *Eur. Phys. J.*, C75(5):188, 2015, arXiv:1501.00888 [hep-th].
- [57] Tobias Henz, Jan Martin Pawłowski, Andreas Rodigast, and Christof Wetterich. Dilaton Quantum Gravity. *Phys. Lett.*, B727:298–302, 2013, arXiv:1304.7743 [hep-th].
- [58] E. Marchais. Ph.D. thesis. *University of Sussex*.
- [59] Gaurav Narain and Roberto Percacci. Renormalization Group Flow in Scalar-Tensor Theories. I. *Class. Quant. Grav.*, 27:075001, 2010, arXiv:0911.0386 [hep-th].

- [60] Julia Borchardt and Benjamin Knorr. Global solutions of functional fixed point equations via pseudospectral methods. *Phys. Rev.*, D91(10):105011, 2015, arXiv:1502.07511 [hep-th]. [Erratum: *Phys. Rev.* D93,no.8,089904(2016)].
- [61] Gaurav Narain and Roberto Percacci. On the scheme dependence of gravitational beta functions. *Acta Phys. Polon.*, B40:3439–3457, 2009, arXiv:0910.5390 [hep-th].
- [62] Djamel Dou and Roberto Percacci. The running gravitational couplings. *Class. Quant. Grav.*, 15:3449–3468, 1998, arXiv:hep-th/9707239 [hep-th].
- [63] Martin Reuter and Frank Saueressig. Renormalization group flow of quantum gravity in the Einstein-Hilbert truncation. *Phys. Rev.*, D65:065016, 2002, arXiv:hep-th/0110054 [hep-th].
- [64] O. Lauscher and Martin Reuter. Ultraviolet fixed point and generalized flow equation of quantum gravity. *Phys. Rev.*, D65:025013, 2002, arXiv:hep-th/0108040 [hep-th].
- [65] O. Lauscher and Martin Reuter. Flow equation of quantum Einstein gravity in a higher derivative truncation. *Phys. Rev.*, D66:025026, 2002, arXiv:hep-th/0205062 [hep-th].
- [66] Daniel F. Litim. Fixed points of quantum gravity. *Phys. Rev. Lett.*, 92:201301, 2004, arXiv:hep-th/0312114 [hep-th].
- [67] Peter Fischer and Daniel F. Litim. Fixed points of quantum gravity in extra dimensions. *Phys. Lett.*, B638:497–502, 2006, arXiv:hep-th/0602203 [hep-th].
- [68] Pedro F. Machado and Frank Saueressig. On the renormalization group flow of $f(R)$ -gravity. *Phys. Rev.*, D77:124045, 2008, arXiv:0712.0445 [hep-th].
- [69] Astrid Eichhorn, Holger Gies, and Michael M. Scherer. Asymptotically free scalar curvature-ghost coupling in Quantum Einstein Gravity. *Phys. Rev.*, D80:104003, 2009, arXiv:0907.1828 [hep-th].
- [70] Alessandro Codello and Roberto Percacci. Fixed points of higher derivative gravity. *Phys. Rev. Lett.*, 97:221301, 2006, arXiv:hep-th/0607128 [hep-th].
- [71] Dario Benedetti, Pedro F. Machado, and Frank Saueressig. Asymptotic safety in higher-derivative gravity. *Mod. Phys. Lett.*, A24:2233–2241, 2009, arXiv:0901.2984 [hep-th].
- [72] Astrid Eichhorn and Holger Gies. Ghost anomalous dimension in asymptotically safe quantum gravity. *Phys. Rev.*, D81:104010, 2010, arXiv:1001.5033 [hep-th].
- [73] Kai Groh and Frank Saueressig. Ghost wave-function renormalization in Asymptotically Safe Quantum Gravity. *J. Phys.*, A43:365403, 2010, arXiv:1001.5032 [hep-th].
- [74] Elisa Manrique, Stefan Rechenberger, and Frank Saueressig. Asymptotically Safe Lorentzian Gravity. *Phys. Rev. Lett.*, 106:251302, 2011, arXiv:1102.5012 [hep-th].
- [75] Stefan Rechenberger and Frank Saueressig. A functional renormalization group equation for foliated spacetimes. *JHEP*, 03:010, 2013, arXiv:1212.5114 [hep-th].
- [76] Dario Benedetti and Francesco Caravelli. The Local potential approximation in quantum gravity. *JHEP*, 06:017, 2012, arXiv:1204.3541 [hep-th]. [Erratum: *JHEP*10,157(2012)].

- [77] Juergen A. Dietz and Tim R. Morris. Asymptotic safety in the $f(R)$ approximation. *JHEP*, 01:108, 2013, arXiv:1211.0955 [hep-th].
- [78] K. Falls, D. F. Litim, K. Nikolakopoulos, and C. Rahmede. A bootstrap towards asymptotic safety. 2013, arXiv:1301.4191 [hep-th].
- [79] Dario Benedetti. On the number of relevant operators in asymptotically safe gravity. *Europhys. Lett.*, 102:20007, 2013, arXiv:1301.4422 [hep-th].
- [80] Nobuyoshi Ohta and Roberto Percacci. Higher Derivative Gravity and Asymptotic Safety in Diverse Dimensions. *Class. Quant. Grav.*, 31:015024, 2014, arXiv:1308.3398 [hep-th].
- [81] Maximilian Demmel, Frank Saueressig, and Omar Zanusso. RG flows of Quantum Einstein Gravity on maximally symmetric spaces. *JHEP*, 06:026, 2014, arXiv:1401.5495 [hep-th].
- [82] Kevin Falls, Daniel F. Litim, Konstantinos Nikolakopoulos, and Christoph Rahmede. Further evidence for asymptotic safety of quantum gravity. *Phys. Rev.*, D93(10):104022, 2016, arXiv:1410.4815 [hep-th].
- [83] Kevin Falls. Renormalization of Newton’s constant. *Phys. Rev.*, D92(12):124057, 2015, arXiv:1501.05331 [hep-th].
- [84] Kevin Falls. Critical scaling in quantum gravity from the renormalisation group. 2015, arXiv:1503.06233 [hep-th].
- [85] Holger Gies, Benjamin Knorr, and Stefan Lippoldt. Generalized Parametrization Dependence in Quantum Gravity. *Phys. Rev.*, D92(8):084020, 2015, arXiv:1507.08859 [hep-th].
- [86] Maximilian Demmel, Frank Saueressig, and Omar Zanusso. A proper fixed functional for four-dimensional Quantum Einstein Gravity. *JHEP*, 08:113, 2015, arXiv:1504.07656 [hep-th].
- [87] Alessandro Codello, Giulio D’Odorico, and Carlo Pagani. Consistent closure of renormalization group flow equations in quantum gravity. *Phys. Rev.*, D89(8):081701, 2014, arXiv:1304.4777 [gr-qc].
- [88] Nicolai Christiansen, Benjamin Knorr, Jan Meibohm, Jan M. Pawłowski, and Manuel Reichert. Local Quantum Gravity. *Phys. Rev.*, D92(12):121501, 2015, arXiv:1506.07016 [hep-th].
- [89] P. Donà, Astrid Eichhorn, and Roberto Percacci. Consistency of matter models with asymptotically safe quantum gravity. *Can. J. Phys.*, 93(9):988–994, 2015, arXiv:1410.4411 [gr-qc].
- [90] Jan Meibohm, Jan M. Pawłowski, and Manuel Reichert. Asymptotic safety of gravity-matter systems. *Phys. Rev.*, D93(8):084035, 2016, arXiv:1510.07018 [hep-th].
- [91] Mikhail Shaposhnikov and Christof Wetterich. Asymptotic safety of gravity and the Higgs boson mass. *Phys. Lett.*, B683:196–200, 2010, arXiv:0912.0208 [hep-th].
- [92] O. Zanusso, L. Zambelli, G. P. Vacca, and R. Percacci. Gravitational corrections to Yukawa systems. *Phys. Lett.*, B689:90–94, 2010, arXiv:0904.0938 [hep-th].
- [93] G. P. Vacca and O. Zanusso. Asymptotic Safety in Einstein Gravity and Scalar-Fermion Matter. *Phys. Rev. Lett.*, 105:231601, 2010, arXiv:1009.1735 [hep-th].

- [94] U. Harst and Martin Reuter. QED coupled to QEG. *JHEP*, 05:119, 2011, arXiv:1101.6007 [hep-th].
- [95] Astrid Eichhorn and Holger Gies. Light fermions in quantum gravity. *New J. Phys.*, 13:125012, 2011, arXiv:1104.5366 [hep-th].
- [96] Astrid Eichhorn. Quantum-gravity-induced matter self-interactions in the asymptotic-safety scenario. *Phys. Rev.*, D86:105021, 2012, arXiv:1204.0965 [gr-qc].
- [97] Kin-ya Oda and Masatoshi Yamada. Non-minimal coupling in Higgs–Yukawa model with asymptotically safe gravity. *Class. Quant. Grav.*, 33(12):125011, 2016, arXiv:1510.03734 [hep-th].
- [98] Mohamed M. Anber and John F. Donoghue. On the running of the gravitational constant. *Phys. Rev.*, D85:104016, 2012, arXiv:1111.2875 [hep-th].
- [99] Nobuyoshi Ohta, Roberto Percacci, and Gian Paolo Vacca. Flow equation for $f(R)$ gravity and some of its exact solutions. *Phys. Rev.*, D92(6):061501, 2015, arXiv:1507.00968 [hep-th].
- [100] Martin Reuter and Holger Weyer. Conformal sector of Quantum Einstein Gravity in the local potential approximation: Non-Gaussian fixed point and a phase of unbroken diffeomorphism invariance. *Phys. Rev.*, D80:025001, 2009, arXiv:0804.1475 [hep-th].
- [101] Sarah Folkerts, Daniel F. Litim, and Jan M. Pawłowski. Asymptotic freedom of Yang-Mills theory with gravity. *Phys. Lett.*, B709:234–241, 2012, arXiv:1101.5552 [hep-th].
- [102] Jan Meibohm and Jan M. Pawłowski. Chiral fermions in asymptotically safe quantum gravity. *Eur. Phys. J.*, C76(5):285, 2016, arXiv:1601.04597 [hep-th].
- [103] Astrid Eichhorn and Aaron Held. Viability of quantum-gravity induced ultraviolet completions for matter. 2017, arXiv:1705.02342 [gr-qc].
- [104] Astrid Eichhorn and Aaron Held. Top mass from asymptotic safety. 2017, arXiv:1707.01107 [hep-th].
- [105] Jan M. Pawłowski. Geometrical effective action and Wilsonian flows. 2003, arXiv:hep-th/0310018 [hep-th].
- [106] Jan Martin Pawłowski. On Wilsonian flows in gauge theories. <http://www.thphys.uni-heidelberg.de/~pawłowski/FRG/literature/review.pdf>.
- [107] Ivan Donkin. On the geometrical effective action. *Diploma thesis, Heidelberg*, 2008.
- [108] O. Lauscher and Martin Reuter. Fractal spacetime structure in asymptotically safe gravity. *JHEP*, 10:050, 2005, arXiv:hep-th/0508202 [hep-th].
- [109] Martin Reuter and Frank Saueressig. Fractal space-times under the microscope: A Renormalization Group view on Monte Carlo data. *JHEP*, 12:012, 2011, arXiv:1110.5224 [hep-th].
- [110] Stefan Rechenberger and Frank Saueressig. The R^2 phase-diagram of QEG and its spectral dimension. *Phys. Rev.*, D86:024018, 2012, arXiv:1206.0657 [hep-th].

- [111] Gianluca Calcagni, Astrid Eichhorn, and Frank Saueressig. Probing the quantum nature of spacetime by diffusion. *Phys. Rev.*, D87(12):124028, 2013, arXiv:1304.7247 [hep-th].
- [112] Giulio D’Odorico and Frank Saueressig. Quantum phase transitions in the Belinsky-Khalatnikov-Lifshitz universe. *Phys. Rev.*, D92(12):124068, 2015, arXiv:1511.00247 [gr-qc].
- [113] Marc H. Goroff and Augusto Sagnotti. The Ultraviolet Behavior of Einstein Gravity. *Nucl. Phys.*, B266:709–736, 1986.
- [114] Maximilian Demmel, Frank Saueressig, and Omar Zanusso. Fixed-Functionals of three-dimensional Quantum Einstein Gravity. *JHEP*, 11:131, 2012, arXiv:1208.2038 [hep-th].
- [115] Juergen A. Dietz and Tim R. Morris. Redundant operators in the exact renormalisation group and in the $f(R)$ approximation to asymptotic safety. *JHEP*, 07:064, 2013, arXiv:1306.1223 [hep-th].
- [116] Gian Paolo Vacca and Luca Zambelli. Multimeson Yukawa interactions at criticality. *Phys. Rev.*, D91(12):125003, 2015, arXiv:1503.09136 [hep-th].
- [117] Daniel F. Litim and Francesco Sannino. Asymptotic safety guaranteed. *JHEP*, 12:178, 2014, arXiv:1406.2337 [hep-th].
- [118] Daniel F. Litim, Matin Mojaza, and Francesco Sannino. Vacuum stability of asymptotically safe gauge-Yukawa theories. *JHEP*, 01:081, 2016, arXiv:1501.03061 [hep-th].
- [119] Holger Gies. Renormalizability of gauge theories in extra dimensions. *Phys. Rev.*, D68:085015, 2003, arXiv:hep-th/0305208 [hep-th].
- [120] L. F. Abbott. The Background Field Method Beyond One Loop. *Nucl. Phys.*, B185:189–203, 1981.
- [121] Maximilian Demmel and Andreas Nink. Connections and geodesics in the space of metrics. *Phys. Rev.*, D92(10):104013, 2015, arXiv:1506.03809 [gr-qc].
- [122] Astrid Eichhorn. On unimodular quantum gravity. *Class. Quant. Grav.*, 30:115016, 2013, arXiv:1301.0879 [gr-qc].
- [123] Astrid Eichhorn. The Renormalization Group flow of unimodular $f(R)$ gravity. *JHEP*, 04:096, 2015, arXiv:1501.05848 [gr-qc].
- [124] Andreas Nink. Field Parametrization Dependence in Asymptotically Safe Quantum Gravity. *Phys. Rev.*, D91(4):044030, 2015, arXiv:1410.7816 [hep-th].
- [125] Christof Wetterich. Exact evolution equation for the effective potential. *Phys. Lett.*, B301:90–94, 1993.
- [126] Tim R. Morris. The Exact renormalization group and approximate solutions. *Int. J. Mod. Phys.*, A9:2411–2450, 1994, arXiv:hep-ph/9308265 [hep-ph].
- [127] Tim R. Morris and Anthony W. H. Preston. Manifestly diffeomorphism invariant classical Exact Renormalization Group. *JHEP*, 06:012, 2016, arXiv:1602.08993 [hep-th].

-
- [128] Tim R. Morris. Derivative expansion of the exact renormalization group. *Phys. Lett.*, B329:241–248, 1994, arXiv:hep-ph/9403340 [hep-ph].
- [129] Tim R. Morris. Elements of the continuous renormalization group. *Prog. Theor. Phys. Suppl.*, 131:395–414, 1998, arXiv:hep-th/9802039 [hep-th].
- [130] Tim R. Morris. Equivalence of local potential approximations. *JHEP*, 07:027, 2005, arXiv:hep-th/0503161 [hep-th].
- [131] Vincenzo Branchina, Krzysztof A. Meissner, and Gabriele Veneziano. The Price of an exact, gauge invariant RG flow equation. *Phys. Lett.*, B574:319–324, 2003, arXiv:hep-th/0309234 [hep-th].
- [132] Maximilian Demmel, Frank Saueressig, and Omar Zanusso. RG flows of Quantum Einstein Gravity in the linear-geometric approximation. *Annals Phys.*, 359:141–165, 2015, arXiv:1412.7207 [hep-th].

This page intentionally left blank.

Appendices

A. Exponential parametrisation

In this appendix we will give some basic results concerning the exponential parametrisation of the metric field. This includes basic definitions, York decomposition, gauge fixing and ghost sector, as well as results for the variations of the Christoffel symbols, Ricci tensor and Ricci scalar curvature in the exponential parametrisation.

The signature of the metric we will use throughout is given by $(-, +, \dots, +)$.

A.1 Basic definitions

In d dimensions, any metric of given signature can be written as

$$g_{\mu\nu} = \theta^\rho{}_\mu \theta^\sigma{}_\nu \bar{g}_{\rho\sigma} \quad (\text{A.1})$$

where $\bar{g}_{\rho\sigma}$ is a fixed metric of the same signature and $\theta^\rho{}_\mu$ is a field with values in the group $GL(d)$. One can write $\theta = e^X$, where $X^\rho{}_\mu$ is a generic matrix. Let $Y_{\mu\nu} = \bar{g}_{\mu\rho} X^\rho{}_\nu$. It is possible to choose the matrix X in such a way that Y is symmetric. Then it is easy to check that

$$\begin{aligned} g &= \exp(X^T) \bar{g} \exp(X) = \exp(Y \bar{g}^{-1}) \bar{g} \exp(\bar{g}^{-1} Y) \\ &= \bar{g} \exp(\bar{g}^{-1} Y) \exp(\bar{g}^{-1} Y) = \bar{g} \exp(2X). \end{aligned} \quad (\text{A.2})$$

We therefore parametrize the metric as

$$g_{\mu\nu} = \bar{g}_{\mu\rho} (e^h)^\rho{}_\nu, \quad (\text{A.3})$$

where $\bar{g}_{\mu\rho}$ is a fixed but arbitrary background and $h = 2X$. We will use the background metric \bar{g} to raise and lower indices. Then due to the symmetry of $g_{\mu\nu}$ and $\bar{g}_{\mu\nu}$ also the tensor $h_{\mu\nu} = \bar{g}_{\mu\rho} h^\rho{}_\nu$ is

symmetric. We may then expand the metric and its inverse in powers of the tensor $h_{\mu\nu}$ around the background $\bar{g}_{\mu\nu}$:

$$g_{\mu\nu} = \bar{g}_{\mu\nu} + h_{\mu\nu} + \frac{1}{2} h_{\mu\lambda} h^{\lambda}_{\nu} + \frac{1}{6} h_{\mu}^{\lambda} h_{\nu}^{\kappa} h_{\kappa\lambda} + \frac{1}{24} h_{\mu}^{\lambda} h_{\nu}^{\kappa} h_{\lambda}^{\rho} h_{\kappa\rho} + \mathcal{O}(h^5), \quad (\text{A.4})$$

$$g^{\mu\nu} = \bar{g}^{\mu\nu} - h^{\mu\nu} + \frac{1}{2} h^{\mu\lambda} h_{\lambda}^{\nu} - \frac{1}{6} h^{\mu\lambda} h^{\nu\kappa} h_{\kappa\lambda} + \frac{1}{24} h^{\mu\lambda} h^{\nu\kappa} h_{\lambda}^{\rho} h_{\kappa\rho} + \mathcal{O}(h^5). \quad (\text{A.5})$$

In contrast to the usual linear split between background and fluctuation of the form $g_{\mu\nu} = \bar{g}_{\mu\nu} + h_{\mu\nu}$, here also the covariant metric is non-polynomial in the quantum field h^{μ}_{ν} . The linear terms above are the same as in the linear parametrisation, but from the second order onwards, they differ.

A.2 York decomposition

We can split the metric fluctuation field in its spin components as follows:

$$h_{\mu\nu} = h_{\mu\nu}^{\text{TT}} + \bar{\nabla}_{\mu} \xi_{\nu} + \bar{\nabla}_{\nu} \xi_{\mu} + \bar{\nabla}_{\mu} \bar{\nabla}_{\nu} \sigma - \frac{1}{d} \bar{g}_{\mu\nu} \bar{\nabla}^2 \sigma + \frac{1}{d} \bar{g}_{\mu\nu} h, \quad (\text{A.6})$$

where $h_{\mu\nu}^{\text{TT}}$ is the transverse and traceless spin-2 field satisfying $\bar{\nabla}^{\mu} h_{\mu\nu}^{\text{TT}} = 0$ and $h^{\text{TT}\mu}_{\mu} = 0$, ξ_{μ} is the transverse spin-1 field satisfying $\bar{\nabla}^{\mu} \xi_{\mu} = 0$, and σ and h are the two spin-0 degrees of freedom. The latter is the trace part of $h_{\mu\nu}$, $\text{Tr} h_{\mu\nu} = h$, which justifies the slight abuse of notation. The above splitting is called York decomposition.

For later convenience we will list several quadratic expressions in $h_{\mu\nu}^{\text{TT}}$, re-expressed in terms of their spin components, here, which will be used to derive the Hessian of the Einstein-Hilbert action. All these expressions hold on any Einstein manifold, in particular the sphere \mathbb{S}^d and flat space \mathbb{R}^d . For the latter we have $\bar{R} = 0$ and $\bar{\nabla}_{\mu} = \partial_{\mu}$.

$$\begin{aligned} \int d^d x \sqrt{\bar{g}} h_{\mu\nu} \bar{\nabla}^2 h^{\mu\nu} &= \int d^d x \sqrt{\bar{g}} \left[h_{\mu\nu}^{\text{TT}} \bar{\nabla}^2 h^{\text{TT}\mu\nu} - 2 \xi_{\mu} \left(\bar{\nabla}^2 + \frac{\bar{R}}{d} \right) \right. \\ &\quad \left. \times \left(\bar{\nabla}^2 + \frac{d+1}{d(d-1)} \bar{R} \right) \xi^{\mu} + \frac{d-1}{d} \sigma \bar{\nabla}^2 \left(\bar{\nabla}^2 + \frac{2\bar{R}}{d-1} \right) \left(\bar{\nabla}^2 + \frac{\bar{R}}{d-1} \right) \sigma + \frac{1}{d} h \bar{\nabla}^2 h \right], \end{aligned} \quad (\text{A.7})$$

$$\begin{aligned} \int d^d x \sqrt{\bar{g}} h_{\mu\nu} \nabla^{\mu} \nabla_{\rho} h^{\rho\nu} &= \int d^d x \sqrt{\bar{g}} \left[-\xi_{\mu} \left(\bar{\nabla}^2 + \frac{\bar{R}}{d} \right)^2 \xi^{\mu} + \frac{(d-1)^2}{d^2} \right. \\ &\quad \left. \times \sigma \bar{\nabla}^2 \left(\bar{\nabla}^2 + \frac{\bar{R}}{d-1} \right)^2 \sigma + \frac{2(d-1)}{d^2} h \bar{\nabla}^2 \left(\bar{\nabla}^2 + \frac{\bar{R}}{d-1} \right) \sigma + \frac{1}{d^2} h \bar{\nabla}^2 h \right], \end{aligned} \quad (\text{A.8})$$

$$\begin{aligned} \int d^d x \sqrt{\bar{g}} h_{\mu\nu} h^{\mu\nu} &= \int d^d x \sqrt{\bar{g}} \left[h_{\mu\nu}^{\text{TT}} h^{\text{TT}\mu\nu} + 2 \xi_{\mu} \left(-\bar{\nabla}^2 - \frac{\bar{R}}{d} \right) \xi^{\mu} \right. \\ &\quad \left. + \frac{d-1}{d} \sigma \bar{\nabla}^2 \left(\bar{\nabla}^2 + \frac{\bar{R}}{d-1} \right) \sigma + \frac{1}{d} h^2 \right]. \end{aligned} \quad (\text{A.9})$$

In order to simplify the form of the propagators for the various spin modes, and to recover the

canonical momentum dependence, we will often use the following redefinitions of the fields:

$$\xi'_\mu = \sqrt{-\bar{\nabla}^2 - \frac{\bar{R}}{d}} \xi_\mu, \quad (\text{A.10})$$

$$\sigma' = \sqrt{(-\bar{\nabla}^2)^2 + \frac{\bar{R}}{d-1} \bar{\nabla}^2} \sigma. \quad (\text{A.11})$$

A.3 Gauge fixing and ghost sector

As in any other gauge theory such as Yang-Mills, in gravity too we have to “factor out” spurious field configurations which are physically equivalent, when integrating over the fluctuation field $h_{\mu\nu}$ in the path integral. This can be done by fixing a gauge. In this section we review various choices to do so in the case of gravity.

A.3.1 Conventional gauge fixing

The conventional way of fixing the gauge in gravity follows the same procedure as in Yang-Mills theory, namely, one adds a term

$$S_{\text{gf}} = \frac{1}{2\alpha} \int d^d x \sqrt{\bar{g}} F_\mu \bar{g}^{\mu\nu} F_\nu, \quad (\text{A.12})$$

to the action, where

$$F_\mu[\bar{g}, h] = \bar{\nabla}_\rho h^\rho{}_\mu - \frac{\beta+1}{d} \bar{\nabla}_\mu h, \quad (\text{A.13})$$

is the gauge condition, fixed on the background manifold, and α and β are gauge parameters. One common choice of these parameters is the de Donder, or harmonic gauge:

$$\alpha = 1 \quad \text{and} \quad \beta = \frac{d}{2} - 1. \quad (\text{A.14})$$

Using the York decomposition and the field redefinitions of the last section, the gauge fixing term can also be expressed in terms of the spin components as follows:

$$S_{\text{gf}} = \frac{1}{2\alpha} \int d^d x \sqrt{\bar{g}} \left[\xi'_\mu \left(-\bar{\nabla}^2 - \frac{\bar{R}}{d} \right) \xi'^\mu + \left(\frac{d-1}{d} \sqrt{-\bar{\nabla}^2 - \frac{\bar{R}}{d-1}} \sigma' + \frac{\beta}{d} \sqrt{-\bar{\nabla}^2} h \right)^2 \right]. \quad (\text{A.15})$$

One then applies the Faddeev-Popov procedure, and exponentiates the resulting Faddeev-Popov determinant by introducing a Grassmann-valued vector field $C^\nu(x)$ with the following action

$$S_{\text{ghost}} = - \int d^d x \sqrt{\bar{g}} \bar{C}^\mu M_{\mu\nu} C^\nu, \quad (\text{A.16})$$

where \bar{C}^μ is the Dirac-conjugate field and the inverse propagator is given by:

$$M[\bar{g}, h]_{\mu\nu} = \bar{g}^{\sigma\lambda} \bar{\nabla}_\lambda (g_{\mu\nu} \nabla_\sigma + g_{\sigma\nu} \nabla_\mu) - \bar{g}^{\rho\sigma} \bar{\nabla}_\mu g_{\sigma\nu} \nabla_\rho. \quad (\text{A.17})$$

One then has to integrate over ghost and anti-ghost configuration in the partition function. This will introduce interactions between graviton and ghost particles. Also note that when applying the functional renormalisation group to theories gauge-fixed in this way, and additional cutoff operator for the ghost sector will have to be introduced.

A.3.2 Gauge transformation properties

In this section we will study the transformation properties of the metric $g_{\mu\nu}$ under local gauge transformations

$$g_{\mu\nu}(x_\mu) \mapsto g'_{\mu\nu}(x_\mu) \quad (\text{A.18})$$

i.e. diffeomorphisms of the space-time manifold. From these properties we will be able to infer how to fix the gauge symmetry when integrating over the metric field in the path integral.

The transformation of the metric under an infinitesimal diffeomorphism ε_μ , a d -dimensional coordinate vector, is given by the Lie derivative

$$\delta_\varepsilon g_{\mu\nu} = \mathcal{L}_\varepsilon g_{\mu\nu} \equiv \varepsilon^\rho \partial_\rho g_{\mu\nu} + g_{\mu\rho} \partial_\nu \varepsilon^\rho + g_{\nu\rho} \partial_\mu \varepsilon^\rho. \quad (\text{A.19})$$

Since we are using the background field method, we now have to choose the transformation of the background metric $\bar{g}_{\mu\nu}$ and the fluctuation field $h_{\mu\nu}$ in such a way, that when using the exponential parametrisation the combined transformations obey the last equation. The simplest way to do this, is to use the background transformation, which in the following we will denote with B. If we treat $\bar{g}_{\mu\nu}$ and $h_{\mu\nu}$ as tensors under infinitesimal gauge transformations, *i.e.*

$$\delta_\varepsilon^{(\text{B})} \bar{g}_{\mu\nu} = \mathcal{L}_\varepsilon \bar{g}_{\mu\nu}, \quad (\text{A.20})$$

$$\delta_\varepsilon^{(\text{B})} h^\mu{}_\nu = \mathcal{L}_\varepsilon h^\mu{}_\nu, \quad (\text{A.21})$$

then it also follows that

$$\delta_\varepsilon^{(\text{B})} (e^h)^\mu{}_\nu = \mathcal{L}_\varepsilon (e^h)^\mu{}_\nu, \quad (\text{A.22})$$

and Eqn. (A.19) is satisfied. A more convenient choice when using the background field method however, is the so-called ‘quantum’ gauge transformation Q, where the background metric $\bar{g}_{\mu\nu}$ is held fixed, and only the fluctuation field $h_{\mu\nu}$ transforms in a non-trivial way:

$$\delta_\varepsilon^{(\text{Q})} \bar{g}_{\mu\nu} = 0, \quad (\text{A.23})$$

$$\bar{g}_{\mu\rho} \delta_\varepsilon^{(\text{Q})} (e^h)^\rho{}_\nu = \mathcal{L}_\varepsilon g_{\mu\nu}. \quad (\text{A.24})$$

The right-hand side of the second transformation may be written as

$$\begin{aligned} \mathcal{L}_\varepsilon g_{\mu\nu} &= (\mathcal{L}_\varepsilon \bar{g}_{\mu\rho}) (e^h)^\rho{}_\nu + \bar{g}_{\mu\rho} (\mathcal{L}_\varepsilon (e^h)^\rho{}_\nu) \\ &= (\bar{\nabla}_\rho \varepsilon_\mu + \bar{\nabla}_\mu \varepsilon_\rho) (e^h)^\rho{}_\nu + g_{\mu\lambda} (e^{-h})^\lambda{}_\rho \mathcal{L}_\varepsilon (e^h)^\rho{}_\nu, \end{aligned} \quad (\text{A.25})$$

where, in the second equation we used the properties of the Lie derivative and rewrote the background metric in terms of the full metric and the fluctuation field. By contracting with the inverse metric, we can use the last expression to re-express the fluctuation field transformation in terms of $h_{\mu\nu}$ and the background metric only:

$$(e^{-h} \delta_\varepsilon^{(\text{Q})} e^h)^\mu{}_\nu = (e^{-h} \mathcal{L}_\varepsilon e^h)^\mu{}_\nu + (e^{-h})^\mu{}_\rho (\bar{\nabla}^\rho \varepsilon_\sigma + \bar{\nabla}_\sigma \varepsilon^\rho) (e^h)^\sigma{}_\nu. \quad (\text{A.26})$$

This way, we can expand the last expression in powers of $h_{\mu\nu}$:

$$\delta_\varepsilon^{(\text{Q})} h^\mu{}_\nu = \bar{\nabla}^\mu \varepsilon_\nu + \bar{\nabla}_\nu \varepsilon^\mu + \mathcal{L}_\varepsilon h^\mu{}_\nu + [\mathcal{L}_\varepsilon \bar{g}, h]^\mu{}_\nu + \mathcal{O}(\varepsilon h^2). \quad (\text{A.27})$$

Note that the first three terms coincide with the quantum transformation when using the linear background decomposition. When using a background field approximation, where one eventually sets $h_{\mu\nu} = 0$, it is sufficient to evaluate the last expression at the lowest order in $h_{\mu\nu}$:

$$\delta_\varepsilon^{(Q)} h^\mu{}_\nu = \bar{\nabla}^\mu \varepsilon_\nu + \bar{\nabla}_\nu \varepsilon^\mu + \mathcal{O}(h). \quad (\text{A.28})$$

In order to extract the transformation properties of single spin modes from this expression, we may split the coordinate transformation ε_μ into its transverse part ε_μ^T and its longitudinal part ε as follows

$$\varepsilon_\mu = \varepsilon_\mu^T + \frac{\bar{\nabla}^\mu}{\sqrt{-\bar{\nabla}^2}} \varepsilon, \quad (\text{A.29})$$

$$\bar{\nabla}^\mu \varepsilon_\mu^T = 0, \quad (\text{A.30})$$

where we introduced the normalisation in the denominator so that ε_μ^T and ε have the same dimensionality. With the above transformation of the full fluctuation field to lowest order and the split of the coordinate transformation ε , one can derive the following infinitesimal gauge transformations for the York-decomposed fields:

$$\delta_\varepsilon h_{\mu\nu}^{\text{TT}} = 0, \quad (\text{A.31})$$

$$\delta_\varepsilon \xi_\mu = \varepsilon_\mu^T, \quad (\text{A.32})$$

$$\delta_\varepsilon h = -2 \sqrt{-\bar{\nabla}^2} \varepsilon, \quad (\text{A.33})$$

$$\delta_\varepsilon \sigma = \frac{2}{\sqrt{-\bar{\nabla}^2}} \varepsilon. \quad (\text{A.34})$$

Note that the transverse, traceless mode $h_{\mu\nu}^{\text{TT}}$ as well as the combination $h - \bar{\nabla}^2 \sigma$ are gauge invariant quantities. In terms of the rescaled fields we have

$$\delta_\varepsilon \xi'_\mu = \sqrt{-\bar{\nabla}^2 - \frac{\bar{R}}{d}} \varepsilon_\mu^T, \quad (\text{A.35})$$

$$\delta_\varepsilon \sigma' = 2 \sqrt{-\bar{\nabla}^2 - \frac{\bar{R}}{d-1}} \varepsilon. \quad (\text{A.36})$$

A.3.3 Unimodular gauge

In the unimodular gauge one fixes the determinant of the (full) metric field to be the one of the background field: $g = \bar{g}$. In conformally reduced gravity, this is done at the kinematic level. Here, however, we want to use it to break diffeomorphism invariance of full gravity, thus introducing a Faddeev-Popov ghost determinant. Using the formula $\det e^{h_{\mu\nu}} = e^{\text{Tr} h_{\mu\nu}}$, one sees that the above gauge can be fixed by setting $h = 0$. Actually, it suffices to demand

$$h = \text{const.}, \quad (\text{A.37})$$

since a constant factor of the path integral can always be reabsorbed into the partition function. Inspecting the transformation property of h in the last section we find that the path integral needs

a ghost determinant $\det \sqrt{-\bar{\nabla}^2}$, which can be obtained by introducing a real, Grassmann-valued scalar ghost field C with action

$$S_{\text{ghost}}^{(h)} = \int d^d x \sqrt{\bar{g}} C (-\bar{\nabla}^2) C. \quad (\text{A.38})$$

The above condition however does not break the subset of gauge symmetries that leave the volume unchanged. Since these diffeomorphism are generated by the transverse part of the infinitesimal gauge transformation ε_μ^T , going back to the last section, we see that we can additionally demand

$$\xi'_\mu = 0. \quad (\text{A.39})$$

This may be achieved by introducing a second ghost field, which is a real, Grassmann-valued transverse vector field C_μ with action

$$S_{\text{ghost}}^{(\xi'_\mu)} = \int d^d x \sqrt{\bar{g}} C_\mu \bar{g}^{\mu\nu} \left(-\bar{\nabla}^2 - \frac{\bar{R}}{d} \right) C_\nu. \quad (\text{A.40})$$

A.4 Variations of Christoffel symbols and curvature invariants

In this section we will list expansions for various curvature invariants in terms of the fluctuation field $h_{\mu\nu}$ around an arbitrary background in the exponential parametrisation. These results will be used later to derive Hessians and vertices in various scalar-tensor theories of gravity.

In our conventions, the Riemann and Ricci tensors are given by

$$R^\alpha{}_{\beta\mu\nu} = \partial_\mu \Gamma_{\beta\nu}^\alpha - \partial_\nu \Gamma_{\beta\mu}^\alpha + \Gamma_{\mu\lambda}^\alpha \Gamma_{\beta\nu}^\lambda - \Gamma_{\nu\lambda}^\alpha \Gamma_{\beta\mu}^\lambda, \quad (\text{A.41})$$

$$R_{\mu\nu} = R^\alpha{}_{\mu\alpha\nu}, \quad (\text{A.42})$$

respectively. In the following, we will denote the expansion of a quantity Q as follows:

$$Q = Q^{(0)} + Q^{(1)} + Q^{(2)} + Q^{(3)} + Q^{(4)} + \dots, \quad (\text{A.43})$$

where $Q^{(n)}$ contains altogether n powers of $h^\mu{}_\nu$. In general we have $Q^{(0)} = \bar{Q}$, i.e. the quantity computed from the background metric. For the Christoffel symbols we will thus write as

$$\Gamma_{\mu\nu}^\kappa = \bar{\Gamma}_{\mu\nu}^\kappa + \Gamma_{\mu\nu}^{\kappa(1)} + \Gamma_{\mu\nu}^{\kappa(2)} + \Gamma_{\mu\nu}^{\kappa(3)} + \Gamma_{\mu\nu}^{\kappa(4)} + \dots, \quad (\text{A.44})$$

where

$$\Gamma_{\mu\nu}^{\kappa(1)} = \frac{1}{2} \bar{g}^{\kappa\rho} (\bar{\nabla}_\mu h_{\rho\nu} + \bar{\nabla}_\nu h_{\rho\mu} - \bar{\nabla}_\rho h_{\mu\nu}), \quad (\text{A.45})$$

$$\begin{aligned} \Gamma_{\mu\nu}^{\kappa(2)} &= -\frac{1}{2} h^{\kappa\rho} (\bar{\nabla}_\mu h_{\rho\nu} + \bar{\nabla}_\nu h_{\rho\mu} - \bar{\nabla}_\rho h_{\mu\nu}) \\ &\quad + \frac{1}{4} (\bar{\nabla}_\mu h_{\nu\sigma} h^{\sigma\kappa} + \bar{\nabla}_\nu h_{\mu\sigma} h^{\sigma\kappa} - \bar{\nabla}^\kappa h_{\mu\sigma} h^\sigma{}_\nu), \end{aligned} \quad (\text{A.46})$$

$$\begin{aligned} \Gamma_{\mu\nu}^{\kappa(3)} &= \frac{1}{12} \left[3 h^\kappa{}_\sigma h^{\sigma\rho} (\bar{\nabla}_\mu h_{\rho\nu} + \bar{\nabla}_\nu h_{\rho\mu} - \bar{\nabla}_\rho h_{\mu\nu}) \right. \\ &\quad - 3 h^{\kappa\rho} (\bar{\nabla}_\mu h_{\rho\sigma} h^\sigma{}_\nu + \bar{\nabla}_\nu h_{\rho\sigma} h^\sigma{}_\mu - \bar{\nabla}_\rho h_{\mu\sigma} h^\sigma{}_\nu) \\ &\quad \left. + \bar{\nabla}_\nu h_{\mu\rho} h^{\rho\sigma} h_\sigma{}^\kappa + \bar{\nabla}_\mu h_{\nu\rho} h^{\rho\sigma} h_\sigma{}^\kappa - \bar{\nabla}^\kappa h_{\mu\rho} h^{\rho\sigma} h_{\sigma\nu} \right], \end{aligned} \quad (\text{A.47})$$

$$\begin{aligned} \Gamma_{\mu\nu}^{\kappa(4)} &= \frac{1}{48} \left[-4 h^{\kappa\alpha} h_{\alpha\sigma} h^{\sigma\rho} (\bar{\nabla}_\mu h_{\rho\nu} + \bar{\nabla}_\nu h_{\rho\mu} - \bar{\nabla}_\rho h_{\mu\nu}) \right. \\ &\quad + 6 h^{\kappa\sigma} h_{\sigma\rho} (\bar{\nabla}_\mu h_{\alpha\nu} h^\alpha{}_\rho + \bar{\nabla}_\nu h_{\mu\alpha} h^\alpha{}_\rho - \bar{\nabla}_\rho h_{\mu\alpha} h^\alpha{}_\nu) \\ &\quad - 4 h^{\kappa\rho} (\bar{\nabla}_\mu h_{\nu\alpha} h^{\alpha\sigma} h_{\sigma\rho} + \bar{\nabla}_\nu h_{\mu\alpha} h^{\alpha\sigma} h_{\sigma\rho} - \bar{\nabla}_\rho h_{\mu\sigma} h^{\alpha\sigma} h_{\sigma\nu}) \\ &\quad \left. + \bar{\nabla}_\nu h_{\mu\sigma} h^{\sigma\alpha} h_{\alpha\rho} h^{\rho\kappa} + \bar{\nabla}_\mu h_{\nu\sigma} h^{\sigma\alpha} h_{\alpha\rho} h^{\rho\kappa} - \bar{\nabla}^\kappa h_{\mu\sigma} h^{\sigma\alpha} h_{\alpha\rho} h^\rho{}_\nu \right]. \end{aligned} \quad (\text{A.48})$$

In here, the covariant derivatives always act on everything to the right of them. In similar fashion, with the definitions above, one finds for the Ricci tensor:

$$\begin{aligned} R_{\mu\nu}^{(1)} &= -\frac{1}{2} (\bar{\nabla}^2 h_{\mu\nu} - \bar{\nabla}_\mu \bar{\nabla}_\rho h^\rho{}_\nu - \bar{\nabla}_\nu \bar{\nabla}_\rho h^\rho{}_\mu + \bar{\nabla}_\mu \bar{\nabla}_\nu h) \\ &\quad + \frac{1}{2} \bar{R}_{\mu\alpha} h^\alpha{}_\nu + \frac{1}{2} \bar{R}_{\nu\alpha} h^\alpha{}_\mu - \bar{g}_{\alpha\rho} \bar{R}^\rho{}_{\beta\nu} h^{\alpha\beta}, \end{aligned} \quad (\text{A.49})$$

$$\begin{aligned} R_{\mu\nu}^{(2)} &= \frac{1}{2} \bar{\nabla}_\mu (h^{\alpha\beta} \bar{\nabla}_\nu h_{\alpha\beta}) - \frac{1}{2} \bar{\nabla}_\alpha (h^{\alpha\beta} (\bar{\nabla}_\mu h_{\nu\beta} + \bar{\nabla}_\nu h_{\mu\beta} - \bar{\nabla}_\beta h_{\mu\nu})) \\ &\quad - \frac{1}{4} (\bar{\nabla}_\mu h^\beta{}_\alpha + \bar{\nabla}_\alpha h^\beta{}_\mu - \bar{\nabla}^\beta h_{\alpha\mu}) (\bar{\nabla}_\beta h^\alpha{}_\nu + \bar{\nabla}_\nu h^\alpha{}_\beta - \bar{\nabla}^\alpha h_{\beta\nu}) \\ &\quad + \frac{1}{4} \bar{\nabla}_\rho h (\bar{\nabla}_\mu h^\rho{}_\nu + \bar{\nabla}_\nu h^\rho{}_\mu - \bar{\nabla}^\rho h_{\mu\nu}) \\ &\quad + \frac{1}{4} \bar{\nabla}_\rho (\bar{\nabla}_\mu (h^{\rho\lambda} h_{\lambda\nu}) + \bar{\nabla}_\nu (h^{\rho\lambda} h_{\lambda\mu}) - \bar{\nabla}^\rho (h_{\mu\lambda} h^\lambda{}_\nu)) - \frac{1}{4} \bar{\nabla}_\mu \bar{\nabla}_\nu (h^{\rho\sigma} h_{\rho\sigma}), \end{aligned} \quad (\text{A.50})$$

$$\begin{aligned} R_{\mu\nu}^{(3)} &= \frac{1}{2} \bar{\nabla}_\lambda (h^{\lambda\sigma} h^\rho{}_\sigma \bar{\nabla}_\mu h_{\rho\nu}) - \frac{1}{4} \bar{\nabla}_\lambda (h^{\lambda\sigma} h^\rho{}_\sigma \bar{\nabla}_\rho h_{\mu\nu}) - \frac{1}{2} \bar{\nabla}_\lambda (h^{\lambda\sigma} \bar{\nabla}_\mu (h_{\rho\sigma} h^\rho{}_\nu)) \\ &\quad + \frac{1}{4} \bar{\nabla}_\lambda (h^{\lambda\sigma} \bar{\nabla}_\sigma (h_{\mu\rho} h^\rho{}_\nu)) + \frac{1}{6} \bar{\nabla}_\lambda \bar{\nabla}_\mu (h^\lambda{}_\sigma h^\sigma{}_\rho h^\rho{}_\nu) - \frac{1}{12} \bar{\nabla}^2 (h_{\mu\rho} h^\rho{}_\sigma h^\sigma{}_\nu) \\ &\quad - \frac{1}{4} h^{\rho\sigma} (\bar{\nabla}_\mu h_{\sigma\nu}) \bar{\nabla}_\rho h + \frac{1}{4} h^{\rho\sigma} (\bar{\nabla}_\sigma h_{\mu\nu}) \bar{\nabla}_\rho h + \frac{1}{4} h^\sigma{}_\nu (\bar{\nabla}_\mu h^{\rho\sigma}) \bar{\nabla}_\rho h \\ &\quad - \frac{1}{4} h_{\mu\sigma} (\bar{\nabla}^\rho h^\sigma{}_\nu) \bar{\nabla}_\rho h + \frac{1}{2} h^{\lambda\sigma} (\bar{\nabla}_\rho h_{\nu\sigma}) \bar{\nabla}_\lambda h^\rho{}_\mu - \frac{1}{2} h^{\lambda\sigma} (\bar{\nabla}_\sigma h_{\nu\rho}) \bar{\nabla}_\lambda h^\rho{}_\mu \\ &\quad - \frac{1}{2} h^\sigma{}_\nu (\bar{\nabla}_\rho h_{\lambda\sigma}) \bar{\nabla}^\lambda h^\rho{}_\mu + \frac{1}{2} h^{\sigma\nu} (\bar{\nabla}^\lambda h_{\rho\sigma}) \bar{\nabla}_\lambda h^\rho{}_\mu, \end{aligned} \quad (\text{A.51})$$

where implicit symmetrizations in μ and ν are understood on the right hand sides, and we again use the notation $\text{Tr } h_{\mu\nu} = h$. For the Ricci scalar we obtain the following results

$$R^{(1)} = \bar{\nabla}_\mu \bar{\nabla}_\nu h^{\mu\nu} - \bar{\nabla}^2 h - \bar{R}_{\mu\nu} h^{\mu\nu}, \quad (\text{A.52})$$

$$\begin{aligned} R^{(2)} &= \frac{3}{4} \bar{\nabla}_\alpha h_{\mu\nu} \bar{\nabla}^\alpha h^{\mu\nu} + h_{\mu\nu} \bar{\nabla}^2 h^{\mu\nu} - \bar{\nabla}_\rho h^\rho_\mu \bar{\nabla}_\sigma h^{\sigma\mu} + \bar{\nabla}_\rho h^\rho_\mu \bar{\nabla}^\mu h - 2 h_{\mu\nu} \bar{\nabla}^\mu \bar{\nabla}_\rho h^{\rho\nu} \\ &+ h_{\mu\nu} \bar{\nabla}^\mu \bar{\nabla}^\nu h - \frac{1}{2} \bar{\nabla}_\mu h_{\nu\alpha} \bar{\nabla}^\alpha h^{\mu\nu} - \frac{1}{4} \bar{\nabla}_\mu h \bar{\nabla}^\mu h + \bar{R}_{\alpha\beta\gamma\delta} h^{\alpha\gamma} h^{\beta\delta} \\ &+ \frac{1}{2} \bar{\nabla}_\mu \bar{\nabla}_\nu (h^{\mu\rho} h_\rho^\nu) - \frac{1}{2} \bar{\nabla}^2 (h^{\mu\rho} h_{\mu\rho}) - \frac{1}{2} \bar{R}_{\mu\nu} h^{\mu\rho} h_\rho^\nu, \end{aligned} \quad (\text{A.53})$$

$$\begin{aligned} R^{(3)} &= -\frac{1}{6} h^\mu_\rho h^\rho_\sigma h^{\sigma\nu} \bar{R}_{\mu\nu} + \frac{1}{4} h^\mu_\rho h^{\rho\nu} \bar{\nabla}^2 h_{\mu\nu} - \frac{1}{4} h^\mu_\rho h^\rho_\nu \bar{\nabla}_\nu \bar{\nabla}_\mu h \\ &+ \frac{1}{2} h^{\mu\nu} (\bar{\nabla}_\lambda h^{\lambda\rho}) \bar{\nabla}_\mu h_{\rho\nu} + \frac{1}{2} h^{\mu\nu} h^{\lambda\rho} \bar{\nabla}_\lambda \bar{\nabla}_\mu h_{\rho\nu} - \frac{1}{2} h^{\mu\nu} (\bar{\nabla}_\lambda h^{\lambda\rho}) \bar{\nabla}_\rho h_{\mu\nu} \\ &- \frac{1}{2} h^{\mu\nu} h^{\lambda\rho} \bar{\nabla}_\lambda \bar{\nabla}_\rho h_{\mu\nu} - \frac{1}{4} h^{\mu\nu} (\bar{\nabla}_\rho h) \bar{\nabla}_\mu h^\rho_\nu - \frac{1}{4} h^{\mu\nu} (\bar{\nabla}_\nu h^\lambda_\rho) \bar{\nabla}_\mu h^\rho_\lambda \\ &- \frac{1}{4} h^{\rho\sigma} (\bar{\nabla}_\mu h_\sigma^\mu) \bar{\nabla}_\rho h + \frac{1}{4} h^{\rho\sigma} (\bar{\nabla}_\sigma h) \bar{\nabla}_\rho h + \frac{1}{2} h^{\mu\sigma} (\bar{\nabla}_\rho h^\lambda_\sigma) \bar{\nabla}^\rho h_{\mu\lambda}, \end{aligned} \quad (\text{A.54})$$

where we have dropped total derivatives in the third variation.

One significant difference between the linear and the exponential parametrisation is that, due to the formula $\det e^{h_{\mu\nu}} = e^{\text{Tr } h_{\mu\nu}}$, only the trace of $h_{\mu\nu}$ enters in the definition of the determinant, at all orders. In particular, the square root of the determinant appearing in integral measure of the action has the following expansion:

$$\sqrt{g} = e^{h/2} \sqrt{\bar{g}} = \sqrt{\bar{g}} \left(1 + \frac{h}{2} + \frac{h^2}{8} + \frac{h^3}{48} + \frac{h^4}{384} + \dots \right). \quad (\text{A.55})$$

A.5 Hessian of the Einstein-Hilbert action and propagators

In this section we will use the results obtained so far to calculate the Hessian of the Einstein-Hilbert action

$$S_{\text{EH}} = \int d^d x \sqrt{g} R \quad (\text{A.56})$$

in the exponential parametrisation. We will also calculate the resulting graviton propagators on a flat background in the gauges we have discussed earlier. The latter will be used to evaluate Feynman diagrams when using the vertex expansion.

A.5.1 Hessian with and without York decomposition

To derive the Hessian of the Einstein-Hilbert action, one combines the expansions of \sqrt{g} and of R and integrates over spacetime. Dropping total derivatives, one can then rewrite the second order terms in the expansion as follows:

$$\begin{aligned} \int d^d x \sqrt{\bar{g}} \left[\frac{1}{4} h_{\mu\nu} \bar{\nabla}^2 h^{\mu\nu} - \frac{1}{2} h_{\mu\nu} \bar{\nabla}^\mu \bar{\nabla}^\rho h_\rho^\nu + \frac{1}{2} h \bar{\nabla}_\mu \bar{\nabla}_\nu h^{\mu\nu} - \frac{1}{4} h \bar{\nabla}^2 h \right. \\ \left. + \frac{1}{2} \bar{R}_{\mu\rho\nu\sigma} h^{\mu\nu} h^{\rho\sigma} - \frac{1}{2} \bar{R}_{\mu\nu} h^{\mu\nu} h + \frac{1}{8} \bar{R} h^2 \right]. \end{aligned} \quad (\text{A.57})$$

We can then rewrite this expression in terms of the independent fields $h_{\mu\nu}^{\text{TT}}$, ξ'_μ , σ' , and h , using the expressions Eqns. (A.7)–(A.9):

$$\int d^d x \sqrt{\bar{g}} \left[\frac{1}{4} h_{\mu\nu}^{\text{TT}} \left(-\bar{\nabla}^2 + \frac{2\bar{R}}{d(d-1)} \right) h^{\text{TT}\mu\nu} - \frac{(d-1)(d-2)}{4d^2} \sigma' (-\bar{\nabla}^2) \sigma' \right. \\ \left. - \frac{(d-1)(d-2)}{2d^2} h \sqrt{(-\bar{\nabla}^2)^2 + \frac{\bar{R}}{d-1} \bar{\nabla}^2} \sigma' - \frac{(d-1)(d-2)}{4d^2} h \left(-\bar{\nabla}^2 + \frac{(d-2)\bar{R}}{2(d-1)} \right) h \right]. \quad (\text{A.58})$$

Note that this expression is independent of the vector mode ξ'_μ , without fixing the gauge. Also note the infamous ‘wrong’ sign of the kinetic terms of the scalar modes for any $d > 2$.

A.5.2 Propagators in the conventional gauges

Adding the conventional gauge fixing terms to the second variation of the action one obtains:

$$\int d^d x \sqrt{\bar{g}} \left[\frac{1}{4} h_{\mu\nu}^{\text{TT}} \left(-\bar{\nabla}^2 + \frac{2\bar{R}}{d(d-1)} \right) h^{\text{TT}\mu\nu} + \frac{1}{2\alpha} \xi'_\mu \left(-\bar{\nabla}^2 - \frac{\bar{R}}{d} \right) \xi'^\mu \right. \\ \left. + \frac{(d-1)[2(d-1) - \alpha(d-2)]}{4\alpha d^2} \sigma' \left(-\bar{\nabla}^2 - \frac{2\bar{R}}{2(d-1) - \alpha(d-2)} \right) \sigma' \right. \\ \left. - \frac{(d-1)[\alpha(d-2) - 2\beta]}{2\alpha d^2} h \sqrt{(-\bar{\nabla}^2)^2 - \frac{\bar{R}}{d-1}} \sigma' \right. \\ \left. - \frac{\alpha(d-1)(d-2) - 2\beta^2}{4\alpha d^2} h \left(-\bar{\nabla}^2 + \frac{\alpha(d-2)^2 \bar{R}}{2[\alpha(d-1)(d-2) - 2\beta^2]} \right) h \right]. \quad (\text{A.59})$$

This shows that for this particular gauge fixing procedure the vector mode will propagate unless we take the limit $\alpha \rightarrow \infty$.

On a flat background \mathbb{R}^4 in four dimensions, using the de Donder gauge where $\alpha = 1$ and $\beta = d/2 - 1 = 1$, the propagators of the four independent fields thus become:

$$\left[\Gamma_k^{(h^{\text{TT}}, h^{\text{TT}})} + R_k^{h^{\text{TT}}} \right]_{\mu\nu\kappa\lambda}^{-1} = \frac{\delta_{\mu\kappa} \delta_{\nu\lambda} + \delta_{\mu\lambda} \delta_{\nu\kappa}}{p^2 + r_k(p^2)}, \quad (\text{A.60})$$

$$\left[\Gamma_k^{(\xi', \xi')} + R_k^{\xi'} \right]_{\mu\nu}^{-1} = \frac{\delta_{\mu\nu}}{p^2 + r_k(p^2)}, \quad (\text{A.61})$$

$$\left[\Gamma_k^{(\sigma', \sigma')} + R_k^{\sigma'} \right]^{-1} = \frac{8}{3} \frac{1}{p^2 + r_k(p^2)}, \quad (\text{A.62})$$

$$\left[\Gamma_k^{(h, h)} + R_k^h \right]^{-1} = -8 \frac{1}{p^2 + r_k(p^2)}. \quad (\text{A.63})$$

Here we assumed the use of a type I cutoff, following the conventions in Ref. [17]. Note that the de Donder gauge also diagonalises the Hessian. The ghost action on a flat background reads

$$S_{\text{ghost}} = \int d^4 x \left[\bar{C}_\mu \bar{g}^{\mu\nu} (-\partial^2) C_\nu \right], \quad (\text{A.64})$$

which yields the following propagator in momentum space:

$$\left[\Gamma_k^{(\bar{C}_\mu, C_\nu)} + R_k^{C_\mu} \right]_{\mu\nu}^{-1} = \frac{1}{2} \frac{\delta_{\mu\nu}}{p^2 + r_k(p^2)}. \quad (\text{A.65})$$

Note that contrary to the case of the unimodular gauge (which we will see shortly), even on a flat background the conventional gauge fixing introduces infinitely many interaction terms amongst ghost fields and the gravitational modes.

A.5.3 Propagators in the unimodular gauge

In the unimodular gauge, where $h = \text{const.}$ and $\xi'_\mu = 0$, the Hessian takes a very simple form:

$$\int d^d x \sqrt{\bar{g}} \left[\frac{1}{4} h_{\mu\nu}^{\text{TT}} \left(-\bar{\nabla}^2 + \frac{2\bar{R}}{d(d-1)} \right) h^{\text{TT}\mu\nu} - \frac{(d-1)(d-2)}{4d^2} \sigma' (-\bar{\nabla}^2) \sigma' \right]. \quad (\text{A.66})$$

On a flat background \mathbb{R}^4 in four dimensions the propagators for $h_{\mu\nu}^{\text{TT}}$ and σ' with a type I cutoff thus become

$$\left[\Gamma_k^{(h^{\text{TT}}, h^{\text{TT}})} + R_k^{h^{\text{TT}}} \right]_{\mu\nu\kappa\lambda}^{-1} = \frac{\delta_{\mu\kappa}\delta_{\nu\lambda} + \delta_{\mu\lambda}\delta_{\nu\kappa}}{p^2 + r_k(p^2)}, \quad (\text{A.67})$$

$$\left[\Gamma_k^{(\sigma', \sigma')} + R_k^{\sigma'} \right]^{-1} = -\frac{16}{3} \frac{1}{p^2}, \quad (\text{A.68})$$

respectively. The ghost sector on a flat background simply reads

$$S_{\text{ghost}} = \int d^4 x \left[C (-\partial^2) C + C_\mu \bar{g}^{\mu\nu} (-\partial^2) C_\nu \right], \quad (\text{A.69})$$

with a real, anti-commuting scalar C , and a real, anti-commuting, transverse vector ghost field C_μ . Introducing an additional type I cutoff operator for each ghost, we find the following propagators in momentum space:

$$\left[\Gamma_k^{(C_\mu, C_\nu)} + R_k^{C_\mu} \right]_{\mu\nu}^{-1} = \frac{1}{2} \frac{\delta_{\mu\nu}}{p^2 + r_k(p^2)}, \quad (\text{A.70})$$

$$\left[\Gamma_k^{(C, C)} + R_k^C \right]^{-1} = \frac{1}{2} \frac{1}{p^2 + r_k(p^2)}. \quad (\text{A.71})$$

B. Scalar-tensor theories

In this Appendix we will derive the Hessian for the model introduced in chapter 3 in some detail, making use of results obtained in the last appendix. We will also give an outline on how to derive the resulting flow equations using heat kernel techniques.

B.1 Derivation of the Hessian

We want to study the following effective average action

$$\Gamma_k[g_{\mu\nu}, \varphi^i] = \int d^d x \sqrt{g} \left[-F(\varphi) R + \frac{1}{2} \sum_{i=1}^{N_S} (\nabla \varphi^i)^2 + V(\varphi) \right] + S_{\text{gf}} + S_{\text{ghost}}, \quad (\text{B.1})$$

where we had previously defined $\varphi = \sqrt{\delta_{ij} \varphi^i \varphi^j}$ and we will use the Einstein summation convention throughout in this appendix. We will use the background field method by writing

$$\varphi^i = \bar{\varphi}^i + \delta\varphi^i, \quad i = 1, \dots, N, \quad (\text{B.2})$$

$$g_{\mu\nu} = \bar{g}_{\mu\rho} (e^h)^{\rho\nu}. \quad (\text{B.3})$$

With this definitions we can expand the full scalar field in powers of its fluctuation field:

$$\varphi = \bar{\varphi} + \frac{\delta_{ij} \bar{\varphi}^i \delta\varphi^j}{\bar{\varphi}} + \frac{1}{2} \frac{\delta_{ij} \delta\varphi^i \delta\varphi^j}{\bar{\varphi}} + \mathcal{O}(\delta\varphi^3) \quad (\text{B.4})$$

and we can expand any $O(N)$ invariant function $U(\varphi)$ about the background configuration as follows

$$U(\varphi) = U(\bar{\varphi}) + U'(\bar{\varphi}) \delta\varphi + \frac{1}{2} U''(\bar{\varphi}) \delta\varphi^2 + \mathcal{O}(\delta\varphi^3), \quad (\text{B.5})$$

where $U' = dU/d\varphi$. Additionally, we will define the radial and perpendicular projectors with respect to the background field configuration as follows

$$P_{\text{R}}^{ij} = \frac{\bar{\varphi}^i \bar{\varphi}^j}{\bar{\varphi}^2}, \quad (\text{B.6})$$

$$P_{\perp}^{ij} = \delta^{ij} - P_{\text{R}}^{ij}. \quad (\text{B.7})$$

Using the above expansion and these latter projectors, we can obtain the effective average action to second order in the scalar field fluctuations

$$\Gamma_k^{(\varphi, \varphi)} = \int d^d x \sqrt{\bar{g}} \frac{1}{2} \delta\varphi_i \left[(-\bar{\nabla}^2 + \bar{V}'' - \bar{F}'' \bar{R}) P_{\text{R}}^{ij} + \left(-\bar{\nabla}^2 + \frac{1}{\bar{\varphi}} (\bar{V}' - \bar{F}' \bar{R}) \right) P_{\perp}^{ij} \right] \delta\varphi_j, \quad (\text{B.8})$$

as well as the mixing between the scalar fields and the gravitational modes

$$\Gamma_k^{(\varphi, h_{\mu\nu})} = \int d^d x \sqrt{\bar{g}} \delta\varphi_i \frac{P_{\text{R}}^{ij} \bar{\varphi}_j}{\bar{\varphi}} \left[\frac{1}{2} h (\bar{V}' - \bar{F}' \bar{R}) - \bar{F}' (\bar{\nabla}_{\mu} \bar{\nabla}_{\nu} h^{\mu\nu} - \bar{\nabla}^2 h - \bar{R}_{\mu\nu} h^{\mu\nu}) \right]. \quad (\text{B.9})$$

Here we used results for the second variation of the Einstein-Hilbert action from the previous appendix, assuming the background to be an Einstein manifold. We also made use of the identity $\varphi_i \delta_{ij} \bar{\varphi}_j = \varphi_i P_{\text{R}}^{ij} \bar{\varphi}_j$.

Without loss of generality we can now separate the radial field component from the Goldstone bosons by fixing the background to be

$$\bar{\varphi}^i = 0, \quad i = 1, \dots, N-1, \quad (\text{B.10})$$

$$\bar{\varphi}^N = \bar{\rho} \quad (\text{B.11})$$

such that $\bar{\varphi} = \bar{\rho}$ and define $\varphi^N = \delta\varphi$. Then we have

$$\varphi_i P_{\text{R}}^{ij} \varphi_j = \delta\varphi^2, \quad (\text{B.12})$$

$$\varphi_i P_{\perp}^{ij} \varphi_j = \sum_{i=1}^{N-1} \varphi^i \varphi^i. \quad (\text{B.13})$$

With these relations, using the York decomposition and field redefinitions of app. A, the mixing between scalars and gravitational scalar modes can be rewritten as

$$\Gamma_k^{(\varphi, h_{\mu\nu})} = \int d^d x \sqrt{\bar{g}} \frac{(d-1)}{d} \bar{F}' \delta\varphi \left[-\sqrt{-\bar{\nabla}^2 \left(-\bar{\nabla}^2 - \frac{\bar{R}}{d-1} \right)} \sigma' + \left(-\bar{\nabla}^2 - \frac{(d-2)\bar{R}}{2(d-1)} + \frac{d\bar{V}'}{2(d-1)\bar{F}'} \right) h \right]. \quad (\text{B.14})$$

Finally, using the unimodular gauge $h = \text{const.}$, $\xi = 0$ and also neglecting the residual constant

mode of h , with the aid of results of the last appendix, we obtain the full Hessian

$$\begin{aligned} \Gamma_k^{(2)} = \int d^d x \sqrt{\bar{g}} \left[\frac{1}{4} \bar{F} h_{\mu\nu}^{\text{TT}} \left(-\bar{\nabla}^2 + \frac{2\bar{R}}{d(d-1)} \right) h^{\text{TT}\mu\nu} - \frac{(d-2)(d-1)}{4d^2} \bar{F} \sigma' (-\bar{\nabla}^2) \sigma' \right. \\ \left. + \frac{1}{2} \delta\varphi \left(-\bar{\nabla}^2 + \bar{V}'' - \bar{F}'' \bar{R} \right) \delta\varphi + \frac{1}{2} \sum_{i=1}^{N-1} \delta\varphi^i \left(-\bar{\nabla}^2 + \frac{1}{\bar{\rho}} (\bar{V}' - \bar{F}' \bar{R}) \right) \delta\varphi^i \right. \\ \left. - \frac{(d-1)}{d} \bar{F}' \delta\varphi \sqrt{-\bar{\nabla}^2 \left(-\bar{\nabla}^2 - \frac{\bar{R}}{d-1} \right)} \sigma' \right]. \quad (\text{B.15}) \end{aligned}$$

The Hessian can then be diagonalised by the transformation

$$\sigma'' = \sigma' - \frac{2d}{d-2} \frac{\bar{F}'}{\bar{F}} \sqrt{\frac{-\bar{\nabla}^2 - \frac{\bar{R}}{d-1}}{-\bar{\nabla}^2}} \delta\varphi, \quad (\text{B.16})$$

and the diagonal Hessian reads

$$\begin{aligned} \Gamma_k^{(2)} = \int d^d x \sqrt{\bar{g}} \left[\frac{1}{4} \bar{F} h_{\mu\nu}^{\text{TT}} \left(-\bar{\nabla}^2 + \frac{2\bar{R}}{d(d-1)} \right) h^{\text{TT}\mu\nu} - \frac{(d-2)(d-1)}{4d^2} \bar{F} \sigma'' (-\bar{\nabla}^2) \sigma'' \right. \\ \left. + \frac{1}{2} \delta\varphi \left(-\bar{\nabla}^2 + \bar{V}'' - \bar{F}'' \bar{R} + 2 \frac{d-1}{d-2} \frac{\bar{F}'^2}{\bar{F}} \left(-\bar{\nabla}^2 - \frac{\bar{R}}{d-1} \right) \right) \delta\varphi \right. \\ \left. + \frac{1}{2} \sum_{i=1}^{N-1} \delta\varphi^i \left(-\bar{\nabla}^2 + \frac{1}{\bar{\rho}} (\bar{V}' - \bar{F}' \bar{R}) \right) \delta\varphi^i \right]. \quad (\text{B.17}) \end{aligned}$$

The ghost action induced by the unimodular gauge fixing was given by:

$$S_{\text{ghost}} = \int d^d x \sqrt{\bar{g}} \left[C (-\bar{\nabla}^2) C + C_\mu \bar{g}^{\mu\nu} \left(-\bar{\nabla}^2 - \frac{\bar{R}}{d} \right) C_\nu \right]. \quad (\text{B.18})$$

B.2 Derivation of the flow equations

To obtain the flow equations of the functions $V(\varphi)$ and $F(\varphi)$, respectively, we will essentially follow the same steps as in Sec. 1.2.2 for scalar field theories. We start with the Hessian given above and define cutoff operators of type I with the help of the following matrix equation

$$\Gamma_k^{(2)} + R_k \equiv \Gamma_k^{(2)} \Big|_{-\bar{\nabla}^2 \mapsto P_k(-\bar{\nabla}^2)}. \quad (\text{B.19})$$

Throughout, we will employ the Litim cutoff, such that the regulated inverse propagator reads $P_k(p^2) = p^2 + (k^2 - p^2) \theta(k^2 - p^2)$. To extract the scale-dependence of the functions $V(\varphi)$ and $F(\varphi)$, we first set the field configuration φ to a constant such that

$$\partial_t \Gamma_k = \left[\partial_t V(\varphi) - \partial_t F(\varphi) \bar{R} \right] \int d^d x \sqrt{\bar{g}}. \quad (\text{B.20})$$

With this result, we can once more use the beta function of the effective average action as a generating functional for the beta functions of $V(\varphi)$ and $F(\varphi)$:

$$\partial_t V = \frac{1}{\text{vol}} \partial_t \Gamma_k \Big|_{\bar{R}=0}, \quad (\text{B.21})$$

$$\partial_t F = -\frac{1}{\text{vol}} \frac{\partial}{\partial \bar{R}} \partial_t \Gamma_k \Big|_{\bar{R}=0}, \quad (\text{B.22})$$

where we abbreviate the volume coefficient $\text{vol} \equiv \int d^d x \sqrt{g}$. To evaluate these expressions, we have to calculate the functional traces on the right hand side of the flow equation for the effective average action as a power series in \bar{R} . To evaluate functional traces on a d -dimensional sphere \mathbb{S}^d , we may use the method of heat kernels. Following Ref. [17], we can write the trace of some operator $W(\Delta)$ as

$$\text{Tr} W(\Delta) = \frac{1}{(4\pi)^{d/2}} \left[B_0(\Delta) Q_{d/2}[W] + B_2(\Delta) Q_{d/2-1}[W] + B_4(\Delta) Q_{d/2-2}[W] + \dots \right] \quad (\text{B.23})$$

where for type I cutoff we have $\Delta = -\bar{\nabla}^2$, and the Q -functionals are the same as defined in Eqn. (1.97). The heat kernel coefficients

$$B_n = \int d^d x \sqrt{g} \text{Tr} \mathbf{b}_n \quad (\text{B.24})$$

depend on the background curvature and scale as $\text{Tr} \mathbf{b}_n \in \mathcal{O}(\bar{R}^{n/2})$ in the curvature invariants. In particular, at the lowest order $\mathcal{O}(\bar{R}^0)$ we have

$$\text{Tr} W(-\bar{\nabla}^2) = \frac{B_0(-\bar{\nabla}^2)}{(4\pi)^{d/2}} Q_{d/2}[W]. \quad (\text{B.25})$$

For all fields Φ in $\Gamma_k^{(2)}$, the most general form of the Hessian we encounter here is $A_k^{(\Phi)}(-\bar{\nabla}^2) + B_k^{(\Phi)}$, with scale-dependent coefficients $A_k^{(\Phi)}$ and $B_k^{(\Phi)}$, of which the latter may depend on \bar{R} . With the cutoff operator (B.19) we thus find

$$\tilde{W}^{(\Phi)} = \frac{\dot{R}_k}{\Gamma_k^{(2)} + R_k} = \frac{(k^2 - z) \partial_t A_k^{(\Phi)} + 2k^2 A_k^{(\Phi)}}{A_k^{(\Phi)} \left[z + (k^2 - z) \theta(k^2 - z) \right] + B_k^{(\Phi)}} \theta(k^2 - z). \quad (\text{B.26})$$

With this expression of $\tilde{W}^{(\Phi)}$ we can calculate $Q_{d/2}[W]$ analytically, and we find for the flow of the potential V

$$\partial_t V = c_d k^d \sum_{\Phi} \left[\frac{A_k^{(\Phi)} + \frac{\partial_t A_k^{(\Phi)}}{d+2}}{A_k^{(\Phi)} + B_k^{(\Phi)}/k^2} \text{Tr} \mathbf{b}_0^{(\Phi)} \right], \quad (\text{B.27})$$

where $B_k^{(\Phi)}$ is evaluated at $\bar{R} = 0$, and $\Phi = \{h_{\mu\nu}^{\text{TT}}, \sigma'', \delta\varphi, \delta\varphi^i, C, C_\mu\}$. Note that the volume coefficient appearing on both sides cancelled. Inserting the coefficients for the various fields and passing to dimensionless variables will then result in Eqn. (3.2). For the function $F(\varphi)$ one proceeds in a similar manner, collecting contributions to (B.23) at $\mathcal{O}(\bar{R})$.

C. Running of interaction vertices

In this appendix we will derive interaction vertices for the effective average action given in Ch. 4, using results from app. A. We will also describe in some detail how to evaluate the Feynman diagrams appearing in Figs. 4.1 and 4.2.

C.1 Interaction vertices

We start with the fiducial action

$$\hat{\Gamma}_k[\bar{g}_{\mu\nu}, h_{\mu\nu}, \varphi] = \int d^4x \sqrt{g} \left[-\frac{R}{16\pi G_N} + \frac{1}{2} \sum_{i=1}^{N_S} (\nabla\varphi^i)^2 \right], \quad (\text{C.1})$$

from which we will derive our truncation as explained in detail in Ch. 4. In particular we will use a flat background in $d = 4$ and use the exponential parametrisation of the metric with the unimodular gauge, as described in app. A.

To calculate the diagrams in Figs. 4.1 and 4.2 we need to find the interaction vertices of two scalar particles interacting with one, two and three gravitons respectively, as well as the vertex of three gravitons. We will denote the momenta of the scalars by q_1 and q_2 and the ones of the gravitons by p_1 , p_2 and p_3 . The direction of the momenta will always be defined towards the vertex, *i.e.* ingoing. For the first class of vertices we only need to consider the kinetic term of the minimally coupled scalar

$$\frac{1}{2} \sum_{i=1}^{N_S} \int d^4x \sqrt{g} g^{\mu\nu} \partial_\mu \varphi^i \partial_\nu \varphi^i, \quad (\text{C.2})$$

since the rest of effective average action given above is independent of φ . We can expand the metric part of the kinetic term to third order in the graviton field $h_{\mu\nu}$, using the expansions for the inverse

metric and the determinant of the metric which were given in app. A. This results in

$$\sqrt{g} g^{\mu\nu} = \delta^{\mu\nu} - \kappa h^{\mu\nu} + \frac{\kappa^2}{2} h^{\mu\lambda} h_{\lambda}{}^{\nu} - \frac{\kappa^3}{6} h^{\mu\lambda} h^{\nu\kappa} h_{\kappa\lambda} + \mathcal{O}(h^4), \quad (\text{C.3})$$

where $\kappa \equiv \sqrt{32\pi G_N}$ and we used the field redefinition $h_{\mu\nu} \mapsto \kappa h_{\mu\nu}$. Then the relevant part for the 2-scalar-1-graviton vertex $V^{(2,1)\mu\nu} = \sqrt{\frac{g_3}{G_N}} \hat{\Gamma}_k^{(2,2)}$ is given by

$$\Gamma_k^{\text{rhs}} \subseteq -\frac{\kappa}{2} \sqrt{\frac{g_3}{G_N}} \sum_{i=1}^{N_S} \int d^4x h^{\mu\nu} \partial_\mu \varphi^i \partial_\nu \varphi^i. \quad (\text{C.4})$$

In order to disentangle the different spin components, one applies the York decomposition to the last expression. Passing to momentum space, we then find the following two vertices:

$$V^{(2,\text{TT})\mu\nu} = \sqrt{32\pi g_3} q_1^{(\mu} q_2^{\nu)}, \quad (\text{C.5})$$

$$V^{(2,\sigma)} = \sqrt{32\pi g_3} \left[\frac{1}{4} (q_1 \cdot q_2) - \frac{(p_1 \cdot q_1)(p_1 \cdot q_1)}{\|p_1\|^2} \right], \quad (\text{C.6})$$

where parenthesis denote complete symmetrizations, and TT and σ the propagating spin-2 and spin-0 modes, respectively. Proceeding in a similar fashion yields the following three flavours of 2-scalar-2-graviton vertices:

$$V^{(2,2\text{TT})\mu\nu\rho\sigma} = -\frac{32\pi g_4}{4} \left(q_1^{(\mu} q_2^{\rho)} \delta^{\nu\sigma} + q_1^{(\mu} q_2^{\sigma)} \delta^{\nu\rho} + q_1^{(\nu} q_2^{\rho)} \delta^{\mu\sigma} + q_1^{(\nu} q_2^{\sigma)} \delta^{\mu\rho} \right), \quad (\text{C.7})$$

$$V^{(2,\text{TT}\sigma)\mu\nu} = \frac{32\pi g_4}{4} \left(q_1^{(\mu} q_2^{\nu)} + \frac{(p_1 \cdot q_2) q_1^{(\mu} p_1^{\nu)}}{\|p_1\|^2} + \frac{(p_1 \cdot q_1) q_2^{(\mu} p_1^{\nu)}}{\|p_1\|^2} \right), \quad (\text{C.8})$$

$$V^{(2,2\sigma)} = -\frac{32\pi g_4}{2} \left(\frac{(p_1 \cdot p_2)(q_1 \cdot p_2)(q_2 \cdot p_1)}{\|p_1\|^2 \|p_2\|^2} + \frac{(p_1 \cdot p_2)(q_1 \cdot p_1)(q_2 \cdot p_2)}{\|p_1\|^2 \|p_2\|^2} \right. \\ \left. - \frac{1}{2} \frac{(q_1 \cdot p_2)(q_2 \cdot p_2)}{\|p_2\|^2} - \frac{1}{2} \frac{(q_1 \cdot p_1)(q_2 \cdot p_1)}{\|p_1\|^2} + \frac{(q_1 \cdot q_2)}{8} \right) \quad (\text{C.9})$$

There are another two flavours of the 2-scalar-3-graviton vertices we will need to evaluate all the diagrams.

$$V^{(2,3\text{TT})\mu\nu\rho\sigma\gamma\delta} = \frac{(32\pi g_5)^{3/2}}{12} \left(q_1^{(\mu} q_2^{\rho)} \mathbb{1}^{\nu\sigma\gamma\delta} + q_1^{(\mu} q_2^{\sigma)} \mathbb{1}^{\nu\rho\gamma\delta} + q_1^{(\mu} q_2^{\gamma)} \mathbb{1}^{\nu\rho\sigma\delta} + q_1^{(\mu} q_2^{\delta)} \mathbb{1}^{\nu\rho\sigma\gamma} \right. \\ \left. q_1^{(\nu} q_2^{\rho)} \mathbb{1}^{\mu\sigma\gamma\delta} + q_1^{(\nu} q_2^{\sigma)} \mathbb{1}^{\mu\rho\gamma\delta} + q_1^{(\nu} q_2^{\gamma)} \mathbb{1}^{\mu\rho\sigma\delta} + q_1^{(\nu} q_2^{\delta)} \mathbb{1}^{\mu\rho\sigma\gamma} \right. \\ \left. q_1^{(\rho} q_2^{\gamma)} \mathbb{1}^{\mu\nu\sigma\delta} + q_1^{(\rho} q_2^{\delta)} \mathbb{1}^{\mu\nu\sigma\gamma} + q_1^{(\sigma} q_2^{\gamma)} \mathbb{1}^{\mu\nu\rho\delta} + q_1^{(\sigma} q_2^{\delta)} \mathbb{1}^{\mu\nu\rho\gamma} \right), \quad (\text{C.10})$$

$$\begin{aligned}
V^{(2, \pi 2\sigma) \mu\nu} = & \frac{(32\pi g_5)^{3/2}}{2} \left(\frac{1}{8} q_1^{(\mu} q_2^{\nu)} - \frac{1}{4} \frac{(p_1 \cdot q_2) q_1^{(\mu} p_1^{\nu)}}{\|p_1\|^2} - \frac{1}{4} \frac{(p_1 \cdot q_1) q_2^{(\mu} p_1^{\nu)}}{\|p_1\|^2} \right. \\
& - \frac{1}{4} \frac{(p_2 \cdot q_2) q_1^{(\mu} p_2^{\nu)}}{\|p_2\|^2} - \frac{1}{4} \frac{(p_2 \cdot q_1) q_2^{(\mu} p_2^{\nu)}}{\|p_2\|^2} + \frac{1}{3} \frac{(q_1 \cdot p_1)(q_2 \cdot p_2) p_1^{(\mu} p_2^{\nu)}}{\|p_1\|^2 \|p_2\|^2} \\
& + \frac{1}{3} \frac{(q_1 \cdot p_2)(q_2 \cdot p_1) p_1^{(\mu} p_2^{\nu)}}{\|p_1\|^2 \|p_2\|^2} + \frac{1}{3} \frac{(p_1 \cdot p_2)(q_2 \cdot p_2) q_1^{(\mu} p_1^{\nu)}}{\|p_1\|^2 \|p_2\|^2} + \frac{1}{3} \frac{(p_1 \cdot p_2)(q_2 \cdot p_1) q_1^{(\mu} p_2^{\nu)}}{\|p_1\|^2 \|p_2\|^2} \\
& \left. + \frac{1}{3} \frac{(p_1 \cdot p_2)(q_1 \cdot p_2) q_2^{(\mu} p_1^{\nu)}}{\|p_1\|^2 \|p_2\|^2} + \frac{1}{3} \frac{(p_1 \cdot p_2)(q_1 \cdot p_1) q_2^{(\mu} p_2^{\nu)}}{\|p_1\|^2 \|p_2\|^2} \right), \tag{C.11}
\end{aligned}$$

Note in particular, that the strength of the interaction is independent of the magnitude of the graviton momenta, and only depends on the angles between the scalar and the graviton momenta. This independence is a consequence of the minimally-coupled form of the interaction and would hold for a truncation as the one considered in Ch. 3.

To derive the pure three- and four-graviton vertices, we first have to find the third and fourth order expansion of the Einstein-Hilbert action. With the results of app. A, on a flat background we find

$$\begin{aligned}
\sqrt{g} R \Big|_{\mathcal{O}(h_{\mu\nu}^3)} = & \frac{1}{4} h^{\mu\nu} \partial_\mu h^{\rho\sigma} \partial_\nu h_{\rho\sigma} - \frac{1}{4} h^{\mu\nu} \partial_\mu h \partial_\nu h + \frac{1}{4} h^{\mu\nu} \partial_\nu h \partial_\rho h_{\mu}{}^\rho \\
& + \frac{1}{4} h^{\mu\nu} \partial_\nu h_{\mu}{}^\rho \partial_\rho h + \frac{1}{8} h \partial_\rho h \partial^\rho h - \frac{1}{4} h \partial^\rho h \partial_\sigma h_{\rho}{}^\sigma \\
& - \frac{1}{2} h^{\mu\nu} \partial_\nu h_{\rho\sigma} \partial^\sigma h_{\mu}{}^\rho + \frac{1}{4} h \partial_\rho h_{\nu\sigma} \partial^\sigma h^{\nu\rho} - \frac{1}{8} h \partial_\sigma h_{\nu\rho} \partial^\sigma h^{\nu\rho}, \tag{C.12}
\end{aligned}$$

$$\begin{aligned}
\sqrt{g} R \Big|_{\mathcal{O}(h_{\mu\nu}^4)} = & \frac{1}{8} h^{\mu\nu} h^{\rho\sigma} \partial_\nu h_{\sigma\gamma} \partial_\rho h_{\mu}{}^\gamma - \frac{1}{8} h_{\mu}{}^\rho h^{\mu\nu} \partial_\nu h^{\sigma\gamma} \partial_\rho h_{\sigma\gamma} + \frac{1}{8} h h^{\nu\rho} \partial_\nu h^{\sigma\gamma} \partial_\rho h_{\sigma\gamma} \\
& + \frac{1}{8} h_{\mu}{}^\rho h^{\mu\nu} \partial_\nu h \partial_\rho h - \frac{1}{8} h h^{\nu\rho} \partial_\nu h \partial_\rho h - \frac{1}{12} h_{\mu}{}^\rho h^{\mu\nu} \partial_\rho h \partial_\sigma h_{\nu}{}^\sigma \\
& + \frac{1}{8} h h^{\nu\rho} \partial_\rho h \partial_\sigma h_{\nu}{}^\sigma - \frac{1}{12} h^{\mu\nu} h^{\rho\sigma} \partial_\nu h_{\mu\rho} \partial_\sigma h - \frac{1}{12} h_{\mu}{}^\rho h^{\mu\nu} \partial_\rho h_{\nu}{}^\sigma \partial_\sigma h \\
& + \frac{1}{8} h h^{\nu\rho} \partial_\rho h_{\nu}{}^\sigma \partial_\sigma h + \frac{1}{32} h^2 \partial_\mu h \partial^\mu h - \frac{1}{16} h^2 \partial^\mu h \partial_\nu h_{\mu}{}^\nu \\
& - \frac{1}{12} h^{\mu\nu} h^{\rho\sigma} \partial_\sigma h_{\nu\gamma} \partial^\gamma h_{\mu\rho} + \frac{1}{24} h^{\mu\nu} h^{\rho\sigma} \partial_\gamma h_{\nu\sigma} \partial^\gamma h_{\mu\rho} + \frac{1}{6} h_{\mu}{}^\rho h^{\mu\nu} \partial_\rho h_{\sigma\gamma} \partial^\gamma h_{\nu}{}^\sigma \\
& - \frac{1}{4} h h^{\nu\rho} \partial_\rho h_{\sigma\gamma} \partial^\gamma h_{\nu}{}^\sigma + \frac{1}{24} h_{\mu}{}^\rho h^{\mu\nu} \partial_\sigma h_{\rho\gamma} \partial^\gamma h_{\nu}{}^\sigma - \frac{1}{24} h_{\mu}{}^\rho h^{\mu\nu} \partial_\gamma h_{\rho\sigma} \partial^\gamma h_{\nu}{}^\sigma \\
& + \frac{1}{16} h^2 \partial_\sigma h_{\rho\gamma} \partial^\gamma h^{\rho\sigma} - \frac{1}{32} h^2 \partial_\gamma h_{\rho\sigma} \partial^\gamma h^{\rho\sigma}. \tag{C.13}
\end{aligned}$$

Note that both of these expressions reduce considerably once the gauge condition $h = 0$ is applied. The result of doing so yields Eqns. (4.3) and (4.4). We then have to decompose the full tensor fields

$h_{\mu\nu}$ into their spin components as before. For the 3-graviton vertices, with gauge fixing, that gives:

$$\sqrt{g} R \Big|_{\mathcal{O}(h_{\text{TT}}^3)} = \frac{1}{4} h^{\text{TT}\mu\nu} \partial_\mu h^{\text{TT}\rho\sigma} \partial_\nu h_{\rho\sigma}^{\text{TT}} - \frac{1}{2} h^{\text{TT}\mu\nu} \partial_\nu h_{\rho\sigma}^{\text{TT}} \partial^\sigma h^{\text{TT}}{}_{\mu}{}^\rho \quad (\text{C.14})$$

$$\begin{aligned} \sqrt{g} R \Big|_{\mathcal{O}(h_{\text{TT}}^2 \sigma)} &= \frac{1}{4} \partial_\mu h^{\text{TT}\rho\alpha} \partial_\nu h_{\rho\alpha}^{\text{TT}} \partial^\nu \partial^\mu \sigma - \frac{1}{2} h_{\rho}^{\text{TT}\alpha} \partial_\mu h_{\nu\alpha}^{\text{TT}} \partial^\rho \partial^\nu \partial^\mu \sigma + \frac{1}{2} h_{\rho}^{\text{TT}\alpha} \partial^\rho \partial^\nu \partial^\mu \sigma \partial_\alpha h_{\mu\nu}^{\text{TT}} \\ &- \frac{1}{2} h_{\nu}^{\text{TT}\alpha} \partial^\rho \partial^\nu \partial^\mu \sigma \partial_\alpha h_{\mu\rho}^{\text{TT}} + \frac{1}{8} h^{\text{TT}\rho\alpha} \partial^\nu \partial_\mu \partial^\mu \sigma \partial_\alpha h_{\nu\rho}^{\text{TT}} - \frac{1}{2} \partial_\mu h_{\rho\alpha}^{\text{TT}} \partial^\nu \partial^\mu \sigma \partial^\alpha h_{\nu}^{\text{TT}\rho} \\ &+ \frac{1}{8} \partial_\mu \partial^\mu \sigma \partial_\rho h_{\nu\alpha}^{\text{TT}} \partial^\alpha h^{\text{TT}\nu\rho} - \frac{1}{16} \partial_\mu \partial^\mu \sigma \partial_\alpha h_{\nu\rho}^{\text{TT}} \partial^\alpha h^{\text{TT}\nu\rho} \end{aligned} \quad (\text{C.15})$$

$$\begin{aligned} \sqrt{g} R \Big|_{\mathcal{O}(h_{\text{TT}} \sigma^2)} &= \frac{1}{4} \partial_\mu \partial^\alpha \partial^\rho \sigma \partial_\nu h_{\rho\alpha}^{\text{TT}} \partial^\nu \partial^\mu \sigma + \frac{1}{4} \partial_\mu h_{\rho\alpha}^{\text{TT}} \partial_\nu \partial^\alpha \partial^\rho \sigma \partial^\nu \partial^\mu \sigma \\ &- \frac{1}{2} \partial_\mu \partial^\alpha \partial^\rho \sigma \partial^\nu \partial^\mu \sigma \partial_\rho h_{\nu\alpha}^{\text{TT}} + \frac{1}{8} h_{\nu\alpha}^{\text{TT}} \partial^\nu \partial_\mu \partial^\mu \sigma \partial_\rho \partial^\alpha \partial^\rho \sigma - \frac{1}{2} h_{\rho\alpha}^{\text{TT}} \partial_\mu \partial^\alpha \partial_\nu \sigma \partial^\rho \partial^\nu \partial^\mu \sigma \\ &+ \frac{1}{4} h_{\rho\alpha}^{\text{TT}} \partial^\rho \partial^\nu \partial^\mu \sigma \partial^\alpha \partial_\nu \partial_\mu \sigma - \frac{1}{2} \partial_\mu h_{\rho\alpha}^{\text{TT}} \partial^\nu \partial^\mu \sigma \partial^\alpha \partial_\nu \partial^\rho \sigma - \frac{3}{32} h_{\nu\alpha}^{\text{TT}} \partial^\nu \partial_\mu \partial^\mu \sigma \partial^\alpha \partial_\rho \partial^\rho \sigma \\ &+ \frac{1}{8} \partial_\mu h_{\nu\alpha}^{\text{TT}} \partial^\nu \partial^\mu \sigma \partial^\alpha \partial_\rho \partial^\rho \sigma + \frac{1}{8} h_{\rho\alpha}^{\text{TT}} \partial^\nu \partial_\mu \partial^\mu \sigma \partial^\alpha \partial^\rho \partial_\nu \sigma + \frac{1}{8} \partial_\mu \partial^\mu \sigma \partial_\nu h_{\rho\alpha}^{\text{TT}} \partial^\alpha \partial^\rho \partial^\nu \sigma \\ &+ \frac{1}{8} \partial_\mu \partial^\mu \sigma \partial_\rho h_{\nu\alpha}^{\text{TT}} \partial^\alpha \partial^\rho \partial^\nu \sigma - \frac{1}{8} \partial_\mu \partial^\mu \sigma \partial_\alpha h_{\nu\rho}^{\text{TT}} \partial^\alpha \partial^\rho \partial^\nu \sigma \end{aligned} \quad (\text{C.16})$$

$$\begin{aligned} \sqrt{g} R \Big|_{\mathcal{O}(\sigma^3)} &= \frac{1}{4} \partial_\mu \partial^\alpha \partial^\rho \sigma \partial_\nu \partial_\alpha \partial_\rho \sigma \partial^\nu \partial^\mu \sigma - \frac{3}{32} \partial_\mu \partial_\rho \partial^\rho \sigma \partial_\nu \partial_\alpha \partial^\alpha \sigma \partial^\nu \partial^\mu \sigma \\ &+ \frac{1}{8} \partial_\mu \partial_\alpha \partial^\alpha \sigma \partial^\nu \partial^\mu \sigma \partial_\rho \partial_\nu \partial^\rho \sigma + \frac{1}{8} \partial_\mu \partial_\nu \partial^\rho \sigma \partial^\nu \partial^\mu \sigma \partial_\rho \partial_\alpha \partial^\alpha \sigma + \frac{3}{128} \partial_\mu \partial^\mu \sigma \partial_\rho \partial_\alpha \partial^\alpha \sigma \partial^\rho \partial_\nu \partial^\nu \sigma \\ &- \frac{1}{32} \partial_\mu \partial^\mu \sigma \partial^\rho \partial_\nu \partial^\nu \sigma \partial_\alpha \partial_\rho \partial^\alpha \sigma - \frac{1}{32} \partial_\mu \partial^\mu \sigma \partial^\rho \partial_\nu \partial^\nu \sigma \partial_\alpha \partial^\alpha \partial_\rho \sigma - \frac{1}{2} \partial_\mu \partial_\rho \partial_\alpha \sigma \partial^\nu \partial^\mu \sigma \partial^\alpha \partial_\nu \partial^\rho \sigma \\ &+ \frac{1}{8} \partial_\mu \partial^\mu \sigma \partial_\nu \partial_\alpha \partial_\rho \sigma \partial^\alpha \partial^\rho \partial^\nu \sigma - \frac{1}{16} \partial_\mu \partial^\mu \sigma \partial_\alpha \partial_\rho \partial_\nu \sigma \partial^\alpha \partial^\rho \partial^\nu \sigma \end{aligned} \quad (\text{C.17})$$

To obtain the vertices in momentum space—which will be necessary for the evaluation of Feynman diagrams—we have to Fourier transform the last expressions and take the derivative with respect to the three respective graviton fields. In the case of three spin-2 modes, this can effectively be achieved by replacing every term using the following rule

$$\begin{aligned} h_{ab}^{\text{TT}} \partial_i h_{cd}^{\text{TT}} \partial_f h_{ef}^{\text{TT}} &\mapsto -p_{1i} \mathbb{1}_{cd}^{\mu\nu} \left[p_{2j} \mathbb{1}_{ef}^{\rho\sigma} \mathbb{1}_{ab}^{\gamma\delta} + p_{3j} \mathbb{1}_{ab}^{\rho\sigma} \mathbb{1}_{ef}^{\gamma\delta} \right] - p_{2i} \mathbb{1}_{cd}^{\rho\sigma} \left[p_{1j} \mathbb{1}_{ef}^{\mu\nu} \mathbb{1}_{ab}^{\gamma\delta} + p_{3j} \mathbb{1}_{ab}^{\mu\nu} \mathbb{1}_{ef}^{\gamma\delta} \right] \\ &- p_{3i} \mathbb{1}_{cd}^{\gamma\delta} \left[p_{1j} \mathbb{1}_{ab}^{\rho\sigma} \mathbb{1}_{ef}^{\mu\nu} + p_{2j} \mathbb{1}_{ef}^{\rho\sigma} \mathbb{1}_{ab}^{\mu\nu} \right], \end{aligned} \quad (\text{C.18})$$

and ensuring energy conservation $\sum_i p_i = 0$. Similar rules for the other combinations of fields are easy to derive and can conveniently be implemented in computer algebra software.¹ For the sake of saving space we will refrain from given the explicit expressions of the vertices in momentum space as well as the York decomposed form of the forth variation of the Einstein-Hilbert action.

¹We used Wolfram Mathematica 10.0 together with the open source extension packages xAct 1.1.2 to obtain all variations and vertices for the calculation of Ch. 4.

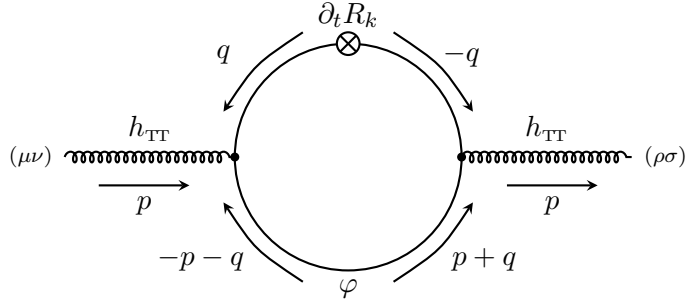


Figure C.1: One of the scalar candy versions contributing to diagram 4 in Fig. 4.1. The other one is symmetric and has the regulator insertion $\partial_t R_k$ in the lower leg in the loop.

C.2 Calculating Feynman diagrams

In this section we want to illustrate how to evaluate the Feynman diagrams of Figs. 4.1 and 4.2, using the rather simple example of the scalar φ candy diagram contributing to the beta function of the wave-function renormalisation Z_{TT} of the graviton, *cf.* diagram 4 in Fig. 4.1.

For the convenience of the reader, we display one of the two versions of the diagram including some additional annotation in Fig. C.1. The second version of this diagram, which is not displayed here, has the regulator insertion on the lower propagator in the loop and will give the same contribution as the first version. The diagram D_4 displayed in Fig. C.1 can be calculated as

$$D_4 = \int \frac{d^4 q}{(2\pi)^4} \left[\partial_t R_k^{(\varphi)}(q^2) G_k^{(\varphi)}(q^2) V^{(2,\text{TT})\mu\nu}(q, -p - q) \right. \\ \left. \times G_k^{(\varphi)}((p + q)^2) V^{(2,\text{TT})\rho\sigma}(p + q, -q) \frac{\mathcal{P}_{\mu\nu\rho\sigma}^{\text{TT}}}{5} \right], \quad (\text{C.19})$$

where we recall that the projector $\mathcal{P}_{\mu\nu\kappa\lambda}^{\text{TT}}$ was given by

$$\mathcal{P}_{\mu\nu\kappa\lambda}^{\text{TT}} = \frac{1}{2} (T_{\mu\kappa} T_{\nu\lambda} + T_{\mu\lambda} T_{\nu\kappa}) - \frac{1}{d-1} T_{\mu\nu} T_{\kappa\lambda}, \quad (\text{C.20})$$

$$T_{\mu\nu} = \delta_{\mu\nu} - \frac{p_\mu p_\nu}{p^2}. \quad (\text{C.21})$$

The latter appears because of the projection rule Eqn. (4.12), and we will have to make sure to evaluate the diagram at $\mathcal{O}(p^2)$. Using the expression of the vertex from the last section and the formula for the projector above, we can evaluate the tensor contraction to be

$$V^{(2,\text{TT})\mu\nu}(q, -(p + q)) V^{(2,\text{TT})\rho\sigma}(p + q, -q) \frac{\mathcal{P}_{\mu\nu\rho\sigma}^{\text{TT}}}{5} = \frac{64\pi}{15} g_3 (x^2 - 1)^2 q^4, \quad (\text{C.22})$$

where the angular variable x is define via

$$x \equiv \frac{p^\mu q_\mu}{p q}. \quad (\text{C.23})$$

Next, using the optimised cutoff and its first derivative

$$R_k^{(\varphi)} = Z_s (k^2 - q^2) \theta(k^2 - q^2) \quad (\text{C.24})$$

$$\partial_t R_k^{(\varphi)}, = \dot{Z}_s (k^2 - q^2) \theta(k^2 - q^2) + 2k^2 Z_s \theta(k^2 - q^2) + 2k^2 Z_s (k^2 - q^2) \delta(k^2 - q^2), \quad (\text{C.25})$$

we see that upon integration we have

$$\partial_t R_k^{(\varphi)}(q^2) G_k^{(\varphi)}(q^2) = Z_s \frac{2k^2 - \eta_s(k^2 - q^2)}{k^2} \theta(k^2 - q^2). \quad (\text{C.26})$$

The third and last contribution to the momentum integral is coming from the second propagator, and has to be expanded up to $\mathcal{O}(p^2)$

$$\begin{aligned} G_k^{(\varphi)}((p+q)^2) &= G_k^{(\varphi)}(q^2) + \frac{1}{2} G_k''^{(\varphi)}(q^2) p^2 + \mathcal{O}(p^4) \\ &= \frac{1}{k^2} - \frac{2x^2 p^2 q^2}{k^6} [2q^2 \delta(k^2 - q^2) + q^2(k^2 - q^2) \delta'(k^2 - q^2)], \end{aligned} \quad (\text{C.27})$$

where the second equality holds upon integration, when multiplied with $\theta(k^2 - q^2)$.

If we now collect the contributions (C.22), (C.26) and (C.27), and integrate over the two independent angular variables in momentum q_μ , such that we replace the measure by

$$\int \frac{d^4 q}{(2\pi)^4} \mapsto \frac{1}{4\pi^3} \frac{1}{2} \int_{-1}^1 dx \sqrt{1-x^2} \int_0^\infty dz z, \quad (\text{C.28})$$

where $z = q^2$, we can evaluate the integral and find

$$D_4 = -\frac{g_3 Z k^2}{24\pi}. \quad (\text{C.29})$$

Using the fact, that we have two diagrams for each and every of the N_s scalar fields, we find from the flow equation

$$\partial_t Z_{\text{TT}} = -\eta_{\text{TT}} Z \subseteq \frac{1}{2} (2N_s D_4), \quad (\text{C.30})$$

that the contribution the gravitational anomalous dimension is given by

$$\eta_{\text{TT}} \subseteq \frac{N_s \bar{g}_3}{24\pi}, \quad (\text{C.31})$$

which agrees with the result listed in Tab. 4.1.

D. The msWI in Yang-Mills theory

In this appendix we briefly want to illustrate the use of the msWI in the case of pure Yang-Mills theory in a covariant gauge using the example of the universal one-loop beta function, *cf.* in particular Ref. [106], Ch. IV C, p. 61ff.

Splitting the full field as $A_\mu = \bar{A}_\mu + a_\mu$, the covariant background gauge reads

$$\bar{D}_\mu a_\mu \equiv (\partial_\mu + i g \bar{A}_\mu) a_\mu = 0. \quad (\text{D.1})$$

The beta function of the coupling g can be read off from that of the running of the kinetic term $\text{Tr } \bar{F}^2$ in the background effective action $\Gamma_k[\bar{A}_\mu] = \Gamma_k[\bar{A}_\mu, a_\mu = 0]$. In particular, one finds

$$\partial_t \Gamma_k[\bar{A}] \Big|_{\text{Tr } \bar{F}^2} = -2 \bar{\beta}_g S_{\text{YM}}[\bar{A}], \quad (\text{D.2})$$

which comes about due to background gauge invariance. It turns out that regulators r_k which scale in the infrared like

$$p^2 r_k(y) \sim k^2 y^{-(n-1)}, \quad (\text{D.3})$$

where $y = p^2/k^2$, lead to a background beta function $\bar{\beta}_g = (1+n) \beta_g|_{1\text{-loop}}$, and are hence regulator-dependent. The beta function computed from the fluctuation diagrams instead is regulator-independent, $\beta_g = \beta_g|_{1\text{-loop}}$, which reflects the one-loop universality of the Yang-Mills beta function.

This puzzle may be resolved as follows. Firstly, let us note that an evaluation of the fluctuation correlation functions yields the correct one-loop beta function. Secondly, in the background field approximation the kinetic term $\text{Tr } \bar{F}^2$ receives contributions from the background field dependence of the regulator, too. This \bar{A} -dependence triggered by the regulator should not be seen as a genuine field dependence. Indeed, for $k \rightarrow 0$ it disappears, *cf.* Eqn. (5.26). This is why we have to disentangle

the regulator field dependence from the genuine one. This may be done by writing the effective action as

$$\Gamma_k[\bar{A}, a] = \Gamma_{k,1}[a] + \Gamma_{k,2}[\bar{A}] + \Gamma_{k,3}[\bar{A}, a], \quad (\text{D.4})$$

where the second term originates from the \bar{A} -dependence of the regulator and the last term accounts for gauge invariance under transformations of the full field. We will see shortly that this term vanishes in the present case.

To extract the regulator dependence, one simply takes a functional derivative of the last expression with respect to the background field. The renormalisation group flow of the resulting object can then be projected onto the relevant coupling to obtain the regulator contribution of the beta function one is interested in. The physical beta function is then given by the difference

$$\beta^{(\text{phys})} = \beta \Big|_{a=0} - \bar{\beta}. \quad (\text{D.5})$$

This is why we will investigate the flow of the background-dependence of the effective action $\partial_t \delta_{\bar{A}} \Gamma_k$

$$\partial_t \int_{y,z} \frac{\delta R_k(y,z)}{\delta \bar{A}(x)} \frac{\delta \Gamma_k}{\delta R_k(y,z)} = \frac{1}{2} \text{Tr} \partial_t \left(\frac{\delta R_k[\bar{A}]}{\delta \bar{A}(x)} G_k[\bar{A}, a] \right). \quad (\text{D.6})$$

The right hand side of this equation can be rewritten as a sum of traces over the spin-0 and spin-1 Laplacians $\bar{\Delta}_0 = -\bar{D}^2$ and $\bar{\Delta}_1 = -\bar{D}^2 - 2g\bar{F}$, respectively. These traces can then be re-expressed as total derivatives as follows

$$\frac{1}{2} \text{Tr} \partial_t \left[\frac{\delta R_k(\bar{\Delta})}{\delta \bar{A}(x)} G_k(\bar{\Delta}) \right] = \frac{1}{2} \frac{\delta}{\delta \bar{A}(x)} \text{Tr} \partial_t F_{\text{RG}}(\bar{\Delta}), \quad (\text{D.7})$$

where we defined the functional

$$F_{\text{RG}}(x) = \int_{x_0}^x dx' \frac{\partial R_k(x')}{\partial x'} G_k(x'). \quad (\text{D.8})$$

Note that the functional $F_{\text{RG}}(x)$ is potentially singular in the infrared, that is for $x \rightarrow 0$. The infrared limit of the regulators is given by (D.3), and it follows that

$$F_{\text{RG}}(x \rightarrow 0) \propto x^{-(n-1)}, \quad (\text{D.9})$$

shows a logarithmic divergence for $n = 1$. Accordingly, the t -derivative in Eqn. (D.6) is required for finiteness.

This shows how the msWI of Eqn. (5.26) can trigger contributions to logarithmically running quantities, even at one-loop: this is because infrared-singular regulators can introduce additional scales for background observables.

Now we want to compute the contributions to $\text{Tr} \bar{F}^2$ that come from the genuine background field dependence of the effective action. This is done by removing the mixed contributions, $\text{Tr} \bar{F} \bar{F}_{R_k}$, and $\text{Tr} \bar{F}_{R_k} \bar{F}_{R_k}$, from the full \bar{A} -dependence. Here, F_{R_k} signals the field strength of the regulator field. To that end we first notice that mixed contributions to $\text{Tr} \bar{F}^2$ are not present: taking a \bar{A} -derivative of Eqn. (D.7) which hits the genuine \bar{A} -dependence will lead to terms proportional to

$$-\partial_t \left[\text{Tr} \int_{x_0}^x dx' \frac{\partial R_k(x')}{\partial x'} G_k(x) \frac{\delta \Gamma_k^{(2)}}{\delta \bar{A}} G_k \Big|_{\text{Tr} \bar{F}^2} \right] = 0. \quad (\text{D.10})$$

Note that the occurrence of G_k^2 leads to an infrared-finite expressions, and hence the trace can be evaluated before taking the t -derivative. Since we focus on field-dependences with dimensionless coefficients, the t -derivative vanishes (this is because no other scale μ is present which could lead to $\log k/\mu$ dependences).

This leaves us with the task to compute Eqn. (D.7). The right hand side of which is a trace over a functional of $\bar{\Delta} = \bar{\Delta}_0, \bar{\Delta}_1$, and can be computed with standard heat-kernel techniques. In case we are interested in powers of $\text{Tr}\bar{F}^2$ only, the simplest way to compute the trace is by using the identity

$$\text{Tr}f(\bar{\Delta}) = f(-\partial_\tau)\text{Tr}e^{-\tau\bar{\Delta}}\Big|_{\tau=0}, \quad (\text{D.11})$$

which is valid a general function f . It is useful, since it avoids the standard Laplace transform. In the case of a Yang-Mills theory this leads to

$$\frac{1}{2}\text{Tr}\partial_t F_{\text{RG}}(\bar{\Delta})\Big|_{\text{Tr}\bar{F}^2} = -2n\beta_g|_{1\text{-loop}}S_{\text{YM}}[\bar{A}]. \quad (\text{D.12})$$

Subtracting this result from Eqn. (D.2) leads us to

$$\dot{\Gamma}_k[\bar{A}] - \frac{1}{2}\text{Tr}\partial_t F_{\text{RG}}(\bar{\Delta})\Big|_{\text{Tr}\bar{F}^2} = -2\beta_g|_{1\text{-loop}}S_{\text{YM}}[\bar{A}]. \quad (\text{D.13})$$

which is indeed the regulator independent, universal beta function.

The above analysis of Yang-Mills theory suggests the following: When using the background field approximation, one should modify second derivatives with respect to the background field in order to account for the regulator dependence of the background field.

This page intentionally left blank.

E. The msWI from heat kernel techniques

In this appendix we present a detailed derivation for the corrections of the background couplings through the use of the modified split Ward identity for Ch. 5. In particular we want to evaluate the following expression through heat kernel techniques:

$$\begin{aligned}
I &\equiv \frac{1}{2} \text{Tr} \left[\frac{1}{\sqrt{\bar{g}}} G_k(\bar{\Delta}) \frac{\delta}{\delta \bar{g}_{\mu\nu}} \left(\sqrt{\bar{g}} R_k(\bar{\Delta}) \right) \right] = \frac{1}{4} \bar{g}^{\mu\nu} \text{Tr} G_k R_k + \frac{1}{2} \text{Tr} \frac{\delta}{\delta \bar{g}_{\mu\nu}} F_{\text{RG}} \\
&= \frac{1}{4} \bar{g}^{\mu\nu} \text{Tr} G_k R_k + \frac{1}{2} \frac{\delta}{\delta \bar{g}_{\mu\nu}} \text{Tr} F_{\text{RG}} - \frac{1}{2} \text{Tr} \left[\frac{1}{\sqrt{\bar{g}}} \left(\frac{\delta}{\delta \bar{g}_{\mu\nu}} \sqrt{\bar{g}} \right) F_{\text{RG}} \right] \\
&= \frac{1}{4} \bar{g}^{\mu\nu} \text{Tr} \left(G_k R_k - F_{\text{RG}} \right) + \frac{1}{2} \frac{\delta}{\delta \bar{g}_{\mu\nu}} \text{Tr} F_{\text{RG}} = \frac{1}{2} \bar{g}^{\mu\nu} \left(I_1 - I_2 \right) + \frac{\delta}{\delta \bar{g}_{\mu\nu}} I_2. \tag{E.1}
\end{aligned}$$

In order to present intermediate results, we introduce the following short hand notations:

$$I_1 = \frac{1}{2} \text{Tr} G_k R_k, \quad I_2 = \frac{1}{2} \text{Tr} F_{\text{RG}}, \quad I_3 = \frac{1}{2} \text{Tr} G_k \dot{R}_k, \tag{E.2}$$

where the last expression is nothing but the background flow. To calculate these functional traces, we will once again follow Ref. [17]. In particular, we can write

$$I_1 = \frac{1}{32\pi^2} \left[B_0(\bar{\Delta}) Q_2(R_k G_k) + B_2(\bar{\Delta}) Q_1(R_k G_k) + B_4(\bar{\Delta}) Q_0(R_k G_k) \right] + \mathcal{O}(\bar{R}^3), \tag{E.3}$$

where the Q -functionals and the heat kernel coefficients were given by

$$Q_n[W] = \frac{1}{\Gamma(n)} \int dx x^{n-1} W(x), \tag{E.4}$$

$$B_n = \int d^d x \sqrt{\bar{g}} \text{tr} b_n. \tag{E.5}$$

To evaluate the Q -functionals, we note that the most general argument function $W(x)$ we encounter here is given by

$$W(x) = \frac{r_k(x)}{[x + r_k(x) + a \lambda k^2]^b}, \quad (\text{E.6})$$

as we will see shortly. The constants a and b will depend on the field component, and we have introduced the dimensionless cosmological constant λ . Using again the optimised cutoff, one finds the following results:

$$Q_2 = \frac{1}{6} \frac{k^{6-2b}}{(1+a\lambda)^b}, \quad Q_1 = \frac{1}{2} \frac{k^{4-2b}}{(1+a\lambda)^b}, \quad Q_0 = \frac{k^{2-2b}}{(1+a\lambda)^b}. \quad (\text{E.7})$$

In the limit $\beta = 0$ and $\alpha \rightarrow 0$, the trace of $R_k G_k$ over the spin components can be evaluated following the procedure in Ref. [85], and is given by the sum of the contributions of the four modes $h_{\mu\nu}^{\text{TT}}, \xi^\mu, h$ and σ . For the case of vanishing anomalous dimensions $\eta_h = \eta_c = 0$ they are given by

$$\text{Tr} R_k G_k \Big|_{h_{\text{TT}}} = \frac{r_k(x)}{x + r_k(x) - 2\lambda k^2} - \frac{2}{3} \bar{R} \frac{r_k(x)}{(x + r_k(x) - 2\lambda k^2)^2} + \frac{4}{9} \bar{R}^2 \frac{r_k(x)}{(x + r_k(x) - 2\lambda k^2)^3}, \quad (\text{E.8})$$

$$\text{Tr} R_k G_k \Big|_{\xi} = \frac{r_k(x)}{x + r_k(x)} + \frac{1}{4} \bar{R} \frac{r_k(x)}{(x + r_k(x))^2} + \frac{1}{16} \bar{R}^2 \frac{r_k(x)}{(x + r_k(x))^3}, \quad (\text{E.9})$$

$$\text{Tr} R_k G_k \Big|_h = \frac{r_k(x)}{x + r_k(x) - \frac{4}{3} \lambda k^2}, \quad (\text{E.10})$$

$$\text{Tr} R_k G_k \Big|_{\sigma} = \frac{r_k(x)}{x + r_k(x)} + \frac{1}{3} \bar{R} \frac{r_k(x)}{(x + r_k(x))^2} + \frac{1}{9} \bar{R}^2 \frac{r_k(x)}{(x + r_k(x))^3}. \quad (\text{E.11})$$

The vector (VG) and scalar ghost (SG) contributions are given by

$$\text{Tr} R_k G_k \Big|_{\text{VG}} = -2 \frac{r_k(x)}{x + r_k(x)} - \frac{1}{2} \bar{R} \frac{r_k(x)}{(x + r_k(x))^2} - \frac{1}{8} \bar{R}^2 \frac{r_k(x)}{(x + r_k(x))^3}, \quad (\text{E.12})$$

$$\text{Tr} R_k G_k \Big|_{\text{SG}} = -2 \frac{r_k(x)}{x + r_k(x)} - \frac{2}{3} \bar{R} \frac{r_k(x)}{(x + r_k(x))^2} - \frac{2}{9} \bar{R}^2 \frac{r_k(x)}{(x + r_k(x))^3}. \quad (\text{E.13})$$

We will now specialise the background to a four-dimensional sphere \mathbb{S}^4 . Then the heat kernel coefficients are given by

$$B_n(\bar{\Delta}) = \sqrt{\bar{g}} \text{Tr} b_n, \quad n = 0, 2, 4, \quad (\text{E.14})$$

where the trace coefficients are given in Tab. E.1. By specialising the coefficients a and b in the

	TTT	VT	S
tr b_0	5	3	1
tr b_2	$-\frac{5}{6}R$	$\frac{1}{4}R$	$\frac{1}{6}R$
tr b_4	$-\frac{1}{432}R^2$	$-\frac{7}{1440}R^2$	$\frac{29}{2160}R^2$

Table E.1: Heat kernel coefficients for transverse traceless tensors (TTT), transverse vectors (VT) and scalars (S) on a four-dimensional sphere \mathbb{S}^4 .

general expression above and evaluating the sum over all spin modes, we find

$$\begin{aligned}
I_1 = \frac{\sqrt{\bar{g}}}{32\pi^2} & \left\{ \left[\frac{5}{6} \frac{1}{1-2\lambda} + \frac{1}{6} \frac{1}{1-\frac{4}{3}\lambda} - \frac{2}{3} \right] k^4 \bar{R}^0 \right. \\
& + \left[-\frac{5}{9} \frac{1}{(1-2\lambda)^2} - \frac{5}{12} \frac{1}{1-2\lambda} + \frac{1}{12} \frac{1}{1-\frac{4}{3}\lambda} - \frac{7}{18} \right] k^2 \bar{R}^1 \\
& \left. + \left[\frac{10}{27} \frac{1}{(1-2\lambda)^3} + \frac{5}{18} \frac{1}{(1-2\lambda)^2} - \frac{1}{432} \frac{1}{1-2\lambda} + \frac{29}{2160} \frac{1}{1-\frac{4}{3}\lambda} - \frac{169}{1440} \right] k^0 \bar{R}^2 \right\}. \tag{E.15}
\end{aligned}$$

With similar methods we can evaluate the trace I_2 . In particular, using the expansion Eqn. (D.11) we may write

$$I_2 = \frac{1}{32\pi^2} F_{\text{RG}} \partial_\tau \left[B_0(\bar{\Delta}_s) \tau^{-2} + B_2(\bar{\Delta}_s) \tau^{-1} + B_4(\bar{\Delta}_s) \tau^0 \right] \Big|_{\tau=0} + \mathcal{O}(\bar{R}^3). \tag{E.16}$$

In particular, by utilising the following identities

$$\frac{1}{\tau^2} = \int_0^\infty dx x e^{-\tau x} \Big|_{\tau=0} \tag{E.17}$$

$$\frac{1}{\tau} = \int_0^\infty dx e^{-\tau x} \Big|_{\tau=0} \tag{E.18}$$

one can evaluate the action of the differential operator of Eqn. (D.8):

$$F_{\text{RG}}(-\partial_\tau) \tau^{-2} = \int_0^\infty dx x F_{\text{RG}}(x) = -\frac{1}{3} \frac{k^{6-2b}}{(1+a\lambda)^b}, \tag{E.19}$$

$$F_{\text{RG}}(-\partial_\tau) \tau^{-1} = \int_0^\infty dx F_{\text{RG}}(x) = -\frac{1}{2} \frac{k^{4-2b}}{(1+a\lambda)^b}, \tag{E.20}$$

$$F_{\text{RG}}(-\partial_\tau) \tau^0 = F_{\text{RG}}(0) = 0, \tag{E.21}$$

where the last equalities respectively hold for the general function

$$F_{\text{RG}}(x) = \int_0^x dy \frac{r'_k(y)}{(y + r_k(y) + a\lambda k^2)^b} = -\frac{x}{(1+a\lambda)^b}, \quad (x \leq k^2), \tag{E.22}$$

using the optimised cutoff as before. Specializing the coefficients a and b for the various spin modes and summing the contributions we find up to $\mathcal{O}(\bar{R}^2)$

$$I_2 = \frac{\sqrt{\bar{g}}}{32\pi^2} \left\{ \left[-\frac{5}{3} \frac{1}{1-2\lambda} - \frac{1}{3} \frac{1}{1-\frac{4}{3}\lambda} + \frac{4}{3} \right] k^4 \bar{R}^0 + \left[\frac{5}{12} \frac{1}{1-2\lambda} - \frac{1}{12} \frac{1}{1-\frac{4}{3}\lambda} + \frac{5}{24} \right] k^2 \bar{R}^1 \right\}. \quad (\text{E.23})$$

Finally, the right-hand side of the flow equation I_3 can be evaluated in the same way as I_1 , where the Q -functionals now depend on another function

$$\tilde{W}(x) = \frac{\dot{r}_k(x)}{[x + r_k(x) + a\lambda k^2]^b}. \quad (\text{E.24})$$

Using $\dot{r}_k(x) = 2k^2\theta(k^2 - x)$ for the optimized cutoff, we find

$$Q_2[\tilde{W}] = \frac{k^{6-2b}}{(1+a\lambda)^b}, \quad Q_1[\tilde{W}] = \frac{2k^{4-2b}}{(1+a\lambda)^b}, \quad Q_0[\tilde{W}] = \frac{2k^{2-2b}}{(1+a\lambda)^b}. \quad (\text{E.25})$$

With these relations, we find for the background flow

$$I_3 = \frac{\sqrt{\bar{g}}}{32\pi^2} \left\{ \left[\frac{5 - \frac{5}{6}\eta_h}{1-2\lambda} + \frac{1 - \frac{1}{6}\eta_h}{1 - \frac{4}{3}\lambda} - 4 - \frac{2}{3}\eta_h + \frac{4}{3}\eta_c \right] k^4 \bar{R}^0 \right. \\ + \left[-\frac{10}{3} \frac{1 - \frac{1}{6}\eta_h}{(1-2\lambda)^2} - \frac{5}{3} \frac{1 - \frac{1}{4}\eta_h}{1-2\lambda} + \frac{1}{3} \frac{1 - \frac{1}{4}\eta_h}{1 - \frac{4}{3}\lambda} - \frac{23}{12} - \frac{7}{18}\eta_h + \frac{14}{18}\eta_c \right] k^2 \bar{R}^1 \\ \left. + \left[\frac{20}{9} \frac{1}{(1-2\lambda)^3} + \frac{10}{9} \frac{1}{(1-2\lambda)^2} - \frac{1}{216} \frac{1}{1-2\lambda} + \frac{29}{1080} \frac{1}{1 - \frac{4}{3}\lambda} - \frac{149}{270} \right] k^0 \bar{R}^2 \right\}. \quad (\text{E.26})$$

In order to evaluate the full expression for I , we have to take first derivatives of the background Ricci scalar \bar{R} with respect to the background field. Carrying out the general variation one finds

$$\frac{\delta \bar{R}}{\delta \bar{g}_{\mu\nu}} = -\frac{1}{d} \bar{R} \bar{g}^{\mu\nu} + \bar{g}^{\alpha\beta} \frac{\delta \bar{R}_{\alpha\beta}}{\delta \bar{g}_{\mu\nu}}, \quad \text{where} \quad \frac{\delta \bar{R}_{\alpha\beta}}{\delta \bar{g}_{\mu\nu}} = \bar{\Delta}_\rho \frac{\delta \Gamma_{\alpha\beta}^\rho}{\delta \bar{g}_{\mu\nu}} - \bar{\Delta}_\alpha \frac{\delta \Gamma_{\rho\beta}^\rho}{\delta \bar{g}_{\mu\nu}}. \quad (\text{E.27})$$

The two right-most terms are total derivatives and will not contribute. Note that this does not hold true any more when the derivative of \bar{R}^2 is evaluated. We thus have in $d = 4$

$$\frac{\delta \sqrt{\bar{g}}}{\delta \bar{g}_{\mu\nu}} = \frac{1}{2} \sqrt{\bar{g}} \bar{g}^{\mu\nu}, \quad \frac{\delta \sqrt{\bar{g}} \bar{R}}{\delta \bar{g}_{\mu\nu}} = \frac{1}{4} \sqrt{\bar{g}} \bar{g}^{\mu\nu} \bar{R}. \quad (\text{E.28})$$

Using these relations, we can finally evaluate I to be

$$I = \frac{\sqrt{\bar{g}} \bar{g}^{\mu\nu}}{32\pi^2} \left\{ \left[\frac{5}{12} \frac{1}{1-2\lambda} + \frac{1}{12} \frac{1}{1 - \frac{4}{3}\lambda} - \frac{1}{3} \right] k^4 \bar{R}^0 \right. \\ + \left[-\frac{5}{18} \frac{1}{(1-2\lambda)^2} - \frac{5}{16} \frac{1}{1-2\lambda} + \frac{1}{16} \frac{1}{1 - \frac{4}{3}\lambda} - \frac{71}{288} \right] k^2 \bar{R}^1 \\ \left. + \left[\frac{10}{27} \frac{1}{(1-2\lambda)^3} + \frac{5}{18} \frac{1}{(1-2\lambda)^2} - \frac{1}{432} \frac{1}{1-2\lambda} + \frac{29}{2160} \frac{1}{1 - \frac{4}{3}\lambda} - \frac{169}{1440} \right] k^0 \bar{R}^2 \right\}.$$

For a pure scalar field we find the following results:

$$I_1^s = \frac{\sqrt{\bar{g}}}{32\pi^2} \left[\frac{1}{6} k^4 + \frac{1}{12} k^2 \bar{R} + \frac{29}{2160} \bar{R}^2 \right] + \mathcal{O}(\bar{R}^3), \quad (\text{E.29})$$

$$I_2^s = \frac{\sqrt{\bar{g}}}{32\pi^2} \left[-\frac{1}{3} k^4 - \frac{1}{12} k^2 \bar{R} \right] + \mathcal{O}(\bar{R}^3), \quad (\text{E.30})$$

$$I_3^s = \frac{\sqrt{\bar{g}}}{32\pi^2} \left[k^4 + \frac{1}{3} k^2 \bar{R} + \frac{29}{1080} \bar{R}^2 \right] + \mathcal{O}(\bar{R}^3). \quad (\text{E.31})$$

This implies

$$I^s = \frac{\sqrt{\bar{g}} \bar{g}^{\mu\nu}}{32\pi^2} \left[\frac{1}{12} k^4 + \frac{1}{16} k^2 \bar{R} + \frac{29}{4320} \bar{R}^2 \right] + \mathcal{O}(\bar{R}^3). \quad (\text{E.32})$$

This page intentionally left blank.

Declaration of Authorship

I, Peter Labus, declare that this thesis titled, “Matter Fields in Asymptotically Safe Quantum Field Theories of Gravity” and the work presented in it are my own. I confirm that:

- This work was done wholly or mainly while in candidature for a PhD degree at SISSA.
- Where any part of this thesis has previously been submitted for a degree or any other qualification at this research institute or any other institution, this has been clearly stated.
- Where I have consulted the published work of others, this is always clearly attributed.
- Where I have quoted from the work of others, the source is always given. With the exception of such quotations, this thesis is entirely my own work.
- I have acknowledged all main sources of help.

Date: 11th September 2017

Signature: